

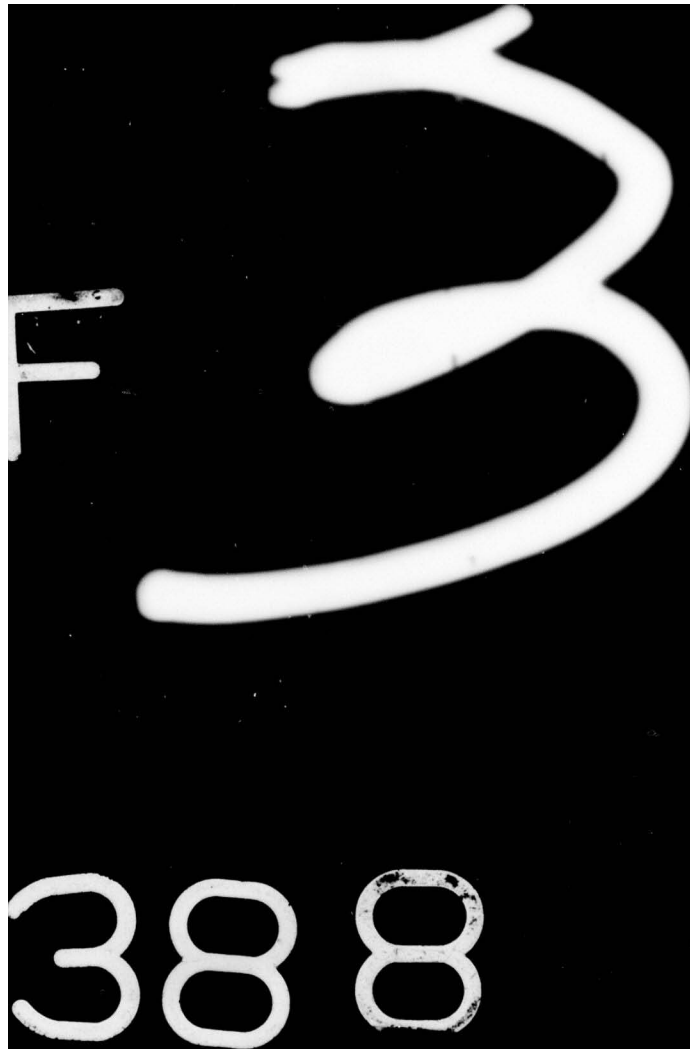
AD-A031 388

NIELSEN ENGINEERING AND RESEARCH INC MOUNTAIN VIEW CALIF F/G 1/3
PREDICTION OF SUPERSONIC STORE SEPARATION CHARACTERISTICS. VOLU--ETC(U)
MAY 76 F K GOODWIN, M M KEIRSTEAD F33615-75-C-3053
NEAR-TR-106 AFFDL-TR-76-41-VOL-2 NL

UNCLASSIFIED

1 OF 3
AD
A031388





AD A031388

AFFDL-TR-76-41
VOLUME II

(12)

**PREDICTION OF SUPERSONIC STORE SEPARATION
CHARACTERISTICS
VOLUME II-USERS MANUAL FOR THE COMPUTER
PROGRAM**

*NIELSEN ENGINEERING & RESEARCH, INC.
MOUNTAIN VIEW, CALIFORNIA 94043*

MAY 1976

**COPY AVAILABLE TO DDC DOES NOT
PERMIT FULLY LEGIBLE PRODUCTION**

FINAL REPORT FEBRUARY 1975 - MARCH 1976

DDC
RECEIVED
NOV 1 1976
B

Approved for public release; distribution unlimited

AIR FORCE FLIGHT DYNAMICS LABORATORY
AIR FORCE WRIGHT AERONAUTICAL LABORATORIES
AIR FORCE SYSTEMS COMMAND
WRIGHT-PATTERSON AIR FORCE BASE, OHIO 45433

NOTICE

When Government drawings, specifications, or other data are used for any purpose other than in connection with a definitely related Government procurement operation, the United States Government thereby incurs no responsibility nor any obligation whatsoever; and the fact that the Government may have formulated, furnished, or in any way supplied the said drawings, specifications, or other data, is not to be regarded by implication or otherwise as in any manner licensing the holder or any other person or corporation, or conveying any rights or permission to manufacture, use, or sell any patented invention that may in any way be related thereto.

This technical report has been reviewed and is approved for publication.

FOR THE COMMANDER

E. H. Flinn

E. H. Flinn, Chief
Control Criteria Branch
Flight Control Division

Calvin L. Dyer

Calvin L. Dyer
Project Engineer
Control Criteria Branch
Flight Control Division

Lt Col Larry M. Hadley, Chief
Flight Control Division

Copies of this report should not be returned unless return is required by security considerations, contractual obligations, or notice on a specific document.

UNCLASSIFIED

SECURITY CLASSIFICATION OF THIS PAGE (When Data Entered)

REPORT DOCUMENTATION PAGE		READ INSTRUCTIONS BEFORE COMPLETING FORM
1. REPORT NUMBER	2. GOVT ACCESSION NO.	3. REPORT TYPE AND DATES COVERED
AFFDL-TR-76-41, Vol. II	(9) Final	Rept. 24 Feb 75-24 Mar 76
4. TITLE (and Subtitle)	5. TYPE OF REPORT & PERIOD COVERED	
PREDICTION OF SUPERSONIC STORE SEPARATION CHARACTERISTICS, Volume II. Users Manual for the Computer Program	Final-Technical 2/24/75 to 3/24/76	
7. AUTHOR(s)	6. PERFORMING ORG. REPORT NUMBER	
Frederick K. Goodwin, Mary M. Keirstead Marnix F. E. Dillenius	NEAR-TR-106	
9. PERFORMING ORGANIZATION NAME AND ADDRESS	8. CONTRACT OR GRANT NUMBER(s)	
Nielsen Engineering & Research, Inc. 510 Clyde Avenue Mountain View, California 94043	F33615-75-C-3053	
11. CONTROLLING OFFICE NAME AND ADDRESS	10. PROGRAM ELEMENT, PROJECT, TASK AREA & WORK UNIT NUMBERS	
Air Force Flight Dynamics Laboratory (FGC) Wright-Patterson Air Force Base Ohio 45433	Program Element 62201 F 8219-01-13	
13. MONITORING AGENCY NAME & ADDRESS (if different from Controlling Office)	12. REPORT DATE	
(16) AF-8219 (12) 274p	(11) May 1976	
16. DISTRIBUTION STATEMENT (of this Report)	14. NUMBER OF PAGES	
(17) 821901 Approved for public release; distribution unlimited.	271	
17. DISTRIBUTION STATEMENT (of the abstract entered in Block 20, if different from Report)	15. SECURITY CLASS. (of this report)	
(18) AFFDL (19) TR-76-41-Vol-2	Unclassified	
15a. DECLASSIFICATION/DOWNGRADING SCHEDULE		
18. SUPPLEMENTARY NOTES		
19. KEY WORDS (Continue on reverse side if necessary and identify by block number)		
Aerodynamic Loads Flow Fields Aerodynamic Interference Store Separation External Stores Supersonic Flow		
20. ABSTRACT (Continue on reverse side if necessary and identify by block number)		
Detailed instructions are presented for using a computer program which calculates the six-degree-of-freedom trajectories of external stores which are separated from fighter-bomber type aircraft flying at supersonic speeds. Single store configurations can be handled by the program. The program uses linear potential-flow theory to model the wing and pylon loading and thickness. Three-dimensional line sources and line doublets are used to model the fuselage and store. The program also calculates the trajectory		

389 783

over
1/B

UNCLASSIFIED

SECURITY CLASSIFICATION OF THIS PAGE(When Data Entered)

20. of the store as it separates from the aircraft. This report describes the program, presents instructions for preparing input for the program, describes the output from the program, and presents a sample case. The program draws heavily on an earlier program for subsonic speeds written by the present authors and described in AFFDL-TR- 74-130.

ACCESSION for	
NTIS	White Section <input checked="" type="checkbox"/>
DDC	Buff Section <input type="checkbox"/>
UNANNOUNCED	<input type="checkbox"/>
JUSTIFICATION	
BY	
DISTRIBUTION/AVAILABILITY CODES	
Dist.	AVAIL. and/or SPECIAL
A	

UNCLASSIFIED

SECURITY CLASSIFICATION OF THIS PAGE(When Data Entered)

FOREWORD

This report, "Prediction of Supersonic Store Separation Characteristics," describes a combined theoretical-experimental program directed toward developing a computer program for predicting the trajectory of an external store separated from an aircraft flying at supersonic speed. Volume I, "Theoretical Methods and Comparisons with Experiment," describes the theoretical approach and presents extensive comparisons with experimental data. This volume, Volume II.- "Users Manual for the Computer Program," presents detailed instructions on the use of the computer program.

The work was carried out by Nielsen Engineering & Research, Inc., 510 Clyde Avenue, Mountain View, California 94043, under Contract No. F33615-75-C-3053. The contract was initiated under Project 8219, Task 821901, of the Air Force Flight Dynamics Laboratory. The Air Force Project Engineer on the contract was Calvin L. Dyer, AFFDL/FGC. The report number assigned by Nielsen Engineering & Research, Inc. is NEAR TR 106.

The authors wish to thank Mr. Dyer, AFFDL/FGC, for his assistance during the course of the investigation. The computer program card deck is available upon request from Mr. Dyer. His address is AFFDL/FGC, Wright-Patterson AFB, Ohio 45433.

The work documented in this report was started on February 24, 1975 and was effectively concluded with the submission of this report. The report was submitted by the authors in March 1976.

TABLE OF CONTENTS

<u>Section</u>	<u>Page No.</u>
1. INTRODUCTION	1
2. GENERAL DESCRIPTION OF THE USE OF THE PROGRAM	3
2.1 Input Section	3
2.2 Wing-Pylon Loading Section	4
2.3 Trajectory Section	5
3. DETAILS OF THE USE OF THE PROGRAM	6
3.1 General Flow Chart	7
3.2 Input Data	10
3.2.1 Input format	10
3.2.2 Sample input data	29
3.3 Output from the Program	34
4. PROGRAM ERROR MESSAGES	38
5. PROGRAM RUNNING TIMES	39
TABLE I	40
APPENDIX I - DETAILS FOR THE PROGRAMMER	117
APPENDIX II - DETERMINATION OF TAIL-FIN LIFT-CURVE SLOPE	262
REFERENCES	264

LIST OF ILLUSTRATIONS

<u>Figure</u>	<u>Page</u>
1. Program listing.	43
2. General flow chart of trajectory program.	81
3. Trajectory program input format.	84
4. Simplified layout of panels for wing-pylon and fuselage combination.	92
5. Fuselage coordinate system.	93
6. Definition of certain wing input variables.	94
7. Example wing.	95
8. Variables describing and locating pylon, input data item number 19.	96
9. Wind-tunnel models used in sample calculations.	97
10. Configuration for sample trajectory.	100
11. Input data deck for sample trajectory calculation.	101
12. Trajectory program output for sample case.	102
13. Coordinate systems fixed in separated store and used in force and moment calculation.	116
14. Coordinate systems used in trajectory calculation.	117

LIST OF SYMBOLS

a_{\max}	maximum store body radius
c_{dC}	section drag coefficient of a circular cylinder normal to airstream
C_A	axial-force coefficient, axial force/ $q_{\infty} S_R$
C_l	rolling-moment coefficient, rolling moment/ $q_{\infty} S_R l_R$
C_m	pitching-moment coefficient, pitching moment/ $q_{\infty} S_R l_R$
C_n	yawing-moment coefficient, yawing moment/ $q_{\infty} S_R l_R$
C_N	normal-force coefficient, normal force/ $q_{\infty} S_R$
C_Y	side-force coefficient, side force/ $q_{\infty} S_R$
d	maximum diameter of store
F_T	thrust force
F_x	total force acting along the store longitudinal axis
g_x	component of the gravitational force acting along the store longitudinal axis
I_{xx}, I_{yy}, I_{zz}	moments of inertia about x, y, z axes of figure 13; taken about store moment center
I_{yz}, I_{xz}, I_{xy}	products of inertia about x, y, z axes of figure 13; taken about store moment center
l	body length
l_R	reference length; store maximum diameter, d
l_s	length of separated store
m	mass of separated store
M_{∞}	aircraft free-stream Mach number
p, q, r	rotational velocities about x, y, z axes of figure 13; positive as shown in figure 14
q_{∞}	free-stream dynamic pressure; $1/2 \rho_{\infty} V_{\infty}^2$

LIST OF SYMBOLS (CONC.)

$q_{\infty S}$	ejected store free-stream dynamic pressure; $1/2 \rho_{\infty} V_{\infty S}^2$
r	local body radius
s	semispan of wing
S_R	reference area taken equal to body frontal area, πa_{\max}^2
t	time
u_+/V_{∞}	strength of a constant u-velocity panel
U_s, V_s, W_s	total velocities as seen by store, positive in x_s, y_s, z_s directions, see figure 13
V_{∞}	aircraft free-stream velocity
$V_{\infty S}$	separated store free-stream velocity
x, y, z	coordinate system with origin at store moment center, see figure 13
x_B, y_B, z_B	coordinate system fixed in fuselage with the origin at nose, see figure 5
$x_{\ell}, y_{\ell}, z_{\ell}$	coordinate system fixed in local airfoil section of wing, see figure 8(b), with x_{ℓ} lying along chord line
x_s, y_s, z_s	coordinate system fixed in separated store with origin at store nose, see figure 13
$x_{s,m}$	x_s coordinate of store moment center
x_w, y_w, z_w	coordinate system fixed in wing with origin at root-chord leading edge, see figure 6
α_{ℓ}	local angle of attack due to wing twist and camber
θ	$\tan \theta$, local slope of wing thickness envelope
ξ, η, ζ	inertial coordinate system fixed in fuselage nose, positive forward along longitudinal axis, positive laterally to the right, and positive vertically downward, respectively, see figure 14
ρ_{∞}	free-stream mass density
ψ, θ, ϕ	store yaw, pitch and roll angles specifying angular orientation of store x, y, z coordinate system relative to ξ, η, ζ inertial system, see figure 14

PREDICTION OF SUPERSONIC STORE SEPARATION CHARACTERISTICS

Volume II.- Users Manual for the Computer Program

1. INTRODUCTION

The purpose of this volume of the report is to describe and present instructions for using the computer program developed in conjunction with the theoretical work presented in Volume I, reference 1. This work represents a first year's effort on the development of an analytical method for predicting the trajectory of a store separated from an aircraft flying at supersonic speeds. As a result, the parent aircraft configuration which can be modeled does not have the generality of the subsonic store separation prediction method and program described in references 2 and 3. Preliminary versions of that method and program are described in references 4, 5, and 6.

In developing the present program every attempt has been made to keep the input data format the same as that used in the program described in reference 3. The printed output also has been kept as similar as possible.

The program as described in this report has been run on the CDC 6600 computer. The program should run with very little, if any, modification on other computers with large enough memory capacity. The program requires approximately 210,000 octal words of core storage on the 6600. No tapes, drums, or disks are used by the program. All input to the program is from cards and all output is printed.

The next sections of this report will describe in more detail the general use of the program and then present instructions for preparing the input data and interpreting the output. A sample case is presented. Details of the program are contained in an appendix.

The method of describing the aircraft components, the aircraft operational parameters, and the dynamical characteristics of the store are of importance. The various parameters which are included in the computer program are:

Wing Panels

Thickness distribution: Specified at large number of chordwise locations and at the same number of spanwise locations as used in the constant u-velocity panel layout which represents the wing as a lifting surface.

Mean camber surface: May have both twist and camber.

Leading-edge shape: Represented by straight line segments of differing sweep.

Trailing-edge shape: Also represented by straight line segments of differing sweep.

Dihedral: None.

Fuselage

Shape: Body of revolution.

Pylon

Thickness distribution: Same method of description as for wing panel

Mean camber surface: Planar.

Orientation: Vertical and streamwise.

Leading-edge shape: Straight but can be swept.

Trailing-edge shape: Straight but can be swept.

Tip: Parallel to pylon root chord.

Number: One pylon per wing panel or one under fuselage centerline.

Store

Shape: Body of revolution.

Number of stores: One.

Attached orientation: Initial pitch angle arbitrary, initial yaw angle zero.

Empennage: Planar or cruciform empennage.

Initial roll orientation: Arbitrary.

Power: Option of specifying a thrust time history.

Airplane Operating Characteristics

Flight path: Straight but not necessarily horizontal.

Flight velocity: Constant.

Density: Constant.

Angle of attack: Constant.

Yaw angle: Zero.

Store Inertial Characteristics

Moments of inertia: Constant.

Products of inertia: Constant.

Center of gravity position: Not necessarily on store longitudinal axis.

Store Ejection Conditions

Initial translational velocities: Arbitrary.

Initial pitching velocity: Arbitrary.

Initial yawing velocity: Arbitrary.

Initial rolling velocity: Arbitrary.

2. GENERAL DESCRIPTION OF THE USE OF THE PROGRAM

The store separation trajectory program consists of three main sections. The first section reads in the input data and calculates quantities from these data, the second section solves for the singularity distribution which represents the wing-pylon loading including interference on the fuselage, and the third section calculates the trajectory.

2.1 Input Section

The input section of the program reads in the following information.

- (1) Aircraft flight conditions
- (2) Indices specifying what aircraft components are present
- (3) Fuselage data
- (4) Wing data
- (5) Pylon data
- (6) Store data

The aircraft flight conditions, item (1) above, which can be varied are the angle of attack, flight path angle, Mach number, free-stream air density, and flight velocity.

Item (2) consists of four indices. The first specifies whether a fuselage is present and the second specifies whether a pylon is present. The third index is not used and has been left in for compatibility with the input data for the subsonic program, reference 3. The fourth index specifies whether a store is present. The program in its present form will only handle one store.

The fuselage input data, item (3) above, are the length, maximum radius, and polynomials specifying the body radius as a function of axial location. Other fuselage input data specify the number of sources and doublets, to be used in representing the fuselage volume and angle of attack effects, and specify the fuselage interference panel layout.

The wing input data, item (4), locate the wing relative to the fuselage and supply information required to lay out the u-velocity panels and the thickness distribution. These data also include the twist and camber distribution and the slope distribution of the thickness envelope. The wing leading and trailing edges can have breaks in sweep.

Similarly, the pylon input data, item (5), locate the pylon and provide information required to lay out the u-velocity panels and the thickness distribution. The pylon is located laterally relative to the fuselage centerline and longitudinally relative to the leading edge of the local wing chord. The data also include the slope distribution of the thickness envelope. The pylon cannot have twist or camber. The leading and trailing edges can be swept at constant but different sweep angles.

Store data, item (6), are input which assign a store number and specify a shape number, length, and maximum radius. The store is located by specifying its lateral position relative to the fuselage centerline and the longitudinal and vertical position of the store nose relative to the wing chord immediately above the store. The incidence of the store relative to the wing root chord is also specified. The store must be under the fuselage centerline or to the left of this line as seen by the pilot. Data used to determine the source and doublet distributions to represent the store volume and angle of attack effects are also input. These data include the number of singularities and polynomials specifying the store shape.

2.2 Wing-Pylon Loading Section

The second main section of the program calculates the singularity distribution representing the wing-pylon loading including interference on the fuselage. This is done using the method described in section 3.3 of reference 1. The coefficient matrix is first calculated and then the right-hand side is determined. Finally, the strengths of the constant u-velocity panels divided by π are calculated by solving the set of simultaneous equations.

2.3 Trajectory Section

The third and last main section of the trajectory program is the trajectory calculation which consists of the following steps:

- (1) Input additional information to describe separated store
- (2) Input empennage data if store has one
- (3) Input thrust time history if powered store
- (4) Initialize for trajectory calculation
- (5) Calculate aerodynamic forces and moments
- (6) Calculate accelerations and rates of change of orientation angles
- (7) Integrate equations of motion
- (8) Repeat steps (5), (6), and (7) to end of trajectory

The additional data describing the store to be separated include indices specifying the store number, the number of segments the body is to be broken into for the force calculation, the flow separation location, whether the store has an empennage and whether it is powered. Also, the store mass and inertia characteristics are read in along with the location of the point about which the aerodynamic moments are to be calculated. This is the point about which the moments and products of inertia were calculated. The location of the store center of mass relative to this point is also specified as are the store axial-force coefficient and the value of the crossflow-drag coefficient to be used in the viscous crossflow force and moment calculation.

Three other indices are input which pertain to options included in the computer program. Provision has been made to include or exclude the damping terms in the velocity field calculation. Also, for a store with an empennage, rolling moment may or may not be included in the acceleration determination. The third option pertains to the calculation of free-flight trajectories as opposed to captive-store trajectories as obtained in the wind tunnel. In wind-tunnel captive-store testing it is customary to change the store pitch and yaw angles to account for translational motion only while measuring the aerodynamic forces and moments. This changes its position in the nonuniform flow field. Provision has been made in the computer program to simulate this.

For a store with an empennage, additional quantities must be specified. These data are an index indicating whether the empennage is planar or cruciform, the tail-fin semispan, the average body radius in the tail-fin region, the initial roll orientation of the fins, and the lift-curve slope

of the fins alone. In addition, the axial position at which the forces are assumed to act must be specified.

For a powered store, a series of polynomials is used to specify the thrust time history.

In the trajectory initialization certain store separation conditions are specified. These are the initial translational velocities and rotational velocities.

The integration of the equations of motion is done by a standard numerical integration technique with the aerodynamic forces and moments calculated at each point required by the integration scheme. The calculation of the nonuniform velocity field and the resulting forces and moments is described in sections 3.4 and 4 of reference 1 and in section 5 of reference 4, respectively.

For a given aircraft-store combination and Mach number, it can be seen that a series of trajectories can be run with only minor changes to the input data deck. For example, the aircraft angle of attack can be varied by changing one number on one card as can the aircraft flight path angle. The altitude can be varied by changing the free-stream density and possibly the free-stream velocity to account for changes in the speed of sound. Among other things easily varied are the store mass and inertia properties, center of gravity location, and ejection conditions.

Provision has also been made for restarting a trajectory. This is accomplished by changing one card which specifies the initial and final times and adding two cards specifying the current values of the dependent variables. These are tabulated in the output at each integration step.

3. DETAILS OF THE USE OF THE PROGRAM

The program consists of a main program and 42 subroutines. Table I lists these subroutines in alphabetical order and gives a one-sentence description of what each subroutine does. A listing of the six-degree-of-freedom trajectory program and its 42 subroutines is presented in figure 1 and a general flow chart of the main program in figure 2. The program listing in figure 1 is specifically for the CDC 6600 computer. To run it on other machines the first card and the three cards following statement number 1000 in the main program may have to be removed or changed. A detailed description of the program and subroutines, including the equations programmed, is presented in Appendix I.

3.1 General Flow Chart

The computer program integrates the six-degree-of-freedom equations of motion which are derived in Appendix II of reference 4. The aerodynamic forces and moments are calculated by the methods presented in section 5.2 of that report.

A general flow chart of the program is presented in figure 2. Page 1 of the flow chart, figure 2(a), is the input section of the program. Constants are defined and heading information is read and printed. The aircraft flight conditions are input as are indices specifying what aircraft components are present. If the fuselage is present, the fuselage data are read in and printed in subroutine FUSEIO. This routine also calls BDYGEN to calculate the source and doublet distributions which represent the fuselage volume and angle of attack effects.

The next steps in the program read in the data required to model the wing. The data locating the wing are first read and then subroutine SWNGIN is called. This routine reads in the data required to lay out the constant u-velocity panels which will represent the loaded wing. In addition it reads in the twist and camber distribution at the panel control points. Subroutine WLYOUT is called to lay out the panels. The last wing input data is the thickness distribution. These data are read in by subroutine WITHIN.

A check is made in the program to determine whether or not a pylon is present. If one is, subroutine PLYOUT is called to read in the data required to lay out the constant u-velocity panels which will represent the pylon loading. This routine also lays out the panels. Subroutine PYTHIN is next called to read in the pylon thickness data.

The next two steps in the program are calls to subroutines THKOUT and THKLYT. These two routines, respectively, print the input data for the wing and pylon thickness and lay out the thickness panels.

A check is now made to see if a fuselage is present. If it is then subroutine BLYOUT is called to lay out the constant u-velocity panels on the fuselage.

Provision has been made for not including a store in the input data. This has been done so that the program can be used to determine the coordinates of the points at which the wing twist and camber distribution must be input. The next step in the program checks to see if there is a store

and if there is not one, the store input section of the program is bypassed. If there is a store, subroutine STORIO is called to read in and print all of the store data. These data consist of the location and incidence of the store and polynomials specifying its shape. This routine also calls subroutine BDYGEN to calculate the source and doublet distributions which represent the store volume and angle of attack effects. Following this the store is located in the fuselage coordinate system.

Boxes 2 through 4 of the left-hand column of figure 2(b) are associated with the calculation of the strengths of the constant u-velocity panels to represent the wing-pylon loading including interference effects on the fuselage. The equations used to solve for the strengths are given in section 3.3 of reference 1. The first step is to call subroutine DPCOEF which calculates the coefficient matrix, that is, the coefficients multiplying the unknown panel strengths divided by π , $(u_+/V_\infty)/\pi$. The next step is to call subroutine DPRHS which calculates the right-hand side of this set of simultaneous equations. The resulting set of equations is then solved by calling subroutine INVERS. The next section of the program prints the resulting panel strengths, control point coordinates, and interference velocities at these points. If a store is not present this ends the calculations and the program returns to the beginning to read another set of input data.

If a store is present the program continues and reads in the additional data required to describe the store to be separated and performs the initialization for the trajectory calculation. The remainder of the flow chart of figure 2(b) shows this part of the program. First the additional data describing the store are read in. These data consist of, among other things, the mass and inertia characteristics, polynomials defining the body shape, and center of gravity location. The next step is to calculate other quantities from these data.

If the store to be separated has an empennage the data required to describe the empennage are input and subroutine SEMPIN is called to initialize for the empennage force and moment calculation.

The program next reads in polynomials specifying the thrust time history if this option is being used.

Provision is made in the program for prescribing initial translational and rotational velocities relative to the parent aircraft. These are next

read in and then the initial values of the 12 dependent variables in the trajectory calculation are computed. These are:

- (1) The three coordinates of the store center of moments relative to the fuselage nose.
- (2) The three translational velocity components of the store center of moments relative to the fuselage.
- (3) The three store rotational velocities.
- (4) The three angles giving the store orientation relative to the fuselage.

Reference positions of the store nose, center of moments, and base are next calculated and the initial and final trajectory times, as well as the integration interval, are input. If the initial time is not zero, then the trajectory is being restarted from a previous run and the current values of the 12 dependent variables obtained from that run are read in. The last step in the initialization is to initialize subroutine ADAMS, the integration routine.

The last page of the flow chart, figure 2(c), is the integration loop of the program. The first steps are to calculate the aerodynamic forces and moments acting on the body and the empennage, if one is present, of the separated store. The body forces and moments are determined by using the equation presented in section 5.2 of reference 4. The empennage forces and moments are determined as discussed in section 5.3 and Appendix I of that reference.

One of the options in the computer program is to calculate a wind-tunnel captive-store trajectory as opposed to a free-flight trajectory. It is customary in the wind tunnel to change the store orientation relative to the parent aircraft while measuring the forces and moments in order to approximately account for the store translational motion relative to the aircraft. The computer program also does this during the force and moment calculation. Thus, if a captive-store trajectory is being calculated, the next step in the program is to put the store back to its correct orientation and call subroutine DIRCOS in order to calculate the free-flight direction cosines between the store body coordinate system and the inertial coordinate system which is fixed in the fuselage.

The next series of steps determines the store translational and rotational accelerations. This involves solving the set of six simultaneous

equations given by equations (II-16) through (II-18) and (II-41) through (II-43) of Appendix II of reference 4 making use of the relationships given in section 6.1 of that reference. The equations in section 6.1 are unchanged except for the expression for the force acting along the store axis, F_x , in equation (65). This now contains a thrust term so that

$$F_x = mg_x - q_{\infty} S_R C_A + F_T \quad (1)$$

The coefficient matrix is first calculated and then the right-hand sides are determined. Subroutine INVERS is called to solve the set of six equations for the accelerations. The rates of change of the orientation angles are next determined from equation (II-1) of Appendix II of reference 4.

A check is next made to see if output is to be printed at the end of an integration step. If output is not required the integration continues by calling subroutine ADAMS. If it is required, subroutine SOUTPT is called. Upon return from this subroutine a check is made to see if the time is equal to the final time which was read in and if so, the trajectory is stopped and control returns to the beginning of the program to read in a new set of data. If it is not, the integration is continued.

3.2 Input Data

This section of the report will describe in detail the preparation of the input data deck for the program. Whenever possible the input format has not been changed from that used in the subsonic store separation program described in reference 3. If an item of input has not been changed, the item number of figure 14 of reference 3 will be given. Other remarks which will aid the user who is familiar with the subsonic program will be made where appropriate.

3.2.1 Input format

The format for the input data for the trajectory program is shown in figure 3. Three lines of information are shown for each item. The first line gives the program variable names, the second line shows the card column fields into which the data are to be punched, and the third line shows the FORTRAN format type. Data punched in I and E formats are right

justified in the fields whereas data in F format can be punched anywhere in the field. A decimal point should be included in both E- and F-type data.

Item number 1 (item no. 1, ref. 3) is an index NCARDS which indicates how many cards of information are to follow to identify the run, item number 2. The value of NCARDS must be one or greater.

Item number 2 (item no. 2, ref. 3) is a set of NCARDS cards containing hollerith information identifying the run and may start and end anywhere on the card. The cards are reproduced in the output just as they are read in.

Item number 3 (item no. 3, ref. 3) consists of one card and contains the following information:

ALFAC	fuselage and wing angle of attack, degrees
GAMF	fuselage flight path angle, degrees
FMACH	Mach number
RHO	air density at flight altitude, slugs per cubic foot
VINF	aircraft free-stream velocity, feet per second

The aircraft is assumed to be flying in a straight line; however, it can be climbing or diving. For climbing flight, GAMF is positive. The Mach number should be between 1.2 and 3.0 and the angle of attack should not exceed 10° . The wing-fuselage flow model is valid within these limits.

Item number 4 contains four indices which specify what aircraft components are present. They are

NFU	fuselage?	NFU = 0, no NFU = 1, yes
NPY	pylon?	NPY = 0, no NPY = 1, yes
NDMY	dummy variable which is not used; input as NDMY = 0	
NSTRS	store?	NSTRS = 0, no NSTRS = 1, yes

Provision has been made for omitting the fuselage. For cases with no fuselage the reference coordinate system is fixed at the wing root-chord leading edge and ALFAC and GAMF of item 3 should be the wing angle of attack and

flight path angle, respectively. The present version of the program is limited to one store, NSTRS = 1. The number of stores can be zero. This allows the input data deck through item 23 to be checked out without running a trajectory. In addition, the program can also be used as an aid in determining the points on the wing and pylon at which the slopes of the camberline and the thickness distribution are to be input.

Item number 5 (item no. 5, ref. 3) consists of two quantities which are

FLTHC length of fuselage, feet

FRMAX maximum fuselage radius, feet

This item and the next five are omitted if NFU = 0.

The next three items of input, items 6, 7, and 8 (item no. 9, 10, and 11, ref. 3) are included in the data deck only when NFU = 1. They are

NFPOLY number of polynomials specifying circular
fuselage shape
 $1 \leq \text{NFPOLY} \leq 7$

FXEND(J) x/l of end points of polynomials specifying
fuselage shape, NFPOLY values

FCOEF(J,K) coefficients of polynomials specifying shape

These data specify the radius distribution of the fuselage and are used in the calculation of the source-sink distribution which represents the fuselage volume and the doublet distribution which represents the fuselage angle of attack effects. Up to seven polynomials may be used. The polynomial programmed is

$$\frac{r}{l} = C_1 + C_7 \sqrt{C_2 \left(\frac{x}{l}\right)^2 + C_3 \left(\frac{x}{l}\right) + C_4} + C_5 \left(\frac{x}{l}\right) + C_6 \left(\frac{x}{l}\right)^2 \quad (2)$$

where C_1 through C_7 are the coefficients, r is the local fuselage radius, and l is the fuselage length. The polynomials must be input for shapes which are made dimensionless by the body length since the trajectory program is written assuming this to be the case.

Item 6 specifies the number of polynomials. Item 7 consists of one card which contains the NFPOLY values of the end points of the polynomials describing the shape. The decimal point can be placed anywhere in the ten-column field.

Item number 8 on figure 3 is a set of NFPOLY cards specifying the values of the coefficients of the polynomials, equation (2). All seven coefficients are input even though some of them may be zero.

Items 9 and 10 specify the body interference panel layout and the number of line sources and line doublets to be used to model the fuselage volume and angle of attack effects. The various quantities are

NCWB	number of rings of body interference panels
NBDCR1	number of panels in a ring lying above the wing on the left half of the fuselage
NBDCR2	number of panels in a ring lying below the wing on the left half of the fuselage
NFSOR	number of line sources and line doublets to be used over the fuselage length
BODYPL	length of fuselage over which body interference panels are to be placed, feet

The definitions of some of the above quantities can be clarified by the use of figure 4. In this simplified layout there are five rings of body interference panels, $NCWB = 5$, laid out over the length $BODYPL$. In each of the rings one panel, $NBDCR1 = 1$, lies above the wing $z_w = 0$ plane and three panels, $NBDCR2 = 3$, lie below this plane. Some general rules for determining the input values of these quantities will now be given.

First, consider the length $BODYPL$. If the wing trailing edge is supersonic, that is, the component of the free-stream Mach number perpendicular to the trailing edge is greater than one, body interference panels should be laid out over the wing root-chord length, CRW , in figure 4. For a subsonic wing trailing edge, (perpendicular Mach number less than one) body interference panels should extend to the x_w coordinate of the wing tip-chord trailing edge. If the base of the store being separated is behind the point selected using the preceeding rules then the body interference panels should be extended to the x_w location of the store base. When a large rearward axial motion of the store is expected during its trajectory, the body panels should be extended aft to cover this motion.

The number of rings of body interference panels and the number of panels in each ring will now be discussed. The number of rings is dependent on the number of panels in a chordwise row on the wing, NCW . This quantity is input as part of item 13 and its selection will be discussed later. Since, if at all possible, the same number of chordwise panels should be

used on both the body and the wing, over the wing root-chord region, CRW in figure 4, the number of rings of body panels can be found using the following relation

$$NCWB = NCW \left(\frac{BODYPL}{CRW} \right)$$

The value of CRW is determined as described under the item 12 input data. In the above expression, the value of BODYPL should be adjusted so that NCWB is an integer.

Two rules can be given for selecting the number of panels in a ring on the left side of the body. If the store to be separated is under the fuselage at least eight panels should be used. If the store is under the wing, six panels is probably sufficient. The two input parameters specifying the number in a ring are NBDCLR1 and NBDCLR2. These are the number of panels above and below the wing $z_w = 0$ plane of figure 4. Assume that six panels are to be used in a ring, for example. Then, the values of NBDCLR1 and NBDCLR2 for three specific wing positions are:

Mid-wing

$$NBDCLR1 = NBDCLR2 = 3$$

Wing tangent with top of fuselage

$$NBDCLR1 = 0, NBDCLR2 = 6$$

Wing tangent with bottom of fuselage

$$NBDCLR1 = 6, NBDCLR2 = 0$$

For wings located intermediate between the mid-wing and high or low wing positions, the panels should be divided above and below the wing so that the panel widths are as equal as possible.

The computer program as documented in this report limits the total number of constant u-velocity panels or interference panels on the fuselage, wing, and pylon to 200. This limit is imposed by the dimensions of certain arrays in the program. Thus, the following relation which is based on the total panel layout must be satisfied.

$$NCWB*(NBDCLR1 + NBDCLR2) + NCW*MSW + NCP*MSP \leq 200 \quad (3)$$

The variables NCW and MSW are input in item 13 and the variables NCP and MSP are input in item 20.

The last input variable in item number 9 is NFSOR, the number of line sources and line doublets to be used to model the fuselage volume and angle of attack effects. The general rule to use in determining NFSOR is that the distance between the origins of successive sources or doublets should be approximately equal to the chordwise length of the wing constant u-velocity panels at the root chord. Therefore,

$$\text{NFSOR} \cong \text{NCW} \left(\frac{\text{FLTHC}}{\text{CRW}} \right) \leq 100$$

The maximum value of 100 is imposed by dimension statements in the program. The fuselage length, FLTHC, was input as part of item 5. The wing root chord length, CRW, will be input as part of item 12 and the number of chordwise panels, NCW, will be input as part of item 13.

Item number 11 (item 15, ref. 3) contains two parameters which specify the wing location relative to the fuselage nose. The two parameters are shown pictorially in figure 5 and are

XBWOC x_B location of intersection of wing leading edge
with fuselage, feet; negative as shown in figure 5

ZBWO z_B location of intersection of wing leading edge
with fuselage, feet; negative as shown in figure 5

Item 12 (item 16, ref. 3) contains

CRW wing root chord length, feet

SSPAN wing semispan, feet

The definitions are shown in figure 6. The wing root chord is the wing chord at the spanwise station, Y(1), at which the wing leading edge intersects the fuselage. Both quantities are input as positive quantities.

Items 13 and 14 (items 17 and 18, ref. 3) are input data describing the left wing panel which are used to lay out the constant u-velocity panels. The quantities are

NCW number of panels in a chordwise row on wing; $\text{NCW} \geq 4$

MSW number of panels in a spanwise row on wing;
also number of thickness strips in a spanwise
row on wing; $\text{MSW} \leq 19$

I wing u-velocity panel side-edge number;
I = 1 to MSW+1

Y(I) y_w location of I^{th} side edge on the left wing panel, feet ($I = 1$ value shown in figure 6, negative for all I's since on left panel; measured in wing planform plane)

PSIWLE(I) leading-edge sweep of wing section to the right of the I^{th} side edge, degrees; positive swept back (measured in wing planform plane)

PSIWTE(I) trailing-edge sweep of wing section to the right of the I^{th} side edge, degrees; positive swept back (measured in wing planform plane)

Based on these input data, the wing is divided chordwise and spanwise into trapezoidal shaped elemental panels and one constant u-velocity panel placed on each panel. All the NCW panels in a chordwise row have equal chords and spans, the spans being determined by the Y(I)'s.

The question arises as to the values to use for NCW and MSW. No specific rules can be given since the number needed is determined to some extent by the wing planform shape and the location of the store being separated. Fewer panels can be used on the wing if the store is under the fuselage than if the store is under the wing. The number of panels in a chordwise row, NCW, is also determined to some extent by the camber distribution, if any, since the camber is specified at the panel control points. If the wing is uncambered except near the leading edge then a fairly large number of panels is required in a chordwise row if this effect is to be included. In general a minimum of eight panels, NCW = 8, should be used.

The number of panels in a spanwise row, MSW, is controlled to some extent by the wing. A panel side edge must coincide with the root chord and each break in leading-edge sweep angle and trailing-edge sweep angle, and if a pylon is present, a trailing leg must coincide with the spanwise location of the pylon. One must also coincide with the wing tip. Consider the example wing alone of figure 7. There is a break in trailing-edge sweep at $y_w/s = -0.2$, a break in leading-edge sweep at -0.4 , and a pylon at -0.6 . To place a panel side edge at each of these positions plus the wing tip and the root chord requires four panels across the semispan. This is the minimum number which can be used for this wing and is probably not sufficient. Experience with the program has shown that in some cases six panels in a spanwise row has given good results.

The only sure way of determining convergence with number of panels, both NCW and MSW, is to examine the results obtained from the trajectory program. For a particular wing various panel layouts should be tried to

assure convergence. The minimum number of panels, consistent with the desired accuracy, should be used in order to minimize the trajectory calculation time.

The maximum number of panels that can be placed on the left wing panel, pylon, and fuselage, is 200. This limit is imposed by dimension statements in the computer program. Thus, limits may be imposed on NCW and NSW in order to satisfy equation (3).

Item number 14 consists of a deck of $MSW+1$ cards. The index I is the panel side-edge number. The side edges are numbered from the root chord, $I = 1$, to the tip, $I = MSW + 1$. Associated with each I are the spanwise location of the side edge, $Y(I)$, and the sweep angles of the leading and trailing edges of the wing segment to the right of the side edge, $PSIWLE(I)$ and $PSIWTE(I)$. When $I = 1$ the sweep angles are zero.

The two indices of item number 15 (item 19, ref. 3) are associated with the wing twist and camber distribution.

NTAC twist and/or camber? NTAC = 0, no
 NTAC = 1, yes

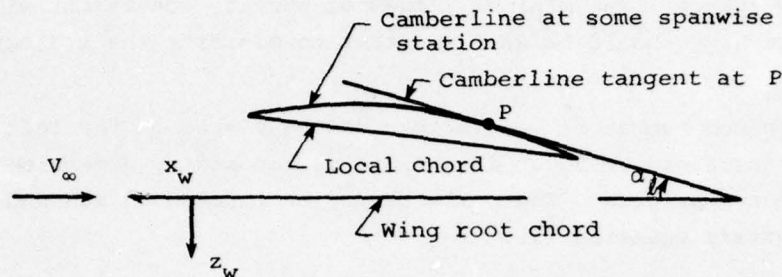
NUNI if wing has no twist, and the camber distribution
 is similar at all spanwise stations, NUNI = 1; for
 all other cases, NUNI = 0 (omit if NTAC = 0)

If NTAC = 1, item number 16 is included in the input data deck. These data specify the wing twist and/or camber distribution in terms of the tangent of the local angle of attack of the camberline for a wing root chord angle of attack of zero degrees. The function of the index NUNI is explained below.

ALPHAL(J) $\tan \alpha$ of the wing camberline at the constant u-velocity panel control points. If NUNI = 1, only data for the chordwise row adjacent to the root chord are input. The first value is for the control point nearest the leading edge. If NUNI = 0, data for all chordwise rows must be input starting nearest the root chord and working outboard. Data for each row start on a new card (omit if NTAC = 0)

The constant u-velocity panel control points are at 95 percent of the chord which passes through the centroid of area (see fig. 2, ref. 1) of each elemental panel laid out by NCW, MSW, and the $Y(I)$'s of items 13 and 14.

The values of ALPHAL(J) are obtained as follows. Consider the following sketch



which shows the cambered and twisted section of the lifting surface at some spanwise station for zero wing angle of attack. At the control point P , a tangent to the camberline is constructed, which makes an angle α_l with the root chord (the x_w axis). The positive sense of α_l is shown. The input value required is $ALPHAL(J) = \tan \alpha_l$. For wings which have the same camber distribution at all spanwise stations and no twist, $NUNIS = 1$, data are only input for the row of control points closest to the root chord. The program assigns these values to all other rows.

The two indices of item number 17 (item 21, ref. 3) are associated with the specification of the wing thickness distribution. They are

NCWS number of thickness panels in a chordwise row on the wing; $NCWS * MSW + NCPS * MSP \leq 400$

NUNIS if wing has a similar thickness distribution at all spanwise stations, $NUNIS = 1$; if not, $NUNIS = 0$

A total of 400 thickness panels can be used on the wing and pylon. The thickness panels are also trapezoidal in shape. The span of each chordwise strip is the same as the corresponding row of constant u -velocity panels. Each of these chordwise strips is divided into NCWS equal chord panels. Usually more thickness panels should be used in a chordwise row than u -velocity panels. Experience with the program has shown 12 to 14 thickness panels usually to be sufficient. Again, this can only be checked by varying the number and examining the resulting store load distributions. The minimum number, consistent with the desired accuracy, should be used to minimize the trajectory calculation time.

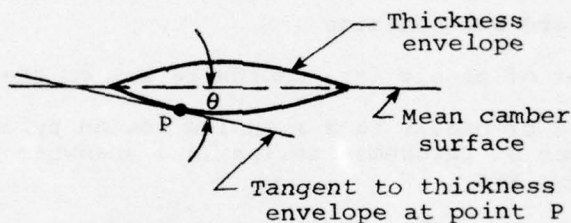
The data contained in item number 18 are

THETAL(J) slope of the wing thickness distribution at the centroid of area of the thickness panels. If $NUNIS = 1$ only data for the chordwise row adjacent to the root chord are input. The first

value is for the panel at the leading edge. If NUNIS = 0, data for all chordwise rows must be input starting at the root chord and working outboard. Data for each row start on a new card.

Note that the values of the thickness slopes are input for the centroid of area of each panel. Also, for wings with similar distributions at all spanwise stations, NUNIS = 1, data are only input for the row of panels adjacent to the root chord. The program assigns these values to all other rows.

The values of THETAL(J) are obtained as follows. Consider the following sketch



which shows the thickness envelope at a spanwise station where the slopes are to be determined. At a point P at which the slope is required, a tangent to the surface of the thickness envelope is constructed which makes an angle θ with the line connecting the leading and trailing edges of the envelope. The input value required is $\text{THETAL}(J) = \tan \theta$. Forward of the point of maximum thickness θ is positive and aft of this point it is negative. In some cases for a wing with a blunt leading edge, the thickness slope should not exceed a certain value. The determination of this value is discussed in detail in section 3.4.1 of reference 1.

The next five items of input data, items 19 through 23, are associated with the pylon if one is present, $\text{NPY} = 1$. Item number 19 (item 23, ref. 3) consists of one card and contains the following quantities

IP	index of the y_w location of the pylon. This must be one of the $Y(I)$'s read in for the wing, item 14, if under the wing. If pylon is under the fuselage centerline, $\text{IP} = 0$.
PSIPLE	sweep angle of the pylon leading edge in the wing coordinate system, degrees. Positive sweep is swept back.
PSIPTE	sweep angle of the pylon trailing edge in the wing coordinate system, degrees. Positive sweep is swept back.

CRP	length of pylon root chord, feet
HP	height of pylon measured from wing chordal plane, feet
XPLE	location of pylon root chord leading edge measured from local wing chord leading edge, feet (negative behind)

The pylon location can be under the fuselage, $IP = 0$, or at one of the wing-panel side-edge locations outboard of the wing-fuselage juncture. The remaining five items are shown in figure 8 for the two cases.

The next two items of input data are associated with the constant u-velocity panels which represent the pylon loading. Item number 20 (item 24, ref. 3) is one card and contains

NCP	number of panels in a chordwise row on the pylon
MSP	number of panels in a spanwise row on pylon; also number of thickness strips in a spanwise row on the pylon; $MSP \leq 19$

For a typical pylon, two or three vortices in a spanwise row are sufficient, $MSP = 2$ or 3 . The number chordwise, NCP , depends on the length of the pylon root chord. The chordwise dimensions of the trapezoidal shaped area elements on the pylon should be approximately the same as those on the wing immediately above the pylon. That is, the local wing chord length divided by NCW of item 13 should be approximately equal to the pylon root chord length divided by NCP .

The program is limited to 200 constant u-velocity panels on the wing-
pylon-fuselage combination. Thus,

$$NCWB*(NBDCR1 + NBDCR2) + NCW*MSW + NCP*MSP \leq 200$$

Item number 21 (item 25, ref. 3) consists of a deck of $MSP+1$ cards which contain the following information

K	pylon-panel side-edge number; $K = 1$ to $MSP+1$
Z(K)	z location of the K^{th} side edge, feet; measured from local wing chord

The first side edge should be placed on the pylon root chord and the last on the tip chord. The remaining side edges should be equally spaced between these two. For a pylon located under the fuselage, figure 8(a), $Z(1)$ should be the z_w location of the pylon root chord, the bottom of the fuselage, and $Z(MSP+1)$ should equal $Z(1) + HP$. For a pylon under the wing, $Z(1) = 0$ and $Z(MSP+1) = HP$.

Items 22 and 23 provide data required to model the pylon thickness distribution. The data are

NCPS	number of thickness panels in a chordwise row on the pylon
NUNIP	if pylon has a similar thickness distribution at all spanwise stations, NUNIP = 1; if not, NUNIP = 0
THETPL(J)	slope of the pylon thickness distribution at the centroids of the thickness panels. If NUNIP = 1 only data for the chordwise row adjacent to the root chord are input. The first value is for the panel at the leading edge. If NUNIP = 0, data for all chordwise rows must be input starting at the root chord and working outboard. Data for each row start on a new card.

These data are prepared in the same manner as were the corresponding data for the wing thickness, items 17 and 18. The comments made there concerning a blunt leading edge also apply to the pylon.

The program is limited to 400 thickness panels on the wing-eylon combination. Thus,

$$NCWS*MSW + NCPS*MSP \leq 400$$

If no store is present, NSTRS of item 4 is equal to zero, this concludes the input data deck. If NSTRS is not zero, then the next five items of input data describe the store to be separated. The store to be separated must be under the fuselage centerline or to the left of this line as seen by the pilot.

Item number 24 (item 32, ref. 3) is one card which contains the following information.

NUMSTR(1)	store number; ≤ 99
NSHAPE(1)	shape number of store; ≤ 99
SLTHC(1)	length of store, feet
SRMAX(1)	maximum radius of store, feet
XSNC(1)	x_l location of store nose measured from wing chord leading edge immediately above store, feet; positive ahead
YSN(1)	y_w location of store nose measured from fuselage centerline, feet; positive to the right

ZSN(1) z/l location of store nose measured from wing
 chord leading edge immediately above store,
 feet; positive below

SIC(1) store incidence angle measured relative to wing
 root chord, degrees; positive nose up

The subscripted form of the above variables is not required since the present program is limited to one store. It is used in anticipation of a future version of the program treating multiple stores.

Item number 25 is one card which contains

NSHPT number of different values of NSHAPE(J) from
 item number 24; since J is limited to one,
 NSHPT is input as NSHPT = 1

Item number 26 is one card. The data are

MSHAPE shape number of store represented by the shape
 data to be read in as item numbers 27, 28, and
 29; input as MSHAPE = NSHAPE(1) which was input
 in item number 24

MSOR number of line sources and line doublets to be
 used to model the store volume and angle of
 attack effects; $MSOR \leq 100$

A value of MSOR of 30 to 40 should be sufficient to model the store. The value can be varied to determine whether increasing the number affects the trajectory.

The next three items of input data, item numbers 27, 28, and 29, specify the store shape. They are

NSPOLJ number of polynomials specifying store shape;
 $1 \leq NSPOLJ \leq 7$

SXNDJ(J) x/l of end points of polynomials specifying
 store shape; NSPOLJ values

SCOFJ(J,K) coefficients of polynomials specifying shape

These data specify the radius distribution of the store and are used in the calculation of the source-sink distribution which represents the store volume and the doublet distribution which represents the store angle of attack effects. Up to seven polynomials may be used. The polynomial programmed is given by equation (2). The polynomials must be input for a shape which is made dimensionless by the store length since the trajectory program is written assuming this to be the case.

Item 27 specifies the number of polynomials. Item 28 consists of one card which contains the NSPOLJ values of the end points of the polynomials describing the shape.

Item number 29 is a set of NSPOLJ cards specifying the values of the coefficients of the polynomials, equation (2). All seven coefficients are input even though some of them may be zero.

The remainder of the input data deck is additional data required to describe the store being separated and other data required for the force and moment and trajectory calculations.

Item number 30 is one card which contains nine indices. They are

NEJECT	number of the store being separated
NSEG	number of equal length segments the body is to be broken into for the force calculation; $NSEG \leq 40$
NSEGXO	number of body segments to the flow separation location
NGAM	trajectory to simulate wind-tunnel captive-store trajectory? NGAM = 0, no NGAM = 1, yes
NPOLY	number of polynomials specifying store shape; $1 \leq NPOLY \leq 7$
NROLL	rolling moment to be calculated? NROLL = 0, no NROLL = 1, yes
NEMP	empennage present? NEMP = 0, no NEMP = 1, yes
NDAMP	damping to be included in force calculation? NDAMP = 0, no NDAMP = 1, yes
NTHRUS	thrust time history to be specified? NTHRUS = 0, no NTHRUS = 1, yes

The index NEJECT must be the store number that was read into NUMSTR(1) in item 24; that is, NEJECT = NUMSTR(1).

In the store body force and moment calculation, the body is divided into NSEG equal length segments. Experience in using the program has shown that 20 body segments, NSEG = 20, usually yields converged forces and moments. This can only be checked for a specific case by varying NSEG

and comparing results. To minimize calculation time NSEG should be kept as small as possible.

No definite rules for the selection of a value of NSEGXO can be given. For stores with cylindrical afterbodies NSEGXO should probably be input as NSEG. For stores with boattailed afterbodies NSEGXO should probably be less than NSEG. In the subsonic store separation program, reference 3, an empirical relationship was given for estimating the flow separation location for boattailed bodies. This relationship was obtained from data taken at low subsonic speeds and is, therefore, probably not valid at supersonic speeds. In using the present program NSEGXO should be set equal to NSEG unless experimental data are available for determining the separation location.

The index NGAM is included as input solely for the purpose of allowing the program to be used to compare with captive store data obtained in the wind tunnel. Since the wind tunnel cannot produce a flow where the store sees a free-stream velocity coming from a different direction than that seen by the parent aircraft the captive store case must be handled differently by the computer program.

The number of polynomials specifying the store shape, NPOLY, is the number required to specify the shape from the store nose to its base. These polynomials are used in the force and moment calculation. The polynomials are of the form given by equation (2). The value of NPOLY should be equal to the value of NSPOLJ read in under item 27.

The next index, NROLL, indicates whether or not the rolling moment for a store with an empennage is to be calculated. NEMP specifies whether there is an empennage. The index, NDAMP, is used by the program to determine whether or not aerodynamic damping in pitch, yaw, and roll is to be included in the force and moment calculation. The last index, NTHRUS, specifies whether a thrust time history is to be read in.

Item number 31 (item 38, ref. 3) is one card and specifies the store mass and inertia characteristics. The quantities are

SMASS store mass, slugs

FIXX I_{xx} moment of inertia, slug-ft²

FIYY	I_{YY}	moment of inertia, slug-ft ²
FIZZ	I_{ZZ}	moment of inertia, slug-ft ²
FIYZ	I_{YZ}	product of inertia, slug-ft ²
FIXZ	I_{XZ}	product of inertia, slug-ft ²
FIXY	I_{XY}	product of inertia, slug-ft ²

The equations defining the moments and products of inertia are given by equation (II-36) of Appendix II of reference 4.

The one card of item number 32 (item 39, ref. 3) contains

XMOM	location along store axis about which the pitching and yawing moments are to be taken, negative behind nose, feet; same point about which moments of inertia are taken
XBAR	x location of store c.g. measured from moment center, feet; positive forward
YBAR	y location of store c.g. measured from store axis, feet; positive to the right
ZBAR	z location of store c.g. measured from store axis, feet; positive below

The next two items of input, items 33 and 34 (items 40 and 41, ref. 3) describe the shape of the separated store. The quantities contained on the cards are

XEND(J)	x/l of end points of polynomials specifying shape of ejected store, NPOLY values
COEF(J,K)	coefficients of polynomials specifying shape

These data are a repeat of the data input as items 28 and 29.

Item number 35 (item 42, ref. 3) contains two quantities which are

CA	store axial-force coefficient; reference area is store maximum cross-sectional area
CDC	crossflow-drag coefficient

The store axial-force coefficient is not calculated by the computer program so it is required input. The crossflow-drag coefficient is used in the viscous crossflow force and moment calculation which is used in place of the slender-body calculation behind the assumed separation location. It is defined as the section drag coefficient of a circular cylinder normal

to the airstream. That is,

$$CDC = c_{d_c} = \frac{\text{drag per unit length}}{q_{\infty}(2r)}$$

where q_{∞} is the free-stream dynamic pressure and r is the cylinder radius. The value commonly used for this parameter is 1.2. If a more accurate value is desired, reference 7 should be used. The crossflow-drag coefficient is presented there as a function of crossflow Mach number and Reynolds number.

The next two items of input data are included in the input data deck if an empennage is present, NEMP = 1 in item 30. Item 36 (item 43, ref. 3) contains

IPLNR	IPLNR = 0, cruciform empennage IPLNR = 1, planar empennage
MSF	number of spanwise control points on each fin; <u>must</u> be odd and $5 \leq MSF \leq 11$

It should be noted that MSF must be odd and in the range $5 \leq MSF \leq 11$. For most stores, MSF = 5 has been found to give accurate results. The larger the fin span to body radius ratio, the more points required.

The next card, item number 37 (item 44, ref. 3) contains

XTAIL	x location at which empennage forces are to act measured from store nose, feet; negative number
RADAV	average store body radius in empennage region, feet; positive number
FINSS	tail fin semispan, measured from body longitudinal axis, feet; positive number
PHIROL	initial fin orientation, degrees; $0 \leq PHIROL \leq 90$; PHIROL = 0 if fins vertical and horizontal for a cruciform empennage or horizontal for a planar empennage.
CLALPH	lift-curve slope of two exposed panels joined together, per radian; reference area is store maximum cross-sectional area

The location at which the empennage forces are assumed to act, XTAIL, is arbitrary. It can be estimated using Chart 10 of reference 8. The lift-curve slope, CLALPH, can be estimated using the method described in Appendix II.

The next three items of input data, item numbers 38, 39, and 40, are included in the input data deck if a thrust time history is to be specified, NTHRUS = 1, in item 30. The input quantities are

NTPOLY number of polynomials specifying thrust time history;
 $1 \leq \text{NTPOLY} \leq 5$

TEND(J) final times over which the NTPOLY polynomials apply

TC(J,K) coefficients of the polynomials

The thrust force as programmed acts along the store longitudinal axis and is specified by a series of polynomials of the form

$$F_T = \sum_{k=1}^6 a_k t^{k-1} \quad (4)$$

where F_T is the thrust force in pounds. Up to five polynomials can be used to specify the time history and item 38 contains the number of polynomials, NTPOLY. Item 39 is one card and contains the NTPOLY values of the final time t over which each of the polynomials applies. That is, the first polynomial is used from $t = 0$ to $t = \text{TEND}(1)$, the second from $t = \text{TEND}(1)$ to $t = \text{TEND}(2)$, and so on. Item 40 is a set of NTPOLY cards which specify the six a_k coefficients, TC(J,K), for the polynomials.

Item number 41 (item 45, ref. 3) is one card which contains the initial velocities of the store relative to the parent aircraft such as might exist at the end of the ejection stroke of a store released from a pylon or rack. The six quantities are

VXZERO store forward ejection velocity parallel to store longitudinal axis, ft/sec

VYZERO store lateral ejection velocity perpendicular to store longitudinal axis, ft/sec

VZZERO store downward ejection velocity perpendicular to store longitudinal axis, ft/sec

VAR(4) store initial rolling rate, p , radians/sec

VAR(5) store initial pitching rate, q , radians/sec

VAR(6) store initial yawing rate, r , radians/sec

At the beginning of the trajectory, the end of the stroke, the store is oriented such that its y-axis is parallel to the y_B fuselage axis shown in figure 5. Thus the x,z store plane is parallel to the x_B, z_B fuselage plane and the initial vertical translational velocity of the store, VZZERO, is in the x,z store plane perpendicular to the store x-axis. The velocities VXZERO, VYZERO, and VZZERO are positive in the positive x,y, and z directions.

The next card, item number 42 (item 46, ref. 3) contains three items. They are:

DTIME	integration interval, seconds
TIMEI	initial time, seconds
TIMEF	final time, seconds

The first, DTIME, is the integration interval to be used in the integration subroutine, ADAMS. The version of this routine which is included in the present program does not adjust this interval to satisfy certain accuracy requirements but uses the input value of DTIME. A value of 0.025 or 0.01 seconds should probably work. However, different values should be tried and the trajectory results compared to determine that a small enough value is being used. Finned stores probably require a smaller value than finless stores because of the large moments produced by the empennage. The initial time, TIMEI, must be input as 0.0 unless a trajectory is to be restarted using the last page of output from a previous run to obtain the initial conditions. Then, TIMEI should be given the value that appears on that page of output. The final time, TIMEF, is the time at which the trajectory calculation is to be terminated. Except for very unusual trajectories, a value of 0.5 to 0.7 second is normally sufficient to determine if a store will or will not clear the aircraft.

If TIMEI and TIMEF are both input as zero, no trajectory calculation will be performed. However, the store load distributions and forces and moments will be calculated with the store in its initial position. This feature can be useful in checking out the entire input data deck prior to running a trajectory or for studying store loadings at specific points.

The last item of input, item number 43 (item 47, ref. 3) is input only if a trajectory is being restarted, TIMEI \neq 0. This item consists of two cards with VAR(1) through VAR(8) on the first card and VAR(9) through VAR(12) on the second. The following table gives the notation used to identify

VAR(1) through VAR(12) on the trajectory program output which will be discussed in section 3.3.

<u>Program Notation</u>	<u>Output Notation</u>
VAR(1)	DXF, ft/sec
VAR(2)	DYF, ft/sec
VAR(3)	DZF, ft/sec
VAR(4)	P, radians/sec
VAR(5)	Q, radians/sec
VAR(6)	R, radians/sec
VAR(7)	XF of XMOM, ft
VAR(8)	YF of XMOM, ft
VAR(9)	ZF of XMOM, ft
VAR(10)	PSI, degrees
VAR(11)	THETA, degrees
VAR(12)	PHI, degrees

3.2.2 Sample input data

A sample input data deck will now be presented. It will utilize the wind tunnel model components shown in figure 9 except that they have been scaled up by a factor of twenty in order to approximate a full-scale aircraft and store. The models were used in the wind tunnel test program described in reference 9.

The configuration for the sample calculation is shown in figure 10. It consists of the wing-fuselage combination of figure 9(a), the pylon of figure 9(b), and the store of figure 9(c). The store is shown in its initial position which is one store body radius below the carriage position on the pylon.

The input data deck is tabulated in figure 11. The item numbers indicated on the figure correspond to those of figure 3. The first item on figure 11 is item number 1 which contains the value of NCARDS, in this case 12. This is followed by item number 2, which consists of these 12 cards of identifying information.

Item number 3 specifies the aircraft flight conditions. The angle of attack is 2.0° , the flight path angle is -30.0° , and the Mach number is 1.5. The free-stream air density is 0.0008907 slugs per cubic foot, which corresponds to a flight altitude of 30,000 feet. The flight velocity is 1,492.0 feet per second.

The aircraft components which are present are specified by item 4. There is a circular fuselage, NFU = 1; there is a pylon, NPY = 1; and there is a store, NSTRS = 1.

Items 5 through 10 are the fuselage input data. Item 5 contains the fuselage length and maximum radius which are shown in figure 10. Items 6, 7, and 8 contain the data for the polynomials specifying the fuselage shape. The fuselage radius distribution, made dimensionless by the fuselage length is tabulated in figure 9(a). Three polynomials, item 6, are required. The nose is a circular arc and ends at $x/l = 0.32$, the centerbody is a cylinder ending at $x/l = 0.7534$, and the aft position is a circular arc ending at $x/l = 1.0$. These three values of x/l are contained in item 7.

The next three cards, item 8, contain the coefficients of the polynomials for the three sections (see eq. (2)). The nose section is a circular arc so that when the following boundary conditions are imposed

$$\frac{x}{l} = 0$$

$$\frac{r}{l} = 0$$

$$\frac{x}{l} = 0.32$$

$$\frac{r}{l} = 0.0457$$

$$\frac{x}{l} = 0.32$$

$$\frac{dr}{dx} = 0$$

the equation of a circle gives

$$\frac{r}{l} = -1.0975 + \sqrt{-\left(\frac{x}{l}\right)^2 + 0.64\left(\frac{x}{l}\right) + 1.2045} \quad (5)$$

The cylindrical section runs from $x/l = 0.32$ to $x/l = 0.7534$ and in this region

$$\frac{r}{l} = 0.0457 \quad (6)$$

The last section is also a circular arc. By imposing the following three boundary conditions

$$\frac{x}{\ell} = 0.7534$$

$$\frac{r}{\ell} = 0.0457$$

$$\frac{x}{\ell} = 0.7534$$

$$\frac{dr}{dx} = 0$$

$$\frac{x}{\ell} = 1.0$$

$$\frac{r}{\ell} = 0.0302$$

we obtain

$$\frac{r}{\ell} = -1.9237 + \sqrt{-\left(\frac{x}{\ell}\right)^2 + 1.5068\left(\frac{x}{\ell}\right) + 3.3109} \quad (7)$$

Equations (5), (6), and (7) are the three polynomials describing the shape of the fuselage and the coefficients are contained in the three cards making up item 8.

Item number 9 contains four indices. The first three specify the constant u-velocity panel layout on the fuselage and the last specifies the number of line sources and line doublets to be used to represent the fuselage volume and angle of attack effects. Twelve (12) rings of panels are to be laid out on the fuselage with eight in each ring. Since this is a mid-wing configuration, four panels in each ring are to be placed above the wing and four below. The number of sources and doublets to be used is 52.

Item number 10 specifies the fuselage length over which the constant u-velocity panels are to be laid out. Since, in this case, the wing trailing edge is supersonic and no rearward motion of the store is expected, BODYPL is input as the length of the wing root chord shown in figure 10.

The next eight items, items 11 through 18, are the wing input data. Item 11 gives the position of the wing root chord leading edge relative to the fuselage and item 12 specifies the root chord length and the semispan. These quantities are shown in figure 10. Items 13 and 14 are data required by the program to lay out the constant u-velocity panels. There are to be 12 panels in each chordwise row and 8 of these rows across the semispan. This requires that the spanwise locations on the left wing panel of nine side edges and the sweep angles to the right of these points be specified.

These data are contained on the nine cards of item 14. Note that the first side edge coincides with the wing-fuselage juncture. Item 15 indicates that the wing has neither twist nor camber, and thus item 16 is omitted from the input data deck. Items 17 and 18 specify the wing thickness distribution. The two indices on item 17 indicate that 20 thickness panels are to be placed in a chordwise row and that the wing has a similar thickness distribution at all spanwise stations. Consequently, item 18 consists of three cards with the 20 values of the slope of the thickness distribution. The airfoil section specification is shown in figure 9(a). The wing leading edge in this case is subsonic. The maximum value of the slope has been selected in accordance with the discussion in section 3.4 of reference 1.

Since there is a pylon, items 19 through 23 are input and contain the pylon data. The pylon is the one shown in figure 9(b), except that it has been scaled up by a factor of 20. Item 19 of the input data specifies that the pylon is located below wing-panel side-edge number 3 ($IP = 3$), the leading-edge and trailing-edge sweep angles are 0.0° , the root chord length is 4.43 feet, the height is 1.65 feet, and the leading edge is 2.51 feet behind the local wing chord leading edge (see fig. 10). Items 20 and 21 are the pylon constant u-velocity panel data. There are to be four panels in a chordwise row and two of these rows spanwise. The three side edge locations are given by item 21. Items 22 and 23 specify the pylon thickness distribution. There are to be 9 thickness panels in a chordwise row and the thickness distribution is similar at all spanwise stations.

Item 24 begins the store data. The store is shown in figure 9(c) but has been scaled up by a factor of twenty. Item 24 contains the number assigned to the store and its shape number. The next five quantities in this item are the store length, maximum radius, and location of the store nose. This information is shown in figure 10. The last number is the store incidence angle which, in this case, is 0.0° .

Item number 25 contains the value of NSHPT. In the present version of this program this variable must be input as NSHPT = 1. Items 26 through 29 contain the shape data for the store. Item 26 contains the value of MSHAPE, which must be equal to the value of NSHAPE(1) read in as part of item 24. It also specifies the number of line sources and line doublets to be used for the store.

Items 27 through 29 contain the data specifying the store shape. The body shape shown in figure 9(c) is defined by two polynomials. The first is a circular arc representing the nose which ends at $x/l = 1.5/6.375 = 0.2353$. The second is one which specifies a constant radius, $r/l = 0.05882$, to the base of the store, $x/l = 1.0$. Item 28 contains the end points and item 29 contains the coefficients of the polynomials (see eq.(2)). The coefficients are determined in the manner previously described for the fuselage.

Item 30 contains nine indices which indicate the following. Store number 10, NEJECT = 10, is the store being separated and the body is to be broken into 20 segments, NSEG = 20, for the force and moment calculation with flow separation occurring at the base of the store, NSEGXO = 20. In addition, a free-flight trajectory is to be calculated, NGAM = 0; two polynomials are to be input describing the body shape, NPOLY = 2; rolling moment is to be calculated, NROLL = 1; the store has an empennage, NEMP = 1; aerodynamic damping is to be included, NDAMP = 1; and a thrust time history is to be specified, NTHRUS = 1.

Item 31 contains the mass and inertia characteristics of the separated store. The particular numbers used in this example have been assigned and have not been determined by specifying a density distribution of the store and performing the required integrations. Item 32 specifies that the inertia characteristics are assumed to have been calculated about a point 7.4 feet behind the store nose and that the store center of gravity is not offset from this point.

Items 33 and 34 contain the end points and coefficients of the polynomials describing the store shape. These data must be identical to the data read in as items 28 and 29.

The store axial force coefficient, 0.65, and crossflow drag coefficient, 0.0, are input in item 35. A crossflow drag coefficient is not used in this example since flow separation is not assumed to occur ahead of the store base.

Items 36 and 37 are data describing the store empennage. Item 36 specifies a cruciform empennage and five control points on each tail panel. Item 37 indicates that the empennage forces act 9.558 feet behind the store nose, the body radius in the fin region is 0.625 feet, the fin semispan is 1.45833 feet, the initial fin orientation is 45° from the vertical and horizontal, and the lift-curve slope is 3.491. The fin details are obtained from figure 9(c) and scaled up by a factor of 20.

Items 38, 39, and 40 specify the thrust time history. Two polynomials of the type given by equation (4) are to be specified. Item 39 indicates that the first polynomial will apply from $t = 0$ seconds to $t = 0.2$ seconds and the second from $t = 0.2$ seconds to $t = 1.0$ second. Item 40 contains the coefficients of the polynomials. The first polynomial is a constant thrust of 1,500 pounds. The second polynomial starts with this value at $t = 0.2$ seconds and allows the thrust to linearly decrease to zero at $t = 1.0$ second.

Item 41 specifies initial axial and lateral translational velocities of the store of 0 feet per second, an initial downward translational velocity of 10 feet per second, and initial rotational velocities of 0.0 radians per second.

The last card on input, item 42, provides the integration interval and the initial and final times. Since the initial time is 0.0, item 43 is not included.

3.3 Output from the Program

Figure 12 presents the output from the computer program for the sample case, the configuration of figure 10, and the data deck of figure 11.

The first page of output, figure 12(a), tabulates the input identifying information, the aircraft flight conditions, and the fuselage input data. Near the bottom of the page, a tabulation of the fuselage shape, as calculated from the input polynomials specifying the shape, and the source and doublet singularity origins and strengths begins. This tabulation is continued on the next page, figure 12(b).

Figure 12(c), 12(d), and 12(e) tabulate most of the wing and pylon input data. Figure 12(c) tabulates the wing data exclusive of the twist and camber and thickness distributions. Figure 12(d) tabulates the pylon data except for the thickness distribution. The input thickness distributions for the wing and pylon are tabulated in figure 12(e).

Figure 12(f) tabulates the input data for the store. Following this, a tabulation of the store shape, as calculated from the input polynomials, and the source and doublet singularity origins and strengths is presented.

The next four pages of output, figure 12(g) through figure 12(j), tabulate quantities associated with the constant u-velocity panel layout on the wing, pylon, and fuselage and the boundary condition at the control

points of these panels. The x, y, z coordinates are those of the control points in the wing coordinate system. The next three columns, $U/VINF$, $V/VINF$, and $W/VINF$, are the sums of the dimensionless perturbation velocities in the x_w, y_w , and z_w directions, respectively, induced at the control points by the other aircraft components. These include fuselage and store on the wing and pylon, wing thickness on pylon, pylon thickness on wing, both wing and pylon thickness on the fuselage, and store on fuselage. $VINF$ is the free-stream velocity. The next to last column tabulates the twist and camber distribution input for the wing. The last column tabulates the singularity strengths of the constant u -velocity panels laid out on the wing, pylon, and fuselage.

Page 11 of the output, figure 12(k), indicates the number of the store separated and tabulates the additional data which were read in to describe this store.

The last three parts of figure 12, parts (l), (m), and (n), are output for three points in the trajectory, the first point, an intermediate point, and the point at which the trajectory is terminated. The complete output from the program will contain a page like this for each integration step, in this case every 0.025 seconds.

At the top of each page is the trajectory time in seconds. Following this, the forces and moments, components as well as totals, and the body load distributions and the velocity distributions along the store axis from which these load distributions were calculated are listed. The load distributions are the sums of those due to buoyancy, slender body, and viscous crossflow. The velocity field calculation is discussed in detail in sections 3.4 of reference 1 and 5.1 of reference 4 and the force and moment calculation in sections 5.2 and 5.3 of reference 4.

The following table relates the program output variables to the x_s, y_s, z_s coordinate system and positive directions shown in figure 13.

<u>Program Notation</u>	<u>Notation of figure 13</u>
CN	C_N
CY	C_Y
CLM	C_m
CLN	C_n
CLL	C_ℓ

<u>Program Notation</u>	<u>Notation of figure 13</u>
X, FT	x_s , feet
X/L	x_s/l_s
DCN/DX	dc_N/dx_s , per foot
DCY/DX	dc_Y/dx_s , per foot
U/VS	U_s/V_{∞_s}
V/VS	V_s/V_{∞_s}
W/VS	W_s/V_{∞_s}

As the store pitches, yaws, and rolls during the trajectory, the x_s, y_s, z_s coordinate system pitches, yaws, and rolls with it. The velocities and forces are always calculated in this coordinate system.

The remaining quantities tabulated on each page of trajectory output specify the store location, orientation, velocities, and accelerations relative to the parent aircraft at that particular time. Before discussing these quantities, the coordinate systems must be mentioned. Figure 13 shows another coordinate system, x, y , and z , which is fixed in the store and moves with the store as it yaws, pitches, and rolls. The origin of this system is fixed at the store moment center. This coordinate system is also shown in figure 14 along with another system, ξ, η, ζ . This latter system is an inertial coordinate system whose origin is fixed in the fuselage nose and is parallel to the x_B, y_B, z_B system of figure 5. At any point in time, the two coordinate systems are orientated with respect to each other by a system of angles. The angles are those shown in figure 14 and consist of three rotations in the yaw, Ψ , pitch, Θ , and roll, Φ , sequence. The positive senses of the three store rotational velocities about the x, y, z axes are also shown in the figure.

Following the load and velocity distribution output on, for example, figure 12(m), the location of the store in the fuselage, or inertial, coordinate system is tabulated. The locations of the store nose, NOSE, moment center, XMOM, and base, BASE, are tabulated relative to the fuselage nose and also relative to the position of the store at time $t = 0$. In this tabulation XF is x_B of figure 5 or ξ of figure 14. Likewise, YF is y_B or η and ZF is z_B or ζ .

The next output are the translational velocities and accelerations of the store relative to the moving aircraft. For example,

$$DXF = \frac{dx_B}{dt} \text{ or } \frac{d\xi}{dt}, \text{ ft/sec}$$

$$D2XF = \frac{d^2x_B}{dt^2} \text{ or } \frac{d^2\xi}{dt^2}, \text{ ft/sec}^2$$

Next the rotational velocities shown in figure 14 are listed as are the rotational accelerations. The notation is

$$P = p, \text{ radians/sec}$$

$$Q = q, \text{ radians/sec}$$

$$R = r, \text{ radians/sec}$$

$$PDOT = \frac{dp}{dt}, \text{ radians/sec}^2$$

$$QDOT = \frac{dq}{dt}, \text{ radians/sec}^2$$

$$RDOT = \frac{dr}{dt}, \text{ radians/sec}^2$$

The last output printed at each integration step are the values of the three orientation angles shown in figure 14 and their time rates of change. The notation is

$$PSI = \psi, \text{ deg.}$$

$$THETA = \theta, \text{ deg.}$$

$$PHI = \phi, \text{ deg.}$$

$$DPSI = \frac{d\psi}{dt}, \text{ radians/sec}$$

$$DTHETA = \frac{d\theta}{dt}, \text{ radians/sec}$$

$$DPHI = \frac{d\phi}{dt}, \text{ radians/sec}$$

As the yaw angle, Ψ , and/or the pitch angle, Θ , increase in magnitude, the velocity field which is used in the store force and moment calculation may not be calculated along the store longitudinal axis. This is the case when all or a portion of the store lies in the region where the velocity field is smoothed as described in section 3.4.2 of reference 1. The velocity field to be smoothed is calculated by making an axial traverse parallel to the fuselage longitudinal axis at the y_B, z_B location of the store center of gravity. When Ψ and Θ are zero the store axis lies along this traverse. As the angles increase in magnitude, this is no longer the case. Except for an extremely long store, sufficiently accurate velocity fields are calculated up to angles of ± 10 degrees.

4. PROGRAM ERROR MESSAGES

The possible occurrence of certain fatal errors during program execution has been anticipated in the store separation trajectory program. If such an error should occur, the program has been designed to print a diagnostic error message and then halt. Each message with the routine in which the corresponding error is detected is presented in the following table. The table is arranged in alphabetical order by the first word of the message.

<u>Routine</u>	<u>Error Message</u>
BDYGEN	at base of body radial distance to Mach cone emanating from body nose is less than maximum body radius; check body input data and Mach number
NUMACH	axial location of traverse above wing chordal plane
INVERS	matrix is singular
NUMACH	no negative velocity due to wing thickness found in traverse to trailing-edge Mach cone
SSTORE	NSTRS input as ($n > 1$); program limited to one store
STORIO	shape polynomials not input for all stores
WITHIN	slope of wing thickness envelope at leading edge not positive for some chordwise row
THRCAL	time greater than end of specified thrust time history

If one of the above messages is printed out during program execution, the user should examine the input data for possible error.

5. PROGRAM RUNNING TIMES

The program described in this report has been run on the CDC 6600. Because of machine differences, the running time varies from one machine to the other. As a consequence, only an approximate running time can be given.

The running time of the trajectory program is a function of a number of factors, some of which are

- (a) Number of sources and doublets required to represent the bodies
- (b) Number of constant u-velocity panels on wing, pylon, and fuselage
- (c) Number of thickness panels on wing and pylon
- (d) Number of body segments and tail fin control points used in force and moment calculation
- (e) Integration interval
- (f) Real time duration of trajectory

All of the above should be kept to a minimum except (e) which should be as large as possible. For the sample trajectory which was presented, the running time was about 5 minutes on the CDC 6600.

TABLE I

SUBROUTINES USED IN COMPUTER PROGRAM

<u>Subroutine Name</u>	<u>Function</u>
ADAMS	numerical integration routine to integrate differential equations
BDYGEN	calculates line sources and doublets to give a required body shape and angle of attack
BLYOUT	lays out fuselage constant u-velocity panels
CEL1	calculates complete elliptic integral of the first kind
CEL2	calculates complete elliptic integral of the second kind
DIRCOS	calculates direction cosines between inertial and store body coordinate systems
DOUBLT	calculates the strength of a linear line doublet
DPCOEF	calculates coefficient matrix of the set of equations to be solved for the wing-pylon-fuselage constant u-velocity panel strengths
DPRHS	calculates right-hand side of the set of equations to be solved for the wing-pylon-fuselage constant u-velocity panel strengths
ELI1	calculates generalized elliptic integral of the first kind
ELI2	calculates generalized elliptic integral of the second kind
FLSQFY	calculates least squares polynomial approximation of specified degree to a given set of data points
FUSEIO	reads and prints fuselage data and calls BDYGEN to calculate line source and doublet distributions
INTOST	transforms a vector with components in the inertial coordinate system to one with component in the store body coordinate system
INVERS	solves a system of simultaneous linear algebraic equations
NUMACH	calculates the local Mach number to be used in calculating the wing-fuselage induced velocities, calculates these velocities and calls FLSQFY to perform a least squares smoothing

TABLE I.- (CONT.)

PLYOUT	reads and prints pylon data and lays out constant u-velocity panels on pylon
PYTHIN	reads pylon thickness data
RESVEL	calculates velocities induced at a field point by all aircraft components
SEMFOR	calculates store empennage forces and moments
SEMPIN	initializes for empennage force and moment calculation
SFORCE	calculates the store-body forces and moments
SHAPE	calculates radius and surface slope at a point on a body from input polynomials
SIMSON	performs a Simpson rule integration
SOURCE	calculates the strength of a linear line source
SOUTPT	prints forces, moments, load distributions, and trajectory data at the end of each integration step
STORIO	reads and prints store data and calls BDYGEN to calculate line source and doublet distributions
STTOIN	transforms a vector with components in the store body coordinate system to one with components in the inertial coordinate system
SWNGIN	reads and prints wing constant u-velocity panel data and twist and camber data, if any
THLYT	lays out wing and pylon thickness panels
THKOUT	prints wing and pylon thickness input data
THRCAL	calculates thrust from input polynomials
VELBD	calculates velocities or influence functions due to fuselage constant u-velocity panels or panel
VELCAL	calculates velocities at a field point due to fuselage or store line sources and doublets
VELO	calculates the influence of a semi-infinite triangle associated with a constant u-velocity panel
VELOTH	calculates the influence of a semi-infinite triangle associated with a thickness source panel
VELPP	calculates velocities or influence functions due to pylon constant u-velocity panels or panel

TABLE I.- (CONC.)

VELPTH	calculates velocities at a field point due to pylon thickness source panels
VELWP	calculates velocities or influence functions due to wing constant u-velocity panels or panel
VELWTH	calculates velocities at a field point due to wing thickness source panels
WTHIN	reads wing thickness data
WLYOUT	lays out constant u-velocity panels on wing

[illegible]

(d) Page 4.


```

IF (TIMEP, 14, 23) GO TO 300
LUNENCR1
LUNENCR2
LUNENCR3
LUNENCR4
LUNENCR5
LUNENCR6
LUNENCR7
LUNENCR8
LUNENCR9
LUNENCR10
LUNENCR11
LUNENCR12
LUNENCR13
LUNENCR14
LUNENCR15
LUNENCR16
LUNENCR17
LUNENCR18
LUNENCR19
LUNENCR20
LUNENCR21
LUNENCR22
LUNENCR23
LUNENCR24
LUNENCR25
LUNENCR26
LUNENCR27
LUNENCR28
LUNENCR29
LUNENCR30
LUNENCR31
LUNENCR32
LUNENCR33
LUNENCR34
LUNENCR35
LUNENCR36
LUNENCR37
LUNENCR38
LUNENCR39
LUNENCR40
LUNENCR41
LUNENCR42
LUNENCR43
LUNENCR44
LUNENCR45
LUNENCR46
LUNENCR47
LUNENCR48
LUNENCR49
LUNENCR50
LUNENCR51
LUNENCR52
LUNENCR53
LUNENCR54
LUNENCR55
LUNENCR56
LUNENCR57
LUNENCR58
LUNENCR59
LUNENCR60
LUNENCR61
LUNENCR62
LUNENCR63
LUNENCR64
LUNENCR65
LUNENCR66
LUNENCR67
LUNENCR68
LUNENCR69
LUNENCR70
LUNENCR71
LUNENCR72
LUNENCR73
LUNENCR74
LUNENCR75

SUBROUTINE CELL(RES, AK, IER)
.....
SUBROUTINE CELL
PURPOSE
CALCULATE COMPLETE ELLIPTIC INTEGRAL OF FIRST KIND
USAGE
CALL CELL(RES, AK, IER)
DESCRIPTION OF PARAMETERS
RES = RESULT VALUE
AK = MODULUS (INPUT)
IER = RESULTANT ERROR CODE WHERE
IER=0 NO ERROR
IER=1 AK NOT IN RANGE -1 TO +1
REMARKS
FOR AK=1 THE RESULT IS SET TO 1.430
FOR MODULUS AK AND COMPLEMENTARY MODULUS CK,
RELATIONSHIP CK=SQRT(1-AK**2) IS USED.
AK MUST BE IN THE RANGE -1 TO +1
SUBROUTINES AND FUNCTION SUBPROGRAMS REQUIRED
NONE
METHOD
DEFINITION
CELL(AR)=INTGRL(1/SQRT(1-(AR**2)), SUMMED
OVER T FROM 0 TO INFINITY)
EQUIVALENT ARE THE DEFINITIONS

```

(g) Page 7.
Figure 1.- Continued.

(o) Page 15.

Figure 1.- Continued.

(p) Page 16.
Figure 1.- Continued.

(q) Page 17.

(r) Page 18.

Figure 1.- Continued.

(s) Page 19.
Figure 1.- Continued.

(t) Page 20.
Figure 1.- Continued.


```

DO 11 J=1,NSTRS
  Y=YS(J)
  IF (VY.GT. 0.0) VY=VY
  101
  102
  103
  104
  105
  106
  107
  108
  109
  110
  111
  112
  113
  114
  115
  116
  117
  118
  119
  120
  121
  122
  123
  124
  125
  126
  127
  128
  129
  130
  131
  132
  133
  134
  135
  136
  137
  138
  139
  140
  141
  142
  143
  144
  145
  146
  147
  148
  149
  150
  151
  152
  153
  154
  155
  156
  157
  158
  159
  160
  161
  162
  163
  164
  165
  166
  167
  168
  169
  170
  171
  172
  173
  174
  175
  176
  177
  178
  179
  180
  181
  182
  183
  184
  185
  186
  187
  188
  189
  190
  191
  192
  193
  194
  195
  196
  197
  198
  199
  200
  201
  202
  203
  204
  205
  206
  207
  208
  209
  210
  211
  212
  213
  214
  215
  216
  217
  218
  219
  220
  221
  222
  223
  224
  225
  226
  227
  228
  229
  230
  231
  232
  233
  234
  235
  236
  237
  238
  239
  240
  241
  242
  243
  244
  245
  246
  247
  248
  249
  250
  251
  252
  253
  254
  255
  256
  257
  258
  259
  260
  261
  262
  263
  264
  265
  266
  267
  268
  269
  270
  271
  272
  273
  274
  275
  276
  277
  278
  279
  280
  281
  282
  283
  284
  285
  286
  287
  288
  289
  290
  291
  292
  293
  294
  295
  296
  297
  298
  299
  300
  301
  302
  303
  304
  305
  306
  307
  308
  309
  310
  311
  312
  313
  314
  315
  316
  317
  318
  319
  320
  321
  322
  323
  324
  325
  326
  327
  328
  329
  330
  331
  332
  333
  334
  335
  336
  337
  338
  339
  340
  341
  342
  343
  344
  345
  346
  347
  348
  349
  350
  351
  352
  353
  354
  355
  356
  357
  358
  359
  360
  361
  362
  363
  364
  365
  366
  367
  368
  369
  370
  371
  372
  373
  374
  375
  376
  377
  378
  379
  380
  381
  382
  383
  384
  385
  386
  387
  388
  389
  390
  391
  392
  393
  394
  395
  396
  397
  398
  399
  400
  401
  402
  403
  404
  405
  406
  407
  408
  409
  410
  411
  412
  413
  414
  415
  416
  417
  418
  419
  420
  421
  422
  423
  424
  425
  426
  427
  428
  429
  430
  431
  432
  433
  434
  435
  436
  437
  438
  439
  440
  441
  442
  443
  444
  445
  446
  447
  448
  449
  450
  451
  452
  453
  454
  455
  456
  457
  458
  459
  460
  461
  462
  463
  464
  465
  466
  467
  468
  469
  470
  471
  472
  473
  474
  475
  476
  477
  478
  479
  480
  481
  482
  483
  484
  485
  486
  487
  488
  489
  490
  491
  492
  493
  494
  495
  496
  497
  498
  499
  500
  501
  502
  503
  504
  505
  506
  507
  508
  509
  510
  511
  512
  513
  514
  515
  516
  517
  518
  519
  520
  521
  522
  523
  524
  525
  526
  527
  528
  529
  530
  531
  532
  533
  534
  535
  536
  537
  538
  539
  540
  541
  542
  543
  544
  545
  546
  547
  548
  549
  550
  551
  552
  553
  554
  555
  556
  557
  558
  559
  560
  561
  562
  563
  564
  565
  566
  567
  568
  569
  570
  571
  572
  573
  574
  575
  576
  577
  578
  579
  580
  581
  582
  583
  584
  585
  586
  587
  588
  589
  590
  591
  592
  593
  594
  595
  596
  597
  598
  599
  600
  601
  602
  603
  604
  605
  606
  607
  608
  609
  610
  611
  612
  613
  614
  615
  616
  617
  618
  619
  620
  621
  622
  623
  624
  625
  626
  627
  628
  629
  630
  631
  632
  633
  634
  635
  636
  637
  638
  639
  640
  641
  642
  643
  644
  645
  646
  647
  648
  649
  650
  651
  652
  653
  654
  655
  656
  657
  658
  659
  660
  661
  662
  663
  664
  665
  666
  667
  668
  669
  670
  671
  672
  673
  674
  675
  676
  677
  678
  679
  680
  681
  682
  683
  684
  685
  686
  687
  688
  689
  690
  691
  692
  693
  694
  695
  696
  697
  698
  699
  700
  701
  702
  703
  704
  705
  706
  707
  708
  709
  710
  711
  712
  713
  714
  715
  716
  717
  718
  719
  720
  721
  722
  723
  724
  725
  726
  727
  728
  729
  730
  731
  732
  733
  734
  735
  736
  737
  738
  739
  740
  741
  742
  743
  744
  745
  746
  747
  748
  749
  750
  751
  752
  753
  754
  755
  756
  757
  758
  759
  760
  761
  762
  763
  764
  765
  766
  767
  768
  769
  770
  771
  772
  773
  774
  775
  776
  777
  778
  779
  780
  781
  782
  783
  784
  785
  786
  787
  788
  789
  790
  791
  792
  793
  794
  795
  796
  797
  798
  799
  800
  801
  802
  803
  804
  805
  806
  807
  808
  809
  810
  811
  812
  813
  814
  815
  816
  817
  818
  819
  820
  821
  822
  823
  824
  825
  826
  827
  828
  829
  830
  831
  832
  833
  834
  835
  836
  837
  838
  839
  840
  841
  842
  843
  844
  845
  846
  847
  848
  849
  850
  851
  852
  853
  854
  855
  856
  857
  858
  859
  860
  861
  862
  863
  864
  865
  866
  867
  868
  869
  870
  871
  872
  873
  874
  875
  876
  877
  878
  879
  880
  881
  882
  883
  884
  885
  886
  887
  888
  889
  890
  891
  892
  893
  894
  895
  896
  897
  898
  899
  900
  901
  902
  903
  904
  905
  906
  907
  908
  909
  910
  911
  912
  913
  914
  915
  916
  917
  918
  919
  920
  921
  922
  923
  924
  925
  926
  927
  928
  929
  930
  931
  932
  933
  934
  935
  936
  937
  938
  939
  940
  941
  942
  943
  944
  945
  946
  947
  948
  949
  950
  951
  952
  953
  954
  955
  956
  957
  958
  959
  960
  961
  962
  963
  964
  965
  966
  967
  968
  969
  970
  971
  972
  973
  974
  975
  976
  977
  978
  979
  980
  981
  982
  983
  984
  985
  986
  987
  988
  989
  990
  991
  992
  993
  994
  995
  996
  997
  998
  999
  1000

```

(w) Page 23.

Figure 1.- Continued.

67

(aa) Page 27.

Figure 1.- Continued.

(ee) Page 31.

ff) Page 32.

Figure 1.- Continued.

(99) Page 33.

(hh) Page 34.

```

SP400117
SP400118
SP400119
SP400120
SP400121
SP400122
SP400123
SP400124
SP400125
SP400126
SP400127
SP400128
SP400129
SP400130
SP400131
SP400132
SP400133
SP400134
SP400135
SP400136
SP400137
SP400138
SP400139
SP400140
SP400141
SP400142
SP400143
SP400144
SP400145
SP400146
SP400147
SP400148
SP400149
SP400150
SP400151
SP400152
SP400153
SP400154
SP400155
SP400156
SP400157
SP400158
SP400159
SP400160
SP400161
SP400162
SP400163
SP400164
SP400165
SP400166
SP400167
SP400168
SP400169
SP400170
SP400171
SP400172
SP400173
SP400174
SP400175
SP400176
SP400177
SP400178
SP400179
SP400180
SP400181
SP400182
SP400183
SP400184
SP400185
SP400186
SP400187
SP400188

IF(XI,GP,AMB(I)) GO TO 100
X=XI+VLC(I)
Y=YI+VLC(I)
CALL VLOC(VELT)
IF(.NOT.FELT) GO TO 10
TUTU=U
TUTV=V
TUTW=W
FELT=TRUE
30 VYI=VLC(I)
IF(.NOT.FELT) GO TO 100
TUTU=U
TUTV=V
TUTW=W
FELT=TRUE
20 IF (FEM2 .LT. 0.0) GO TO 19
C ***** CORNER 3 *****
C CORNER 3 FOR FEM2 .GE. 0 ---- PANEL TRAILING EDGE SHEET MACH
C ***** CORNER 3 *****
IF(XI,GP,AMB(I)) GO TO 40
FEM2=
X=XI+VLC(I)
Y=YI+VLC(I)
CALL VLOC(VELT)
IF(.NOT.FELT) GO TO 51
TUTU=U
TUTV=V
TUTW=W
FELT=TRUE
51 VYI=VLC(I)
CALL VLOC(VELT)
IF(.NOT.FELT) GO TO 30
TUTU=U
TUTV=V
TUTW=W
FELT=TRUE
GO TO 30
C ***** CORNER 3 FOR FEM2 .LT. 0 ---- PANEL TRAILING EDGE SHEET MACH
C ***** CORNER 3 *****
19 FEM2=
IF(XI,GP,AMB(I)) GO TO 40
X=XI+VLC(I)
Y=YI+VLC(I)
CALL VLOC(VELT)
IF(.NOT.FELT) GO TO 53
TUTU=U
TUTV=V
TUTW=W
FELT=TRUE
53 VYI=VLC(I)
CALL VLOC(VELT)
IF(.NOT.FELT) GO TO 21
TUTU=U
TUTV=V
TUTW=W
FELT=TRUE
GO TO 21
C ***** CORNER 4 *****
C ***** CORNER 4 FOR FEM2 .GE. 0 *****
30 CONTINUE
FEM2=
X=XI+VLC(I)
Y=YI+VLC(I)
CALL VLOC(VELT)
IF(.NOT.FELT) GO TO 35
TUTU=U
TUTV=V
TUTW=W
FELT=TRUE
35 VYI=VLC(I)
CALL VLOC(VELT)
IF(.NOT.FELT) GO TO 40
TUTU=U
TUTV=V
TUTW=W
FELT=TRUE
GO TO 40

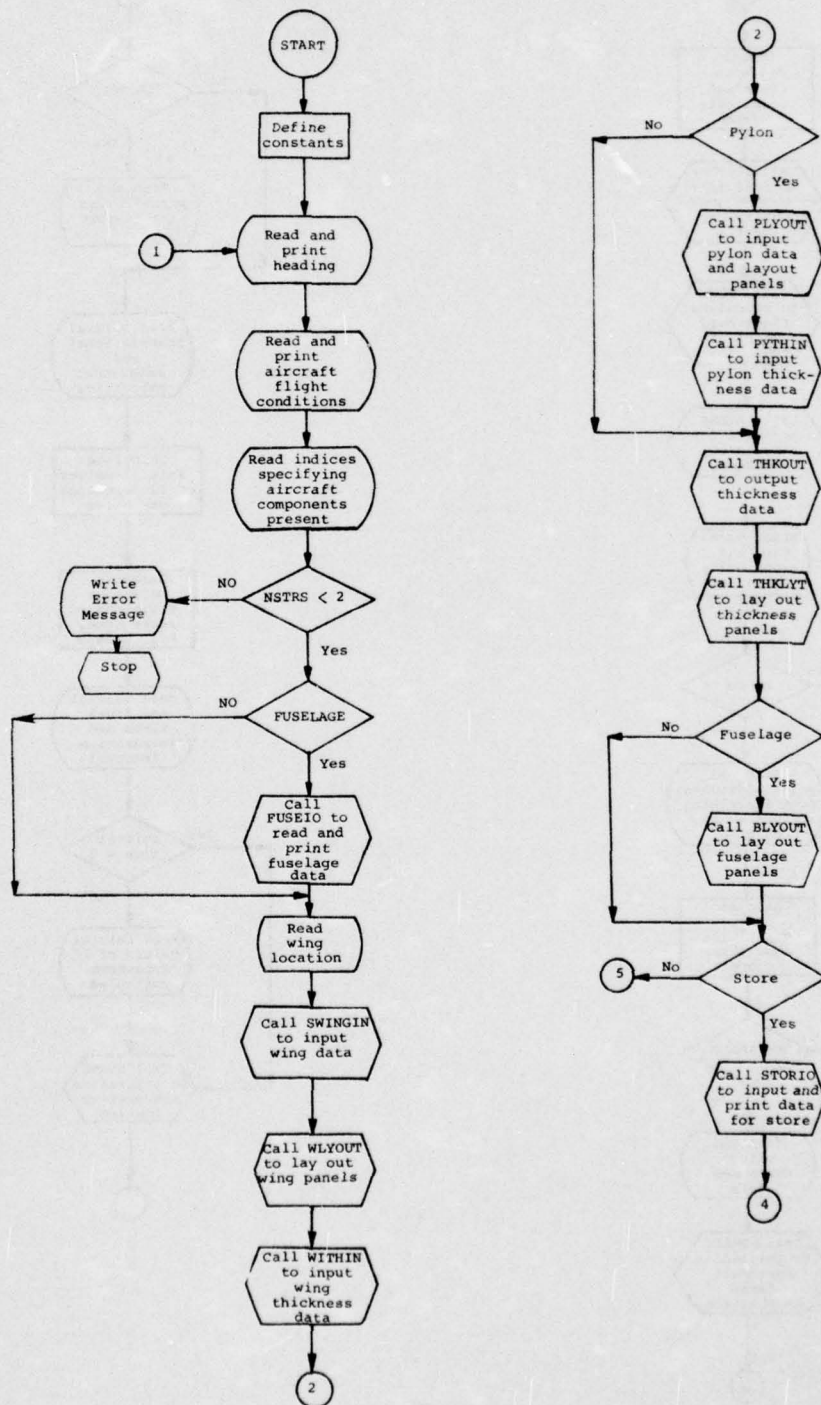
```

(11) Page 35.

Figure 1.- Continued.

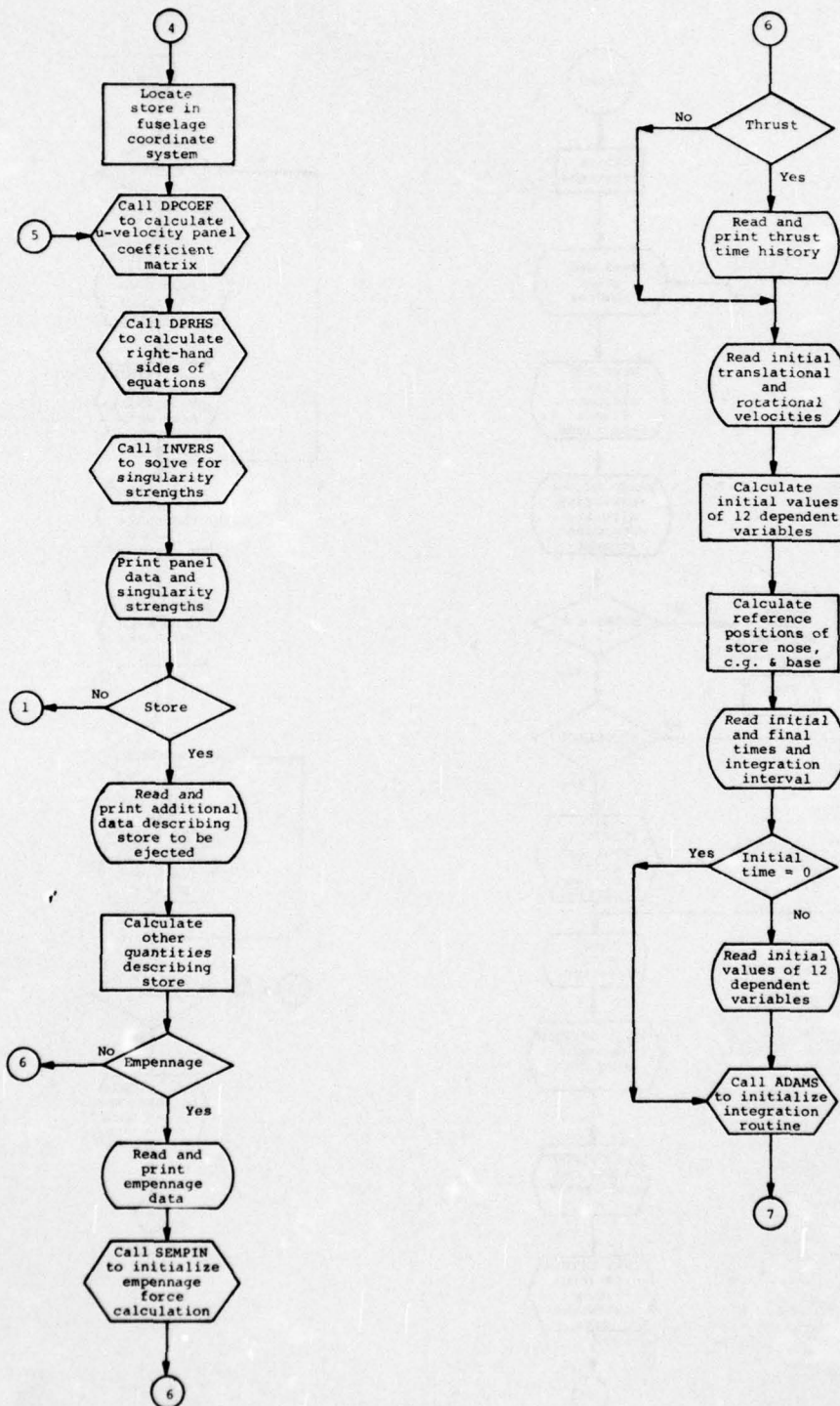
(kk) Page 37.

Figure 1.- Continued.

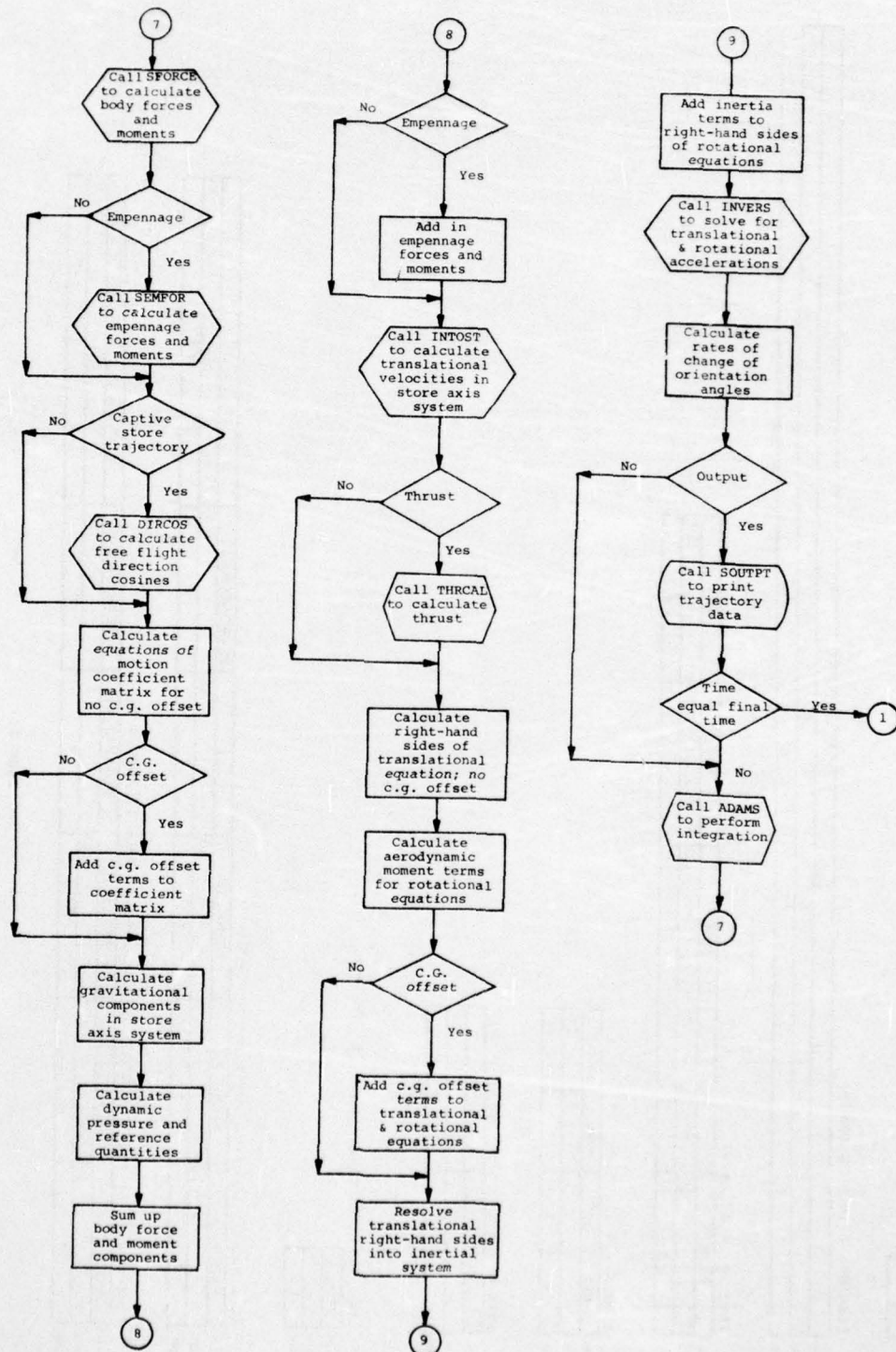


(a) Page 1.

Figure 2.- General flow chart of trajectory program.



(b) Page 2.
Figure 2.- Continued.



(c) Page 3.

Figure 2.- Concluded.

Item No. 1 (1 card)

Variable	NCARDS
Card Column	5
Format Type	I

Item No. 2 (NCARDS cards)

Variable	HEAD		
Card Column	1		
Format Type	A		
	80		

Item No. 3 (1 card)

Variable	ALFAC	10	GAMF	20	FWACH	30	RHO	40	VINF	50
Card Column										
Format Type	F		F		F		F		F	

Item No. 4 (1 card)

Variable	NFU	NPY	NMY	NSTRS
Card Column	5	10	15	20
Format Type	I	I	I	I

Item No. 5 (1 card, omit if NFU = 0)

Variable	FLTHC	FRMAX
Card Column	10	20
Format Type	F	F

Item No. 6 (1 card, omit if NFU = 0)

Variable	NFPOLY
Card Column	5
Format Type	I

Item No. 7 (1 card, omit if NFU = 0)

Variable	FXEND(1)	FXEND(2)	FXEND(3)	...	FXEND(NFPOLY)
Card Column	10	20	30	40	50
Format Type	F	F	F	F	F
					70

Item No. 8 (J = 1 to NFPOLY; NFPOLY cards. Omit if NFU = 0)

Variable	FCOEF(J,1)	FCOEF(J,2)	FCOEF(J,3)	FCOEF(J,4)	FCOEF(J,5)	FCOEF(J,6)	FCOEF(J,7)
Card Column	10	20	30	40	50	60	70
Format Type	F	F	F	F	F	F	F

(a) Page 1.

Figure 3.- Trajectory program input format.

Item No. 9 (1 card. Omit if NFU = 0)

Variable	NCWB	NBDCR1	NBDCR2	NFSOR
Card Column	5	10	15	20
Format Type	I	I	I	I

Item No. 10 (1 card. Omit if NFU = 0)

Variable	BODYPL
Card Column	10
Format Type	F

Item No. 11 (1 card)

Variable	XBWOC	ZBWO
Card Column	10	20
Format Type	F	F

Item No. 12 (1 card)

Variable	CRW	SSPAN
Card Column	10	20
Format Type	F	F

Item No. 13 (1 card)

Variable	NCW	MSW
Card Column	5	10
Format Type	I	I

Item No. 14 (I = 1 to MSW+1; MSW+1 cards)

Variable	I	Y(I)	PSIWLE(I)	PSIWTE(I)
Card Column	5	15	25	35
Format Type	I	F	F	F

(b) Page 2.

Figure 3.- Continued.

Item No. 15 (1 card)

Variable	NTAC	NUNI
Card Column	5	10
Format Type	I	I

Item No. 16 (NCW values, eight to a card. Omit if NTAC = 0. One set of cards if NUNI = 1; MSW sets if NUNI = 0.)

Variable	ALPHAL(1)	ALPHAL(2)	...	ALPHAL(NCW)			
Card Column	10	20		40	50	60	70
Format Type	F	F	F	F	F	F	F

Item No. 17 (1 card)

Variable	NCWS	NUNIS
Card Column	5	10
Format Type	I	I

Item No. 18 (NCWS values, eight to a card. One set of cards if NUNIS = 1; MSW sets if NUNIS = 0.)

[illegible]

Item No. 19 (1 card. Omit if NPY = 0.)

Variable	PSIPL	PSIPLT	CRP	HP	XPLE
Card Column	5	15	25	35	45
Format Type	I	F	F	F	F

Item No. 20 (1 card. Omit if NPY = 0.)

Variable	NCP	MSP
Card Column	5	10
Format Type	I	I

(c) Page 3.

Figure 3.- Continued.

Item No. 21 (K = 1 to MSP+1; MSP+1 cards. Omit if NPY = 0.)

Variable	K	Z(K)
Card Column	5	15
Format Type	I	F

Item No. 22 (1 card. Omit if NPY = 0.)

Variable	NCPS	NUNIP
Card Column	5	10
Format Type	I	I

Item No. 23 (NCPS values, eight to a card. Omit if NPY = 0. One set of cards if NUNIP = 1; MSP sets if NUNIP = 0.)

Variable	THETPL(1)	THETPL(2)	...	THETPL(NCPS)					
Card Column	10	20	30	40	50	60	70	80	
Format Type	F	F	F	F	F	F	F	F	F

Note: If NSTRS = 0 this completes the input data.

Item No. 24 (1 card)

Variable	NUMSTR(1)	NSHAPE(1)	SLTBC(1)	SRMAX(1)	XSNC(1)	YSN(1)	ZSN(1)	SIC(1)
Card Column	5	10	20	30	40	50	60	70
Format Type	I	I	F	F	F	F	F	F

Item No. 25 (1 card)

Variable	NSHPT
Card Column	5
Format Type	I

Item No. 26 (1 card)

Variable	MSHAPE	MSOR
Card Column	5	10
Format Type	I	I

(d) Page 4.

Figure 3.- Continued.

AD-A031 388

NIELSEN ENGINEERING AND RESEARCH INC MOUNTAIN VIEW CALIF F/G 1/3
PREDICTION OF SUPERSONIC STORE SEPARATION CHARACTERISTICS. VOLU--ETC(U)
MAY 76 F K GOODWIN, M M KEIRSTEAD F33615-75-C-3053
NEAR-TR-106 AFFDL-TR-76-41-VOL-2 NL

UNCLASSIFIED

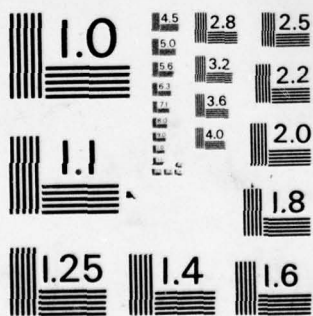
2 OF 3
AD A031388



OF

3

31388



MICROCOPY RESOLUTION TEST CHART
NATIONAL BUREAU OF STANDARDS-1963-A

Item No. 27 (1 card)

Variable	NSPOLJ
Card Column	5
Format Type	I

Item No. 28 (1 card)

Variable	SXNDJ(1)	SXNDJ(2)	...	SXNDJ(NSPOLJ)			
Card Column	10	20	30	40	50	60	70
Format Type	F	F	F	F	F	F	F

Item No. 29 (J=1, NSPOLJ; NSPOLJ cards)

Variable	SCOFJ(J,1)	SCOFJ(J,2)	SCOFJ(J,3)	SCOFJ(J,4)	SCOFJ(J,5)	SCOFJ(J,6)	SCOFJ(J,7)
Card Column	10	20	30	40	50	60	70
Format Type	F	F	F	F	F	F	F

Item No. 30 (1 card)

Variable	NEJECT	NSEG	NSECKO	NGAM	NPOLY	NROLL	NEMP	NDAMP	NTHRUS
Card Column	5	10	15	20	25	30	35	40	45
Format Type	I	I	I	I	I	I	I	I	I

Item No. 31 (1 card)

Variable	SMASS	FIXX	FIYY	FIZZ	FIYZ	FIXZ	FIFY
Card Column	10	20	30	40	50	60	70
Format Type	F	F	F	F	F	F	F

Item No. 32 (1 card)

Variable	XMOM	XBAR	YBAR	ZBAR
Card Column	10	20	30	40
Format Type	F	F	F	F

Item No. 33 (1 card)

Variable	XEND(1)	XEND(2)	...	XEND(NPOLY)			
Card Column	10	20	30	40	50	60	70
Format Type	F	F	F	F	F	F	F

(e) Page 5.

Figure 3.- Continued.

Item No. 34 (J = 1 to NPOLY; NPOLY cards)

Variable	COEF(J,1)	COEF(J,2)	COEF(J,3)	COEF(J,4)	COEF(J,5)	COEF(J,6)	COEF(J,7)
Card Column	10	20	30	40	50	60	70
Format Type	F	F	F	F	F	F	F

Item No. 35 (1 card)

Variable	CA	CDC
Card Column	10	20
Format Type	F	F

Item No. 36 (1 card. Omit if NEMP = 0)

Variable	IPLNR	MSF
Card Column	5	10
Format Type	I	I

Item No. 37 (1 card. Omit if NEMP = 0)

Variable	XTAIL	RADAV	FINSS	PHIROL	CLALPH
Card Column	10	20	30	40	50
Format Type	F	F	F	F	F

Item No. 38 (1 card. Omit if NTHRUS = 0)

Variable	NTPOLY
Card Column	5
Format Type	I

Item No. 39 (1 card. Omit if NTHRUS = 0)

Variable	TEND(1)	TEND(2)	...	TEND(NTPOLY)
Card Column	10	20	30	40
Format Type	F	F	F	F

Item No. 40 (J = 1, NTPOLY; NTPOLY cards. Omit if NTHRUS = 0)

Variable	TC(J,1)	TC(J,2)	TC(J,3)	TC(J,4)	TC(J,5)	TC(J,6)
Card Column	10	20	30	40	50	60
Format Type	F	F	F	F	F	F

(f) Page 6.

Figure 3.- Continued.

Item No. 41 (1 card)

Variable	VXZERO	VYZERO	VZZERO	VAR(4)	VAR(5)	VAR(6)
Card Column	10	20	30	40	50	60
Format Type	F	F	F	F	F	F

Item No. 42 (1 card)

Variable	DTIME	TIMEI	TIMEF
Card Column	10	20	30
Format Type	F	F	F

Item No. 43 (2 cards. Omit if TIMEI = 0)

Variable	VAR(1)	VAR(2)	...	VAR(12)					
Card Column	10	20	30	40	50	60	70	80	
Format Type	F	F	F	F	F	F	F	F	

(g) Page 7.

Figure 3.- Concluded.

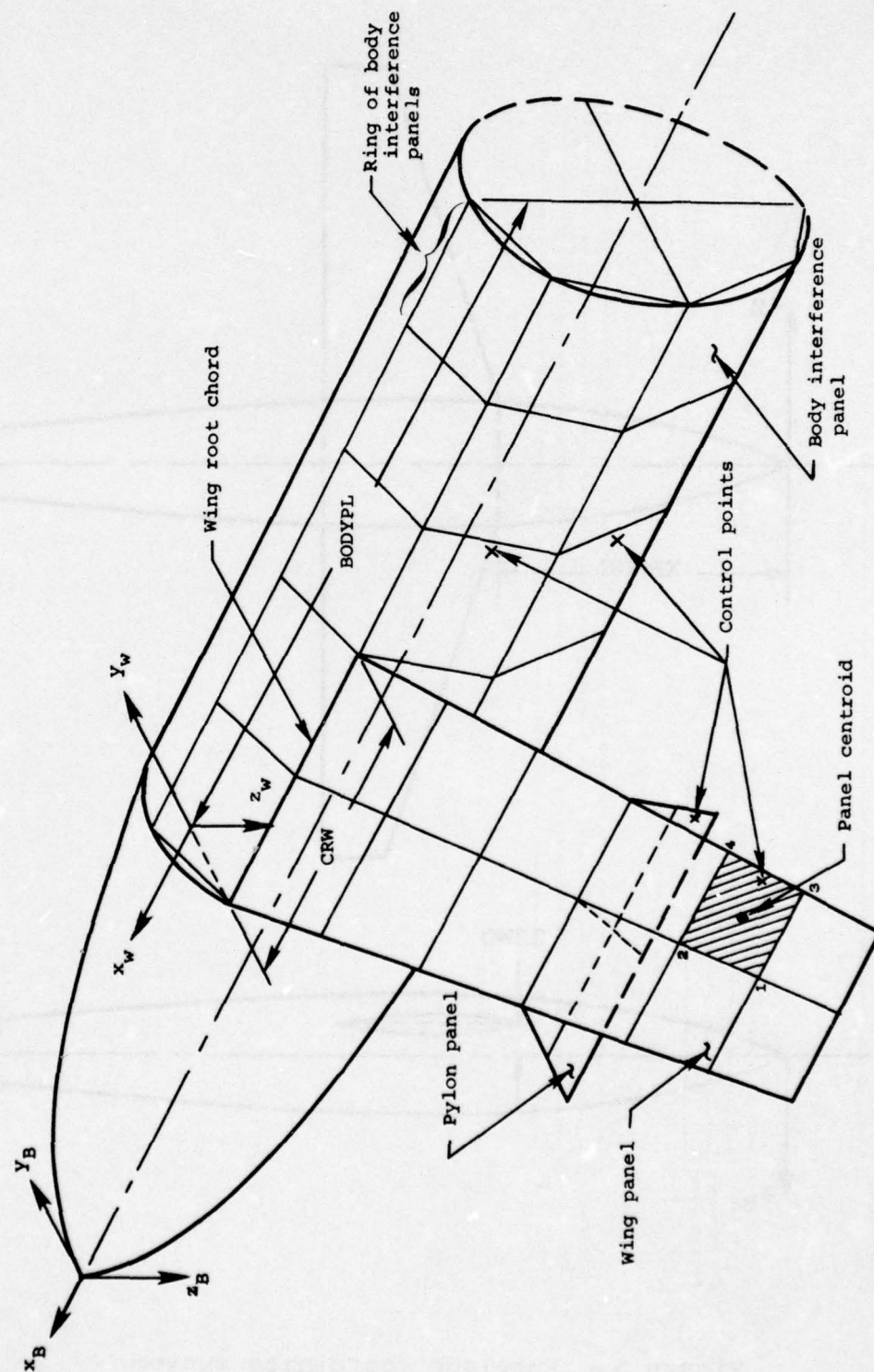


Figure 4.- Simplified layout of panels for wing-pylon and fuselage combination.

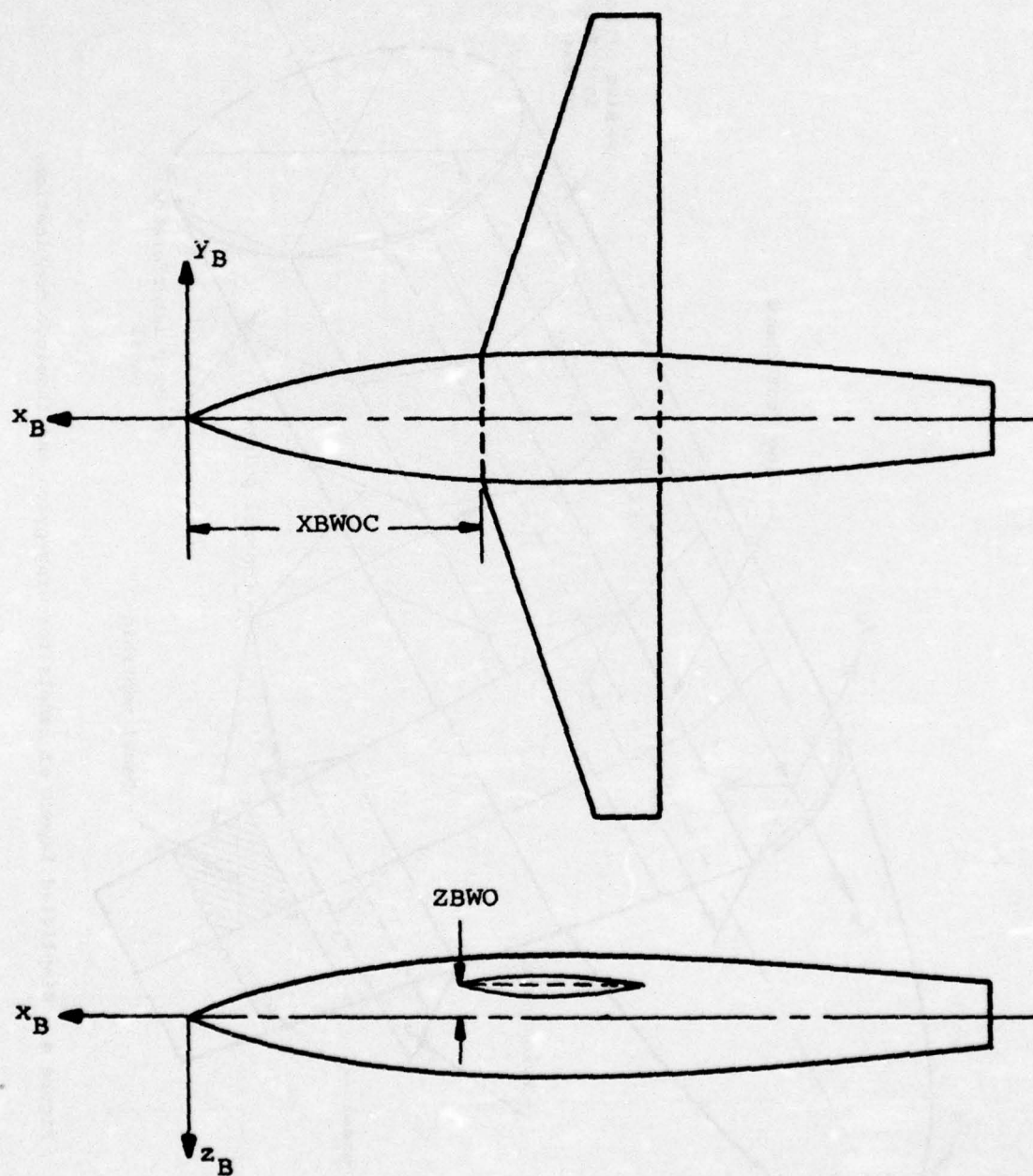


Figure 5.- Fuselage coordinate system.

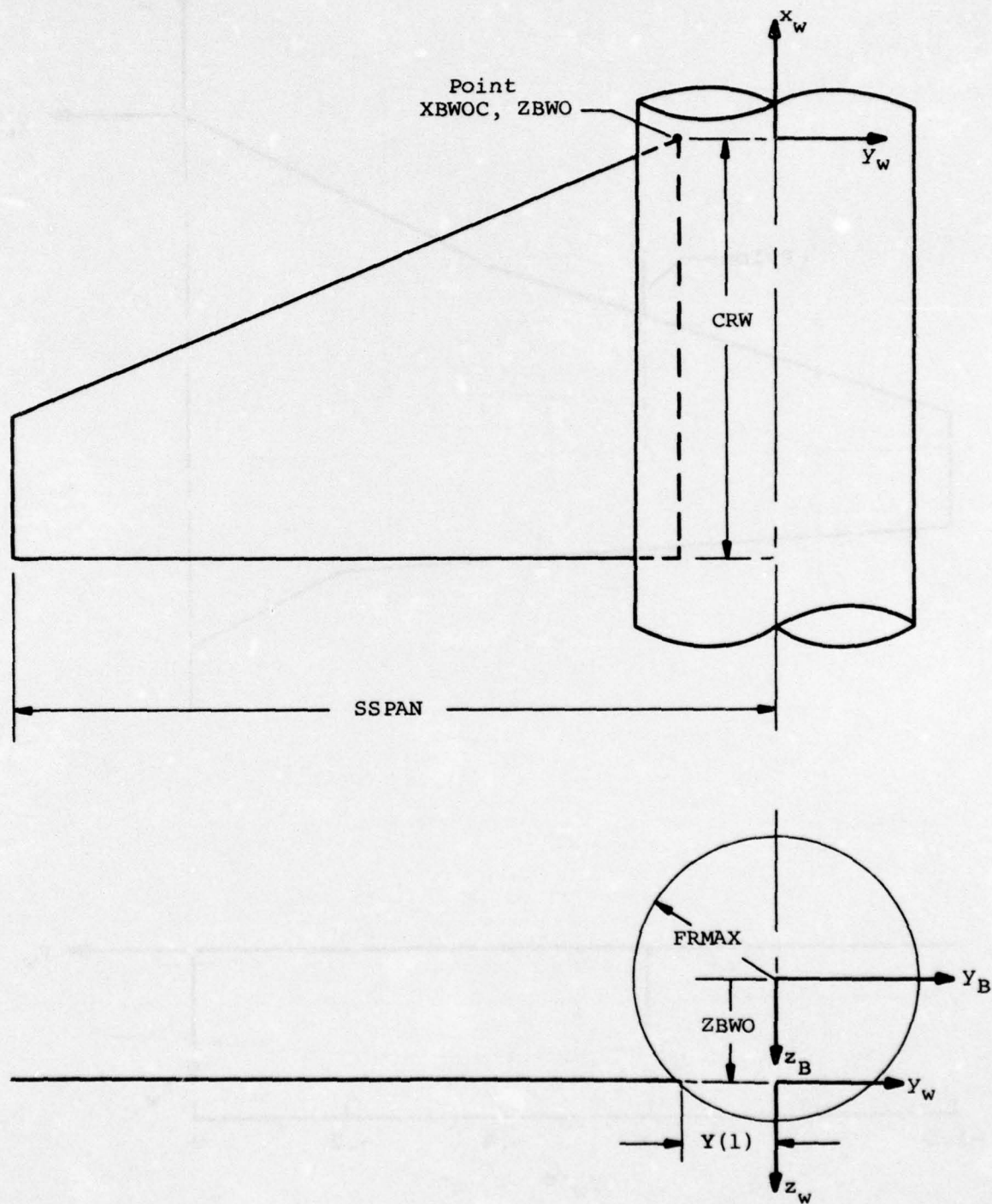


Figure 6.- Definition of certain wing input variables.

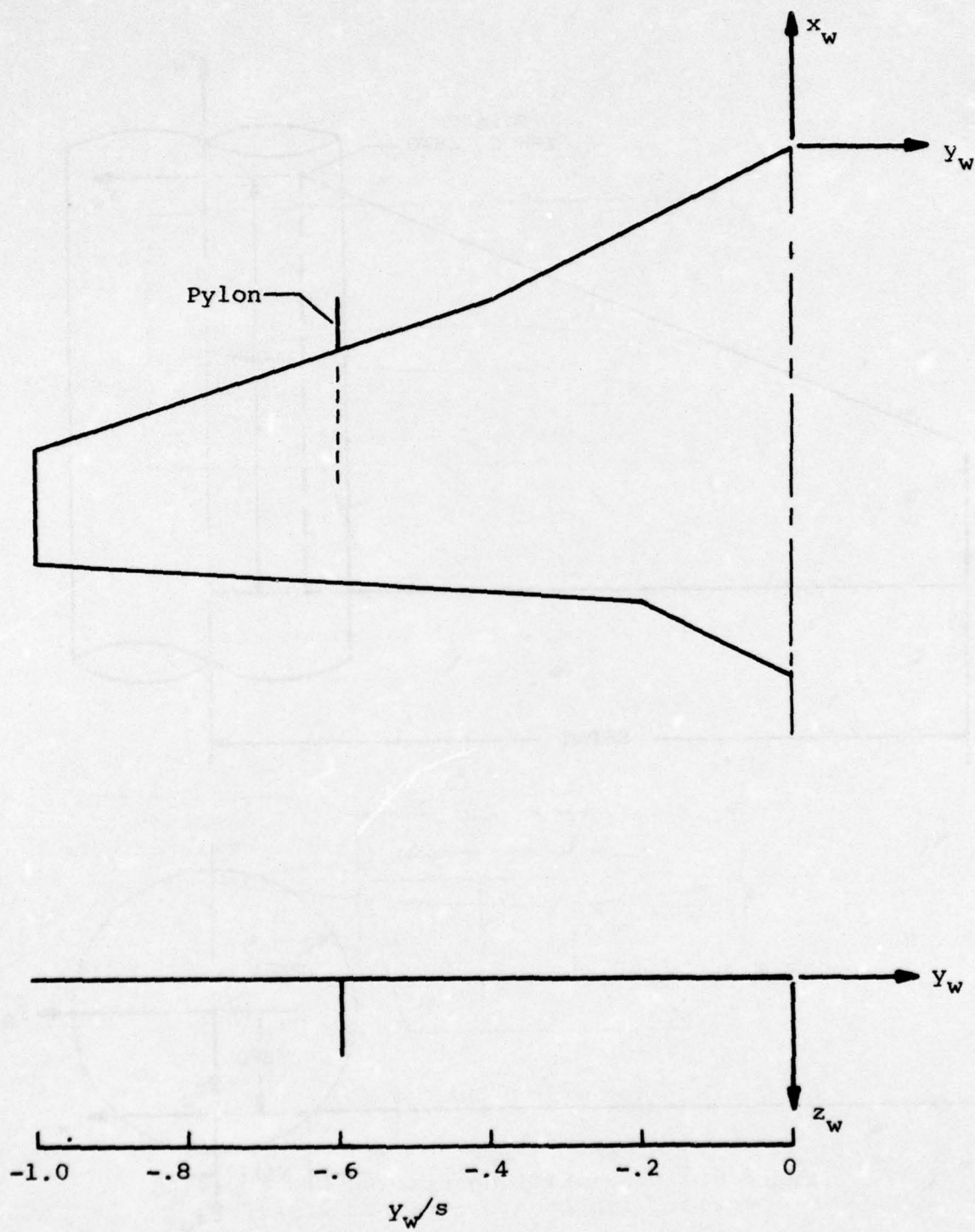
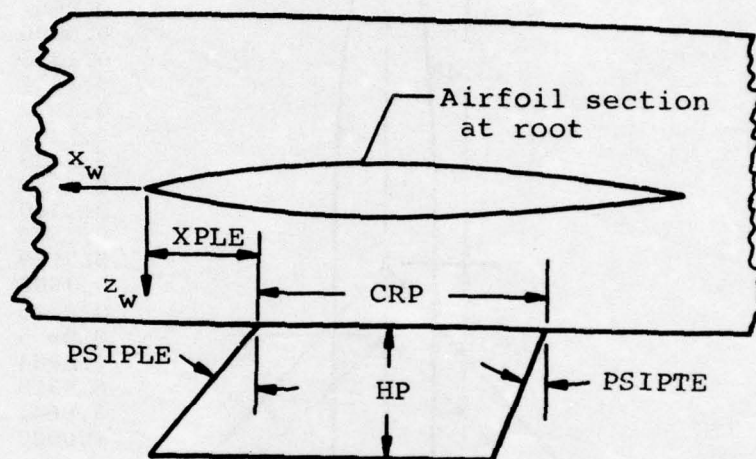
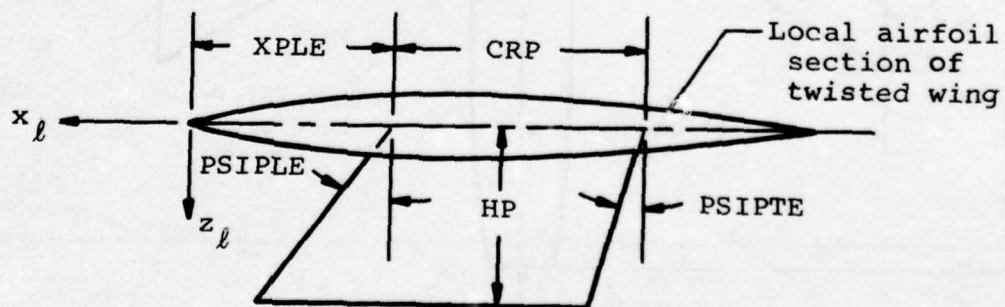


Figure 7 .- Example wing.

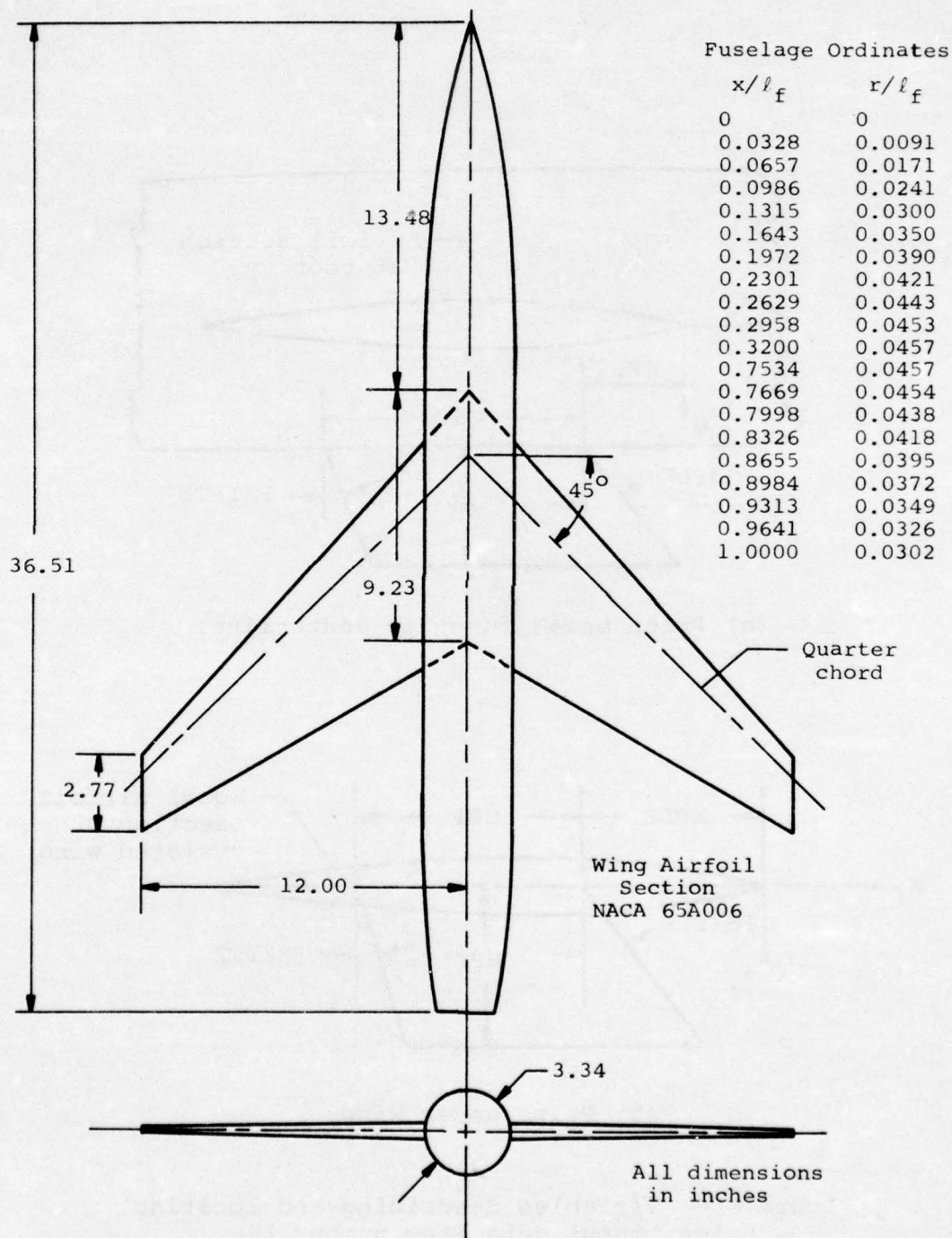


(a) Pylon under fuselage centerline.



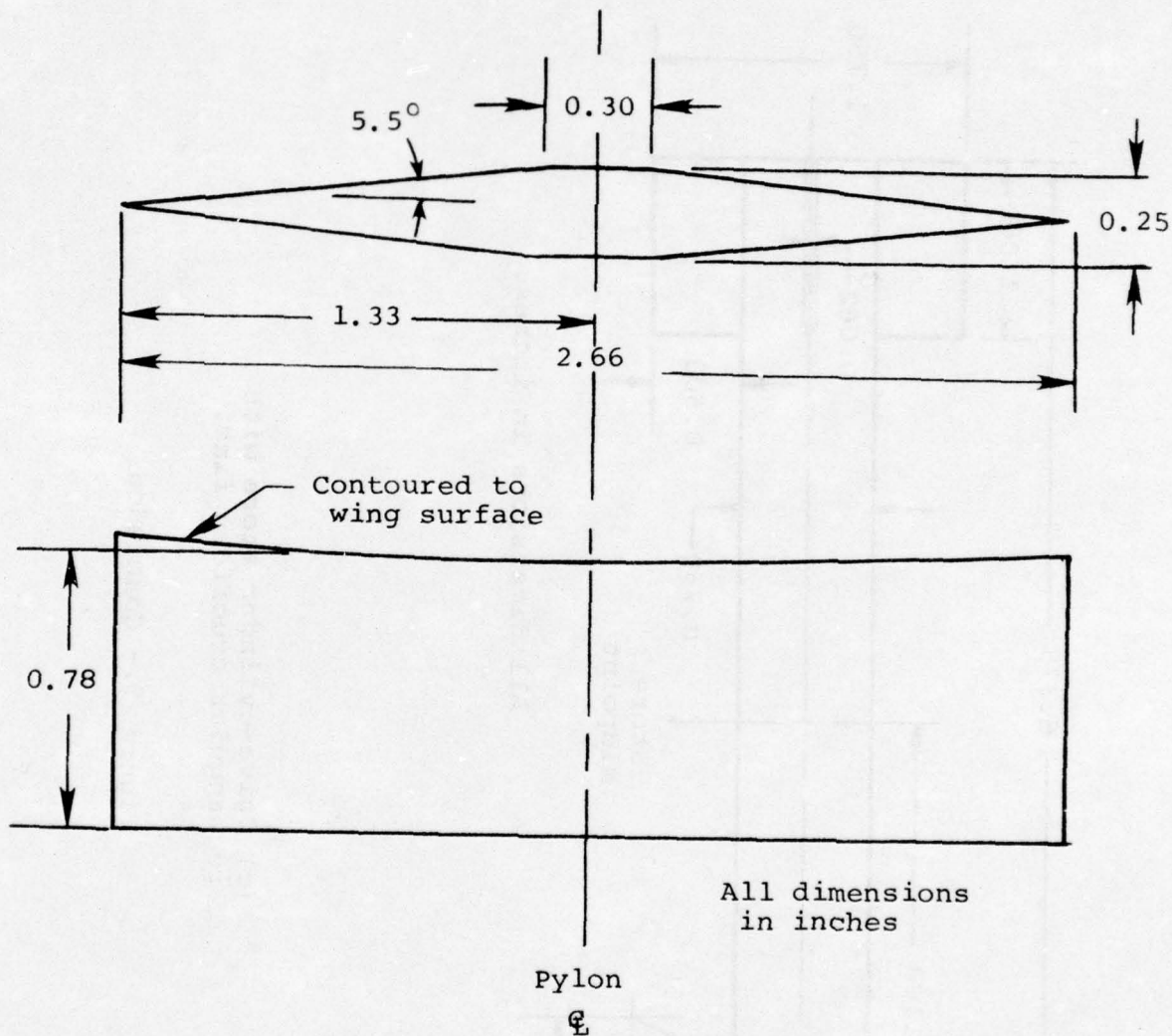
(b) Pylon under wing.

Figure 8.- Variables describing and locating pylon, input data item number 19.



(a) Wing-fuselage combination.

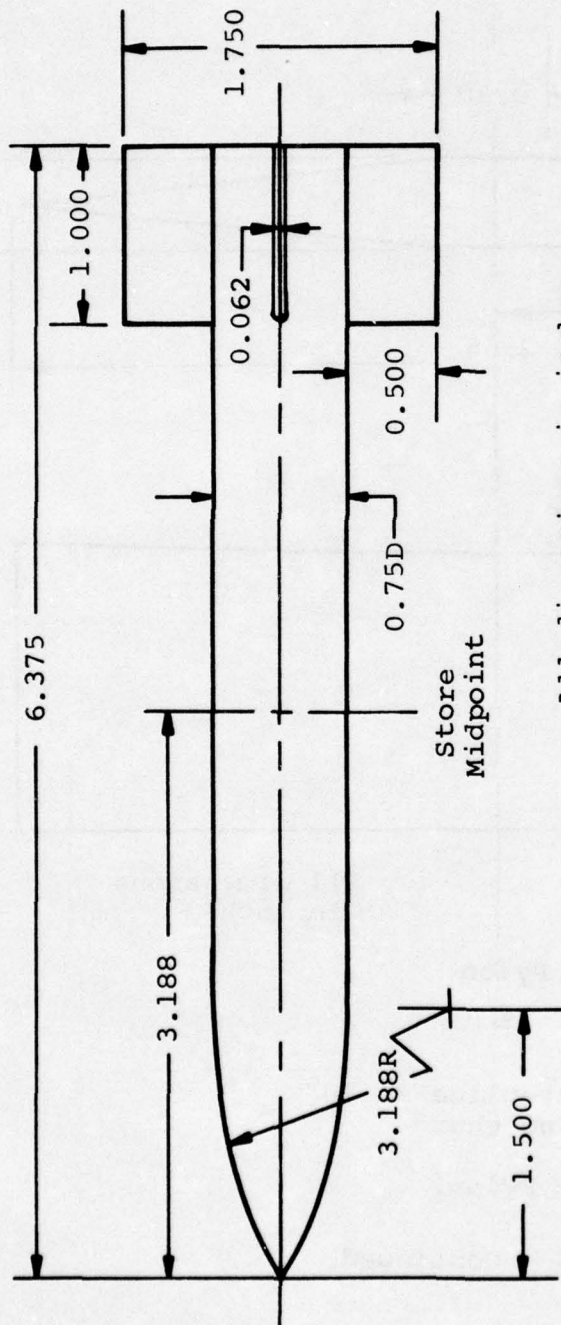
Figure 9.- Wind-tunnel models used in sample calculation.



Pylon centerline at 40°
of wing chord

(b) Pylon.

Figure 9.- Continued.



All dimensions in inches.

(c) Ogive-cylinder store with rectangular cruciform fins.

Figure 9.- Concluded.

										Item No.	
12										1	
SAMPLE TRAJECTORY CALCULATION											
AIRCRAFT AND STORE ARE SCALED UP VERSIONS OF MODELS USED IN EXPERIMENTAL											
PROGRAM CONDUCTED IN CONJUNCTION WITH THIS WORK											
MODELS SCALED UP BY A FACTOR OF 20 TO APPROXIMATE A FULL SCALE AIRCRAFT											
TRAJECTORY STARTS WITH THE STORE ONE RADIUS BELOW THE CARRIAGE POSITION											2
THE STORE FINS ARE ROLLED 45 DEGREES FROM THE VERTICAL AND HORIZONTAL											
THE AIRCRAFT IS DIVING AT A FLIGHT PATH ANGLE OF -30 DEGREES											
IT IS A FREE-FLIGHT TRAJECTORY											
ROLLING MOMENT IS CALCULATED											
AERODYNAMIC DAMPING IS INCLUDED											
THE STORE IS POWERED, THE THRUST STARTS AT T=0.0 SECONDS											
THE STORE HAS AN INITIAL DOWNWARD VELOCITY OF 10 FEET PER SECOND											
2.0	-30.0	1.5	0.0008907	1492.0						3	
1	1	0	1								4
60.85	2.78									5	
3										6	
0.32	0.7534	1.0								7	
-1.0975	-1.0	0.64	1.2045	0.0	0.0	1.0					
0.0457	0.0	0.0	0.0	0.0	0.0	0.0				8	
-1.9237	-1.0	1.5068	3.3109	0.0	0.0	1.0					
12	4	4	52							9	
13.91										10	
-25.62	0.0									11	
13.91	20.0									12	
12	8									13	
1	-2.78	0.0	0.0								
2	-4.725	48.6	30.75								
3	-6.667	48.6	30.75								
4	-8.888	48.6	30.75								
5	-11.112	48.6	30.75							14	
6	-13.333	48.6	30.75								
7	-15.555	48.6	30.75								
8	-17.778	48.6	30.75								
9	-20.000	48.6	30.75								
0										15	
20	1										17
0.209	0.109	0.077	0.057	0.043	0.029	0.017	0.006				
-0.005	-0.014	-0.024	-0.034	-0.044	-0.053	-0.061	-0.066			18	
-0.067	-0.067	-0.067	-0.067								
3	0.0	0.0	4.43	1.65	-2.51					19	
4	2										20
1	0.0										
2	0.825										21
3	1.85										
9	1										22
0.09629	0.09629	0.09629	0.09629	0.0	-0.09629	-0.09629	0.09629			23	
-0.09629											
10	2	10.625	0.625	0.59	-6.667	2.90	0.0			24	
1										25	
2	30										26
2										27	
0.2353	1.0										28
-0.4413	-1.0	0.4706	0.1947	0.0	0.0	1.0				29	
0.05882	0.0	0.0	0.0	0.0	0.0	0.0					
10	20	20	0	2	1	1	1			30	
15.53	16.0	400.0	400.0	0.0	0.0	0.0				31	
-7.4	0.0	0.0	0.0							32	
0.2353	1.0										33
-0.4413	-1.0	0.4706	0.1947	0.0	0.0	1.0				34	
0.05882	0.0	0.0	0.0	0.0	0.0	0.0					
0.65	0.0										35
0	5										36
-9.558	0.625	1.45833	45.0	3.491						37	
2										38	
0.2	1.0										39
1500.0	0.0	0.0	0.0	0.0	0.0					40	
1875.0	-1875.0	0.0	0.0	0.0	0.0						
0.0	0.0	10.0	0.0	0.0	0.0					41	
0.025	0.0	0.4								42	

Figure 11.- Input data deck for sample trajectory calculation.

SUPERBUNIC SIX-DEGREE-OF-FREEDOM TRAJECTORY PROGRAM

SAMPLE TRAJECTORY CALCULATION

AIRCRAFT AND STORE ARE SCALED UP VERSIONS OF MODELS USED IN EXPERIMENTAL PROGRAM CONDUCTED IN CONJUNCTION WITH THIS WORK
 MODELS SCALED UP BY A FACTOR OF 20 TO APPROXIMATE A FULL SCALE AIRCRAFT
 TRAJECTORY STARTS WITH THE STORE ONE RADIUS BELOW THE CARRIAGE POSITION
 THE STORE FINS ARE MOVED 45 DEGREES FROM THE VERTICAL AND HORIZONTAL
 THE AIRCRAFT IS DIVING AT A FLIGHT PATH ANGLE OF -30 DEGREES
 IT IS A FREE-FLIGHT TRAJECTORY
 ROLLING MOMENT IS CALCULATED
 AERODYNAMIC DAMPING IS INCLUDED
 THE STORE IS POWERED. THE THRUST STARTS AT 100.0 SECONDS
 THE STORE HAS AN INITIAL DOWNWARD VELOCITY OF 10 FEET PER SECOND

AIRCRAFT FLIGHT CONDITIONS

ANGLE OF ATTACK = 2.00 DEGREES
 FLIGHT PATH ANGLE = -30.00 DEGREES
 MACH NUMBER = 1.50
 FREE STREAM MASS DENSITY = .000907 SLUGS PER CUBIC FOOT
 FREE STREAM VELOCITY = 1492.00 FEET PER SECOND

FUSELAGE INPUT DATA

FUSELAGE LENGTH = 60.85000 FEET
 MAXIMUM RADIUS = 2.78000 FEET

POLYNOMIALS SPECIFYING FUSELAGE SHAPE

X/L OF END OF EACH SECTION

SECTION	X/L
1	.12000
2	.75360
3	1.00000

COEFFICIENTS OF POLYNOMIALS DESCRIBING EACH SECTION

SECTION	C1	C2	C3	C4	C5	C6	C7
1	-1.09750	-1.00000	.84000	1.20450	0.00000	0.00000	1.00000
2	.04570	0.00000	0.00000	0.00000	0.00000	0.00000	0.00000
3	-1.92370	-1.00000	1.50660	3.31090	0.00000	0.00000	1.00000

12 RINGS OF D-VELOCITY PANELS ARE TO BE LAID OUT ON THE FUSELAGE FROM X=0 FEET TO X=60.85 FEET
 THERE ARE 8 PANELS IN EACH RING ON THE LEFT HALF OF THE FUSELAGE, 4 ABOVE THE WING AND 4 BELOW THE WING
 TOTAL NUMBER OF PANELS IS 48

FUSELAGE SHAPE AS CALCULATED FROM THE INPUT POLYNOMIALS, ORIGINS OF SOURCES AND DOUBLETS REPRESENTING THE FUSELAGE, AND VALUES OF THE SOURCE AND DOUBLET CONSTANTS

BODY SHAPE				SINGULARITY		SOURCE		DOUBLET	
X, FT	R, FT	DR/DX	N	ORIGIN X(IN), FT	CONSTANTS K(IN)	CONSTANTS K(IN)	CONSTANTS K(IN)	CONSTANTS K(IN)	CONSTANTS K(IN)
0.00000	-0.00017	.29157	0	.00019	7.39679E-02	4.46090E-03			
1.17019	.32895	.27270	1	.80129	-1.35779E-02	-6.65444E-04			
2.34038	.63816	.25410	2	1.62690	-9.44987E-03	-2.94702E-04			
3.51058	.92874	.23574	3	2.47669	-9.91233E-03	-5.21890E-04			
4.68077	1.18997	.21761	4	3.35034	-9.07424E-03	-4.30348E-04			
5.85096	1.43410	.19967	5	4.24759	-8.58031E-03	-4.54834E-04			
7.02115	1.65735	.18192	6	5.16618	-8.02313E-03	-4.44529E-04			

(a) Page 1.

Figure 12.- Trajectory program output for sample case.

8.19135	1.85993	.16434	7	6.11188	-7.00932-03	-4.43262-04
9.36154	2.04202	.14690	8	7.07849	-6.95794-03	-4.38422-04
10.53173	2.20379	.12959	9	8.06782	-6.42446-03	-4.32971-04
11.70192	2.34537	.11240	10	9.07972	-5.88518-03	-4.25552-04
12.87212	2.46689	.09531	11	10.11405	-5.33609-03	-4.16071-04
14.04231	2.56845	.07829	12	11.17669	-4.77280-03	-4.03915-04
15.21250	2.65015	.06135	13	12.24954	-4.19089-03	-3.88484-04
16.38269	2.71205	.04445	14	13.35053	-3.58568-03	-3.69048-04
17.55288	2.75420	.02760	15	14.47359	-2.95229-03	-3.44739-04
18.72306	2.77665	.01077	16	15.61869	-2.28550-03	-3.14521-04
19.89327	2.78085	0.00000	17	16.78419	1.93781-02	-2.77311-05
21.06346	2.78085	0.00000	18	17.95438	4.95587-01	3.65240-04
22.23365	2.78085	0.00000	19	19.12457	3.24829-01	3.81268-04
23.40384	2.78085	0.00000	20	20.29477	1.62555-01	3.87400-04
24.57404	2.78085	0.00000	21	21.46496	1.31340-01	3.42922-04
25.74423	2.78085	0.00000	22	22.63515	9.09252-01	2.88421-04
26.91442	2.78085	0.00000	23	23.80534	6.52339-01	2.30360-04
28.08462	2.78085	0.00000	24	24.97554	4.77028-01	1.76141-04
29.25481	2.78085	0.00000	25	26.14573	3.25373-01	1.28657-04
30.42500	2.78085	0.00000	26	27.31592	2.86511-01	8.92176-05
31.59519	2.78085	0.00000	27	28.48611	2.05736-01	5.78490-05
32.76538	2.78085	0.00000	28	29.65631	1.59347-01	3.39141-05
33.93556	2.78085	0.00000	29	30.82650	1.24676-01	1.64161-05
35.10577	2.78085	0.00000	30	31.99669	9.84444-01	4.28052-06
36.27596	2.78085	0.00000	31	33.16688	7.83970-01	-2.71543-06
37.44615	2.78085	0.00000	32	34.33707	6.59182-01	-6.45400-06
38.61635	2.78085	0.00000	33	35.50727	5.08595-01	-1.08392-05
39.78654	2.78085	0.00000	34	36.67746	4.13905-01	-1.58261-05
40.95673	2.78085	0.00000	35	37.84765	3.38972-01	-1.12485-05
42.12692	2.78085	0.00000	36	39.01784	2.79314-01	-1.02651-05
43.29712	2.78085	0.00000	37	40.18804	2.31447-01	-8.48372-06
44.46731	2.78085	0.00000	38	41.35823	1.82816-01	-7.51646-06
45.63750	2.78085	0.00000	39	42.52842	1.40215-01	-2.51642-05
46.80769	2.77659	.00804	40	43.70337	9.81787-01	-2.51974-04
47.97788	2.76147	.01781	41	44.89047	-1.81966-01	-3.16028-04
49.14808	2.73492	.07584	42	46.09015	-1.71651-01	-2.93819-04
50.31827	2.69492	.05734	43	47.30302	9.17161-01	-2.51972-04
51.48846	2.64748	.04713	44	48.52849	7.16923-01	-1.94203-04
52.65865	2.58657	.03945	45	49.76678	4.65034-01	-1.24312-04
53.82885	2.51417	.06678	46	51.01791	9.33168-01	-6.04166-05
54.99904	2.43028	.07662	47	52.28190	1.37706-01	1.01154-05
56.16923	2.33486	.08646	48	53.55878	1.80666-01	8.08870-05
57.33942	2.22748	.09637	49	54.84858	2.23283-01	1.50817-04
58.50962	2.10931	.10628	50	56.15133	2.66003-01	2.18912-04
59.67981	1.97912	.11623	51	57.46708	3.09192-01	2.80005-04
60.85000	1.83726	.12621	52	58.79586	0.	0.

(b) Page 2.

Figure 12.- Continued.

WING INPUT DATA

LOCATION OF WING ROOT CHORD LEADING EDGE RELATIVE TO FUSELAGE NOSE
 XF = -25.02000 FEET
 ZF = 0.00000 FEET
 LENGTH OF WING ROOT CHORD
 CR = 13.91000 FEET
 WING SEMISPAN
 SSPAN = 20.00000 FEET

96 U-VELOCITY PANELS ARE TO BE LAID OUT ON EACH WING PANEL
 8 CHORDWISE ROWS WITH 12 IN EACH ROW

SPANWISE LOCATIONS OF PANEL SIDE EDGES AND SWEEP ANGLES OF
 WING SECTION TO THE RIGHT

I	SPANWISE LOCATION FEET	LE SWEEP DEGREES	TE SWEEP DEGREES
1	-2.78000	0.00000	0.00000
2	-4.72500	48.60000	30.75000
3	-6.66700	48.60000	30.75000
4	-8.60800	48.60000	30.75000
5	-11.11800	48.60000	30.75000
6	-13.33300	48.60000	30.75000
7	-15.55500	48.60000	30.75000
8	-17.77800	48.60000	30.75000
9	-20.00000	48.60000	30.75000

160 THICKNESS PANELS ARE TO BE LAID OUT ON EACH WING PANEL
 8 CHORDWISE ROWS WITH 20 IN EACH ROW
 THE CHORDWISE ROWS COINCIDE WITH THOSE USED
 FOR THE U-VELOCITY PANELS

(c) Page 3.

Figure 12.- Continued.

PYLON INPUT DATA

LEADING EDGE OF PYLON ROOT CHORD IS AT X = -2.51000 FEET (MEASURED FROM LOCAL XING LEADING EDGE)

SPANWISE LOCATION IS Y = 0.68700 FEET

ROOT CHORD = 0.43000 FEET

HEIGHT = 1.65000 FEET

LEADING EDGE SHEEP ANGLE = 0.00000 DEGREES

TRAILING EDGE SHEEP ANGLE = 0.00000 DEGREES

8 U-VELOCITY PANELS ARE TO BE LAID OUT ON THE PYLON

2 CHORDWISE ROWS WITH 4 IN EACH ROW

SPANWISE LOCATIONS OF PANEL SIDE EDGES

N	Z	FEET
1		0.00000
2		0.82500
3		1.65000

16 THICKNESS PANELS ARE TO BE LAID OUT ON THE PYLON

2 CHORDWISE ROWS WITH 9 IN EACH ROW

THE CHORDWISE ROWS COINCIDE WITH THOSE USED

FOR THE U-VELOCITY PANELS

(d) Page 4.

Figure 12.- Continued.

RING THICKNESS DATA		SLIPS			
ROW	NO	10000	07700	05700	02900
1	20800	01000	07700	05700	02900
	-00350	-01400	-02400	-03400	-05300
2	20500	00870	06700	04700	02500
	-00350	-01400	-02400	-03400	-05300
3	20600	00900	06700	04700	02500
	-00350	-01400	-02400	-03400	-05300
4	20800	01000	07700	05700	02900
	-00350	-01400	-02400	-03400	-05300
5	20900	00870	06700	04700	02500
	-00350	-01400	-02400	-03400	-05300
6	20800	01000	06700	04700	02500
	-00350	-01400	-02400	-03400	-05300
7	20900	00870	06700	04700	02500
	-00350	-01400	-02400	-03400	-05300
8	20900	01000	07700	05700	02900
	-00350	-01400	-02400	-03400	-05300

PYLON THICKNESS DATA		SLIPS			
ROW	NO	10000	09629	06629	040000
1	00629	00629	09629	06629	00629
	-09629	-09629	-09629	-09629	-09629
2	00629	00629	09629	06629	00629
	-09629	-09629	-09629	-09629	-09629

STORE INPUT DATA

STORE SHAPE NO	LENGTH FT	MAXIMUM RADIUS FT	STORE LOCATION RELATIVE TO LOCAL RING CHORD LEADING EDGE	INCIDENCE ANGLE DEG
NO	NO	FT	X, FT Y, FT Z, FT	DEG
10	2	10.62500	.62500 -6.66700 2.90000	0.00000

POLYNOMIALS SPECIFYING STORE SHAPE NO 2

SECTION	X/L	Y/L	Z/L
1	.23330		
2	1.00000		

COEFFICIENTS OF POLYNOMIALS DESCRIBING EACH SECTION

SECTION	C1	C2	C3	C4	C5	C6	C7
1	.44130	-1.00000	.47060	.19470	0.00000	0.00000	1.00000
2	.05882	0.00000	0.00000	0.00000	0.00000	0.00000	0.00000

STORE SHAPE 2 AS CALCULATED FROM THE INPUT POLYNOMIALS. ORIGINS OF SOURCES AND DOUBLETS REPRESENTING THE STORE, AND VALUES OF THE SOURCE AND DOUBLET CONSTANTS

BODY SHAPE			SINGULARITY ORIGIN		SOURCE CONSTANTS		DOUBLET CONSTANTS	
X, FT	R, FT	DR/DX	X(N), FT	K(N)	X(N), FT	K(N)	X(N), FT	K(N)
0.00000	.00055	.53326	0	.00061	2.22348E-01	1.12251E-02		
.35417	.17177	.44140	1	.16212	-9.18550E-02	-2.17962E-03		
.70833	.31317	.58620	2	.35820	-5.61088E-02	-1.65146E-03		
1.06250	.42622	.68105	3	.58597	-4.92491E-02	-2.08928E-03		
1.41667	.51276	.76848	4	.84338	-3.96957E-02	-2.06210E-03		
1.77083	.57411	.83856	5	1.12696	-3.26082E-02	-2.16444E-03		
2.12500	.61114	.90777	6	1.44173	-2.55567E-02	-2.26491E-03		
2.47917	.62435	.96393	7	1.78112	-1.90142E-02	-2.46161E-03		
2.83333	.62496	.00393	8	2.13460	-1.26155E-02	-7.58620E-05		
3.18750	.62496	0.00000	9	2.48877	3.22892E-03	8.21709E-04		
3.54167	.62496	0.00000	10	2.84294	5.33093E-03	8.92286E-04		
3.89583	.62496	0.00000	11	3.19710	2.18199E-03	6.33311E-04		
4.25000	.62496	0.00000	12	3.55127	1.55488E-03	4.69918E-04		
4.60417	.62496	0.00000	13	3.90544	9.48609E-04	4.97912E-04		
4.95833	.62496	0.00000	14	4.25960	6.39481E-04	3.41629E-04		
5.31250	.62496	0.00000	15	4.61377	4.32884E-04	2.16013E-04		
5.66667	.62496	0.00000	16	4.96794	3.01172E-04	1.22535E-04		
6.02083	.62496	0.00000	17	5.32210	2.13648E-04	5.76487E-05		
6.37500	.62496	0.00000	18	5.67627	1.54426E-04	1.66581E-05		
6.72917	.62496	0.00000	19	6.03044	1.13107E-04	-7.82336E-06		
7.08333	.62496	0.00000	20	6.38460	8.39571E-05	-1.90303E-05		
7.43750	.62496	0.00000	21	6.73877	6.31417E-05	-2.30202E-05		
7.79167	.62496	0.00000	22	7.09294	4.80195E-05	-2.24196E-05		
8.14583	.62496	0.00000	23	7.44710	3.69102E-05	-1.94792E-05		
8.50000	.62496	0.00000	24	7.80127	2.86546E-05	-1.56647E-05		
8.85417	.62496	0.00000	25	8.15544	2.24317E-05	-1.18494E-05		
9.20833	.62496	0.00000	26	8.50960	1.77495E-05	-8.88987E-06		
9.56250	.62496	0.00000	27	8.86377	1.41472E-05	-5.76490E-06		
9.91667	.62496	0.00000	28	9.21794	1.13843E-05	-3.70486E-06		
10.27083	.62496	0.00000	29	9.57210	9.19641E-06	-2.22647E-06		
10.62500	.62496	0.00000	30	9.92627	0.	0.		

(f) Page 6.

Figure 12.- Continued.

U-VELOCITY PANEL CONTROL POINT COORDINATES,
INTERFERENCE VELOCITIES INDUCED AT THESE POINTS,
INPUT TWIST AND CAMBER SLOPE AT THESE POINTS,
AND PANEL SINGULARITY STRENGTHS
(-ING COORDINATE SYSTEM)

ING CONTROL POINTS	ROM PANEL	X, FT	Y, FT	Z, FT	U/VINF	V/VINF	W/VINF	ALPHA	UPLUS/VINF
1	1	-2.1764	-3.76520	0.00000	-.01284	.00156	-.02072	0.00000	.05051
2	1	-2.20152	-3.76520	0.00000	-.01135	.00132	-.02047	0.00000	.03697
3	1	-2.40641	-3.76520	0.00000	-.01010	.00111	-.02025	0.00000	.02817
4	1	-5.52130	-3.76520	0.00000	-.00903	.00094	-.02005	0.00000	.02556
5	1	-6.3616	-3.76520	0.00000	-.00812	.00081	-.01987	0.00000	.02348
6	1	-7.75107	-3.76520	0.00000	-.00733	.00070	-.01973	0.00000	.02140
7	1	-8.6594	-3.76520	0.00000	-.00645	.00064	-.01940	0.00000	.02048
8	1	-9.6884	-3.76520	0.00000	-.00548	.00053	-.01730	0.00000	.02028
9	1	-11.09573	-3.76520	0.00000	-.00466	.00047	-.02220	0.00000	.00596
10	1	-12.21062	-3.76520	0.00000	-.04099	.03045	-.01615	0.00000	.00153
11	1	-13.32550	-3.76520	0.00000	-.04321	.04031	-.00670	0.00000	-.02611
12	1	-14.44039	-3.76520	0.00000	-.02438	.02519	-.01185	0.00000	-.00395
1	2	-4.29028	-5.70974	0.00000	-.01080	.00296	-.00932	0.00000	.07027
2	2	-5.32674	-5.70974	0.00000	-.00968	.00253	-.00917	0.00000	.04184
3	2	-6.35423	-5.70974	0.00000	-.00873	.00219	-.00904	0.00000	.01181
4	2	-7.38172	-5.70974	0.00000	-.00774	.00238	-.00532	0.00000	.0059
5	2	-8.40821	-5.70974	0.00000	-.00674	.0024	-.00538	0.00000	.00532
6	2	-9.43570	-5.70974	0.00000	-.00574	.0024	-.00538	0.00000	.00449
7	2	-10.46319	-5.70974	0.00000	-.00465	.00235	-.00704	0.00000	-.00610
8	2	-11.49068	-5.70974	0.00000	-.00362	.00230	.03927	0.00000	.03204
9	2	-12.51817	-5.70974	0.00000	-.00261	.01033	-.01654	0.00000	.02209
10	2	-13.54566	-5.70974	0.00000	-.01132	.00850	-.03752	0.00000	.03752
11	2	-14.57315	-5.70974	0.00000	-.00122	.00158	-.00341	0.00000	.01742
12	2	-15.60064	-5.70974	0.00000	-.00311	.00084	-.00751	0.00000	.00351
1	3	-6.57766	-7.79727	0.00000	-.00437	.00350	-.00518	0.00000	.06320
2	3	-7.51162	-7.79727	0.00000	.04911	.02076	-.00659	0.00000	.11676
3	3	-8.44529	-7.79727	0.00000	.03356	.05510	-.03101	0.00000	.05754
4	3	-9.37898	-7.79727	0.00000	-.00213	.02866	-.01139	0.00000	.03229
5	3	-10.31262	-7.79727	0.00000	-.04191	.02016	-.00363	0.00000	.02504
6	3	-11.24629	-7.79727	0.00000	-.07456	.06198	-.03640	0.00000	.02268
7	3	-12.17995	-7.79727	0.00000	-.04007	.04235	-.0246	0.00000	-.00103
8	3	-13.11362	-7.79727	0.00000	-.03519	.01105	-.00824	0.00000	.03476
9	3	-14.04728	-7.79727	0.00000	-.00245	.00089	-.00671	0.00000	.02761
10	3	-14.98095	-7.79727	0.00000	-.00231	.00096	-.00425	0.00000	.02850
11	3	-15.91461	-7.79727	0.00000	-.00346	.00161	-.00372	0.00000	.02187
12	3	-16.84828	-7.79727	0.00000	-.00377	.00179	-.00356	0.00000	.01723
1	4	-9.00664	-10.02220	0.00000	.04135	.03862	-.04032	0.00000	.14066
2	4	-9.84031	-10.02220	0.00000	.01440	.01830	-.02889	0.00000	.08959
3	4	-10.67397	-10.02220	0.00000	.01937	.03358	-.04000	0.00000	.02666
4	4	-11.50764	-10.02220	0.00000	.00487	.01118	-.00528	0.00000	.04312
5	4	-12.34131	-10.02220	0.00000	.00151	.01365	-.00562	0.00000	.03759
6	4	-13.17497	-10.02220	0.00000	-.07239	.07041	-.00804	0.00000	.00551
7	4	-14.00864	-10.02220	0.00000	-.03557	.03522	-.00574	0.00000	.00399
8	4	-14.84230	-10.02220	0.00000	-.02445	.02607	-.00316	0.00000	.01384
9	4	-15.67597	-10.02220	0.00000	.00874	.01083	-.00647	0.00000	.03331
10	4	-16.50964	-10.02220	0.00000	-.00129	.00082	-.00352	0.00000	.02815
11	4	-17.34330	-10.02220	0.00000	-.00303	.00093	-.00308	0.00000	.02915
12	4	-18.17697	-10.02220	0.00000	-.00351	.00147	-.00294	0.00000	.0221
1	5	-11.43500	-12.24764	0.00000	-.03424	.03691	-.02485	0.00000	.15930
2	5	-11.6954	-12.24764	0.00000	-.00059	.00552	-.00746	0.00000	.07403

(g) Page 7.

Figure 12.- Continued.

8	-9.21538	-2.67419	-53193	-01454	.01313	.02999
8	-9.21538	-2.26707	-1.51481	-.00401	-.00055	.02386
8	-9.21538	-1.51481	-2.26707	-.00166	-.00805	.00429
8	-9.21538	-53193	-2.67419	-.00047	-.01154	.00444
8	-9.21538	-53193	2.67419	-.00047	.01154	.01714
8	-9.21538	-1.51481	2.26707	-.00166	.00805	.02161
8	-9.21538	-2.26707	1.51481	.05046	.01672	-.05261
8	-9.21538	-2.67419	53193	.03283	.04133	-.05874
8	-10.37484	-2.67419	-53193	.00826	-.00973	-.00380
8	-10.37484	-2.26707	-1.51481	-.00835	.00625	.01469
8	-10.37484	-1.51481	-2.26707	-.00359	-.00268	.01442
8	-10.37484	-53193	-2.67419	-.00118	-.00640	.00970
8	-10.37484	-53193	2.67419	-.00118	.00640	-.02453
8	-10.37484	-1.51481	2.26707	.04073	.00324	-.04687
8	-10.37484	-2.26707	1.51481	.00087	.01021	-.01597
8	-10.37484	-2.67419	53193	-.01569	-.02533	-.00552
10	-11.53371	-2.67419	-53193	-.01200	.02336	.01296
10	-11.53371	-2.26707	-1.51481	.01403	-.01505	.00663
10	-11.53371	-1.51481	-2.26707	-.00593	.00334	.00916
10	-11.53371	-53193	-2.67419	-.00161	-.00143	.01457
10	-11.53371	-53193	2.67419	.03561	.00036	-.04071
10	-11.53371	-1.51481	2.26707	-.01891	.00281	-.00434
10	-11.53371	-2.26707	1.51481	-.02138	.01075	-.00128
10	-11.53371	-2.67419	53193	.02340	-.02740	-.02240
11	-12.69288	-2.67419	-53193	-.02807	.02309	.00370
11	-12.69288	-2.26707	-1.51481	.00094	.01225	.00630
11	-12.69288	-1.51481	-2.26707	-.00708	.01632	.01241
11	-12.69288	-53193	-2.67419	-.00241	.00449	-.00482
11	-12.69288	-53193	2.67419	-.01652	.00480	-.01936
11	-12.69288	-1.51481	2.26707	.01423	.00935	-.02583
11	-12.69288	-2.26707	1.51481	-.00099	.01391	-.01782
11	-12.69288	-2.67419	53193	.02294	-.02653	.04015
12	-13.85204	-2.67419	-53193	-.06787	.03731	.05075
12	-13.85204	-2.26707	-1.51481	-.00846	.01642	.00917
12	-13.85204	-1.51481	-2.26707	.00490	.00868	-.01379
12	-13.85204	-53193	-2.67419	.02083	.01177	-.00396
12	-13.85204	-53193	2.67419	-.00884	-.01076	-.01815
12	-13.85204	-1.51481	2.26707	.00505	.00963	-.01508
12	-13.85204	-2.26707	1.51481	-.04118	-.02249	-.03694
12	-13.85204	-2.67419	53193	-.15399	-.02550	.10017

(j) Page 10.

Figure 12.- Continued.

STORE NUMBER 10 IS THE STORE EJECTED

ADDITIONAL INPUT FOR THIS STORE

STORE MASS = 15,53000 SLUGS

MOMENTS AND PRODUCTS OF INERTIA, SLUG - SQ FT

IXX = 16.00000

IYY = 400.00000

IZZ = 400.00000

IYZ = 0.00000

IYX = 0.00000

IYZ = 0.00000

IXY = 0.00000

STORE MOMENT CENTER IS -7.40000 FEET BEHIND NOSE

STORE CENTER OF GRAVITY OFFSET FROM MOMENT CENTER, FEET

XBAR = 0.00000

YBAR = 0.00000

ZBAR = 0.00000

POLYNOMIALS SPECIFYING STORE SHAPE

X/L OF END OF EACH SECTION

SECTION	X/L	C1	C2	C3	C4	C5	C6	C7
1	.23510							
2	1.00000							
COEFFICIENTS OF POLYNOMIALS DESCRIBING EACH SECTION								
SECTION	C1	C2	C3	C4	C5	C6	C7	
1	-.44130	-1.00000	.47060	.19470	0.00000	0.00000	1.00000	
2	.05882	0.00000	0.00000	0.00000	0.00000	0.00000	0.00000	

SEPARATION ASSUMED 10.62500 FEET FROM NOSE

AXIAL-FORCE COEFFICIENT IS .05000

CROSSFLOW-DRAG COEFFICIENT IS 0.00000

THIS STORE HAS A CRUCIFORM PENNAGE

THE EMPENNAGE FORCES ACT -9.55000 FEET BEHIND NOSE

THE AVERAGE BODY RADIUS IN THE EMPENNAGE REGION IS .62500 FEET

THE TAIL FIN SPAN MEASURED FROM THE BODY AXIS IS 1.45833 FEET

THE FINS ARE INITIALLY ROLLED 45.00 DEGREES FROM THE VERTICAL AND HORIZONTAL

THE FIN LIST-CURVE SLOPE IS 3.49100 PER RADIAN

POLYNOMIALS SPECIFYING STORE THRUST TIME HISTORY

TIME AT END OF EACH POLYNOMIAL

POLYNOMIAL	TIME, SEC	C1	C2	C3	C4	C5	C6	C7
1	.20000							
2	1.00000							
COEFFICIENTS OF POLYNOMIALS								
POLYNOMIAL	C1	C2	C3	C4	C5	C6	C7	
1	1500.000	0.000	0.000	0.000	0.000	0.000	0.000	
2	1875.000	-1875.000	0.000	0.000	0.000	0.000	0.000	

(k) Page 11.

Figure 12.- Continued.

TIME = 0.00000 SECONDS

FORCE AND MOMENT COEFFICIENTS

	CX	CY	CLM	CLN	CLL
BUOYANCY	.07250	.11984	-.25975	-.51491	
SLINDER BODY	.09273	.04026	-.13025	-.06018	
CROSSFLOW	0.00000	0.00000	0.00000	0.00000	
EXPERIENCE	.43352	.05682	-.74843	-.09809	
TOTAL	.54675	.21696	-1.13843	-.15664	
				-.02310	
				-.02310	

STORE THRUST IS 1500.000 POUNDS

LOAD AND VELOCITY DISTRIBUTIONS

X, FT	XVL	DCN/DX	DCV/DX	U/VX	V/VX	W/VX
.26563	.02500	.02934	-.00100	1.01149	.00043	.04791
.79658	.07500	-.06973	-.26354	1.00346	-.00601	.04412
1.32813	.12500	-.05286	-.00477	.90960	-.07967	.01963
1.85938	.17500	-.04784	.05866	.91896	-.06260	.02507
2.39063	.22500	-.02361	.09412	.92761	-.04802	.02861
2.92188	.27500	-.00733	.08440	.93577	-.03573	.03041
3.45313	.32500	.00419	-.06923	.94349	-.02555	.03060
3.98438	.37500	.01461	.05546	.95075	-.01729	.02933
4.51563	.42500	-.12069	.04333	.95325	-.01077	.03168
5.04688	.47500	-.06162	.03293	.94304	-.00572	.04936
5.57813	.52500	-.02121	.02625	.94370	-.00193	.05425
6.10938	.57500	.03181	.02311	.94659	.00141	.05556
6.64063	.62500	.29236	.01672	.94423	.00401	.02652
7.17188	.67500	.33799	.01839	1.00691	.00632	.01543
7.70313	.72500	.19874	.01377	1.03063	.00867	.04679
8.23438	.77500	.08349	-.00207	1.04457	.00936	.07029
8.76563	.82500	-.10553	-.00693	1.04157	.00661	.07424
9.29688	.87500	-.11120	-.00845	1.01285	.00761	.04623
9.82813	.92500	-.03192	-.00653	1.00501	.00852	.03871
10.35938	.97500	-.00613	-.00183	1.00254	.00597	.03640

LOCATION OF STORE IN FUSELAGE COORDINATE SYSTEM, DIMENSIONS OF FEET

RELATIVE TO FUSELAGE NOSE	RELATIVE TO INITIAL POSITION		
	DEL XF	DEL YF	DEL ZF
NOSE	-29.81894	-6.66700	2.90000
XCM	-36.83884	-6.66700	2.90000
BASE	-40.86394	-6.66700	2.90000

TRANSLATIONAL VELOCITIES AND ACCELERATIONS OF STORE IN FUSELAGE COORDINATE SYSTEM

	RELATIVE TO FUSELAGE MOTION	DEL XF	DEL YF	DEL ZF
DXF	0.00000	0.00000	0.00000	0.00000
DYF	0.00000	0.00000	0.00000	0.00000
DZF	0.00000	0.00000	0.00000	0.00000

ROTATIONAL VELOCITIES AND ACCELERATIONS OF STORE IN STORE COORDINATE SYSTEM

	DEL X	DEL Y	DEL Z
W	0.00000	0.00000	0.00000
P	0.00000	0.00000	0.00000
R	0.00000	0.00000	0.00000

STORE ANGULAR ORIENTATION IN FUSELAGE COORDINATE SYSTEM AND RATES OF CHANGE OF THESE ANGLES

	DEL X	DEL Y	DEL Z
PSI	0.00000	0.00000	0.00000
THETA	0.00000	0.00000	0.00000
DPHI	0.00000	0.00000	0.00000

Figure 12.- Continued.

TIME = .20000 SECONDS

FORCE AND MOMENT COEFFICIENTS

	CN	CT	CLP	CLN	CLL
BUOYANCY	-.06191	-.00457		-.20215	
SLENDER BODY	-.16233	-.04355	-.102266	-.37721	
CROSSFLOW	0.00000	0.00000	0.00000	0.00000	
EMPELLAGE	-.09438	-.16287	1.54405	-.28117	.00219
TOTAL	-1.11862	-.21999	.00211	-.29816	.00219

STORE THRUST IS 1500.000 POUNDS

LOAD AND VELOCITY DISTRIBUTIONS

X, FT	X/L	DCN/RX	DCY/RX	UVX	UVS	WVS
.28563	.02500	-.03056	-.01049	1.01451	-.01656	-.04859
.79486	.07500	-.05998	-.02140	1.01396	-.01673	-.04896
1.32813	.12500	-.05958	-.02213	1.01253	-.01760	-.04984
1.85938	.17500	-.04069	-.01636	1.01190	-.01785	-.05027
2.39063	.22500	-.01062	-.00529	1.01085	-.01850	-.05098
2.92188	.27500	-.00417	-.00321	1.01030	-.01875	-.05141
3.45313	.32500	-.00900	-.00983	1.00941	-.01928	-.05204
3.98438	.37500	-.29197	-.30549	1.00578	-.02156	-.05339
4.51563	.42500	-.06617	-.04143	.94374	-.05814	-.09841
5.04688	.47500	-.05053	-.03776	.94220	-.05289	-.10414
5.57813	.52500	-.03605	-.03426	.94034	-.04810	-.10987
6.10938	.57500	-.02272	-.03091	.94001	-.04378	-.11376
6.64063	.62500	-.01056	-.02772	.94106	-.03989	-.11595
7.17188	.67500	-.00445	-.02469	.94334	-.03641	-.11660
7.70313	.72500	-.01830	-.02162	.94671	-.03332	-.11587
8.23438	.77500	-.08637	-.04141	.94296	-.03045	-.12134
8.76563	.82500	-.02687	-.01833	.93843	-.02762	-.12798
9.29688	.87500	-.00543	-.01771	.93909	-.02546	-.12991
9.82813	.92500	.15830	.01171	.94624	-.02326	-.12575
10.35938	.97500	.21766	.04834	.97966	-.02214	-.09628

LOCATION OF STORE IN FUSELAGE COORDINATE SYSTEM, DIMENSIONS OF FEET

	XF	YF	ZF	RELATIVE TO INITIAL POSITION
NOSE	-28.20105	-6.81485	5.81553	DEL XF DEL YF DEL ZF
XWOM	-35.50068	-6.66748	5.05791	1.23786 -1.4785 2.91553
BASE	-38.76810	-6.60325	4.72873	1.27825 -.00048 2.15791
				1.29584 .06375 1.82773

TRANSLATIONAL VELOCITIES AND ACCELERATIONS OF STORE IN FUSELAGE COORDINATE SYSTEM

	DXF	DYF	DZF	D2XF	D2YF	D2ZF
12.98350	-.57574	15.23875	64.02201	-14.87566	110.06979	

ROTATIONAL VELOCITIES AND ACCELERATIONS OF STORE IN STORE COORDINATE SYSTEM

	P	Q	R	POUT	WOOT	HOOT
-.04042	-.90265	-.24448	.21163	.01767	-1.18940	

STORE ANGULAR ORIENTATION IN FUSELAGE COORDINATE SYSTEM AND RATES OF CHANGE OF THESE ANGLES

	PSI	THETA	PHT	DPHI	DTMETHA	DPHPI
-1.14721	-5.87628	-.20446	-.24250	-.90353	-.01559	

(m) Page 13.

Figure 12.- Continued.

TIME = .40000 SECONDS

FORCE AND MOMENT COEFFICIENTS

	CN	CY	CLM	CLN	CLL
BUOYANCY	.03035	.02446	.11146	.06679	
SLENDER BODY	-.33540	-.12739	-.17277	-.07645	
CROSSFLOW	0.00000	0.00000	0.00000	0.00000	
EMERGENCE	-.11509	-.03545	1.99242	.75174	.00015
TOTAL	-.145914	-.55338	.37812	.16210	.00015

STORE THRUST IS 125,000 POUNDS

LOAD AND VELOCITY DISTRIBUTIONS

X, FT	X/L	DN/DX	DCY/DX	U/V/S	V/V/S	M/V/S
2.563	.02500	-.11373	-.04750	.96013	-.07654	-.18257
1.7988	.07500	-.21218	-.08724	.96320	-.07557	-.18123
1.37813	.12500	-.19891	-.08031	.96644	-.07449	-.17976
1.85936	.17500	-.11604	-.04432	.97021	-.07314	-.17797
2.39063	.22500	-.00940	.00110	.97313	-.07212	-.17661
2.92180	.27500	.01176	.00906	.97724	-.07054	-.17455
3.45313	.32500	.01951	.01219	.98092	-.06909	-.17270
3.98438	.37500	.01340	.01064	.98435	-.06771	-.17095
4.51563	.42500	.01071	.01184	.98824	-.06608	-.16992
5.04688	.47500	.01486	.01215	.99147	-.06470	-.16721
5.57813	.52500	.01374	.01144	.99537	-.06296	-.16510
6.10938	.57500	.01521	.01280	.99876	-.06140	-.16324
6.64063	.62500	.01348	.01155	1.00224	-.05975	-.16129
7.17188	.67500	.01312	.01076	1.00139	-.06003	-.16166
7.70313	.72500	-.00817	.00148	1.00004	-.06054	-.16232
8.23438	.77500	-.00599	.00473	.99869	-.06110	-.16303
8.76563	.82500	-.00364	-.00272	.99603	-.06132	-.16335
9.29688	.87500	-.00348	-.00259	.99677	-.06184	-.16401
9.82813	.92500	-.00367	-.00277	.99822	-.06203	-.16431
10.35938	.97500	-.00262	-.00186	.99519	-.06247	-.16488

LOCATION OF STORE IN FUSELAGE COORDINATE SYSTEM, DIMENSIONS OF FEET

	XF	YF	ZF	DEL XF	DEL YF	DEL ZF
NOSE	-24.80190	-7.87210	12.59828	4.61703	-1.20510	9.69028
XMGW	-31.98907	-7.38477	10.80499	4.84987	-.71777	8.00499
BASE	-35.12131	-7.17238	10.16903	4.94263	-.50538	7.26703

TRANSLATIONAL VELOCITIES AND ACCELERATIONS OF STORE IN FUSELAGE COORDINATE SYSTEM

	DXF	DYF	DZF	D2XF	D2YF	D2ZF
21.38756	-7.48757	43.36490	22.75717	-40.56573	139.27963	

ROTATIONAL VELOCITIES AND ACCELERATIONS OF STORE IN STORE COORDINATE SYSTEM

	P	Q	R	PDOT	QDOT	RDOT
	-.04648	-.39283	-.15702	.01439	1.49022	.61834

STORE ANGULAR ORIENTATION IN FUSELAGE COORDINATE SYSTEM AND RATES OF CHANGE OF THESE ANGLES

	THETA	PHI	DPSI	OTMETA	DPHI
	-3.87905	-13.22779	-.21302	-.19680	-.36321
					-.00999

(n) Page 14.

Figure 12.- Concluded.

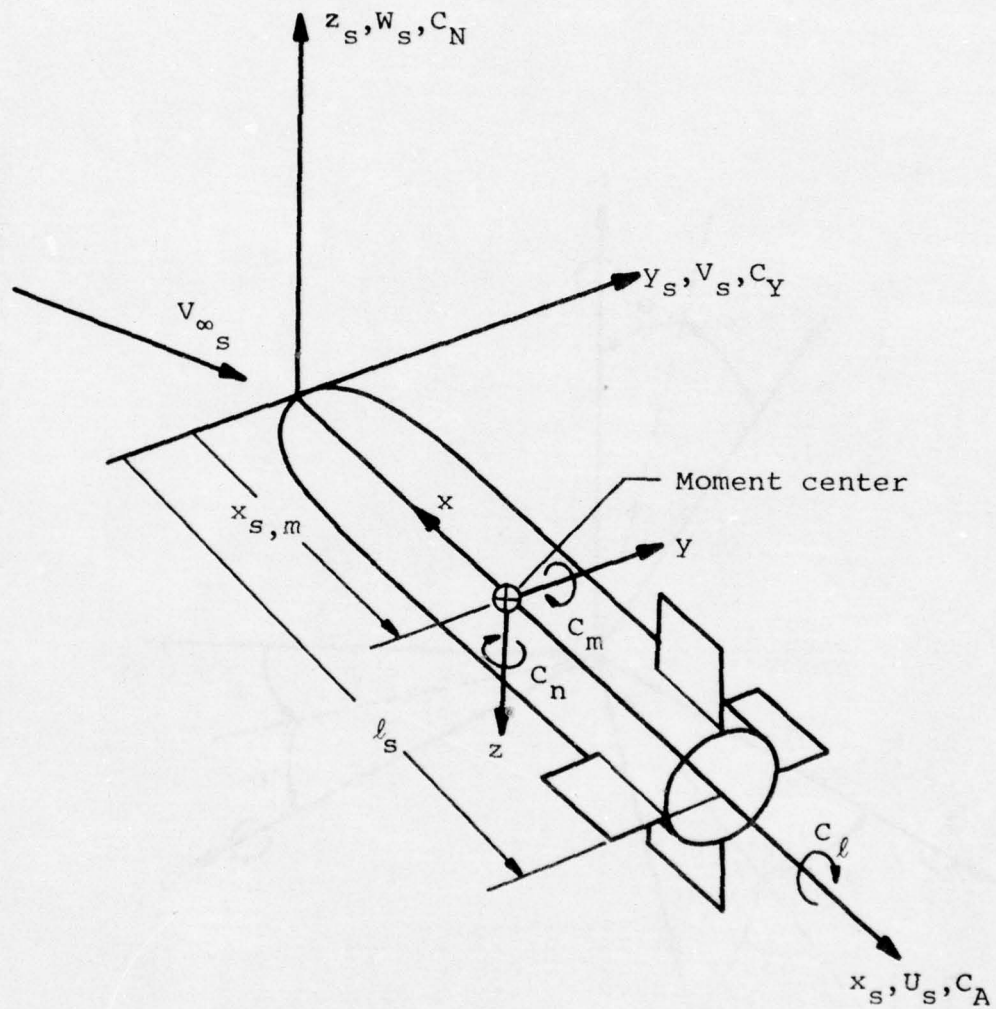


Figure 13.- Coordinate systems fixed in separated store and used in force and moment calculation.

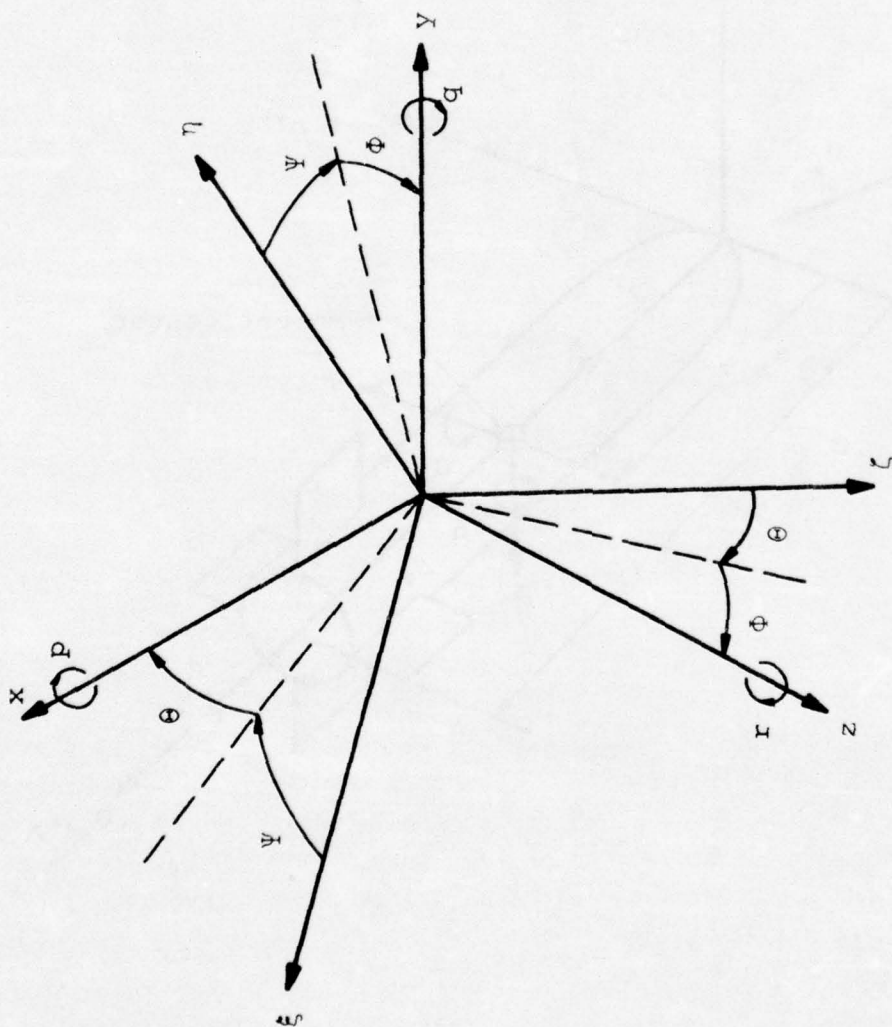


Figure 14.- Coordinate systems used in trajectory calculation.

APPENDIX I

DETAILS OF STORE SEPARATION TRAJECTORY PROGRAM

I-1. INTRODUCTION

The purpose of this appendix is to provide more detailed information on the store separation trajectory program which was described in section 2. A listing of the program was presented in figure 1 and a general flow chart in figure 2. This appendix will present a cross-reference chart showing the subroutines and the common statements contained in each, a schematic description of the subroutine calling sequence, more detailed flow charts, and tables equating the program notation to the algebraic notation. The program consists of a main program and 42 subroutines. The main program will first be described and then the subroutines will be described in alphabetical order. The subroutines and their functions were listed in Table I.

The cross-reference chart showing the subroutines and the common statements contained in each is presented in figure I-1. Across the top of the chart are the subroutine names including the main program SSTORE. Down the side of the page are the common names. The last one is blank common. The schematic showing the subroutine calling sequence is presented in figure I-2.

I-2. MAIN PROGRAM

The first two pages of the flow chart which was presented in figure 2 are quite complete and will therefore not be expanded in this appendix. Using those pages, the description in section 3.1, the input data discussion in section 3.2, and the dictionary of notation in Table I-1, there should be sufficient information to understand the flow of the program.

The last page of the flow chart of figure 2 has been expanded and is presented in figure I-3. This portion of the program begins with FORTRAN statement 62 of the main program (fig. 1(c)), and is the integration loop of the program. The first step in the loop is to call subroutine SFORCE to calculate the aerodynamic forces and moments acting on the store body. If the store has an empennage then subroutine SEMFOR is called to calculate the empennage forces and moments.

The next portion of the program solves for the translational and rotational accelerations. The set of six simultaneous equations which are solved are given in Appendix II of reference 4, equations (II-16) through (II-18) and (II-41) through (II-43). The coefficient matrix and right-hand side are stored in the FVN array. The first subscript of FVN is the equation number. The correspondence is

<u>Subscript Value</u>	<u>Equation Number</u>
1	II-16
2	II-17
3	II-18
4	II-41
5	II-42
6	II-43

The second subscript of FVN is the term in the equation. Here the correspondence is

<u>Subscript Value</u>	<u>Term</u>
1	$\ddot{\xi}$
2	$\ddot{\eta}$
3	$\ddot{\zeta}$
4	\dot{p}
5	\dot{q}
6	\dot{r}
7	Right-Hand Side

Thus, for example, FVN(3,5) is the coefficient of \dot{q} in equation (II-18). Certain parts of this section of the program are bypassed if the store center of gravity, c.g., lies on the store moment center. If this is the case, \bar{x}, \bar{y} and \bar{z} are zero and NASYM equals zero.

After calculating the coefficient matrix and right-hand side of the set of equations, subroutine INVERS is called to solve for the accelerations and the values are transferred to the DVAR array. The next steps of the program put the values of $\ddot{\xi}, \ddot{\eta}$, and $\ddot{\zeta}$ into the DVAR array and calculate the values of $\dot{\psi}, \dot{\theta}$, and $\dot{\phi}$, which are also put in the DVAR array. The DVAR array contains

DVAR(1)	$\ddot{\xi}$
DVAR(2)	$\ddot{\eta}$
DVAR(3)	$\ddot{\zeta}$
DVAR(4)	\dot{p}
DVAR(5)	\dot{q}
DVAR(6)	\dot{r}
DVAR(7)	$\dot{\xi}$
DVAR(8)	$\dot{\eta}$
DVAR(9)	$\dot{\zeta}$
DVAR(10)	$\dot{\psi}$
DVAR(11)	$\dot{\theta}$
DVAR(12)	$\dot{\phi}$

These are the derivatives of the twelve dependent variables.

The program next checks to see if the integration procedure has reached the end of an integration step. If it has $NOUT = 1$ and subroutine SOUTPT is called to print the output. Next a check is made to see if the end of the trajectory has been reached, that is, is the current value of the time equal to the final time which was input. If it is then the program transfers to the first input statement and attempts to read another set of input data. If the end has not been reached, then the integration routine, subroutine ADAMS, is called.

NDIFEQ is a control index used by subroutine ADAMS. If $NDIFEQ = 1$ upon returning to the main program, an error condition has been encountered in ADAMS, the calculation is to be terminated, and the next set of input data is to be read. If $2 \leq NDIFEQ \leq 7$, the program is at some intermediate point in the integration from one point to the next. When $NDIFEQ > 7$, the integration of one step has been completed and $NOUT$ is set equal to 1 so that the output subroutine will be called after the derivatives are calculated.

I-3. SUBROUTINE ADAMS

Subroutine ADAMS is the subroutine which integrates the set of differential equations. The subroutine will not be described in detail, however, an examination of the flow chart (fig. I-4) and the program listing (fig. 1(d)) will indicate how it functions. All returns from the subroutine are to the main program.

Consider the following set of n differential equations:

$$\begin{aligned}\dot{y}_1 &= f_1(t, y_1, y_2, \dots, y_n) \\ &\vdots \\ \dot{y}_n &= f_n(t, y_1, y_2, \dots, y_n)\end{aligned}$$

This subroutine uses a fourth-order Adams predictor-corrector method (ref. 10) to solve the above set of equations. To find the value of y_i at the $(j+4)^{\text{th}}$ step, the following formula is used to predict the value

$$y_{i,j+4}^{(p)} = y_{i,j+3} + \frac{h}{24} (55\dot{y}_{i,j+3} - 59\dot{y}_{i,j+2} + 37\dot{y}_{i,j+1} - 9\dot{y}_{i,j}) \quad (\text{I-1})$$

This assumes that all of the \dot{y}_i 's are known for the j , $(j+1)$, $(j+2)$, and $(j+3)$ steps. The quantity h is the interval in the independent variable between these points. After the values of the $y_{i,j+4}^{(p)}$ have been found, the following equation is used to obtain the corrected values:

$$y_{i,j+4} = y_{i,j+3} + \frac{h}{24} (9\dot{y}_{i,j+4}^{(p)} + 19\dot{y}_{i,j+3} - 5\dot{y}_{i,j+2} + \dot{y}_{i,j+1}) \quad (\text{I-2})$$

The use of the above equations requires that four evenly spaced values of the dependent variables be known. These are found in this subroutine by means of a fourth-order Runge-Kutta method (ref. 10). To find the values of the y_i 's at the $(j+1)^{\text{th}}$ step, the following equation is used:

$$y_{i,j+1} = y_{i,j} + \frac{1}{6} (k_{i,1} + 2k_{i,2} + 2k_{i,3} + k_{i,4}) \quad (\text{I-3})$$

where

$$\left. \begin{aligned}
k_{i,1} &= hf_i(t_j, x_{1,j}, x_{2,j}, \dots, x_{n,j}) \\
k_{i,2} &= hf_i(t_j + \frac{1}{2}h, x_{1,j} + \frac{1}{2}k_{1,1}, \dots, x_{n,j} + \frac{1}{2}k_{n,1}) \\
k_{i,3} &= hf_i(t_j + \frac{1}{2}h, x_{1,j} + \frac{1}{2}k_{1,2}, \dots, x_{n,j} + \frac{1}{2}k_{n,2}) \\
k_{i,4} &= hf_i(t_j + h, x_{1,j} + k_{1,3}, \dots, x_{n,j} + k_{n,3})
\end{aligned} \right\} \quad (I-4)$$

Thus, given initial values of the dependent variables, the y_i 's, the independent variable, t , and the integration interval size, h , the differential equations are integrated three steps using equations (I-3) and (I-4). At this point, the integration is continued using equations (I-1) and (I-2).

A discussion of both the Adams and Runge-Kutta methods is presented in reference 10. From this reference, the truncation error, Δy , at a given step can be shown to be

$$\Delta y = \left(\frac{y_{i,j+4} - y_{i,j+4}^{(p)}}{14.2} \right) \quad (I-5)$$

so that the absolute error is

$$\Delta y_{\text{ABS}} = |\Delta y|$$

and the relative error is

$$\Delta y_{\text{REL}} = \frac{\Delta y_{\text{ABS}}}{|y_{i,j+4}|} \quad (I-6)$$

At the end of each integration step, error tests could be performed and the integration interval, h , adjusted accordingly. This procedure is described in the flow chart (fig. I-4). In the present version of the program,

however, a fixed interval size is used and no attempt is made to satisfy error specifications.

The quantities in the parameter list are:

H	current value of the integration interval
DS	integration interval
Y	array containing current values of the dependent variables
DY	array containing current values of the derivatives of the dependent variables
NEQ	number of equations being integrated; routine dimensioned for a maximum of 12
NDIFEQ	control index
S	current value of independent variable

I-4. SUBROUTINE BDYGEN

Subroutine BDYGEN calculates the line source and doublet strengths using control points on the surface of the fuselage and store. The method used is described in Appendix I of reference 1. A listing of the subroutine is presented in figure 1(e), a flow chart in figure I-5, and a table equating the algebraic and program notation in Table I-2 of this report. The variables appearing in the subroutine parameter list are included in this table. The coordinate system associated with the subroutine is shown in the sketches of Appendix I of reference 1.

At the beginning of the subroutine a test is performed to determine if, at the base of the body, the radial distance to the Mach cone emanating from the body nose is less than the maximum radius of the body. If so, an error message is printed out (see section 4 of this report) and the program stops.

Next, as the flow chart indicates, N is set equal to NXBODY - 1 and the body axis is divided into N segments of equal length. The x locations of the body definition points, XBODY(J), are determined at these equally spaced axis points and, inside a short DO loop, subroutine SHAPE is called to calculate the radius of the body, RBODY, and the surface slope, RPBODY, at each body definition point. Subroutine SHAPE requires that the shape definition quantities be made dimensionless by body length. Subroutine BDYGEN accounts for this before and after the

calls to subroutine SHAPE. Next, the control points are located effectively midway between the body definition points. Subroutine SHAPE calculates the body radius, RF, and the surface slope, DRDX, at each control point. Finally, the axis points, TX, which are the origins of the conical line sources and doublets, are determined.

The next section of the subroutine is a routine for dropping control points that are located outside the Mach cone emanating from the body nose. The routine is a loop in which the first control point is tested. If it is found to be outside the Mach cone, the second body definition point is dropped and a new first control point is determined as described above. The remaining control points and conical line source and doublet origins are redefined so that the second point of each set is dropped. The loop is repeated until a control point is found within the nose Mach cone.

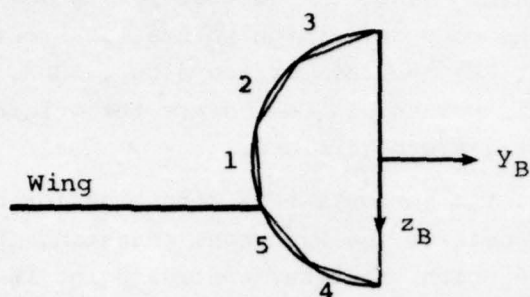
The remainder of the subroutine calculates the source and doublet strengths at the control points. Subroutine SOURCE is called and the source strength at the first control point is calculated using equation (I-14) and at the remaining control points using equation (I-17) of reference 1. One should note that the I^{th} source strength, $T(I)$, is the constant K_{I-1} in the algebraic notation of the equations. Similarly, using subroutine DOBLT, the doublet strengths are calculated using equation (I-27) for the first control point and equation (I-28) for the remaining control points. Here, the I^{th} doublet strength, $TC(I)$, equals $K_{d,I-1}$.

After calculating the source and doublet strengths, the subroutine prints the body definition point data, the singularity origins, and the singularity strengths.

I-5. SUBROUTINE BLYOUT

Subroutine BLYOUT calculates quantities needed to define the constant u-velocity panels on the fuselage and to locate the panel control points. The corner and control point coordinates calculated for the body panels are stored in arrays in locations which follow the same quantities calculated for the wing and pylon constant u-velocity panels. All coordinates are in the wing coordinate system which is shown in figure 6 of this report. A listing of the subroutine is presented in figure 1(f), a flow chart in figure I-6, and a table equating algebraic and program notations in Table I-3.

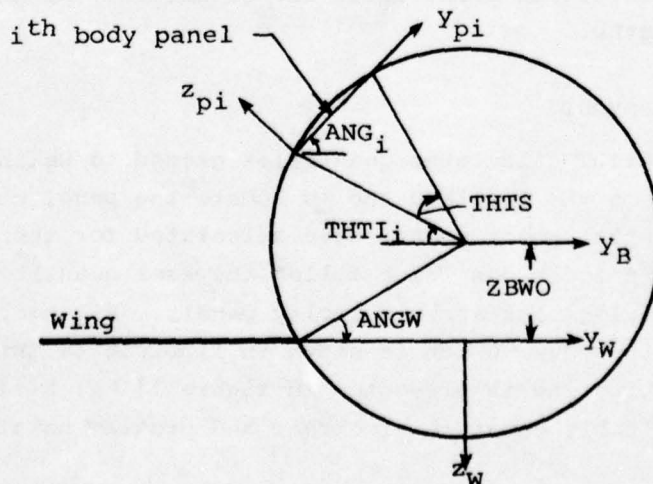
The fuselage interference panels are laid out on the left-half of the fuselage surface, as shown in figure 4. The panel numbering convention employed in a typical ring containing five panels, three above the wing and two below, is shown in the following sketch.



At the beginning of the subroutine quantities DX , NBD , $NBIP$, and $ANGW$, associated with the geometry of the entire panel layout, are calculated. Next, the variable $ANGW$ is tested to determine if the wing is tangent to the fuselage, either at the top or at the bottom. As the flow chart shows, this tangency condition determines the initialization procedure performed before the main loop calculations.

The main part of the subroutine is a double DO loop with the outer loop index running over the rows above or below the wing and the inner loop index over the $NCWB$ panels in a lengthwise row. If the wing is not tangent, this double loop is performed first for the panels above the wing, then repeated for the panels below the wing.

For a given lengthwise row the y, z coordinates of the panel corners and the control points are first obtained in the panel coordinate system. The following sketch shows the coordinate system and certain quantities associated with a panel located above the wing.



Within the inner DO loop the coordinates are transformed into the wing coordinate system and stored in appropriate array locations. Polar angle, THTI and quantities SNT2 and CST2 , necessary for panel-wing transformations, are saved in arrays for subsequent use by other routines. The corner and control point x_w coordinates are calculated and stored; no transformations are necessary for these quantities.

The convention employed in labeling the corner coordinates for the fuselage interference panels is that the right side of the panel is located in clockwise rotation from the left side, when looking forward.

I-6. SUBROUTINE CEL1

Subroutine CEL1 calculates the complete elliptic integral of the first kind. This subroutine has been taken directly from reference 11. For a description of the routine that reference should be consulted. A listing of the routine is presented in figure 1(g). The comment cards give a brief explanation of the use of the routine.

I-7. SUBROUTINE CEL2

Subroutine CEL2 calculates the complete elliptic integral of the second kind. This subroutine has been taken directly from reference 11. For a description of the routine that reference should be consulted. A listing of the routine is presented in figure 1(g). The comment cards give a brief explanation of the use of the routine.

I-8. SUBROUTINE DIRCOS

Subroutine DIRCOS computes the direction cosines which relate the store body coordinate system to the inertial coordinate system. The direction cosines are given by equation (28) of reference 4. A listing of the routine is presented in figure 1(h). The three angles Ψ, θ , and Φ are brought into the subroutine in $A(10)$, $A(11)$, and $A(12)$, respectively, and the direction cosines are returned in the D array.

I-9. SUBROUTINE DOUBLT

Subroutine DOUBLT calculates coefficients used in the determination of the line doublet strengths. They occur as terms in equations (I-27) and (I-28) of reference 1. The relation of the coefficients to perturbation velocities, $u_{B,d}/V_\infty$ and $v_{B,d}/V_\infty$, induced by a number of line doublets

distributed along the body centerline is shown in the first two of equation (I-30) in which the coefficients occur as the multipliers of $K_{d,n} \cos \theta$. A listing of the subroutine is presented in figure 1(h) of this report. The subroutine is called by subroutine BDYGEN and section I-4 should be referred to for further details concerning the doublet strength calculations.

For a specified control point, x_B , r_B , and singularity origin ξ , the subroutine calculates quantities U and V according to the following equations:

$$U = \beta \sqrt{\left(\frac{x_B - \xi}{\beta r_B}\right)^2 - 1}$$

$$V = -\frac{\beta^2}{2} \left[\cosh^{-1}\left(\frac{x_B - \xi}{\beta r_B}\right) + \left(\frac{x_B - \xi}{\beta r_B}\right) \sqrt{\left(\frac{x_B - \xi}{\beta r_B}\right)^2 - 1} \right]$$

At the beginning of the subroutine a test is performed to determine if the control point is ahead of the Mach cone from the doublet origin. If so, U and V are set to zero and control is returned to the calling program.

The following table of definitions contains most of the variable names used in the subroutine:

BETA	$\beta = \sqrt{M_\infty^2 - 1}$
RFIELD	r_B ; radius of body at control point
TX	ξ ; location on body axis of doublet origin, positive measured from tip of nose
U	coefficient defined by first equation above
V	coefficient defined by second equation above
XFIELD	x_B ; x location of control point, positive measured from tip of nose

I-10. SUBROUTINE DPCOEF

Subroutine DPCOEF calculates the coefficient matrix of the set of simultaneous boundary condition equations which are to be solved for the constant u-velocity panel singularity strengths. A listing of the

subroutine is presented in figure 1(h), a flow chart in figure I-7, and a table equating the algebraic and program notation in Table I-4 of this report.

The elements of the matrix are the aerodynamic influence coefficients described in section 3.3.4 of reference 1. They occur indirectly in the summation terms in the left-hand side of equations (9), (10), and (11) of that reference. The actual coefficients which the subroutine calculates, $FVN(v,n)$, are related to the summation terms through the panel strengths, u_{+n}/V_∞ , by the following equations in which n is the index of the influencing panel and v is the control point index:

$$\frac{w_w^{v,n}}{V_\infty} = \frac{u_{+n}}{\pi V_\infty} FVN(v,n) \quad v = 1, 2, \dots, N_{PANLS},$$

$$\frac{-w_w^{v,n}}{V_\infty} = \frac{u_{+n}}{\pi V_\infty} FVN(v,n) \quad v = N1P, N1P+1, \dots, N2,$$

$$\frac{w_N^{v,n}}{V_\infty} = \frac{u_{+n}}{\pi V_\infty} FVN(v,n) \quad v = N2P, N2P+1, \dots, NPTOT,$$

for $n = 1, 2, \dots, NPTOT$.

The subroutine consists of three double DO loops. The first loop uses subroutine VELWP to calculate the influence of the wing panels at the wing, pylon, and fuselage control points. The second loop is bypassed if there is no pylon, $NPY = 0$. If a pylon is present, the influence coefficients for the pylon panels are calculated by means of subroutine VELPP. The third double loop is bypassed if there is no fuselage, $NFU = 0$. Otherwise, the influence coefficients for the fuselage panels are calculated using subroutine VELBD.

Within each outer loop are three inner loops in series, which fix the control point location on the wing, pylon, or fuselage, respectively. On the flow chart, only the first occurrence of the first inner loop is shown in detail, which includes the call to subroutine VELWP. The remaining inner loops have the same logical structure and are not shown. If the

control point is on a fuselage panel, the influence coefficient is the component normal to the body surface at the control point. This is obtained by a rotation through the panel orientation angle using quantities calculated previously in subroutine BLYOUT.

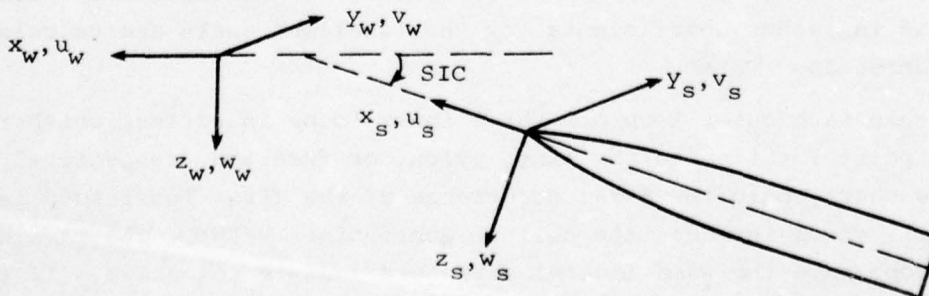
I-11. SUBROUTINE DPRHS

Subroutine DPRHS calculates the right-hand-side vector of the set of simultaneous boundary condition equations which are to be solved in order to determine the constant u-velocity panel singularity strengths. The boundary conditions are specified in equations (9), (10), and (11) of reference 1. A listing of the subroutine is presented in figure 1(i), a flow chart in figure I-8, and a table equating the algebraic and program notation in Table I-5 of this report.

The major portion of the subroutine is devoted to evaluating the externally induced perturbation velocities, $u_{w_i, v}/V_\infty$, $v_{w_i, v}/V_\infty$, and $w_{w_i, v}/V_\infty$, at all of the wing, pylon, and fuselage control points.

The first section calculates velocities induced at wing and pylon control points by the fuselage line sources, sinks, and line doublets if a fuselage is present ($NFU \neq 0$). A control point is located in the fuselage coordinate system (see figure 5) and subroutine VELCAL is called to calculate the velocities at this point. These velocities are summed in the UEI, VEI, and WEI arrays.

The perturbation velocities induced by the store are calculated next in a double DO loop. (The subroutine has been written to accommodate multiple stores although in the present program the number of stores is limited to one.) The velocities induced at the fuselage control points are included in these calculations. A control point is first located in the store coordinate system shown in the sketch below.



Subroutine VELCAL then computes the perturbation velocities which are resolved into the wing system and added to the appropriate array.

If a pylon is present, $NPY \neq 0$, its thickness distribution produces perturbation velocities at the wing control points. Subroutine VELPTH is called for the purpose of calculating these velocities which are added to the UEI, VEI, and WEI arrays. Similarly, subroutine VELWTH is called to calculate the wing thickness perturbation velocities at the pylon control points. Following this, each subroutine is called a second time to compute velocities at the fuselage control points if a fuselage is present.

The last three loops in the subroutine calculate the right-hand sides of equations (9), (10), and (11). If the pylon is located below the fuselage centerline, $CENTER = TRUE$, VEI is set to zero for all pylon control points.

It should be noted that for a fuselage control point the perturbation velocity normal to the fuselage surface at the control point is used for the right-hand side.

I-12. SUBROUTINE ELI1

Subroutine ELI1 calculates the general elliptic integral of the first kind. This subroutine has been taken directly from reference 11. For a description of the routine that reference should be consulted. A listing of the routine is presented in figure 1(j). The comment cards give a brief explanation of the use of the routine.

I-13. SUBROUTINE ELI2

Subroutine ELI2 calculates the general elliptic integral of the second kind. This subroutine has been taken directly from reference 11. For a description of the routine that reference should be consulted. A listing of the routine is presented in figure 1(k). The comment cards give a brief explanation of the use of the routine.

I-14. SUBROUTINE FLSQFY

Subroutine FLSQFY performs a weighted least square orthogonal polynomial curve fit of a set of x, y data. The routine is based on reference 12. A listing of the subroutine is presented in figure 1(l) of this report.

Given a set of points (x_i, y_i) , $i = 1, 2, \dots, M$ and corresponding positive weights w_i , there exist orthogonal polynomials $P_r(x)$ of degree r , $r = 0, 1, \dots, M-1$, and coefficients C_0, C_1, \dots, C_N such that, for any $k \leq N$,

$$Q(x) = C_0 + C_1 P_1(x) + \dots + C_k P_k(x)$$

is that polynomial of degree k for which the scalar

$$\sum_{i=1}^M w_i [Q(x_i) - y_i]^2$$

has its minimum value.

The subroutine calculates an array A of $N+1$ coefficients of the least squares polynomial in standard form $[A(i+1) = a_i]$:

$$Q(x) = a_0 + a_1 x + \dots + a_N x^N$$

Best results are obtained from the subroutine if a preliminary coordinate transformation is performed on the x data points so that the origin lies in the middle of the x data. This is performed in the calling program.

The quantities in the parameter list are

M	number of data points
N	degree of polynomial desired; $0 < N < M$
X	array of independent variable
Y	array of dependent variable
W	array of positive weights in correspondence to the x array; for an unweighted fit, $w_i = 1$ for all i
MN1	row dimension of scratch array S1; $MN1 \geq M+N+1$
S1	scratch array

A array of computed coefficients in order of
 increasing degree

IER error indicator (not used)

I-15. SUBROUTINE FUSEIO

Subroutine FUSEIO reads and prints the input data which describe the fuselage and calculates the line source and doublet distributions as described in Appendix I of reference 1. A listing of the subroutine is presented in figure 1(m), a flow chart in figure I-9, and a table equating the algebraic and program notation in Table I-6 of this report.

The subroutine first reads in and prints input items 5, 6, 7, and 8 which consist of the fuselage length, the maximum radius, and the polynomials specifying the fuselage shape. Next, the data used to lay out the body interference panels, input items 9 and 10, are read and printed. Finally, subroutine BDYGEN is called for the purpose of calculating the source and doublet distributions.

I-16. SUBROUTINE INTOST

Subroutine INTOST (see fig. 1(m) for a listing) takes a vector with components specified in the inertial ξ, η, ζ coordinate system directions and transforms it into a vector with components in the store x, y, z coordinate system directions, see figure 14 of this report. That is,

$$\begin{bmatrix} s_x \\ s_y \\ s_z \end{bmatrix} = [A]' \begin{bmatrix} s_\xi \\ s_\eta \\ s_\zeta \end{bmatrix}$$

The matrix $[A]'$ is the transpose of the direction cosine matrix given by equation (II-2) of reference 4. The transpose is equal to the inverse since $[A]$ is orthogonal. The matrix $[A]$ was calculated in subroutine DIRCOS.

In terms of the above notation, the quantities in the parameter list of the subroutine are

XI	s_ξ
ETA	s_η
ZETA	s_ζ
X	s_x
Y	s_y
Z	s_z
DC	[A]

I-17. SUBROUTINE INVERS

Subroutine INVERS (see fig. 1(m) for a listing) solves a set of simultaneous linear algebraic equations by Gaussian elimination. This routine comes from reference 13 which contains a flow chart. Not all of the options shown in that flow chart are in the present routine. The quantities in the parameter list are

A	array containing coefficient matrix and right-hand sides
NSYS	number of right-hand sides
N	number of equations
NMAX	first dimension of A array in calling program
MMAX	second dimension of A array in calling program

If the coefficient matrix is found to be singular an error message is printed out (see section 4) and the program stops.

I-18. SUBROUTINE NUMACH

Subroutine NUMACH determines a local Mach number at a given field point lateral and vertical position based on the first occurrence of an induced downward flow velocity behind the free stream Mach cone associated with wing thickness. The method used is described in section 3.4 of reference 1. The routine also calculates least-squares polynomials which approximate the velocities at the specified y_w, z_w location. The velocities are based on the local Mach number and represent the sum of velocities induced at each point of the traverse by the wing-fuselage aircraft components. A listing of the program is presented in figure 1(n), a flow chart in figure I-10, and a table equating the algebraic and program notation in Table I-7 of this report.

At the beginning of the subroutine a test is performed to determine if the specified z_w location (Z) is below the wing. If not, an error message is printed (see section 4) and the program stops.

Next, the subroutine calculates the local wing chord, CHRD, at the specified y_w location (Y). Quantities previously determined by subroutine WLYOUT are used in this calculation. As shown in the flow chart, if the field point is below the fuselage, CHRD equals the wing root-chord; outboard of the wing tip CHRD equals the tip-chord.

After initializing certain control variables, the subroutine next begins the calculation of an x traverse aft of $x_w = 0$. At each point the velocity due to wing thickness is calculated (subroutine VELWTH). The point at which wing thickness first induces a downward velocity is determined using an x -interval size, DELX1, equal to one-tenth CHRD. The search is refined twice, each time backing up one step and repeating the calculations using DELX1 equal to one-third the previous interval size. Once the point in the traverse is isolated (XT3,Y,Z) at which the downward velocity is first felt, the local Mach number, M_ℓ , specified by equations (27) and (28) of reference 1 is computed from the velocity components.

The search for XT3 described above is next repeated with velocity calculations based on M_ℓ (specified when INUMCH = 1). The new value of XT3 defines the beginning of the range of influence associated with the wing thickness panels. The subroutine next determines the end of this range by searching for the point in the traverse (XT4,Y,Z) at which a 50 percent decrease in the magnitude of the downward velocity due to wing thickness occurs. The traverse begins at seven-tenths CHRD aft of XT3. The search is very similar to that for XT3.

The remainder of the subroutine calculates the flow field, based on M_ℓ , at a series of NCW points in the XT3, XT4 range. Contributions from all singularities associated with the wing and fuselage are included in the calculations. The flow field is then smoothed by fitting each velocity component with a least-squares cubic polynomial over the data points in the XT3, XT4 range. Subroutine FLSQFY is called for this purpose. The returned polynomial coefficients are stored in the array WSCOE.

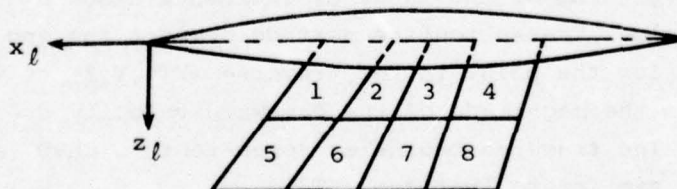
I-19. SUBROUTINE PLYOUT

Subroutine PLYOUT reads in data which describe the geometric characteristics of the pylon and calculates quantities which specify the pylon constant u-velocity panels. The pylon input variables are shown in figure 8 of this report. A listing of the subroutine is presented in figure 1(P), a flow chart in figure I-11, and a table defining the program notation in Table I-8 of this report.

The first part of the subroutine reads in and prints input items 19, 20, and 21. The total number, MP, of pylon constant u-velocity panels is calculated. Next, the pylon leading and trailing edge sweeps and their difference, PSLPDF, are calculated. The variables PLEX and CSIDE are initialized for the calculation of the first chordwise row of panels.

The remainder of the subroutine is a double DO loop within which panel leading-edge and trailing-edge sweeps, corner coordinates, and control point coordinates are calculated. These quantities for the pylon are stored in arrays following the same quantities calculated by subroutine WLYOUT for the NPANLS constant u-velocity panels on the wing.

The following sketch shows the numbering convention associated with the pylon panels for a typical pylon-under-wing layout with four chordwise and two spanwise panels.



In the subroutine notation, the panel corners labeled left are those farther from the pylon root chord.

I-20. SUBROUTINE PYTHIN

Subroutine PYTHIN reads in the pylon thickness data, input item 22 and 23. A listing of the subroutine is presented in figure 1(p) of this report.

The number of panels in a chordwise row, NCPS, is first read in along with an index, NUNIP, which indicates whether the thickness distribution is similar at all spanwise stations. If it is similar, NUNIP = 1, the values of $\tan \theta_p$ are read in for the first row and then the values of $\tan \theta_p$ for the other rows are set equal to those of the first row. If the distribution is not similar, NUNIP = 0, the values of $\tan \theta_p$ for all rows are read in.

The following table contains most of the variable names used in the subroutine. Section 3.2.1 should be referred to for the definition of a variable that is an input quantity.

MPS	number of thickness panels on the pylon; MSP*NCPS
MSP	input, item 20
NCPS	input, item 22
NUNIP	input, item 22
THETPL(I)	input, item 23

I-21. SUBROUTINE RESVEL

Subroutine RESVEL, along with other subroutines which it calls, calculates the perturbation velocities at a specified field point due to all aircraft components other than the store. A listing of the subroutine is presented in figure 1(q), a flow chart in figure I-12, and a table equating the algebraic and program notation in Table I-9 of this report. The variables appearing in the subroutine parameter list are defined in this table.

The subroutine first transforms the field point coordinates into the wing coordinate system and initializes the velocity sums to zero. Next, a test is performed to determine whether the wing-fuselage velocities are to be calculated using a least-squares polynomial approximation, described in section I-18, or in accordance with equations in section 3 of reference 1. If ISMTH = 0, the program calculates and sums velocities using the latter methods. First, if a fuselage is present, NFU = 1, velocities induced by the source and doublet distributions are calculated using subroutine VELCAL and velocities due to the fuselage interference panels using subroutine VELBD. Next, the wing constant u-velocity panel and wing thickness panel velocities are calculated using subroutines VELWP and VELWTH, respectively.

Finally, if a pylon is present, $NPY = 1$, the pylon velocities are calculated by calling VELPP for constant u-velocity panels and VELPTH for thickness panels.

If $ISMTH = 1$, a second test is performed to determine whether the x_w coordinate of the field point is within the range of x , at a specified y, z location, for which a smoothed velocity field has been previously calculated by subroutine NUMACH (see section I-18). This range is referred to in the flow chart as the XT3, XT4 range since these quantities are the limiting x_w values of the range. If the field point x_w coordinate is inside this range, wing-fuselage induced velocities are calculated using the least-squares polynomials. Pylon velocities are calculated as described above for $ISMTH = 0$. If the field point x_w coordinate is outside the XT3, XT4 range, all velocities are calculated as described for $ISMTH = 0$.

I-22. SUBROUTINE SEMFOR

Subroutine SEMFOR calculates the empennage forces and moments by the method described in section 5.3 and Appendix I of reference 4. A listing of the subroutine is presented in figure 1(q), a flow chart in figure I-13, and a table equating the algebraic and program notation in Table I-10 of this report.

An examination of the flow chart shows that the first steps in the routine are to locate the point at which the empennage forces act relative to the store moment center and to set JMAX equal to 2 or 4 depending on whether the empennage is planar or cruciform.

The next part of the subroutine calculates the perturbation velocity field at the MSF control points on each of the JMAX fins. After the velocities are calculated by subroutine RESVEL they are resolved into the store-body coordinate system by subroutine INTOST. The free-stream components are then calculated, resolved into the store-body coordinate system, and added to the perturbation velocities. The resultant velocities are made dimensionless by the store free-stream velocity and the pitch and yaw damping terms are added if aerodynamic damping is being included. From these velocities the components normal to the fin surfaces are determined. Positive directions are shown in figure 10 of reference 4.

The remainder of the routine calculates the empennage forces and moments. First W_0 and V_0 shown in figure 10 of reference 4 are determined from the velocity field used in the store body force and moment

calculation. Then, the normal force and the side force, if the empennage is cruciform, are calculated using equations (I-13) and (I-18) of reference 4. The spanwise integrations are performed using Simpson's rule. It is to be noted that in the present program all four fins are assumed to have the same span, $s_h = s_v$. The pitching moment and yawing moment are calculated using equations (I-21) and (I-22).

These forces and moments are in the fin coordinate system. They are resolved into the body coordinate system using equations (58) through (61) of reference 4.

Finally, if rolling moment is to be calculated this is done using equation (I-30) or (I-52) of reference 4. Equation (I-30) is for a planar empennage and (I-52) is for a cruciform empennage.

I-23. SUBROUTINE SEMPIN

Subroutine SEMPIN initializes certain quantities which will be used repeatedly in the empennage force and moment calculation, subroutine SEMFOR. The equations programmed are given in Appendix I of reference 4. A listing of the subroutine is presented in figure 1(r), a flow chart in figure I-14, and a table equating the algebraic and program notation in Table I-11 of this report.

The flow chart indicates that the first calculation performed is to determine the radial distance outward from the body axis to the MSF fin control points. The first point is at the body-fin juncture, $r_f = a$ (see fig. 10, ref. 4), and the last is at $r_f = s_h = s_v$. The others are equally spaced in between these two points. Next, a check is made to determine that XTAL was input as a negative quantity and then the angular orientation of the fins in the store-body coordinate system is determined. Referring to figure 10 of reference 4, these angles are measured in the clockwise direction from the z_s axis.

JMAX is next set equal to 2 or 4 depending on whether the empennage is planar or cruciform and then the y_s and z_s coordinates of the control points on all of the fins are determined. Next, certain constants are calculated and then the values of $(cc_l)_3$ are calculated at the control points. They are the same for all panels since $s_h = s_v$ (see eqs. (I-14) and (I-19), ref. 4).

If rolling moment is not to be calculated, NROLL = 0, control is returned to the calling program. If rolling moment is to be calculated, and the empennage is planar, IPLNR = 1, $(cc_\ell)_5$ given by equation (I-29) of reference 4 is calculated at the control points. Note that in the program the following substitution is made

$$\cosh^{-1}(x) = \ln(x + \sqrt{x^2 - 1})$$

For a cruciform empennage, IPLNR = 0, equation (I-51) of reference 4 is used for the first control point where $y_f = a$. For the other control points equation (I-38) is used. The following substitution is made in the program

$$\tanh^{-1}(x) = \frac{1}{2} \ln \frac{(1+x)}{(1-x)}$$

I-24. SUBROUTINE SFORCE

Subroutine SFORCE calculates the store-body forces and moments by the methods described in section 5.2 of reference 4. A listing of the subroutine is presented in figure 1(s), a flow chart in figure I-15, and a table equating the algebraic and program notation in Table I-12 of this report.

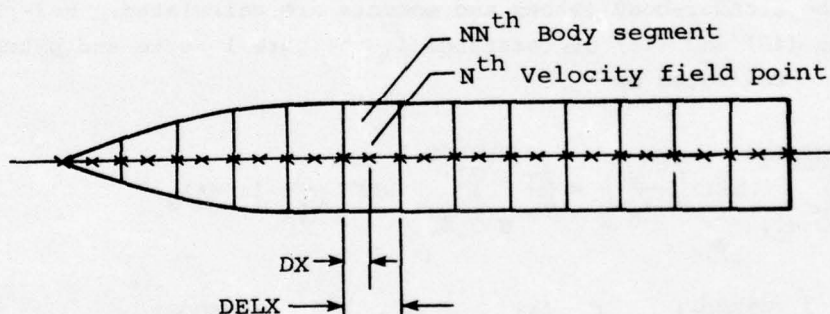
An examination of the flow chart shows that the first step in the routine is to check to see if the trajectory being calculated is to simulate a wind-tunnel captive-store trajectory. If it is, NGAM = 1, then the store attitude relative to the parent aircraft is changed. In wind-tunnel captive-store testing the yaw and pitch angles of the store are changed, only while measuring the aerodynamic forces and moments, to account for translational motion relative to the aircraft. The new angles are

$$\Psi_{cs} = \Psi_{ff} - \tan^{-1} \left(\frac{\dot{\eta}}{V_\infty \cos \alpha_f + \dot{\xi}} \right)$$

$$\Theta_{cs} = \Theta_{ff} + \tan^{-1} \left(\frac{\dot{\zeta}}{V_\infty \cos \alpha_f + \dot{\xi}} \right)$$

The subscript *cs* refers to captive store and *ff* refers to free flight. The direction cosines between this new body coordinate system and the inertial or fuselage system are calculated in DIRCOS. If the trajectory is a free-flight case, the direction cosines between the true body coordinate system and the inertial system are calculated.

In the next section of the program subroutine NUMACH is called (see section I-18). Following this, the program calculates the velocity field given by equation (40) of reference 4 at specified points along the separated store longitudinal axis. The store is removed from the flow field during this calculation. One of the input parameters was NSEG which is the number of equal length segments the body is to be broken into. These segments are of length DELX as shown in the following sketch.



The velocities are calculated at the midpoint of each segment as well as at the two ends, the points indicated by *x* in the sketch. There are thus $NHSEG = 2 * NSEG + 1$ points. The perturbation velocity field is first calculated for all NHSEG points. These velocities are the *u*, *v*, and *w* components given by equation (37) of reference 4. After the velocities are calculated by subroutine RESVEL, they are resolved into the store-body coordinate system by subroutine INTOST. The free-stream velocity components are next determined, resolved into the store-body coordinate system and added to the perturbation velocities given by equation (38). At this time the velocities are made dimensionless by V_{∞} . If damping is being included the damping terms in equation (40) are added.

The routine next calculates the forces and moments. The buoyancy forces and moments are first determined. From equations (42) and (44) of reference 4 the normal force and the pitching moment can be approximated by

$$(C_N)_{BY} = \sum_{N=2,4..}^{NHSEG-1} DELX \left(\frac{dC_N}{dx_s} \right)_N = \frac{2\pi}{S_R} \sum_{N=2,4..}^{NHSEG-1} DELX \left[a_N^2 \frac{(W_{s_{N+1}}^* - W_{s_{N-1}}^*)}{DELX} \right]$$

$$(C_m)_{BY} = \frac{1}{\ell_R} \sum_{N=2,4..}^{NHSEG-1} DELX \left[(x_{s,m} - x_s) \left(\frac{dC_N}{dx_s} \right)_N \right]$$

These are the equations which are programmed. Similar equations can be written for the side force and yawing moment.

Next the slender-body forces and moments are calculated. Referring to equations (46) and (48) of reference 4, the normal force and pitching moment are approximated by

$$\begin{aligned} (C_N)_{SB} &= \sum_{N=2,4..}^{NHSEGO-1} DELX \left(\frac{dC_N}{dx_s} \right)_N = \frac{2\pi}{S_R} \sum_{N=2,4..}^{NHSEGO-1} DELX \frac{d}{dx_s} (a^2 W_s^*)_N \\ &= \frac{2\pi}{S_R} \left\{ \sum_{N=2,4...}^{NHSEGO-1} DELX \left[a_N^2 \frac{(W_{s_{N+1}}^* - W_{s_{N-1}}^*)}{DELX} \right] + \sum_{N=2,4...}^{NHSEGO-1} DELX \left(a_N \frac{da_N}{N dx_s} W_{s_N}^* \right) \right\} \\ (C_m)_{SB} &= \frac{1}{\ell_R} \sum_{N=2,4...}^{NHSEGO-1} DELX \left[(x_{s,m} - x_s) \left(\frac{dC_N}{dx_s} \right)_N \right] \end{aligned}$$

Here the summations are terminated at the assumed separation location as specified by NSEGXO of item 30 of the input data since $NHSEGO = 2 * NSEGXO + 1$. Note that the quantity in the first summation of $(C_N)_{SB}$ is the same as that in $(C_N)_{BY}$. Use has been made of this fact in the program. Similar expressions can be written for $(C_Y)_{SB}$ and $(C_n)_{SB}$.

If separation is assumed to occur ahead of the base of the store, $NHSEGO < NHSEG$, the viscous crossflow forces and moments in this region are calculated using equations (51) through (54) of reference 4. The normal force and pitching moment are approximated by

$$(C_N)_{CF} = \sum_{N=NHSEGO+1, +3..}^{NHSEG-1} DELX \left(\frac{dC_N}{dx_s} \right)_N = \frac{2c_d c}{s_R} \sum_{N=NHSEGO+1, +3..}^{NHSEG-1} DELX \left(a_N V_N^* W_N^* s_N \right)$$

$$(C_m)_{CF} = \frac{1}{l_R} \sum_{N=NHSEGO+1, +3..}^{NHSEG-1} DELX \left[(x_{s,m} - x_s) \left(\frac{dC_N}{dx_s} \right)_N \right]$$

I-25. SUBROUTINE SHAPE

The purpose of this subroutine is to calculate the body radius and surface slope at a specified axial station. The body shape is specified by a series of polynomials of the form of equation (2) of this report. A flow chart of subroutine SHAPE is presented in figure I-16 and a listing of the subroutine in figure 1(t).

The quantities in the parameter list are:

X	value of x/l at which radius and surface slope are to be calculated
NS	number of polynomials describing body shape
XE	array containing values of x/l for the end points of the NS polynomials
C	array containing the coefficients of the NS polynomials
R	calculated value of r/l at $x/l = X$
DRDX	calculated value of dr/dx at $x/l = X$

The calculation performed by this subroutine consists of two steps. The first step is to determine which of the NS polynomials describes the shape at the value of X where the radius and surface slope are required. Once this is determined, the appropriate set of coefficients is used in equation (2) to determine r/l . The value of dr/dx is found by differentiating equation (2).

$$\frac{dr}{dx} = \frac{C_7}{2} \left[\frac{2C_2 \frac{x}{l} + C_3}{\sqrt{C_2 \left(\frac{x}{l} \right)^2 + C_3 \frac{x}{l} + C_4}} \right] + C_5 + 2C_6 \frac{x}{l}$$

It should be noted that r/l and dr/dx are calculated using the coefficients of the NS^{th} polynomial if x/l is greater than $XE(NS)$.

I-26. SUBROUTINE SIMSON

Subroutine SIMSON calculates the value of a definite integral using Simpson's rule. This can be found in any elementary numerical analysis book, for example, reference 14. As programmed here

$$I = \int_{x_0}^{x_0+m\Delta x} f(x) dx \approx \frac{\Delta x}{3} \left\{ f(x_0) + 4f(x_0 + \Delta x) + 2f(x_0 + 2\Delta x) + 4f(x_0 + 3\Delta x) \right. \\ \left. + 2f(x_0 + 4\Delta x) + \dots + 4f[x_0 + (m-1)\Delta x] + f(x_0 + m\Delta x) \right\}$$

where m must be an even number and 4 or greater. The subroutine is listed in figure 1(u) of this report. Referring to the listing and the above equation, the quantities in the subroutine parameter list are

N	$m + 1$
F	$f(x)$
DX	Δx
SUM	I

I-27. SUBROUTINE SOURCE

Subroutine SOURCE calculates coefficients used in the determination of the line source strengths. They occur as terms in equations (I-14) and (I-17) of reference 1. The relation of the coefficients to perturbation velocities, $u_{B,a}/V_\infty$ and $v_{B,a}/V_\infty$, induced by a number of line sources distributed along the body centerline is shown in the first two of equation (I-30) in which the coefficients occur as the multipliers of K_n . A listing of the subroutine is presented in figure 1(u) of this report. The subroutine is called by subroutine BDYGEN and section I-4 should be referred to for further details concerning the source strength calculations.

For a specified control point, x_B, r_B , and singularity origin, ξ , the subroutine calculates quantities U and V according to the following equations:

$$U = - \cosh^{-1} \left(\frac{x_B - \xi}{\beta r_B} \right)$$

$$V = \beta \sqrt{\left(\frac{x_B - \xi}{\beta r_B} \right)^2 - 1}$$

At the beginning of the subroutine a test is performed to determine if the control point is ahead of the Mach cone from the source origin. If so, U and V are set to zero and control is returned to the calling program.

The following table of definitions contains most of the variable names used in the subroutine:

BETA	$\beta = \sqrt{M_\infty^2 - 1}$
RFIELD	r_B ; radius of body at control point
TX	ξ ; location on body axis of source origin; positive measured from tip of nose
U	coefficient defined by first equation above
V	coefficient defined by second equation above
XFIELD	x_B ; x location of control point, positive measured from tip of nose

I-28. SUBROUTINE SOUTPT

Subroutine SOUTPT prints the output at the end of each integration step. A listing of the subroutine is presented in figure 1(u), a flow chart in figure I-17, and a table equating the algebraic and program notation in Table I-13 of this report.

The current value of the time is first printed and then the force and moment components calculated in subroutines SFORCE and SEMFOR are summed up. The components and totals are then printed. If store thrust has been calculated (NTHRUS not equal to zero) the thrust force is printed. Next the normal-force and side-force distributions and the velocity field along the store centerline are printed. The x_s locations are the midpoints of the body segments.

The next section of the subroutine locates the store nose, moment center, and base in the fuselage or inertial system. These points are

located relative to the fuselage nose and also relative to where they would be had the store remained in the $t = 0$ position on the aircraft. These positions are printed.

The remainder of the subroutine prints the store moment center translational velocities and accelerations, the store rotational velocities and accelerations, and the store angular orientation and rates of change of these angles.

I-29. SUBROUTINE STORIO

Subroutine STORIO reads and prints the data which describe and locate the store and calculates the store source and doublet distribution. Although the number of stores in the present version of the program is restricted to one, subroutine STORIO has been written in a general form that will, with minor changes, accommodate multiple stores. A listing of the program is presented in figure 1(v), a flow chart in figure I-18, and a table equating the algebraic and program notation in Table I-14 of this report.

The subroutine first reads in and prints data for each store, including a shape number, NSHAPE(J). The next section of the program is a double DO loop. The outer loop reads in and prints polynomials specifying a particular store shape. In the inner loop this shape is assigned to the store with matching shape number, and subroutine BDYGEN is called to calculate the source and doublet distributions for this store. At the end of the double loop a check is made to see if the index NCOUNT is equal to the number of stores, NSTRS. If it is not, data are missing for some store. This causes the message "shape polynomials not input for all stores" to be printed and the program stops. The last part of the subroutine locates all the stores in the wing coordinate system. The wing coordinate system is shown in figure 6.

I-30. SUBROUTINE STTOIN

Subroutine STTOIN (see fig. 1(w) for a listing) takes a vector with components specified in the store x, y, z coordinate system directions and transforms it into a vector with components in the inertial ξ, η, ζ coordinate system directions, see figure 14 of this report. That is,

$$\begin{bmatrix} s_{\xi} \\ s_{\eta} \\ s_{\zeta} \end{bmatrix} = [A] \begin{bmatrix} s_x \\ s_y \\ s_z \end{bmatrix}$$

The matrix $[A]$ is given by equation (II-2) of reference 4 and was calculated in subroutine DIRCOS.

In terms of the above notation, the quantities in the parameter list of the subroutine are

X	s_x
Y	s_y
Z	s_z
XI	s_{ξ}
ETA	s_{η}
ZETA	s_{ζ}
DC	$[A]$

I-31. SUBROUTINE SWNGIN

Subroutine SWNGIN reads in data required to describe the geometric characteristics of the wing and to lay out the wing constant u-velocity panels. A listing of the subroutine is presented in figure 1(w) of this report.

The first part of the subroutine reads in and prints input items 12, 13, and 14, which consist of wing geometry data and quantities used to locate the trapezoidal-shaped elemental panels. Next, the wing twist and camber distribution, if any, is read, input items 15 and 16. Two indices, NTAC and NUNI, are first input. If $NTAC = 0$ there is no twist and camber. The index NUNI indicates whether the twist and camber distribution is similar at all spanwise stations. If it is similar, $NUNI = 1$, the values of $\tan \alpha_{\ell}$ are read in for the first row and then the values of $\tan \alpha_{\ell}$ for the other rows are set equal to those of the first row. If the distribution is not similar, $NUNI = 0$, the values of $\tan \alpha_{\ell}$ for all rows are read in.

The following table contains definitions of most of the variable names used in the subroutine. Section 3.2.1 of this report should be referred to for the definition of a variable that is an input quantity.

ALPHAL(I)	$\tan \alpha_l$; input, item 16
CRW	length of wing root chord; input, item 12
MSW	input, item 13
MSWP	MSW + 1
NCW	input, item 13
NPANLS	number of constant u-velocity panels on wing; NCW*MSW
NTAC	input, item 15
NUNI	input, item 15
PSIWLE(I)	input, item 14
PSIWTE(I)	input, item 14
SSPAN	semispan of wing; input, item 12
Y(I)	input, item 14

I-32. SUBROUTINE THKLYT

Subroutine THKLYT calculates quantities which characterize the wing and pylon thickness source panels. These quantities are stored in arrays in each of which the wing panel variables precede the pylon variables. All panel coordinates are expressed in the wing coordinate system which is shown in figure 6. A listing of the subroutine is presented in figure 1(w), a flow chart in figure I-19, and a table equating the algebraic and program notation in Table I-15 of this report.

The first part of the subroutine calculates the layout of the wing panels. After the variables CSIDEP, SLPDIF, and WLEX are initialized for the first chordwise row of panels, the remaining calculations are performed within a double DO loop. The outer loop index, I, specifies the chordwise row and the inner loop index, K, the panel location in the Ith row. Within the inner loop the panel leading-edge and trailing-edge slopes and the corner coordinates are calculated and stored. The panels are numbered consecutively in chordwise rows beginning with panel number

one of row one adjacent to the wing root-chord at the leading edge. The sequence proceeds in increasing numbers to the trailing edge. Then back to the leading edge for the second chordwise row. The process continues until the last panel, numbered MS, is located adjacent to the wing tip at the trailing edge.

If a pylon is present (NPY = 1), the remainder of the subroutine calculates the panel leading-edge and trailing-edge slopes and the corner coordinates for the pylon source panels. The procedure used differs very little from the wing panel calculations. The value of PSLPDF, previously calculated by subroutine PLYOUT, is constant for all chordwise rows because no breaks in leading-edge or trailing-edge sweep angles may occur on the pylon. Also, the initial value of PLEX depends upon the pylon location; the index IP is tested for this purpose. The numbering convention associated with the pylon thickness panels is the same as that used for pylon constant u-velocity panels. It is described in section I-19. In describing corner coordinates for both wing and pylon panels, the corners closer to the respective root-chord are designated right corners; those farther from the root-chord are designated left corners.

I-33. SUBROUTINE THKOUT

Subroutine THKOUT prints the slopes of the wing and pylon thickness distributions which were read in as items 18 and 23 of the input data, see section 3.2.1. After the thickness slopes are printed, they are divided by π and saved in a combined array, DZDX, for subsequent velocity calculations. A listing is presented in figure 1(x) of this report.

The following list defines most of the variables used in the subroutine:

DZDX	array containing wing and pylon thickness slopes after dividing by π
MPS	number of pylon thickness panels
MS	number of wing thickness panels
NCPS	number of thickness panels in a chordwise row on the pylon; input, item 22
NCWS	number of thickness panels in a chordwise row on the wing; input, item 17
NPY	index indicating whether a pylon is (NPY = 1) or is not (NPY = 0) present; input, item 4

PI	π
THETAL	array containing wing thickness slopes; input, item 18
THETPL	array containing pylon thickness slopes; input, item 23

I-34. SUBROUTINE THRCAL

Subroutine THRCAL calculates the store thrust at a given time. A listing of the subroutine is presented in figure 1(x) of this report.

The thrust force acts along the store longitudinal axis and is specified by a series of polynomials of the form

$$F_T = \sum_{n=1}^6 a_n t^{n-1}$$

where F_T is the thrust in pounds at time t . The time history is specified by one of NTPOLY polynomials each of which is applicable for a range of t . The subroutine first determines which polynomial should be used for the given time value t . Once this is determined, the appropriate set of coefficients, a_n , is used in the above equation to calculate F_T . If t is greater than the end of the specified thrust time history, an error message is printed (see section 4) and the program stops.

The following table of definitions contains most of the variable names used in the subroutine. Section 3.2.1 should be consulted for the definition of a variable which is an input item.

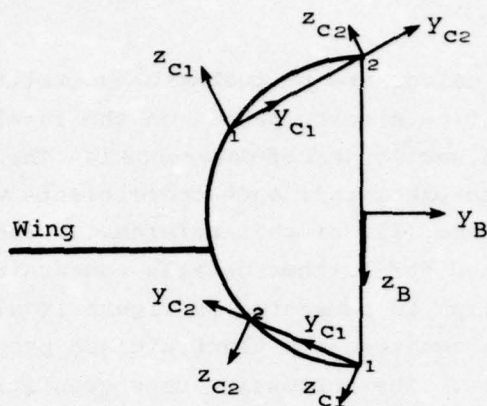
FTHRUS	F_T ; store thrust at time t
NTPOLY	input, item 38
T	t ; time at which thrust force is to be calculated
TC(J,I)	input, item 40
TEND(J)	input, item 39

I-35. SUBROUTINE VELBD

Subroutine VELBD calculates perturbation velocities at a given field point due to the constant u-velocity panels on the fuselage, according to the methods described in section 3.3 of reference 1. The subroutine is also used to obtain the single-panel influence coefficients which occur indirectly in equations (9), (10), and (11) of that reference. Section I-10 of this report should be consulted for further details concerning these coefficients. A listing of the subroutine is presented in figure 1(y), a flow chart in figure I-20, and a table equating the algebraic and program notation in Table I-16 of this report. The subroutine uses quantities calculated in subroutine BLYOUT which is described in section I-5. The wing coordinate system is shown in figure 6.

At the beginning of the subroutine the logical variable PYPNL is set equal to FALSE, the velocity totals UP, VP, and WP are initialized to zero, and the panel leading-edge and trailing-edge slopes, EM, are defined as zero. The remainder of the subroutine consists of a DO loop in which the influence functions for the four corners of the I^{th} panel are calculated and superposed. The superposition scheme is described in section 3.3.4 of reference 1 and that reference should be consulted for further details. In the corner numbering convention for fuselage panels corner one is the left front, corner two the right front, corner three the left rear, and corner four the right rear panel corner. The right corners are clockwise from the left when viewed from the rear.

At the beginning of the DO loop the corner influence function totals TU, TV, and TW are initialized to zero. Next, a test is performed to determine if the point at which velocities are to be calculated lies ahead of the panel leading edge; if so, all calculations for the I^{th} panel are skipped. If the point is not ahead of the leading edge, a test is performed next to determine in which fuselage quadrant the panel lies. As the flow chart indicates, two similar but distinct transformation and superposition procedures are followed, depending upon the panel location. In each procedure, the field point is first located relative to corner one in a corner coordinate system which is shown in the sketch below. Each panel corner has an associated coordinate system. The x_c axis, not shown in the sketch, is positive to the rear.



If corner one is in the upper left quadrant the sign of the y_C coordinate of the field point is reversed and subroutine VELO is called to calculate the influence of the corner on the image of the point with respect to the x_C, z_C plane. The sign of V , which is the returned influence function in the y_C direction, is then reversed. The functions U, V, W are resolved back into the wing system and superposed in the same manner as that used for wing panels with positive sweep (see fig. 4, ref. 1). Panels in the lower left quadrant are treated in the same manner as wing panels with negative sweep. No further coordinate change is necessary and subroutine VELO returns U, V , and W which are resolved into the wing system and superposed.

Next, in each procedure, the influence of the mirror image of corner one with respect to the aircraft vertical plane of symmetry is calculated. This is accomplished by the equivalent method of calculating the direct influence of corner one on the field point image. Following the call to subroutine VELO the sign of V is reversed in the superposition.

Corner one calculations are repeated in a similar manner for corners two, three, and four, but only corner one is detailed in the flow chart. After superposition of the four corner influence functions for the I^{th} panel is completed, a test is performed to determine if perturbation velocities are to be calculated. If $II = IF$, the influence coefficients for the I^{th} fuselage panel and the given control point are returned by the subroutine. If $II \neq IF$, the coefficients are multiplied by the strength of the I^{th} panel, divided by π , to obtain the perturbation velocities induced by that panel at the given field point. These velocities are computed and summed for all fuselage panels.

I-36. SUBROUTINE VELCAL

Subroutine VELCAL calculates perturbation velocities at a given field point due to the fuselage and store source and doublet distributions, according to equation (I-32) of reference 1. A listing of the subroutine is presented in figure 1(aa) of this report. The fuselage coordinate system is shown in figure 5. The store coordinate system is shown in the sketch of section I-11.

The coordinates of the field point are given as formal parameters in the appropriate body coordinate system. The subroutine first transforms these coordinates into the VELCAL system by changing the sign of X and Z, and then into the polar coordinates XFIELD, RFIELD, and THETA.

The major part of the program consists of a DO loop within which the axial, radial, and tangential velocities due to the N sources and doublets are calculated and summed. A test is made to determine whether the field point is ahead of the Mach cone from the I^{th} source origin, TX(I). If so, all remaining perturbation velocities are equal to zero and no further calculations are performed within the loop. At the end of the subroutine, the velocities are resolved back into the directions of the body coordinate system.

The variables in the subroutine parameter list are:

T	array containing the source strengths
TC	array containing the doublet strengths
TX	array containing the x locations of the origins of the singularities; positive, measured aft from tip of nose
N	number of line sources and doublets
XP	x coordinate of field point in body system
Y	y coordinate of field point in body system
ZP	z coordinate of field point in body system
U1	u/V_{∞} perturbation velocity at field point; body system
V1	v/V_{∞} perturbation velocity at field point; body system
W1	w/V_{∞} perturbation velocity at field point; body system

I-37. SUBROUTINE VELO

Subroutine VELO calculates the aerodynamic influence functions of a semi-infinite triangle associated with a constant u-velocity panel, as described in section II-2.1 of Appendix II of reference 1. The influence functions relate the panel singularity strength to the perturbation velocities induced by the triangle at a given point. They occur as the coefficients of $1/\pi(u_+/V_\infty)$ in equations (II-4) and (II-12) of reference 1. A listing of the subroutine is presented in figure 1(bb), a flow chart in figure I-21, and a table equating the algebraic and program notation in Table I-17 of this report. The coordinate system used by the subroutine is shown in figure 3 of reference 1.

At the beginning of the subroutine the quantity BETA is set equal to BETANU or to BETAOL depending on the values of INUMCH and PYPNL (section I-18 of this report should be referred to for further details concerning this choice). Next, the logical variable FELT is initialized to TRUE and a test is performed to determine if the field point is located ahead of the influencing triangle ($X \leq 0$). If so, the influence functions U,V,W are set to zero, FELT is set to FALSE, and control is returned to the calling program.

Next, the variable PYPNL is tested and, if the triangle is on the pylon, a transformation is performed which rotates the triangle into the VELO x,y plane. After the calculation of the logical variable INSIDE and other frequently used quantities, the remainder of the subroutine consists of four major sections in which the influence function terms, F1, F2, F4, F5, and F7, are calculated. Each section corresponds to a condition of the slope, EML, of the leading edge associated with the semi-infinite triangle. The subroutine requires that $EML \geq 0$ and this is accounted for in the VELO calling programs. The four leading-edge conditions are described fully, with accompanying sketches in section II-2.1 of reference 1. All equation numbers mentioned in the following paragraphs are from section II-2.1 of reference 1.

The first section of the subroutine corresponds to a subsonic leading edge, $BTSQ < EMLSQ$. Equation (II-5) is used if the point is inside the Mach cone from the origin, $INSIDE = TRUE$. If not, U,V, and W are set to zero. In this section as in the remaining ones, discontinuities in some of the equations may occur for certain field point locations. In such cases the affected influence function is set to zero. The quantities

YYEDGE and TLRNC, as well as Y and Z, are used to test the singularity locations.

If BETASQ = EMLSQ, the leading edge is a sonic leading edge. The equations used are the same as for the subsonic case except for the function F2, which is given by equation (II-7). If the point lies outside the Mach cone from the origin, the influence functions equal zero.

The third section of the subroutine is used if the triangle leading edge is supersonic, BTSQ > EMLSQ. Equations (II-5) and (II-9) calculate the terms of the influence functions if INSIDE = TRUE. If not, a second test is performed and equation (II-11) is used if the point is inside the Mach cone whose origin is on the leading edge at the field point y location. Otherwise the functions U,V,W are set to zero.

The fourth section of the subroutine is executed if the leading edge is unswept, EML = 0. For this special case the perturbation velocity equations are given by (II-12). If INSIDE = TRUE, the influence function terms are given by (II-5) and (II-13). Outside the Mach cone from the origin but inside the cone from the leading edge equation (II-14) is used. Otherwise, U,V,W are set to zero.

The last part of the subroutine calculates the function U,V,W from the component terms, in the case of a leading edge with positive sweep, using equation (II-4). If the triangle is located on the pylon, V and W are rotated back into pylon orientation.

I-38. SUBROUTINE VELOTH

Subroutine VELOTH calculates the aerodynamic influence functions of a semi-infinite triangle associated with a wing or pylon thickness panel, as described in section II-2.2 of Appendix II of reference 1. The influence functions relate the panel source strength to the perturbation velocities induced by the triangle at a given point. They occur as the coefficients of $1/\pi(\tan \theta)$ in equations (II-15) and (II-16) of reference 1. A listing of the subroutine is presented in figure 1(cc) of this report. The subroutine is very similar in logic to subroutine VELO which is described in detail in section I-37 and represented by a flow chart in figure I-21.

In subroutine VELOTH, three component terms, F1, F2, and F5, need to be calculated in order to determine the influence functions UTH,VTH, and WTH. Referring to section II-2.1 and II-2.2 of reference 1, function F1, F2, and F5 are specified in equation (II-5) for the case of a subsonic

leading edge, in equations (II-5) and II-7) for a sonic leading edge, and in equations (II-5), (II-9), and (II-11) for a supersonic leading edge. For the special case of an unswept leading edge ($EML = 0$), the general perturbation velocity equations are given by (II-16). If the given point lies inside the Mach cone from the origin of the triangle, function $F1$ is given by equation (II-13), function $F5$ by equation (II-5), and function $F2$ by equation (II-17). If the point lies outside the Mach cone from the origin but inside the Mach cone from the triangle leading edge at the field point y location, functions $F1$, $F2$, and $F5$ are given by equation (II-16). In all leading edge cases, the function $F1$, $F2$, and $F5$ are singular for certain field point locations. When this occurs, the affected influence function is set to zero.

A table equating the algebraic and program notation for subroutine VELO is presented in Table I-17 of this report. Almost all of the notation used in subroutine VELOTH is defined in this table. One should note that the influence functions, U, V, W and the point coordinates, YS, ZS , in VELO are named UTH, VTH, WTH, YTH , and ZTH , respectively in subroutine VELOTH.

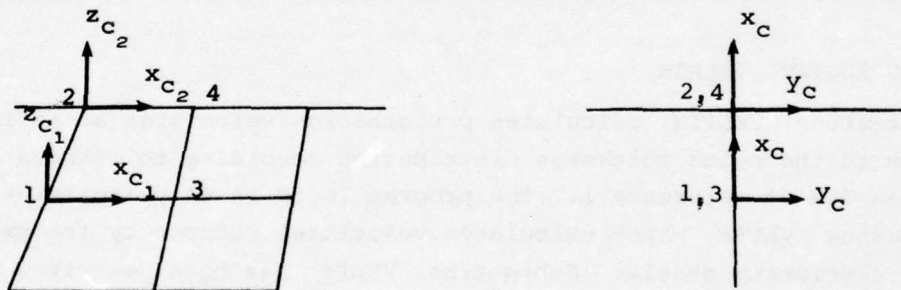
I-39. SUBROUTINE VELPP

Subroutine VELPP calculates perturbation velocities at a field point due to the constant u -velocity panels on the pylon according to methods described in section 3.3 of reference 1. The subroutine is also used to obtain the single panel influence coefficients which form the coefficients of $1/\pi(u_+/V_\infty)$ in equation (12) of reference 1. A listing of the subroutine is presented in figure 1(ee), a flow chart in figure I-22, and a table equating the algebraic and program notation in Table I-18 of this report. The quantities in the subroutine parameter list are contained in this table. The wing coordinate system is shown in figure 6.

At the beginning of the subroutine, the logical variable $PYPNL$ is set equal to $TRUE$, indicating to subroutine VELO that calculations are to be performed for a pylon panel. The quantities $YDIR$ and $YIMG$ are calculated and the velocity totals, UP, VP, WP , are initialized to zero. The remainder of the subroutine consists of a DO loop in which the influence functions for the four corners of the I^{th} panel are calculated and superposed. The superposition scheme is described in section 3.3.4 of reference 1 and that reference should be consulted for further details.

The corner numbering convention for pylon panels associates corners one and two with the leading edge left and right corners, respectively; corners three and four with the trailing edge left and right corners, respectively. The left corners are those farther from the pylon root chord.

At the beginning of the DO loop the influence function totals are initialized to zero and the leading-edge slope, $EM1$, and trailing-edge slope, $EM2$, are defined. Next, a test of the sign of $EM1$ is performed and two distinct transformation and superposition procedures are followed depending on the results of this test, as the flow chart indicates. In each procedure a test is performed first to determine if the field point lies ahead of the most forward leading-edge corner; if so, all calculations for the I^{th} panel are skipped. If the point is not ahead of the leading edge, the point is located relative to corner one in a corner coordinate system which is illustrated in the sketch below. Each panel corner has an associated coordinate system.



For a panel with swept back leading edge, $EM1 \geq 0$ the superposition scheme is the same as for a wing panel with positive sweep (see figure 4, reference 1). The field point z_c coordinate is reversed and subroutine VELO is called to calculate the influence of corner one on the image of the point with respect to the x_c, y_c plane. The sign of W is then reversed. The functions U, V, W are resolved back into the wing system and superposed. If the panel leading edge is swept forward, superposition is the same as for wing panels with negative sweep. The sign of $EM1$ is reversed and subroutine VELO returns U, V, W which are resolved into the wing system and superposed. It should be noted that the subroutine code combines superposition and transformation steps and that the final sign changes of U and W are made at the end of the DO loop.

The next calculations are omitted if the pylon is located under the fuselage centerline. Otherwise, the influence of the mirror image of corner one with respect to the vertical plane of symmetry is calculated. This is accomplished by the equivalent method of calculating the direct influence of corner one on the image of the field point and then reversing the sign of V .

Corner one calculations are repeated in a similar manner for corners two, three, and four, but only corner one is described in detail in the flow chart. After superposition of the four corner influence functions for the I^{th} panel is completed, a test is performed to determine if perturbation velocities are to be calculated. If $II = IF$, the influence coefficient for the I^{th} pylon panel and the given control point is returned by the subroutine. If $II \neq IF$, the coefficients are multiplied by the strength of the I^{th} panel, divided by π , to obtain the perturbation velocities induced by that panel at the given field point. These velocities are computed and summed for all pylon constant u-velocity panels.

I-40. SUBROUTINE VELPTH

Subroutine VELPTH calculates perturbation velocities at a field point due to the pylon thickness distribution according to methods described in section 3.3 of reference 1. The program logic is very similar to that of subroutine VELPP which calculates velocities induced by the pylon constant u-velocity panels. Subroutine VELPP has been described in detail in section I-39 and is represented by a flow chart in figure I-22 of this report. Only those details, therefore, in which subroutine VELPTH differs from subroutine VELPP are included in this description. A listing of the subroutine is presented in figure 1(gg) and a table equating the algebraic and program notation in Table I-19. The quantities in the subroutine parameter list are contained in this table.

The coordinates of the field point are given as formal parameters in the wing coordinate system. The point is located relative to each of the four panel corners using the same transformation scheme as in VELPP. However, the corner coordinate arrays which define the pylon thickness panels and which have been previously calculated by subroutine THKLYT (see section I-32) are used in the transformations. Subroutine VELOTH is called to calculate the corner influence functions, U, V, W , which are then superposed in the same manner as in VELPP.

Finally, the subroutine calculates perturbation velocities only and is not used to obtain single panel influence coefficients. Thus, after the calculation of the influence coefficients for the I^{th} panel is completed, no test is performed to determine if $II = IF$. The influence coefficients are multiplied by $DZDX(I)$ to obtain perturbation velocities induced by the I^{th} panel at the given point. These velocities are calculated and summed for all pylon thickness panels.

I-41. SUBROUTINE VELWP

Subroutine VELWP calculates perturbation velocities induced at a given field point by the constant u-velocity panels on the wing according to methods described in section 3.3 of reference 1. The subroutine is also used to obtain single panel influence coefficients which occur in equation (12) of reference 1 as the coefficients of $1/\pi(u_+/V_\infty)$. A listing of the subroutine is presented in figure 1(hh), a flow chart in figure I-23, and a table equating the algebraic and program notation in Table I-20 of this report. The quantities in the subroutine parameter list are contained in this table. The wing coordinate system is shown in figure 6.

At the beginning of the subroutine, the logical variable PYPNL is set equal to FALSE indicating to subroutine VELO that calculations are for a horizontal rather than a pylon panel. After the velocity totals, UP,VP,WP, are initialized to zero, the remainder of the subroutine consists of a DO loop within which the influence functions for the four corners of the I^{th} panel are calculated and superposed. The superposition scheme is described in section 3.3.4 of reference 1 and that reference should be consulted for further details. The corner numbering convention for wing panels is shown in figure 4 of reference 1.

At the beginning of the DO loop the influence totals, TU,TV, and TW are initialized to zero and the leading-edge slope, EM1, and trailing-edge slope, EM2, are defined. Next, a test of the sign of EM1 is performed and two distinct transformation and superposition procedures are followed depending on the results of this test, as the flow chart indicates. In each procedure the point is first located relative to corner one in the corner coordinate system described in section I-39 of this report. The z_c location of the field point is constant for all wing panels and is defined outside the DO loop. If $EM1 \geq 0$, the sign of the y_c coordinate of the point is reversed and subroutine VELO is called to calculate

the influence of corner one on the image of the point with respect to the x_c, z_c plane. The sign of V is then reversed. The functions U, V, W are resolved back into the wing system and superposed. If $EM1 < 0$, the sign of $EM1$ is reversed. After the call to $VELO$, the functions U, V, W are resolved back into the wing system and superposed. In the subroutine code transformation and superposition steps are combined and the final sign change of U and W are made at the end of the DO loop.

Next, in each procedure, the influence of the image of corner one with respect to the aircraft vertical plane of symmetry is calculated. This is accomplished by the equivalent method of calculating the direct influence of corner one on the field point image and then reversing the sign of V .

Corner one calculations are repeated in a similar manner for corners two, three, and four, but only corner one is detailed in the flow chart. After superposition of the four corner influence functions for the I^{th} panel is completed, a test is performed to determine if perturbation velocities are to be calculated. If $II = IF$, the influence coefficient for the II^{th} panel and the given control point is returned by the subroutine. If $II \neq IF$, the coefficients are multiplied by the strength of the I^{th} panel, divided by π , to obtain the perturbation velocities induced by that panel at the given field point. These velocities are computed and summed for all pylon constant u-velocity panels.

I-42. SUBROUTINE VELWTH

Subroutine $VELWTH$ calculates perturbation velocities at a given field point due to the wing thickness distribution, according to methods described in section 3.3 of reference 1. The program logic is very similar to that of the corresponding subroutine $VELWP$, which calculates velocities induced by the wing constant u-velocity panels. Subroutine $VELWP$ has been described in detail in section I-41 and is represented by a flow chart in figure I-23 of this report. Only those details, therefore, in which subroutine $VELWTH$ differs from subroutine $VELWP$ are included in this description. A listing of the subroutine is presented in figure 1(jj) and a table equating the algebraic and program notation in Table I-21. The quantities in the subroutine parameter list are contained in this table.

The coordinates of the field point are given as formal parameters in the wing coordinate system. The point is located relative to each of the four corners of the trapezoidal shaped thickness panels using the same transformation schemes as in VELWP. However, the corner coordinate arrays which define the wing thickness panels and which have been previously calculated by subroutine THKLYT (see section I-32) are used in the transformations. Subroutine VELOTH is called to calculate the corner influence functions, U,V,W, which are then superposed in the same manner as in VELWP.

Finally, the subroutine calculates perturbation velocities only and is not used to obtain single panel influence coefficients. Thus, after the calculation of the influence coefficients for the I^{th} panel is completed, no test is performed to determine if $II = IF$. The influence coefficients are multiplied by $DZDX(I)$ to obtain the perturbation velocities induced by the I^{th} panel at the given field point. These velocities are calculated and summed for all wing thickness panels.

I-43. SUBROUTINE WITHIN

Subroutine WITHIN reads in the wing thickness data, input items 17 and 18. A listing of the subroutine is presented in figure 1(kk) of this report.

The number of panels in a chordwise row, NCWS, is first read in along with an index, NUNIS, which indicates whether the thickness distribution is similar at all spanwise stations. If it is similar, NUNIS = 1, the values of $\tan \theta$ are read in for the first row of panels and then the values of $\tan \theta$ for the other rows are set equal to those of the first row. If the thickness distribution is not similar, NUNIP = 0, the values of θ for all rows are read in.

After the thickness slopes are read in, an input error check is performed. If any of the $\tan \theta$ values is zero or negative at the wing leading edge, an error message is printed (see section 4) and the program halts.

The following table contains definitions of most of the variable names used in the subroutine. Section 3.2.1 should be referred to for the definition of a variable that is an input quantity.

JLE	index of first wing thickness panel in a chordwise row
MS	number of thickness panels on wing; $MSW \times NCWS$
MSW	input, item 13
NCWS	input, item 17
NUNIS	input, item 17
THETAL(I)	input, item 18

I-44. SUBROUTINE WLYOUT

Subroutine WLYOUT calculates quantities which characterize the constant u-velocity panels on the wing. An example of a wing trapezoidal panel is shown in figure 2 of reference 1. Similar routines PLYOUT and BLYOUT calculate these quantities for the pylon and fuselage panels, respectively. The arrangement of variables in any single coordinate array is wing panels first, pylon panels second, and fuselage panels last. All coordinates are in the wing coordinate system which is shown in figure 6. A listing of the subroutine is presented in figure 1(10), a flow chart in figure I-24, and a table equating the algebraic and program notation in Table I-22 of this report.

As indicated by the flow chart, the first part of the subroutine tests whether the wing leading-edge and trailing-edge sweep angles are constant at all spanwise Y-stations. If breaks in sweep occur, the indicator LVSWP is set equal to one; otherwise, $LVSWP = 0$ and the quantity SLPDIF, the difference between leading-edge and trailing-edge slopes for a chordwise row, is computed outside the main DO loop.

After initializing the quantities CSIDEP and WLEX, the remainder of the subroutine consists of a double DO loop. The outer loop index, I, controls the chordwise row; the inner loop index, K, specifies the panel location in the I^{th} row. Within the inner loop, the panel leading-edge and trailing-edge slopes, the corner coordinates, and the control point coordinates are calculated and stored. The convention used in numbering the NPANLS wing constant u-velocity panels is the same as that used for the wing thickness panels. Section I-32 should be referred to for details. In the subroutine notation, the right-hand side of the panel is the one closer to the root-chord.

TABLE I-1

DICTIONARY OF NOTATION IN MAIN PROGRAM

The following list presents most of the variable names used in the main program. Those which appear in common statements or parameter lists of subroutines but are not used in the main program are not included. Where possible a variable name is identified by a symbol in the list of symbols or an equation number in reference 4. If the symbol or equation number is from another reference, the reference number is given. Where a variable is an input quantity, it is so identified and section 3.2.1 of this report should be referred to for the definition. The x_B, y_B, z_B coordinate system is shown in figure 5 of this report.

<u>PROGRAM NOTATION</u>	<u>ALGEBRAIC NOTATION</u>
ACCG	g , 32.174 feet/second
ALFAC	α_f , degrees; input, item 3
ALFACR	α_f , radians
ALPHAL(N)	$\tan \alpha_l$; input, item 16
BETA	$\beta = \sqrt{M_\infty^2 - 1}$
BETASQ	β^2
CA	C_A ; input, item 35
CAPG	$\cos(\alpha_f + \gamma_f)$
CDC	c_{dc} ; input, item 35
CENTER	logical variable which is TRUE for a pylon under the fuselage centerline
CLALPH	lift-curve slope of tail panels; input, item 37
CLLEM	$(C_l)_E$, equations (62) and (I-30) or equations (63) and (I-52)
CLMBY	$(C_m)_{BY}$, equation (44)
CLMCF	$(C_m)_{CF}$, equation (53)
CLMEM	$(C_m)_E$, equation (60)

Table I-1.- Continued.

CLMSB	$(C_m)_{SB}$, equation (48)
CLNBY	$(C_n)_{BY}$, equation (45)
CLNCF	$(C_n)_{CF}$, equation (54)
CLNEM	$(C_n)_E$, equation (61)
CLNSB	$(C_n)_{SB}$, equation (49)
CNBY	$(C_N)_{BY}$, equation (42)
CNCF	$(C_N)_{CF}$, equation (51)
CNEM	$(C_N)_E$, equation (58)
CNORM	total C_N
CNSB	$(C_N)_{SB}$, equation (46)
COEF(I,J)	coefficients of polynomials specifying separated store shape; input, item 34
CPITCH	total C_m
CROLL	total C_l
CSIBCR(N)	$\cos[SIBCR(N)]$
CSIDE	total C_Y
CYAW	total C_n
CYBY	$(C_Y)_{BY}$, equation (43)
CYCF	$(C_Y)_{CF}$, equation (52)
CYEM	$(C_Y)_E$, equation (59)
CYSB	$(C_Y)_{SB}$, equation (47)
DC(I,J)	$[A]$, equation (28)
DDTIME	input value of integration interval; set equal to DTIME of item 42

Table I-1.- Continued.

DELTP(N)	$1/\pi(u_+/V_\infty)$; equation 15, reference 1
DELX	length of body segment used in force calculation
DTIME	current value of integration interval
DTOR	degrees to radians conversion factor, 1/57.29578
DVAR(N) N = 1,2,...12	$\ddot{\xi}, \ddot{\eta}, \ddot{\zeta}, \dot{p}, \dot{q}, \dot{r}, \dot{\xi}, \dot{\eta}, \dot{\zeta}, \dot{\psi}, \dot{\theta}, \dot{\phi}$ respectively
EDRDX(I)	da/dx_s at the midpoint of the i^{th} segment of the separated store
ERAD(I)	a at the midpoint of the i^{th} segment of the separated store
ESTLGC	l_s of separated store
ESTRMX	a_{max} of separated store
EXST(I)	x_s location of the i^{th} half segment on the separated store
FINSS	tail fin semispan; input, item 37
FIXX	I_{xx} ; input, item 31
FIXY	I_{xy} ; input, item 31
FIXZ	I_{xz} ; input, item 31
FIYY	I_{yy} ; input, item 31
FIYZ	I_{yz} ; input, item 31
FIZZ	I_{zz} ; input, item 31
FLTHC	fuselage length; input, item 5
FMACH	M_∞ ; input, item 3
FMCHSQ	M_∞^2
FTHRUS	thrust force, F_T , reference 1
GAMF	fuselage flight path angle, γ_f ; input, item 3
GXX,GYY,GZZ	g_x, g_y, g_z , equation (67)
IPLNR	empennage type; input, item 36

Table I-1.- Continued.

MP	number of u-velocity panels on pylon, $MP = NCP * MSP$
MPS	number of pylon thickness panels, $MPS = NCPS * MSP$
MS	number of wing thickness panels, $MS = NCWS * MSW$
MSF	input, item 36
MSP	input, item 20
MSW	input, item 13
NBD	$NBD = NBD CR1 + NBD CR2$ which were input in item 9
NBIP	number of u-velocity panels on fuselage; $NBIP = NBD * NCWB$
NCP	input, item 20
NCPS	input, item 22
NCW	input, item 13
NCWB	input, item 9
NCWS	input, item 17
NDAMP	input, item 30
NDIFEQ	control index used in subroutine ADAMS
NEJECT	number of store being separated; input, item 30
NEJSTR	subscript associated with separated store; $1 \leq NEJSTR \leq NSTRS$
NEMP	input, item 30
NEQ	number of differential equations being integrated by subroutine ADAMS; $NEQ = 12$
NFPOLY	input, item 6
NFU	input, item 4
NGAM	input, item 30
NHSEG	number of points along store axis where velocity field is to be calculated; $NHSEG = 2 * NSEG + 1$

Table I-1.- Continued.

NHSEGO	number of points along store axis ahead of separation point where velocity field is to be calculated; $NHSEGO = 2 * NSEG XO + 1$
NPANLS	number of u-velocity panels on left wing panel; $NCW * MSW$
NPOLY	input, item 30
NPTOT	$NPANLS + MP + NBIP$
NPTOTP	$NPTOT + 1$
NPY	input, item 4
NROLL	input, item 30
NSEG	input, item 30
NSEG XO	input, item 30
NSTRS	input, item 4
NTHP	$MS + MPS$
NTHRUS	input, item 30
NTPOLY	input, item 38
NUMSTR(I)	number associated with i^{th} store; input, item 24
N1P	$NPANLS + 1$
N2	$NPANLS + MP$
N2P	$N2 + 1$
PHIROL	input, item 37
Q SREF	$q_{\infty S} S_R$
Q SREFL	$q_{\infty S} S_R l_R$
Q STORE	$q_{\infty S}$, equation (69)
RADAV	input, item 37
REFL	l_R , equation (72)
RHO	ρ_{∞} ; input, item 3

Table I-1.- Continued.

SAPG	$\sin(\alpha_f + \gamma_f)$
SIBCR(I)	incidence angle of i^{th} store relative to fuselage axis, radians; $\text{SIC}(I) \cdot \text{DTOR}$
SIC(I)	incidence angle of the i^{th} store; input, item 24
SLTHC(I)	length of i^{th} store; input, item 24
SMASS	m, mass of separated store; input, item 31
SREF	S_R , equation (70)
SRMAX(I)	maximum radius of i^{th} store; input, item 24
SSIBCR(I)	$\sin[\text{SIBCR}(I)]$
SSPAN	input, item 12
TC(I,J)	input, item 40
TEND(I)	input, item 39
TIME	t, current value of time
TIMEF	final time; input, item 42
TIMEI	initial time; input, item 42
TIPY	exposed wing span
UU	\dot{x}_O
VAR(N), N = 1,2,...12	$\dot{\xi}, \dot{\eta}, \dot{\zeta}, p, q, r, \dot{\xi}, \dot{\eta}, \dot{\zeta}, \Psi, \Theta, \Phi$ respectively
VINF	V_∞ ; input, item 3
VSTORE	$V_{\infty s}$, equation (41)
VV	\dot{y}_O
VXZERO	input, item 41
VYZERO	input, item 41
VZZERO	input, item 41
WW	\dot{z}_O

Table I-1. Concluded.

XBAR	\bar{x} ; input, item 32
XBASEI	ξ coordinate of separated store base at $t = 0$
XBSO(I)	x_B coordinate of tip of nose of i^{th} store
XBWOC	$x_{B_{\text{item 11}}}$ coordinate of wing root-chord leading edge; input, item 11
XCGI	ξ coordinate of separated store moment center at $t = 0$
XEND(N)	end points of polynomials specifying separated store shape; input, item 33
XMOM	$x_{s,m}$; input, item 32
XNOSEI	ξ coordinate of tip of separated store nose at $t = 0$
XTAIL	input, item 37
XWSOC(I)	x coordinate of tip of nose of i^{th} store measured from wing root-chord leading edge
YBAR	\bar{y} ; input, item 32
YBASEI	η coordinate of separated store base at $t = 0$
YBSO(I)	y_B coordinate of i^{th} store
YCGI	η coordinate of separated store moment center at $t = 0$
YNOSEI	η coordinate of tip of separated store nose at $t = 0$
YPL	y_B coordinate of pylon root-chord leading edge
YWSO(I)	y location of i^{th} store in wing coordinate system
ZBAR	\bar{z} ; input, item 32
ZBASEI	ζ coordinate of separated store base at $t = 0$
ZBSO(I)	z_B coordinate of tip of nose of i^{th} store
ZBWO	$z_{B_{\text{item 11}}}$ coordinate of wing root-chord leading edge; input, item 11
ZCGI	ζ coordinate of separated store moment center at $t = 0$
ZNOSEI	ζ coordinate of tip of separated store nose at $t = 0$
ZWSO(I)	z location of tip of i^{th} store nose measured relative to wing root-chord leading edge

TABLE I-2

DICTIONARY OF NOTATION IN SUBROUTINE BDYGEN

The following list presents most of the variable names used in subroutine BDYGEN. Where possible a variable name is identified by a symbol in the list of symbols or an equation number in reference 1. Where a variable is an input quantity it is so identified and section 3.2.1 of this report should be referred to for the definition.

<u>PROGRAM NOTATION</u>	<u>ALGEBRAIC NOTATION</u>
A(J)	coefficient of $K_{d,J-1}$ in equation (I-28), or of K_{J-1} in equation (I-17), for a given control point.
ALPHA	angle measured between the body centerline and the free-stream direction
BETA	$\sqrt{M_\infty^2 - 1}$
DEL	LBODY/N
DRDX(I)	slope of body surface at I^{th} control point
LBODY	length of body for which source and doublet distribution is to be calculated
MACH	M_∞ ; input, item 3
N	NXBODY - 1
NSEG	number of polynomials used to specify body shape
NXBODY	number of body definition points
RADIUS	maximum radius of body
RBODY(I)	radius of body at I^{th} body definition point
RF(I)	radius of body at I^{th} control point
RFIELD	radius of body at a control point
ROL	body radius at a specified axis point, made dimensionless by body length
RPBODY(I)	slope of body surface at I^{th} body definition point

Table I-2.- Concluded.

SCOEF	array containing coefficients of polynomials used to specify body shape
SLOPE	slope of body surface at a control point
SUM	quantity represented by summation expression in right-hand side of the first of equations (I-17) and (I-28)
T	array containing source strengths; $T(J)$ is the quantity K_{J-1} calculated by equations (I-14) and (I-17)
TC	array containing doublet strengths; $TC(J)$ is the quantity $K_{d,J-1}$ calculated by equations (I-27) and (I-28)
TX	array containing x locations of origins of conical line sources and doublets; positive, measured from tip of nose
U	quantities from equations (I-14), (I-17), (I-27), and (I-28), calculated by subroutines SOURCE and DOUBLT
V	terms from equations (I-14), (I-17), (I-27), and (I-28), calculated by subroutines SOURCE and DOUBLT
XBODY(I)	x location of I^{th} body definition point; positive back, measured from tip of nose
XEND	array containing x locations of end points of polynomial sections specifying body shape, made dimensionless by body length
XF(I)	x location of I^{th} control point; positive, measured from tip of nose
XFIELD	x location of a control point; positive, measured from tip of nose
XOL	x location of a specified axis point, made dimensionless by body length

TABLE I-3

DICTIONARY OF NOTATION IN SUBROUTINE BLYOUT

The following list presents most of the variable names used in subroutine BLYOUT. Where possible a variable name is identified by a symbol in the list of symbols or an equation number in reference 1. Where a variable is an input quantity it is so identified and section 3.2.1 of this report should be referred to for the definition. The x_W, y_W, z_W coordinate system is shown in figure 6.

<u>PROGRAM NOTATION</u>	<u>ALGEBRAIC NOTATION</u>
ANG	fuselage panel orientation angle relative to x_B, y_B plane; negative measured in counterclockwise rotation from positive y_B direction
ANGW	$\sin^{-1}(ZBWO/FRMAX)$
BODYPL	input, item 10
CPY	y coordinate of a fuselage control point in panel coordinate system (see section I-5)
CS	$\cos(\text{THT})$
CST2(J)	$\cos(\text{ANG}_J)$; ANG_J is the value of ANG associated with J^{th} panel
DX	panel length; $\text{BODYPL}/\text{NCWB}$
FAC	0.95; constant used to locate $\text{XCPT}(J)$ at 95 percent of chord containing panel centroid
FRMAX	input, item 5
IL,IU	initial and final values, respectively, of loop index over ring of body interference panels
ITIMES	control constant: $\text{ITIMES} = 1$, panel is above non-tangent wing; $\text{ITIMES} = 2$, wing is tangent, or panel is below wing
NBD	number of panels in a ring of body interference panels; $\text{NBD} = \text{NBD}1 + \text{NBD}2$
NBD1	input, item 9
NBD2	input, item 9

Table I-3.- Continued.

NBIP	total number of body interference panels; $NCWB \cdot NBD$
NCWB	input, item 9
N2	number of constant u-velocity panels on wing and pylon
PI	π
PI2	$\pi/2$
RTOD	radians to degrees conversion factor; $180/\pi$
SN	$\sin(\text{THT})$
SNT2(J)	$\sin(\text{ANG}_J)$; ANG_J is value of ANG associated with J^{th} body panel
THT	polar angle in cross-sectional plane, defining the origin of panel coordinate system relative to fuselage center; positive in clockwise rotation from negative y_B axis
THTI(J)	$(\pi - \text{THT}_J) \cdot \text{RTOD}$; THT_J is value of THT associated with J^{th} panel
THTS	central angle in cross-sectional plane, defined by radial lines drawn from center of fuselage to panel edges (see section I-5)
WBIP	y location of right edge of panel, in panel coordinate system (see section I-5)
XCPT(I)	x_W coordinate of I^{th} control point
XFBIP	x_W location of front edge of panels in a ring of body interference panels
XLB(I)	x_W coordinate of left rear corner of I^{th} constant u-velocity panel
XLF(I)	x_W coordinate of left front corner of I^{th} constant u-velocity panel
XRB(I)	x_W coordinate of right rear corner of I^{th} constant u-velocity panel
XRF(I)	x_W coordinate of right front corner of I^{th} constant u-velocity panel
YCPT(I)	y_W coordinate of I^{th} control point
YLC(I)	y_W coordinate of left edge of I^{th} constant u-velocity panel

Table I-3.- Concluded.

YRC(I)	y_W coordinate of right edge of I^{th} constant u-velocity panel
ZBWO	input, item 11
ZCPT(I)	z_W coordinate of I^{th} control point
ZLC(I)	z_W coordinate of left edge of I^{th} constant u-velocity panel
ZRC(I)	z_W coordinate of right edge of I^{th} constant u-velocity panel

TABLE I-4

DICTIONARY OF NOTATION IN SUBROUTINE DPCOEF

The following list presents most of the variable names used in subroutine DPCOEF. Where possible a variable name is identified by a symbol in the list of symbols or an equation number in reference 1. Where a variable is an input quantity it is so identified and section 3.2.1 of this report should be referred to for the definition.

<u>PROGRAM NOTATION</u>	<u>ALGEBRAIC NOTATION</u>
CST2(I)	cosine of orientation angle of I^{th} fuselage panel (see section I-5)
FVN(J,K)	aerodynamic influence coefficient representing the influence of the K^{th} panel at the J^{th} control point
II,IF	index of the influencing panel; $II = IF$
NFU	input, item 4; $NFU = 0$, no fuselage
NPANLS	number of constant u-velocity panels on left wing panel.
NPTOT	total number of constant u-velocity panels
NPY	input, item 4; $NPY = 0$, no pylon
N1P	$NPANLS + 1$
N2	number of constant u-velocity panels on wing and pylon
N2P	$N2 + 1$
SNT2(I)	sine of orientation angle of I^{th} fuselage panel (see section I-5)
VP	influence coefficient associated with function F_v of equation (12)
WP	influence coefficient associated with function F_w of equation (12)
WW	influence coefficient normal to the body surface at a specified fuselage control point
XCPT(I)	x_w coordinate of I^{th} control point
YCPT(I)	y_w coordinate of I^{th} control point
ZCPT(I)	z_w coordinate of I^{th} control point

TABLE I-5

DICTIONARY OF NOTATION IN SUBROUTINE DPRHS

The following list presents most of the variable names used in subroutine DPRHS. Where possible a variable name is identified by a symbol in the list of symbols or an equation number in reference 1. Where a variable is an input quantity it is so identified and section 3.2.1 of this report should be referred to for the definition. The store coordinate system is shown in the sketch in section I-11, the fuselage coordinate system in figure 5, and the wing coordinate system in figure 6.

<u>PROGRAM NOTATION</u>	<u>ALGEBRAIC NOTATION</u>
ALFACR	α_f , radians; α_f in degrees was input in item 3
ALPHAL(J)	$\tan(\alpha_j)$; input, item 16
CENTER	logical variable, TRUE, if pylon is located under the fuselage centerline
CIR	array containing the right-hand sides of equations (9), (10), and (11)
CSIBCR(K)	$\cos[SIC(K)]$; SIC(K) was input, item 24
CST2(I)	cosine of the orientation angle of I^{th} fuselage interference panel
FDS	array containing the strengths of the fuselage doublet distribution
FSS	array containing the strengths of the fuselage source distribution
FXL	array containing the x positions of the fuselage singularity origins; positive, measured from tip of nose
II,IF	initial and final values, respectively, of thickness panel index
MS	number of wing thickness panels
NFSOR	input, item 9
NFU	input, item 4; NFU = 0, no fuselage
NPANLS	number of constant u-velocity panels on wing
NPTOT	number of constant u-velocity panels on wing, pylon, and fuselage

Table I-5.- Continued.

NPY	input, item 4; NPY = 0, no pylon
NSSOR(K)	MSOR associated with K^{th} store; MSOR was input in item 26
NSTRS	input, item 4; NSTRS limited to one in present program
NTHP	number of thickness panels on wing and pylon
N1P	NPANLS + 1
N2	number of constant u-velocity panels on wing and pylon
N2P	N2 + 1
SDS	array containing the strengths of the doublet distribution for the K^{th} store
SLTHC(K)	input, item 24
SNT2(I)	sine of the orientation angle of the I^{th} fuselage interference panel
SSIBCR(K)	$\sin[\text{SIC}(K)]$; SIC(K) was input, item 24
SSS	array containing the strengths of the source distribution for the K^{th} store
SXL	array containing the x positions of the singularity origins for the K^{th} store; positive, measured from tip of store nose
UEI(I)	$u_{w_{i,v}}/V_{\infty}$ at $v = I^{\text{th}}$ control point
UP	u/V_{∞} perturbation velocity at a control point due to pylon or wing thickness
UQ	u/V_{∞} perturbation velocity at a control point due to fuselage or store body singularities
US	store induced u/V_{∞} perturbation velocity, not corrected for store incidence
VEI(I)	$v_{w_{i,v}}/V_{\infty}$ at the $v = I^{\text{th}}$ control point
VP	v/V_{∞} perturbation velocity at a control point due to wing or pylon thickness
VQ	v/V_{∞} perturbation velocity at a control point due to fuselage or store body singularities

Table I-5.- Concluded.

WEI(I)	$w_{W_{i,v}}/V_{\infty}$ at the $v = I^{th}$ control point
WP	w/V_{∞} perturbation velocity at a control point due to wing or pylon thickness
WQ	w/V_{∞} perturbation velocity at a control point due to fuselage or store body singularities
WS	store induced w/V_{∞} perturbation velocity, not corrected for store incidence
WW	perturbation velocity normal to fuselage surface at a fuselage control point
XBWOC	input, item 11
XCPT(I)	x_W coordinate of I^{th} control point
XVC	x_B coordinate of a control point
XVCS	x coordinate of a control point in store coordinate system
XWSOC(K)	x_W coordinate of tip of nose of K^{th} store
YCPT(I)	y_W coordinate of I^{th} control point
YVCS	y coordinate of a control point in the store coordinate system
YWSO(K)	y_W coordinate of tip of nose of K^{th} store
ZBWO	input, item 11
ZCPT(I)	z_W coordinate of I^{th} control point
ZVC	z_B coordinate of a control point
ZVCS	z coordinate of a control point in the store coordinate system
ZWSO(K)	z_W coordinate of tip of nose of K^{th} store

TABLE I-6

DICTIONARY OF NOTATION IN SUBROUTINE FUSEIO

The following list presents most of the variable names used in subroutine FUSEIO. Where possible a variable name is identified by a symbol in the list of symbols. Where a variable is an input quantity it is so identified and section 3.2.1 of this report should be referred to for the definition.

<u>PROGRAM NOTATION</u>	<u>ALGEBRAIC NOTATION</u>
ALFACR	α_f , radians; α_f in degrees was input in item 3
BODYPL	input, item 10
FCOEF	input, item 8
FDS	array containing the strengths of the fuselage doublet distribution
FLTHC	input, item 5
FRMAX	input, item 5
FSS	array containing the strengths of the fuselage source distribution
FXEND	input, item 7
FXL	array containing the x positions of the fuselage sources; positive, measured from tip of nose
NBD	number of constant u-velocity panels in a ring on fuselage; NBD CR1 + NBD CR2
NBDCR1	input, item 9
NBDCR2	input, item 9
NCWB	input, item 9
NFPOLY	input, item 6
NFSOR	input, item 9
NXBODY	NFSOR + 1

TABLE I-7

DICTIONARY OF NOTATION IN SUBROUTINE NUMACH

The following list presents most of the variable names used in subroutine NUMACH. Where possible a variable name is identified by a symbol in the list of symbols or an equation number in reference 1. Where a variable is an input quantity it is so identified and section 3.2.1 of this report should be referred to for the definition. The x_W, y_W, z_W coordinate system is shown in figure 6.

<u>PROGRAM NOTATION</u>	<u>ALGEBRAIC NOTATION</u>
ANGNU1	v_1 , degrees, equation (26)
ANGNU2	v_2 , degrees, equation (25)
BETA	$(M_\infty^2 - 1)^{1/2}$
BETANU	$(M_\ell^2 - 1)^{1/2}$
CHRD	length of local wing chord at field point y_W location
DELTW	change in downward velocity induced by wing thickness at points in XT4 traverse
DELX	$(XT4 - XT3)/20$
DELX1	x interval size used in velocity traverse in determining XT3 and XT4
FDS	array containing fuselage doublet strengths
FNUMCH	M_ℓ , equation (28)
FSS	array containing fuselage source strengths
FXL	array containing x locations of fuselage singularity origins; positive, measured from tip of nose
IF	final index value of panels included in sum of induced velocities representing a particular aircraft component
II	initial index value of panels included in sum of induced velocities representing a particular aircraft component
INUMCH	control constant; INUMCH = 0, velocity calculations performed using M_∞ ; INUMCH = 1, velocity calculations performed using M_ℓ
MS	number of thickness panels on the wing

Table I-7.- Continued.

MSWP	MSW + 1; MSW was input item 13
NCW	input, item 13
NFSOR	input, item 9
NFU	input, item 4; NFU = 0, no fuselage
NORDWS	3; degree of least squares polynomials used to smooth velocities
NPANLS	number of wing constant u-velocity panels
NPTOT	number of constant u-velocity panels on wing, pylon, and fuselage
NPTSSM	number of velocity data points included in least squares fit
N2P	N2 + 1; N2 is the number of constant u-velocity panels on wing and pylon
S	scratch array required by subroutine FLSQFY
TANNU	$\tan \Delta v$, equation (23)
TNU	$\tan^{-1}(\text{TANNU})$, degrees
UP	u/V_{∞} perturbation velocity at a point due to an aircraft component
UTU	sum of u/V_{∞} perturbation velocities at a point due to wing-fuselage aircraft components
VEL	array containing the three velocity component vectors to be fit by least squares polynomial
VP	v/V_{∞} perturbation velocity at a point due to an aircraft component
VTV	sum of v/V_{∞} perturbation velocities at a point due to wing-fuselage aircraft components
W	array of positive weights used in calculating least squares fit; $w_i = 1$, $i = 1, \dots, \text{NPTSSM}$
WLEX	x_w coordinate of wing leading edge at field point y_w location
WP	w/V_{∞} perturbation velocity at a point due to an aircraft component
WSAVE	test value of w/V_{∞} velocity at a traverse point due to wing thickness; used in determining XT3 and XT4

Table I-7.- Continued.

WSCOE	array containing three column vectors of least squares polynomial coefficients, in row order of increasing degree
WTEX	x_W coordinate of wing trailing edge at field point y_W location
WTW	sum of w/V_∞ perturbation velocity at a point due to wing-fuselage aircraft components
X	x_W coordinate of point at which velocities due to wing thickness are calculated in determining XT3 and XT4
XBWOC	input, item 11
XLB(I)	x_W coordinate of left rear corner of I^{th} constant u-velocity panel
XLF(I)	x_W coordinate of left front corner of I^{th} constant u-velocity panel
XRBI(I)	x_W coordinate of right rear corner of I^{th} constant u-velocity panel
XRF(I)	x_W coordinate of right front corner of I^{th} constant u-velocity panel
XSAVE	x_W location of traverse point at which perturbation velocity WSAVE occurs
XSHFTW	midpoint of XT3, XT4 range based on local Mach number
XSM	vector of x coordinates of data points to be fit by least squares polynomial
XT3	x_W location of point on traverse at which first non-zero w/V_∞ velocity due to wing thickness is calculated
XT4	x_W location of point on traverse at which magnitude of decrease in w/V_∞ velocity due to wing thickness is at least 50 percent; $XT4 \leq XT3 - 0.7 \cdot CHRD$
Y	y_W location of field point at which flow field is to be calculated
YLC(I)	y_W coordinate of left edge of I^{th} constant u-velocity panel
YNU	p, equation (27)

Table I-7.- Concluded.

Z	z_w location of field point at which flow field is to be calculated
ZB	z in fuselage coordinate system
ZBWO	input, item 11

TABLE I-8

DICTIONARY OF NOTATION IN SUBROUTINE PLYOUT

The following list presents most of the variable names used in subroutine PLYOUT. Where possible a variable name is identified by a symbol in the list of symbols. Where a variable is an input quantity it is so identified and section 3.2.1 of this report should be referred to for the definition. The x_w, y_w, z_w coordinate system is shown in figure 6. If not specified, the panels referred to in this dictionary are constant u-velocity panels located on the pylon.

<u>PROGRAM NOTATION</u>	<u>ALGEBRAIC NOTATION</u>
CRP	length of pylon root-chord; input, item 19
CSIDE	length of local pylon chord along outboard side of chordwise row
CSIDEP	length of local pylon chord along inboard side of chordwise row
DTOR	degrees to radians conversion factor; $\pi/180$
FAC	FAC = 0.95; used to locate control point at 95 percent of chord containing panel centroid
HP	pylon height; input, item 19
IP	input, item 19
JLE	array index of first pylon panel in a chordwise row
KMAX	MSP + 1
MP	number of constant u-velocity panels on pylon
MSP	input, item 20
NCP	input, item 20
NCW	number of panels in a chordwise row on wing; input, item 13
NPANLS	number of constant u-velocity panels on wing
PLEX	XLF(JLE)
PSIPLE	sweep angle of pylon leading edge; input, item 19
PSIPTE	sweep angle of pylon trailing edge; input, item 19

Table I-8.- Concluded.

PSLPDF	SLLE-SLTE
SLLE	$\tan(\text{PSIPLE})$
SLTE	$\tan(\text{PSIPTE})$
SWIPPLE(I)	leading-edge slope of I^{th} panel
SWPTE(I)	trailing-edge slope of I^{th} panel
XCPT(I)	x_W coordinate of control point on I^{th} panel
XLB(I)	x_W coordinate of left rear corner of I^{th} panel
XLF(I)	x_W coordinate of left front corner of I^{th} panel
XPLE	input, item 19
XRB(I)	x_W coordinate of right rear corner of I^{th} panel
XRF(I)	x_W coordinate of right front corner of I^{th} panel
Y(IP)	Y_W location of pylon
YCPT(I)	Y_W coordinate of control point on I^{th} panel
YLC(I)	Y_W location of left edge of I^{th} panel
YPL	$Y(\text{IP})$, $\text{IP} \geq 1$; 0, $\text{IP} = 0$
YRC(I)	Y_W location of right edge of I^{th} panel
Z(K)	input, item 21
ZBAR	z_W location of panel centroid
ZCPT(I)	z_W coordinate of control point on I^{th} panel
ZLC(I)	z_W coordinate of left edge of I^{th} panel
ZRC(I)	z_W coordinate of right edge of I^{th} panel

AD-A031 388

NIELSEN ENGINEERING AND RESEARCH INC MOUNTAIN VIEW CALIF F/G 1/3
PREDICTION OF SUPERSONIC STORE SEPARATION CHARACTERISTICS. VOLU--ETC(U)
MAY 76 F K GOODWIN, M M KEIRSTEAD F33615-75-C-3053

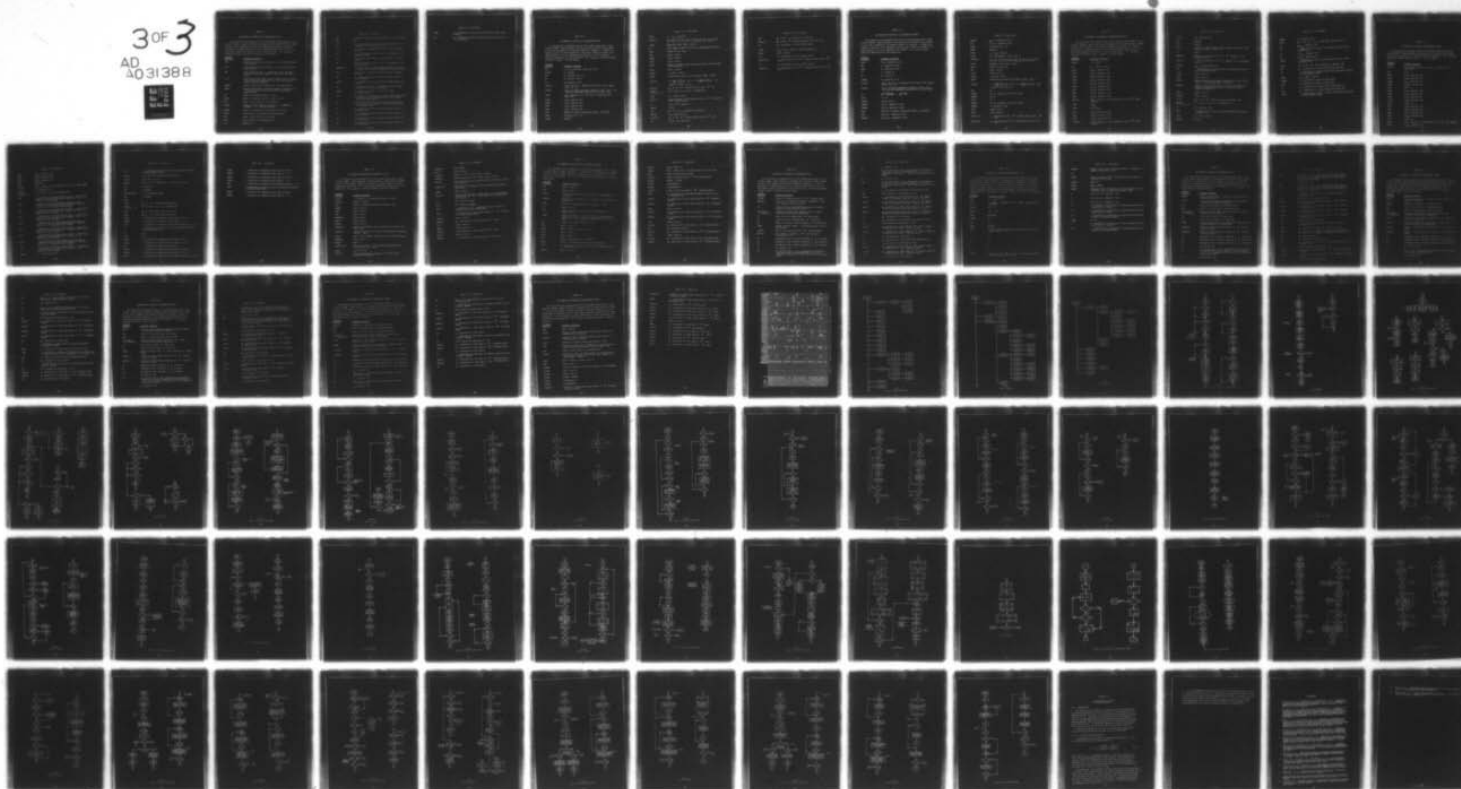
UNCLASSIFIED

NEAR-TR-106

AFFDL-TR-76-41-VOL-2

NL

3 OF 3
AD
A031388



END

DATE
FILMED
12-76

388

TABLE I-9

DICTIONARY OF NOTATION IN SUBROUTINE RESVEL

The following list presents most of the variable names used in subroutine RESVEL. Where possible a variable name is identified by a symbol in the list of symbols or an equation number in reference 1. Where a variable is an input quantity it is so identified and section 3.2.1 of this report should be referred to for the definition. The x_W, y_W, z_W coordinate system is shown in figure 6 of this report.

<u>PROGRAM NOTATION</u>	<u>ALGEBRAIC NOTATION</u>
FDS	array containing the strengths of the fuselage doublet distribution
FSS	array containing the strengths of the fuselage source distribution
FXL	array containing the x positions of the fuselage singularity origins; positive, measured from tip of nose
II,IF	initial and final index values, respectively, of panels which induce perturbation velocities representing a given aircraft component
INUMCH	control index used in subroutines VELO and VELOTH
ISMTH	control index used to determine whether velocities are to be calculated using least-squares polynomial approximation
MS	number of thickness panels on wing
NFSOR	number of fuselage sources; input, item 9
NFU	input, item 4; NFU = 0, no fuselage
NORDWS	degree of least squares polynomial; $1 \leq \text{NORDWS} \leq 5$ (NORDWS = 3 in present program)
NPANLS	number of constant u-velocity panels on wing
NPTOT	total number of constant u-velocity panels
NPY	input, item 4; NPY = 0, no pylon
NTHP	total number of thickness panels
N1P	NPANLS + 1

Table I-9.- Continued.

N2	number of constant u-velocity panels on wing and pylon
N2P	$N2 + 1$
UP	u/V_{∞} perturbation velocity at field point due to a component of the parent aircraft
UTU	sum of u/V_{∞} perturbation velocities due to parent aircraft
VP	v/V_{∞} perturbation velocity due to a component of the parent aircraft
VTU	sum of v/V_{∞} perturbation velocities due to parent aircraft
WP	w/V_{∞} perturbation velocity due to a component of the parent aircraft
WSCOE(I,J)	I^{th} coefficient in least squares polynomial used to calculate J^{th} velocity component; $1 \leq I \leq 6, J=1,2,3$
WTW	sum of w/V_{∞} perturbation velocities due to parent aircraft
XB	$x_{B_{\text{be}}}$ coordinate of point at which velocity field is to be calculated
XBWOC	$x_{B_{\text{item 11}}}$ coordinate of wing root-chord leading edge; input
XP	x location, relative to XSHFTW, of point at which velocity field is to be calculated
XSHFTW	x_w location of center of XT3, XT4 range; $1/2(XT3 + XT4)$
XT3	x_w location of beginning of region within which velocity field is to be calculated using least squares polynomial approximation
XT4	x_w location of end of region within which velocity field is to be calculated using least square polynomial approximation
XW	$x_{w_{\text{be}}}$ coordinate of point at which velocity field is to be calculated
YB	$y_{B_{\text{be}}}$ coordinate of point at which velocity field is to be calculated
YW	$y_{w_{\text{be}}}$ coordinate of point at which velocity field is to be calculated
ZB	$z_{B_{\text{be}}}$ coordinate of point at which velocity field is to be calculated

Table I-9.- Concluded.

ZBWO	z_B coordinate of wing root-chord leading edge; input item 11
ZW	z_W coordinate of point at which velocity field is to be calculated

Table I-10

DICTIONARY OF NOTATION IN SUBROUTINE SEMFOR

The following list presents most of the variable names used in subroutine SEMFOR. Where possible a variable name is identified by a symbol in the list of symbols or an equation number in reference 4. Symbols in figures 8 and 10 of that reference are also used. Where a variable is an input quantity, it is so identified and section 3.2.1 of this report should be referred to for the definition. The x_B, y_B, z_B coordinate system is shown in figure 5 of this report.

<u>PROGRAM NOTATION</u>	<u>ALGEBRAIC NOTATION</u>
ABU	$\alpha_u + \beta_u$, equations (I-28) and (I-37)
ALFACR	α_f , radians
ANG	ϕ_f , radians (fig. 10)
AS	α_s , equation (I-16)
BS	β_s , equation (I-20)
CCL3(K)	$(cc_\ell)_3$ and $(cc_\ell)_4$, equations (I-14) and (I-19); equal since $s_h = s_v$
CCL5(K)	$(cc_\ell)_5$ if planar empennage, equation (I-29); $(cc_\ell)_6$ if cruciform empennage, equations (I-38) and (I-51)
CLLEM	$(C_\ell)_E$, equations (62) and (I-30) or equations (63) and (I-52)
CLMEM	$(C_m)_E$, equation (60)
CLNEM	$(C_n)_E$, equation (61)
CNEM	$(C_N)_E$, equation (58)
CYEM	$(C_Y)_E$, equation (59)
DTOR	degrees to radians conversion factor, 1/57.29578
FCONA	$(dC_L/d\alpha)_H / \pi (s_h - a)^2$
FCONB	$FCONA / l_R$

Table I-10.- Continued.

FCONC	$l_f - x_{s,m}$, figure 8
FROLE(K)	$\phi_f + 90^\circ$ for fin 1, $\phi_f + 270^\circ$ for fin 2, $\phi_f + 180^\circ$ for fin 3, ϕ_f for fin 4; radians; see figure 10
IPLNR	empennage type; input, item 36
IT	body segment number at which the empennage forces act
JMAX	number of tail fins
MSF	input, item 36
NDAMP	input, item 30
NGAM	input, item 30
NHSEG	number of points along store axis where velocity field was calculated
NROLL	input, item 30
PHIROL	ϕ_f ; input, item 37
RADAV	average body radius in fin region; input, item 37
RFIN(K)	$a + \left(\frac{K-1}{MSF-1}\right)(s_h - a)$ or $a + \left(\frac{K-1}{MSF-1}\right)(s_v - a)$; figure 10 with $s_h = s_v$
UTL(K,J)	U_s^* at the k^{th} control point on the j^{th} fin
VAR(N) N = 1,2,...12	$\xi, \dot{\eta}, \dot{\zeta}, p, q, r, \xi, \eta, \zeta, \psi, \theta, \phi$, respectively
VINF	V_∞ ; input, item 3
VN(K,J)	velocity normal to the surface of the j^{th} fin at the k^{th} control point
VO	$V_O/V_{\infty s}$, see figure 10
VRATIO	$V_\infty/V_{\infty s}$
VSO	V_s^* in the y_s direction of figure 10
VSTORE	$V_{\infty s}$, equation (41)
VTL(K,J)	V_s^* at the k^{th} control point on the j^{th} fin
WO	$W_O/V_{\infty s}$, see figure 10

Table I-10.- Concluded.

WSO	W_s^* in the z_s direction of figure 10
WTL(K,J)	W_s^* at the k^{th} control point on the j^{th} fin
XB	x_B coordinate of a fin control point
XMOM	$x_{s,m}$; input, item 32, positive quantity
XTAIL	input, item 37
YB	y_B coordinate of a fin control point
YTAIL(K,J)	$y_{s_{fin}}$ coordinate of the k^{th} control point on the j^{th}
ZB	z_B coordinate of a fin control point
ZTAIL(K,J)	$z_{s_{fin}}$ coordinate of the k^{th} control point on the j^{th}

TABLE I-11

DICTIONARY OF NOTATION IN SUBROUTINE SEMPIN

The following list presents most of the variable names used in subroutine SEMPIN. Where possible a variable name is identified by a symbol in the list of symbols or an equation number in reference 4. Symbols in figures 8 and 10 of that reference are also used. Where a variable is an input quantity, it is so identified and section 3.2.1 of this report should be referred to for the definition.

<u>PROGRAM NOTATION</u>	<u>ALGEBRAIC NOTATION</u>
AKK1	$K(k_1)$, equation (I-43)
AK1	k_1 , equation (I-42)
ARG3	A_1 , equation (I-44)
A2	a^2 , figure 10
A4	a^4 , figure 10
CAPRSQ	R^2 , equation (I-39)
CCL3(K)	$(cc)_3$ and $(cc)_4$, equations (I-14) and (I-19); equal since $s_h = s_v$
CCL5(K)	$(cc)_5$ if planar empennage, equation (I-29); $(cc)_6$ if cruciform empennage, equations (I-38) and (I-51)
CK	$\sqrt{1 - AK1*AK1} = \sqrt{1 - k_1^2}$
CKCK	$1 - k_1^2$
CLALPH	input, item 37
CTWGAM	$\cos 2\gamma$, equation (I-41)
CTWTHE	$\cos 2\theta$, equation (I-40)
DTOR	degrees to radians conversion factor, 1/57.29578
EAK	$E(A_1, k_1)$, equation (I-49)
EPIO2K	$E(\pi/2, k_1)$, equation (I-48)

Table I-11.- Concluded.

ESTRMX	a_{\max} of separated store
FAK	$F(A_1, k_1)$, equation (I-47)
FCONA	$(dC_L/d\alpha)_H/\pi(s_h - a)^2$
FCONB	$FCONA/l_R$
FCONC	$l_f - x_{s,m}$, figure 8
FINSS	tail fin semispan; input, item 37
FROLE(K)	$\phi_f + 90^\circ$ for fin 1, $\phi_f + 270^\circ$ for fin 2, $\phi_f + 180^\circ$ for fin 3, ϕ_f for fin 4; radians; see figure 10
IPLNR	empennage type; input, item 36
JMAX	number of tail fins
MSF	input, item 36
NROLL	input, item 30
PHIROL	ϕ_f ; input, item 37
RADAV	average body radius in fin region; input, item 37
RFIN(K)	$a + \left(\frac{K-1}{MSF-1} \right) (s_h - a)$ or $a + \left(\frac{K-1}{MSF-1} \right) (s_v - a)$; figure 10 with $s_h = s_v$
SHS	s_h^2
STWGAM	$\sin 2\gamma$, equations (I-41) and (I-42)
STWTHE	$\sin 2\theta$
TOVPI	$2/\pi$
TTWGAM	$\tan 2\gamma$, equations (I-41) and (I-42)
TWOTHE	2θ , equation (I-40)
XMOM	input, item 32
XTAIL	input, item 37
YTAIL(K,J)	y_s coordinate of the k^{th} control point on the j^{th} fin
ZTAIL(K,J)	z_s coordinate of the k^{th} control point on the j^{th} fin

TABLE I-12

DICTIONARY OF NOTATION IN SUBROUTINE SFORCE

The following list presents most of the variable names used in subroutine SFORCE. Where possible a variable name is identified by a symbol in the list of symbols or an equation number in reference 4. Where a variable is an input quantity, it is so identified and section 3.2.1 of this report should be referred to for the definition. The x_B, y_B, z_B coordinate system is shown in figure 5 of this report.

<u>PROGRAM NOTATION</u>	<u>ALGEBRAIC NOTATION</u>
ALFACR	α_f , radians
CDC	c_{d_c} ; input, item 35
CLMBY	$(C_m)_{BY}$, equation (44)
CLMCF	$(C_m)_{CF}$, equation (53)
CLMSB	$(C_m)_{SB}$, equation (48)
CLNBY	$(C_n)_{BY}$, equation (45)
CLNCF	$(C_n)_{CF}$, equation (54)
CLNSB	$(C_n)_{SB}$, equation (49)
CNBY	$(C_N)_{BY}$, equation (42)
CNCF	$(C_N)_{CF}$, equation (51)
CNSB	$(C_N)_{SB}$, equation (46)
CNX(NN)	total dC_N/dx_s at the midpoint of the NN^{th} body segment
CONA	$2/a_{max}^2$
CONB	$2c_{d_c}/\pi a_{max}^2$
CYBY	$(C_Y)_{BY}$, equation (43)
CYCF	$(C_Y)_{CF}$, equation (52)
CYSB	$(C_Y)_{SB}$, equation (47)
CYX(NN)	total dC_Y/dx_s at the midpoint of the NN^{th} body segment

Table I-12.- Continued.

DC(I,J)	[A], equation (28)
DCN	dC_N/dx_s
DCY	dC_Y/dx_s
DELX	length of a body segment; store length divided by NSEG which was input in item 30
DX	DELX/2
EDRDX(I)	da/dx_s at the midpoint of the i^{th} segment of the separated store
ERAD(I)	a at the midpoint of the i^{th} segment of the separated store
ESTRMX	a_{max} of separated store
ETA	η coordinate of point on store axis measured relative to store moment center
NDAMP	input, item 30
NGAM	input, item 30
NHSEG	number of points along store axis where velocity field is to be calculated; $NHSEG = 2*NSEG + 1$
NHSEGO	number of points along store axis ahead of separation point where velocity field is to be calculated; $NHSEGO = 2*NSEG + 1$
NSEG	input, item 30
NSEGXO	input, item 30
UT(N)	U_s^* at the N^{th} point along body, equation (40)
VAR(N), N = 1,2,...12	$\dot{\xi}, \dot{\eta}, \dot{\zeta}, p, q, r, \xi, \eta, \zeta, \psi, \theta, \phi$ respectively
VC	V_c^* , equation (55)
VETA	η component of the store free-stream velocity vector, equation (32)
VINF	V_∞ ; input, item 3
VRATIO	$V_\infty/V_{\infty s}$

Table I-12.- Concluded.

VSTORE	$V_{\infty s}$, equation (41)
VT(N)	V_s^* at the N^{th} point along body, equation (40)
VX	$U_{\infty s, x_s}$ equation (35)
VXI	ξ component of the store free-stream velocity vector, equation (32)
VY	$-V_{\infty s, y_s}$ equation (35)
VZ	$W_{\infty s, z_s}$ equation (35)
VZETA	ζ component of the store free-stream velocity vector, equation (32)
WT(N)	W_s^* at the N^{th} point along body, equation (40)
XB	x_B coordinate of a point along store body axis
XI	ξ coordinate of a point on store axis measured relative to store moment center
XMOM	$x_{s, m}$; input, item 32
XSTOR	x_s coordinate of point on store axis
XXX	x coordinate of point on store axis
YB	y_B coordinate of a point along store body axis
ZB	z_B coordinate of a point along store body axis
ZETA	ζ coordinate of a point on store axis measured relative to store moment center

TABLE I-13

DICTIONARY OF NOTATION IN SUBROUTINE SOUTPT

The following list presents most of the variable names used in sub-routine SOUTPT. Where possible a variable name is identified by a symbol in the list of symbols or an equation number in reference 4. The x_B, y_B, z_B coordinate system is shown in figure 5 of this report.

<u>PROGRAM NOTATION</u>	<u>ALGEBRAIC NOTATION</u>
CLLEM	$(C_\ell)_E$, equations (62) and (I-30) or equations (63) and (I-52)
CLLT	total C_ℓ
CLMBY	$(C_m)_{BY}$, equation (44)
CLMCF	$(C_m)_{CF}$, equation (53)
CLMEM	$(C_m)_E$, equation (60)
CLMSB	$(C_m)_{SB}$, equation (48)
CLMT	total C_m
CLNBY	$(C_n)_{BY}$, equation (45)
CLNCF	$(C_n)_{CF}$, equation (54)
CLNEM	$(C_n)_E$, equation (61)
CLNSB	$(C_n)_{SB}$, equation (49)
CLNT	total C_n
CNBY	$(C_N)_{BY}$, equation (42)
CNCF	$(C_N)_{CF}$, equation (51)
CNEM	$(C_N)_E$, equation (58)
CNSB	$(C_N)_{SB}$, equation (46)
CNT	total C_N
CNX(K)	total dC_N/dx_s at the midpoint of the K^{th} body segment
CYBY	$(C_Y)_{BY}$, equation (43)

Table I-13. - Continued.

CYCF	$(C_Y)_{CF}$, equation (52)
CYEM	$(C_Y)_E$, equation (59)
CYSB	$(C_Y)_{SB}$, equation (47)
CYT	total C_Y
CYX(K)	total dC_Y/dx_s at the midpoint of the K^{th} body segment
DC(I,J)	$[A]$, equation (28)
DVAR(N), N=1,2,...12	$\ddot{\xi}, \ddot{\eta}, \ddot{\zeta}, \dot{p}, \dot{q}, \dot{r}, \dot{\xi}, \dot{\eta}, \dot{\zeta}, \dot{\psi}, \dot{\theta}, \dot{\phi}$ respectively
DXB	ξ coordinate of the store base at time t relative to where it would have been had it remained in the $t = 0$ position on the aircraft
DXCG	ξ coordinate of the store moment center at time t relative to where it would have been had it remained in the $t = 0$ position on the aircraft
DXN	ξ coordinate of the store nose at time t relative to where it would have been had it remained in the $t = 0$ position on the aircraft
DYB	η coordinate of the store base at time t relative to where it would have been had it remained in the $t = 0$ position on the aircraft
DYCG	η coordinate of the store moment center at time t relative to where it would have been had it remained in the $t = 0$ position on the aircraft
DYN	η coordinate of the store nose at time t relative to where it would have been had it remained in the $t = 0$ position on the aircraft
DZB	ζ coordinate of the store base at time t relative to where it would have been had it remained in the $t = 0$ position on the aircraft
DZCG	ζ coordinate of the store moment center at time t relative to where it would have been had it remained in the $t = 0$ position on the aircraft
DZN	ζ coordinate of the store nose at time t relative to where it would have been had it remained in the $t = 0$ position on the aircraft
ESTLGC	l_s of separated store

Table I-13.- Continued.

ETA	η coordinate of point on store axis measured relative to store moment center
EXST(J)	x_s at the J^{th} point along store axis
FTHRUS	store thrust force
NTHRUS	input, item 30; NTHRUS = 0, no thrust calculated
PHI	ϕ , degrees
PSI	ψ , degrees
SLTHC(NEJSTR)	ℓ_s of separated store
THA	θ , degrees
TIME	t
UT(J)	U_s^* at J^{th} point along store axis
VAR(N), N = 1,2,...12	$\dot{\xi}, \dot{\eta}, \dot{\zeta}, p, q, r, \xi, \eta, \zeta, \psi, \theta, \phi$ respectively
VT(J)	V_s^* at J^{th} point along store axis
WT(J)	W_s^* at J^{th} point along store axis
XBASE	ξ coordinate of separated store base at time t
XBASEI	ξ coordinate of separated store base at $t = 0$
XCGI	ξ coordinate of separated store moment center at $t = 0$
XI	ξ coordinate of point on store axis measured relative to store moment center
XL	x_s / ℓ_s
XMOM	$x_{s,m}$
XNOSE	ξ coordinate of separated store nose at time t
XNOSEI	ξ coordinate of separated store nose at $t = 0$
XXX	x coordinate of point on store axis
YBASE	η coordinate of separated store base at time t
YBASEI	η coordinate of separated store base at $t = 0$
YCGI	η coordinate of separated store moment center at $t = 0$

Table I-13.- Concluded.

YNOSE	η coordinate of separated store nose at time t
YNOSEI	η coordinate of separated store nose at $t = 0$
ZBASE	ζ coordinate of separated store base at time t
ZBASEI	ζ coordinate of separated store base at $t = 0$
ZCGI	ζ coordinate of separated store moment center at $t = 0$
ZETA	ζ coordinate of point on store axis measured relative to store moment center
ZNOSE	ζ coordinate of separated store nose at time t
ZNOSEI	ζ coordinate of separated store nose at $t = 0$

TABLE I-14

DICTIONARY OF NOTATION IN SUBROUTINE STORIO

The following list presents most of the variable names used in subroutine STORIO. Where possible a variable name is identified by a symbol in the list of symbols. Where a variable is an input quantity it is so identified and section 3.2.1 of this report should be referred to for the definition. The x_W, y_W, z_W coordinate system is shown in figure 6.

<u>PROGRAM NOTATION</u>	<u>ALGEBRAIC NOTATION</u>
ALFACR	α_f , radians; α_f in degrees was input in item 3
ALFAS(K)	ALFACR + SIBCR(K)
DTOR	degrees to radians conversion constant; $\pi/180$
MSHAPE	input, item 26
MSOR	input, item 26
NCW	input, item 13
NSHAPE(K)	input, item 24
NSHPT	input, item 25
NSPOLJ	input, item 27
NSPOLY(K)	number of polynomials used to specify the shape of the K^{th} store
NSSOR(K)	number of sources in the source distribution representing the K^{th} store
NSTRS	input, item 4; NSTRS limited to one in present program
NUMSTR(K)	input, item 24
NXBODY	MSOR + 1
SCOEF(I,J,K)	J^{th} coefficient of I^{th} polynomial describing the shape of the K^{th} store
SCOFJ	input, item 29
SDS(L,K)	array containing the strengths of the K^{th} store doublet distribution

Table I-14.- Concluded.

SIBCR(K)	SIC(J)*DTOR
SIC(K)	input, item 24
SLTHC(K)	length of J th store; input, item 24
SRMAX(K)	maximum radius of J th store; input, item 24
SSS(L,K)	array containing the strengths of the K th store source distribution
SXEND(I,K)	end points of polynomial sections specifying shape of K th store
SXNDJ	input, item 28
SXL(L,K)	array containing the x positions of the singularity origins for the K th store; positive, measured from tip of nose
T(J)	J th source strength
TC(J)	J th doublet strength
TX(J)	x location of J th singularity origin; positive, measured from tip of body nose
XRF(J)	x _W coordinate of right front corner of J th constant u-velocity wing panel
XSNC(J)	input, item 24
XWSOC(J)	x _W coordinate of tip of nose of J th store
Y(I)	input, item 14
YSN(J)	input, item 24
YWSO(J)	y _W coordinate of tip of nose of J th store
ZSN(J)	input, item 24
ZWSO(J)	z _W coordinate of tip of nose of J th store

TABLE I-15

DICTIONARY OF NOTATION IN SUBROUTINE THKLYT

The following list presents most of the variable names used in subroutine THKLYT. Where possible a variable name is identified by a symbol in the list of symbols. Where a variable is an input quantity it is so identified and section 3.2.1 of this report should be referred to for the definition.

<u>PROGRAM NOTATION</u>	<u>ALGEBRAIC NOTATION</u>
CRP	input, item 19
CRW	input, item 12
CSIDE	length of local chord on left side of a chordwise row of panels
CSIDEP	length of local chord on right side of a chordwise row of panels
DTOR	degrees to radians conversion constant; $\pi/180$
IP	input, item 19
JLE	index of array location of the first panel in a chordwise row
LVSWP	control variable; if wing leading-edge and trailing-edge sweep angles constant at all spanwise stations, LVSWP = 0; if not constant, LVSWP = 1
MS	number of thickness panels on wing
MSP	input, item 20
MSWP	MSW + 1; MSW was input, item 13
NCPS	input, item 22
NCWS	input, item 17
NPY	input, item 4; NPY = 0, no pylon
NTHP	number of thickness panels on wing and pylon
PLEX	x_w coordinate of pylon leading edge on right side of a chordwise row
PSIWLE	input, item 19

Table I-15.- Concluded.

PSIWTE	input, item 19
PSLPDF	SLLE - SLTE; SLTE is slope of pylon trailing edge
SLLE	slope of pylon leading edge
SLLET(I)	slope of leading edge of I^{th} thickness panel
SLPDIF	SLPWLE - SLPWTE
SLPWLE	$\tan[\text{PSIWLE}(I)]$
SLPWTE	$\tan[\text{PSIWTE}(I)]$
SLTET(I)	slope of trailing edge of I^{th} thickness panel
WLEX	x_{W_a} coordinate of wing leading edge on right side of chordwise row
XLBT(I)	$x_{W_{\text{panel}}}$ coordinate of left rear corner of I^{th} thickness panel
XLFT(I)	$x_{W_{\text{panel}}}$ coordinate of left front corner of I^{th} thickness panel
XPLE	input, item 19
XRBT(I)	$x_{W_{\text{panel}}}$ coordinate of right rear corner of I^{th} thickness panel
XRFT(I)	$x_{W_{\text{panel}}}$ coordinate of right front corner of I^{th} thickness panel
Y(K)	input, item 14
YLCT(I)	y_W coordinate of left side of I^{th} thickness panel
YPL	y_W location of pylon
YRCT(I)	y_W coordinate of right side of I^{th} thickness panel
Z(K)	input, item 21
ZLCT(I)	z_W coordinate of left side of I^{th} thickness panel
ZRCT(I)	z_W coordinate of right side of I^{th} thickness panel

TABLE I-16

DICTIONARY OF NOTATION IN SUBROUTINE VELBD

The following list presents most of the variable names used in subroutine VELBD. Where possible a variable name is identified by a symbol in the list of symbols or an equation number in reference 1. Where a variable is an input quantity it is so identified and section 3.2.1 of this report should be referred to for the definition. The wing coordinate system is shown in figure 6 of this report.

<u>PROGRAM NOTATION</u>	<u>ALGEBRAIC NOTATION</u>
CST2(K)	cosine of orientation angle of k^{th} fuselage panel
DELTP(I)	$1/\pi(u_{+I}/V_{\infty})$; singularity strength, divided by π , of i^{th} constant u-velocity panel
EM	slope of leading edge and trailing edge of fuselage constant u-velocity panels; $EM = 0$
FELT, FELT α $\alpha = A, AI, B, BI$	logical variables; TRUE whenever non-zero corner influence functions are calculated
IF	final value of fuselage panel DO loop index
II	initial value of fuselage panel DO loop index
N2	number of constant u-velocity panels on wing and pylon
PYPNL	logical variable; FALSE if influencing panel is not a pylon panel
SNT2(K)	sine of orientation angle of k^{th} fuselage panel
THTI(K)	polar angle in degrees of k^{th} fuselage panel (see section I-5)
TU	superposed corner influence functions in x_w direction
TV	superposed corner influence functions in y_w direction
TW	superposed corner influence functions in z_w direction
U	F_u , equation (12)
UP	if $II \neq IF$, sum of u/V_{∞} perturbation velocities at field point due to fuselage panels, if $II = IF$, influence coefficient of II^{th} panel and given control point

Table I-16.- Concluded.

V	F_v , equation (12)
VP	if $II \neq IF$, sum of v/V_∞ perturbation velocities at field point due to fuselage panels; if $II = IF$, influence coefficient of II^{th} panel and given control point
W	F_w , equation (12)
WP	if $II \neq IF$, sum of w/V_∞ perturbation velocities at field point due to fuselage panels; if $II = IF$, influence coefficient of II^{th} panel and given control point
X	x_c coordinate of field point (see section I-35)
XI	local subroutine equivalent of XX
XLB(I)	x_w coordinate of left rear corner of I^{th} panel; right is clockwise from left, looking forward
XLF(I)	x_w coordinate of left front corner of I^{th} panel; right is clockwise from left, looking forward
XRBI(I)	x_w coordinate of right rear corner of I^{th} panel; right is clockwise from left, looking forward
XRF(I)	x_w coordinate of right front corner of I^{th} panel; right is clockwise from left, looking forward
XX	x_w coordinate of field point
Y	y_c coordinate of field point (see section I-35)
YI	local subroutine equivalent of YY
YLC(I)	y_w coordinate of left edge of I^{th} panel; right is clockwise from left, looking forward
YRC(I)	y_w coordinate of right edge of I^{th} panel; right is clockwise from left, looking forward
YY	y_w coordinate of field point
Z	z_c coordinate of field point (see section I-35)
ZI	local subroutine equivalent of ZZ
ZLC(I)	z_w coordinate of left edge of I^{th} panel; right is clockwise from left, looking forward
ZRC(I)	z_w coordinate of right edge of I^{th} panel; right is clockwise from left, looking forward
ZZ	z_w coordinate of field point

TABLE I-17

DICTIONARY OF NOTATION IN SUBROUTINE VELO

The following list presents most of the variable names used in subroutine VELO. Where possible a variable name is identified by a symbol in the list of symbols or an equation number in reference 1. Symbols defined in section II-2.1 of that reference are also used. Where a variable is an input quantity it is so identified and section 3.2.1 of this report should be referred to for the definition. The coordinate system associated with a semi-infinite triangle is shown in figure 3 of reference 1.

<u>PROGRAM NOTATION</u>	<u>ALGEBRAIC NOTATION</u>
ARG1	$x^2 - \beta^2(y^2 + z^2)$
BETA	β ; BETANU, if INUMCH = 1 and PYPNL = FALSE; BETAOL otherwise
BETANU	$(M_{\ell}^2 - 1)^{1/2}$
BETAOL	$(M_{\infty}^2 - 1)^{1/2}$
BTSQ	BETA*BETA
BTSQOL	$M_{\infty}^2 - 1$
EML	$M_{\ell e}$
EMLSQ	EML*EML
FELT	logical variable, FALSE when returning from the subroutine with $U = V = W = 0$
F1	F_1
F2	F_2
F4	F_4
F5	F_5
F7	F_7
INSIDE	logical variable; TRUE if point is located inside Mach cone from origin of triangle

Table I-17.- Concluded.

INUMCH	control index used to determine choice of BETANU or BETAOL (see section I-18)
PI	π
PYPNL	logical variable, TRUE if semi-infinite triangle is located on the pylon
ROOTA1	$(\text{ARG1})^{1/2}$
STEST	BTSQ - EMLSQ
TLRNC	tolerance factor related to the wing semispan; used to represent zero in subroutine logical tests
U	$F_u(x,y,z,\beta,\psi)$, equation (12)
V	$F_v(x,y,z,\beta,\psi)$, equation (12)
W	$F_w(x,y,z,\beta,\psi)$, equation (12)
X	x coordinate of field point in system associated with semi-infinite triangle
Y	y coordinate of field point in system associated with semi-infinite triangle
YS	y coordinate of field point in system associated with corner of influencing panel
YZSQ	$y^2 + z^2$
Z	z coordinate of field point in system associated with semi-infinite triangle
ZS	z coordinate of field point in system associated with corner of influencing panel

TABLE I-18

DICTIONARY OF NOTATION IN SUBROUTINE VELPP

The following list presents most of the variable names used in subroutine VELPP. Where possible a variable name is identified by a symbol in the list of symbols or an equation number in reference 1. Where a variable is an input quantity it is so identified and section 3.2.1 of this report should be referred to for the definition. The x_W, y_W, z_W coordinate system is shown in figure 6.

<u>PROGRAM NOTATION</u>	<u>ALGEBRAIC NOTATION</u>
CENTER	logical variable; TRUE if pylon is located under the fuselage centerline
DELTP	$u_+/\pi V_\infty$; array containing constant u-velocity panel singularity strengths, divided by π
EM1	slope of leading edge of influencing panel
EM2	slope of trailing edge of influencing panel
FELT, FELT α $\alpha = A, AI, B, BI$	logical variables; TRUE whenever non-zero influence functions are calculated
IF	final value of panel DO loop index
II	initial value of panel DO loop index
PYPNL	logical variable required by subroutine VELO; TRUE if influencing panel is a pylon panel
SWPPLE(I)	tangent of leading-edge sweep angle of I^{th} constant u-velocity panel
SWPPTE(I)	tangent of trailing-edge sweep angle of I^{th} constant u-velocity panel
TU	superposed corner influence functions in x_W direction
TV	superposed corner influence functions in y_W direction
TW	superposed corner influence functions in z_W direction
U	F_u , equation (12)
UP	if $II \neq IF$, sum of u/V_∞ perturbation velocities at field point due to pylon constant u-velocity panels; if $II = IF$, influence coefficient of II^{th} panel and given control point
V	F_v , equation (12)

Table I-18.- Concluded.

VP	if $II \neq IF$, sum of v/V_∞ perturbation velocities at field point due to pylon constant u-velocity panels; if $II = IF$, influence coefficient of II^{th} panel and given control point
W	F_w , equation (12)
WP	if $II \neq IF$, sum of w/V_∞ perturbation velocities at field point due to pylon constant u-velocity panels; if $II = IF$, influence coefficient of II^{th} panel and given control point
X	x coordinate of field point in system required by subroutine VELO
XI	local subroutine equivalent of XX
XLB(I)	x_w coordinate of left rear corner of I^{th} constant u-velocity panel
XLF(I)	x_w coordinate of left front corner of I^{th} constant u-velocity panel
XRB(I)	x_w coordinate of right rear corner of I^{th} constant u-velocity panel
XRF(I)	x_w coordinate of right front corner of I^{th} constant u-velocity panel
XX	x_w coordinate of field point
Y	y coordinate of field point in system required by subroutine VELO
YDIR	y_c coordinate of field point (see section I-39)
YIMG	y_c coordinate of image of field point with respect to aircraft vertical plane of symmetry (see section I-39)
YPL	y_w location of pylon
YY	y_w coordinate of field point
Z	z coordinate of field point in system required by subroutine VELO
ZI	local subroutine equivalent of ZZ
ZLC(I)	z_{wpanel} coordinate of left edge of I^{th} constant u-velocity panel
ZRC(I)	z_{wpanel} coordinate of right edge of I^{th} constant u-velocity panel
ZZ	z_w coordinate of field point

TABLE I-19

DICTIONARY OF NOTATION IN SUBROUTINE VELPTH

The following list presents most of the variable names used in subroutine VELPTH. Where possible a variable name is identified by a symbol in the list of symbols or an equation number in reference 1. Where a variable is an input quantity it is so identified and section 3.2.1 of this report should be referred to for the definition. The x_W, y_W, z_W coordinate system is shown in figure 6.

<u>PROGRAM</u> <u>NOTATION</u>	<u>ALGEBRAIC NOTATION</u>
CENTER	logical variable; TRUE if pylon is located under the fuselage centerline
DZDX(I)	THETPL(I)/ π ; THETPL(I) was input item 23
EM1	slope of leading edge of influencing panel
EM2	slope of trailing edge of influencing panel
FELT, FELT α $\alpha = A, AI, B, BI$	logical variables; TRUE whenever non-zero corner influence functions are calculated
II, IF	initial and final values, respectively, of influencing panel DO loop index
PYPNL	logical variable used by subroutine VELOTH; TRUE if influencing panel is a pylon panel
SLLET(I)	tangent of leading-edge sweep angle of I^{th} thickness panel
SLTET(I)	tangent of trailing-edge sweep angle of I^{th} thickness panel
TU	superposed corner influence functions in x_W direction
TV	superposed corner influence functions in y_W direction
TW	superposed corner influence functions in z_W direction
U	F_{u_t} , equation (14)
UP	sum of u/V_∞ perturbation velocities at the field point due to pylon thickness panels
V	F_{v_t} , equation (14)

Table I-19.- Concluded.

VP	sum of v/V_∞ perturbation velocities at the field point due to pylon thickness panels
W	F_{w_t} , equation (14)
WP	sum of w/V_∞ perturbation velocities at the field point due to pylon thickness panels
X	x coordinate of field point in system required by subroutine VELOTH
XI	local subroutine equivalent of XX
XLBT(I)	$x_{w_{panel}}$ coordinate of left rear corner of I^{th} thickness
XLFT(I)	$x_{w_{panel}}$ coordinate of left front corner of I^{th} thickness
XRBT(I)	$x_{w_{panel}}$ coordinate of right rear corner of I^{th} thickness
XRFT(I)	$x_{w_{panel}}$ coordinate of right front corner of I^{th} thickness
XX	x_w coordinate of field point
Y	y coordinate of field point in system required by subroutine VELOTH
YDIR	y_c coordinate of field point (see section I-39)
YIMG	y_c coordinate of image of field point with respect to aircraft vertical plane of symmetry (see section I-39)
YPL	y_w location of pylon in wing coordinate system
YY	y_w coordinate of field point
Z	z coordinate of field point in system required by subroutine VELOTH
ZI	local subroutine equivalent of ZZ
ZLCT(I)	z_w coordinate of left edge of I^{th} thickness panel
ZRCT(I)	z_w coordinate of right edge of I^{th} thickness panel
ZZ	z_w coordinate of field point

TABLE I-20

DICTIONARY OF NOTATION IN SUBROUTINE VELWP

The following list presents most of the variable names used in subroutine VELWP. Where possible a variable name is identified by a symbol in the list of symbols or an equation number in reference 1. Where a variable is an input quantity it is so identified and section 3.2.1 of this report should be referred to for the definition. The x_W, y_W, z_W coordinate system is shown in figure 6.

<u>PROGRAM NOTATION</u>	<u>ALGEBRAIC NOTATION</u>
DELTP	$u_+ / (\pi V_\infty)$; array containing constant u-velocity panel singularity strengths, divided by π
EM1	slope of influencing panel leading edge
EM2	slope of influencing panel trailing edge
FELT, FELT α $\alpha = A, AI, B, BI$	logical variable; TRUE whenever non-zero corner influence functions are calculated
IF	final value of panel DO loop index
II	initial value of panel DO loop index
PYPNL	logical variable; TRUE if influencing panel is a pylon panel
SWPPLE(I)	tangent of leading-edge sweep angle of I^{th} constant u-velocity panel
SWPPTE(I)	tangent of trailing-edge sweep angle of I^{th} constant u-velocity panel
TU	superposed corner influence in x_W direction
TV	superposed corner influence in y_W direction
TW	superposed corner influence in z_W direction
U	F_u , equation (12)
UP	if $II \neq IF$, sum of u/V_∞ perturbation velocities at field point due to wing constant u-velocity panels; if $II = IF$, influence coefficient for II^{th} panel and given control point
V	F_v , equation (12)

Table I-20.- Concluded.

VP	if $II \neq IF$, sum of v/V_∞ perturbation velocities at field point due to wing constant u-velocity panels; if $II = IF$, influence coefficient for II^{th} panel and given control point
W	F_w , equation (12)
WP	if $II \neq IF$, sum of w/V_∞ perturbation velocities at field point due to wing constant u-velocity panels; if $II = IF$, influence coefficient for II^{th} panel and given control point
X	x coordinate of field point in system required by subroutine VELO
XI	local subroutine equivalent of XX
XLB(I)	x_w coordinate of left rear corner of I^{th} panel, viewed from the rear
XLF(I)	x_w coordinate of left front corner of I^{th} constant u-velocity panel
XRB(I)	x_w coordinate of right rear corner of I^{th} constant u-velocity panel
XRF(I)	x_w coordinate of right front corner of I^{th} constant u-velocity panel
XX	x_w coordinate of field point
Y	y coordinate of field point in system required by subroutine VELO
YI	local subroutine equivalent of YY
YLC(I)	y_w coordinate of left edge of I^{th} constant u-velocity panel
YRC(I)	y_w coordinate of right edge of I^{th} constant u-velocity panel
YY	y_w coordinate of field point
Z	z coordinate of field point in system required by subroutine VELO
ZZ	z_w coordinate of field point

TABLE I-21

DICTIONARY OF NOTATION IN SUBROUTINE VELWTH

The following list presents most of the variable names used in subroutine VELWTH. Where possible a variable name is identified by a symbol in the list of symbols or an equation number in reference 1. Where a variable is an input quantity it is so identified and section 3.2.1 of this report should be referred to for the definition. The x_w, y_w, z_w coordinate system is shown in figure 6.

PROGRAM
NOTATIONALGEBRAIC NOTATION

DZDX(I)	THETAL(I)/ π ; THETAL(I) was input, item 23
EM1	slope of leading edge of influencing panel
EM2	slope of trailing edge of influencing panel
FELT, FELT α $\alpha = A, AI, B, BI$	logical variable; TRUE whenever non-zero corner influence functions are calculated
II, IF	initial and final values, respectively, of influencing panel DO loop index
PYPNL	logical variable used by subroutine VELOTH; FALSE if influencing panel is a wing panel
SLLET(I)	tangent of leading-edge sweep angle of I^{th} thickness panel
SLTET(I)	tangent of trailing-edge sweep angle of I^{th} thickness panel
TU	superposed corner influence functions in x_w direction
TV	superposed corner influence functions in y_w direction
TW	superposed corner influence functions in z_w direction
U	F_{u_t} , equation (14)
UP	sum of u/V_∞ perturbation velocities due to wing thickness panels
V	F_{v_t} , equation (14)
VP	sum of v/V_∞ perturbation velocities due to wing thickness panels
W	F_{w_t} , equation (14)

Table I-21.- Concluded.

WP	sum of w/V_∞ perturbation velocities due to wing thickness panels
X	x coordinate of field point in system required by sub-routine VELOTH
XI	local subroutine equivalent of XX
XLBT(I)	x_w coordinate of left rear corner of I^{th} thickness panel
XLFT(I)	x_w coordinate of left front corner of I^{th} thickness panel
XRBT(I)	x_w coordinate of right rear corner of I^{th} thickness panel
XRFT(I)	x_w coordinate of right front corner of I^{th} thickness panel
XX	x_w coordinate of field point
Y	y coordinate of field point in system required by sub-routine VELOTH
YI	local subroutine equivalent of YY
YLCT(I)	y_w coordinate of left edge of I^{th} thickness panel
YRCT(I)	y_w coordinate of right edge of I^{th} thickness panel
YY	y_w coordinate of field point
Z	z coordinate of field point in system required by sub-routine VELOTH
ZLCT(I)	z_w coordinate of left edge of I^{th} thickness panel
ZRCT(I)	z_w coordinate of right edge of I^{th} thickness panel
ZZ	z_w coordinate of field point

TABLE I-22

DICTIONARY OF NOTATION IN SUBROUTINE WLYOUT

The following list presents most of the variable names used in subroutine WLYOUT. Where possible a variable name is identified by a symbol in the list of symbols. Where a variable is an input quantity it is so identified and section 3.2.1 of this report should be referred to for the definition. If not specified, panels referred to in this dictionary are constant u-velocity panels. The x_w, y_w, z_w coordinate system is shown in figure 6.

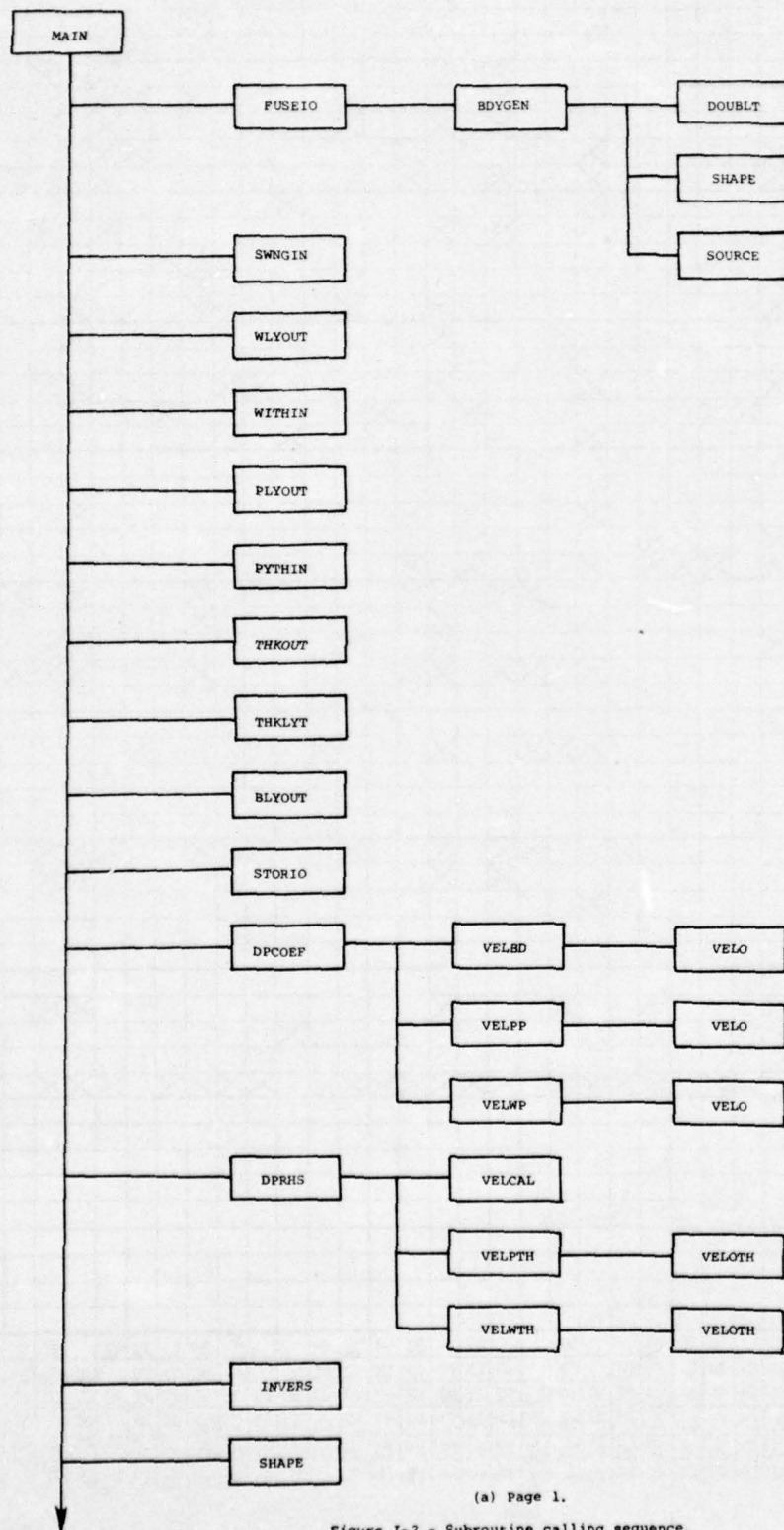
<u>PROGRAM NOTATION</u>	<u>ALGEBRAIC NOTATION</u>
CRW	input, item 12
CSIDE	length of local wing chord along outboard edge of a chordwise row of panels
CSIDEP	length of local wing chord along inboard edge of a chordwise row of panels
DTOR	degrees to radians conversion constant; $\pi/180$
FAC	constant used to locate XCPT(J) at 95 percent of the chord containing the panel centroid; FAC = 0.95
JLE	index of front panel in a chordwise row
LVSWP	control variable; if leading-edge and trailing-edge sweep angles constant for entire wing, LVSWP = 0; if not constant, LVSWP = 1
MSWP	MSW + 1; MSW is input, item 13
NCW	input, item 13
NPANLS	number of constant u-velocity panels on wing; NCW*MSW
PSIWLE	input, item 14
PSIWTE	input, item 14
SLPDIF	SLPWLE - SLPWTE
SLPWLE	$\tan[\text{PSIWLE}(I)]$
SLPWTE	$\tan[\text{PSIWTE}(I)]$
SWPPLE(I)	tangent of leading-edge sweep angle of I^{th} constant u-velocity panel

Table I-22.- Concluded.

SWPTE(I)	tangent of trailing-edge sweep angle of I^{th} constant u-velocity panel
WLEX	x_w coordinate of wing leading edge on right edge of a chordwise row
XCPT(I)	x_w coordinate of I^{th} control point
XLB(I)	x_w coordinate of left rear corner of I^{th} panel
XLF(I)	x_w coordinate of left front corner of I^{th} panel
XRBI(I)	x_w coordinate of right rear corner of I^{th} panel
XRF(I)	x_w coordinate of right front corner of I^{th} panel
Y(I)	input, item 14
YBAR	y_w coordinate of centroid of I^{th} panel
YCPT(I)	y_w coordinate of I^{th} control point
YLC(I)	y_w coordinate of left edge of I^{th} panel
YRC(I)	y_w coordinate of right edge of I^{th} panel
ZCPT(I)	z_w coordinate of I^{th} control point
ZLC(I)	z_w coordinate of left edge of I^{th} panel
ZRC(I)	z_w coordinate of right edge of I^{th} panel

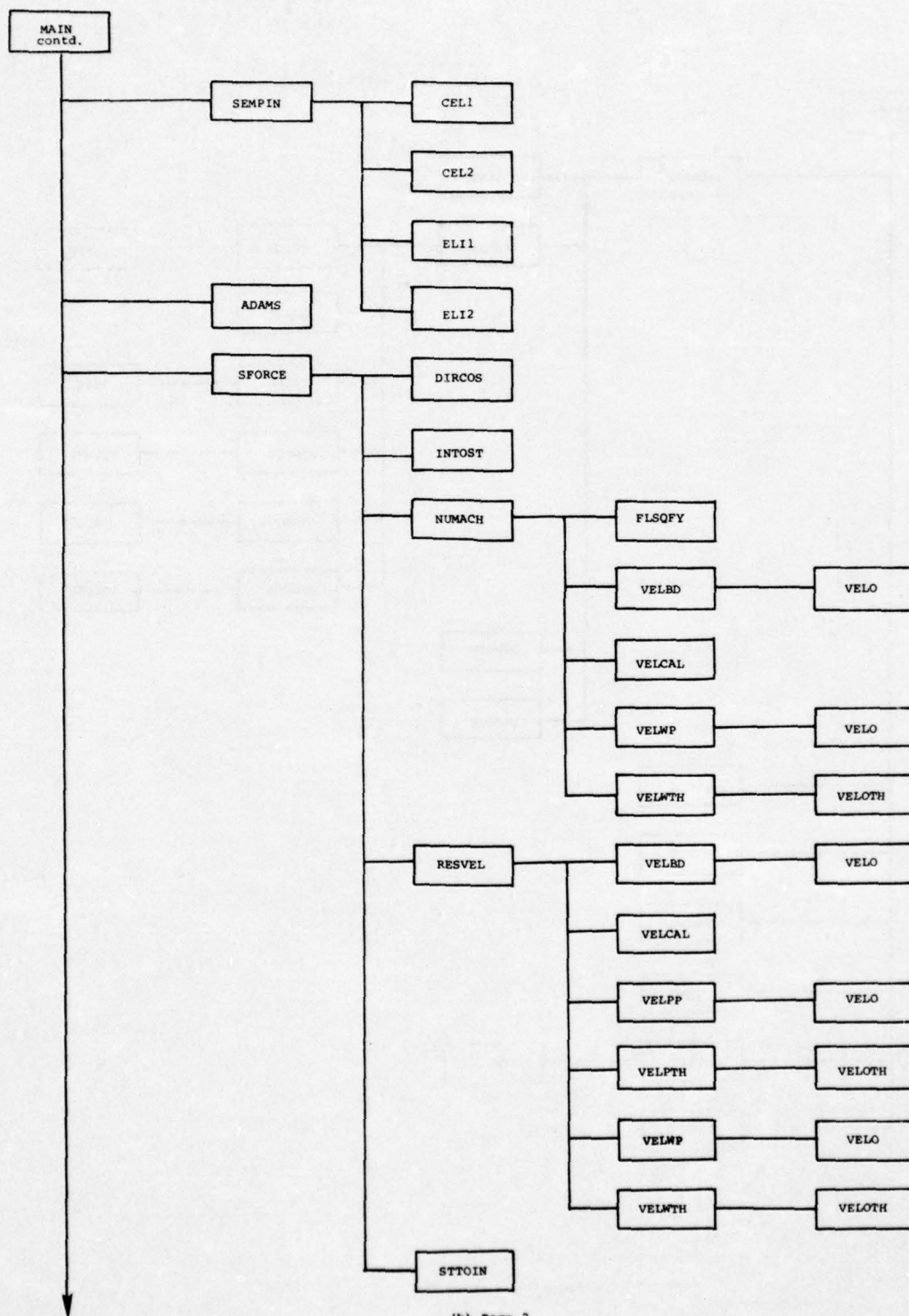
[illegible]

Figure I-1.- Common statements and the routines in which they appear.



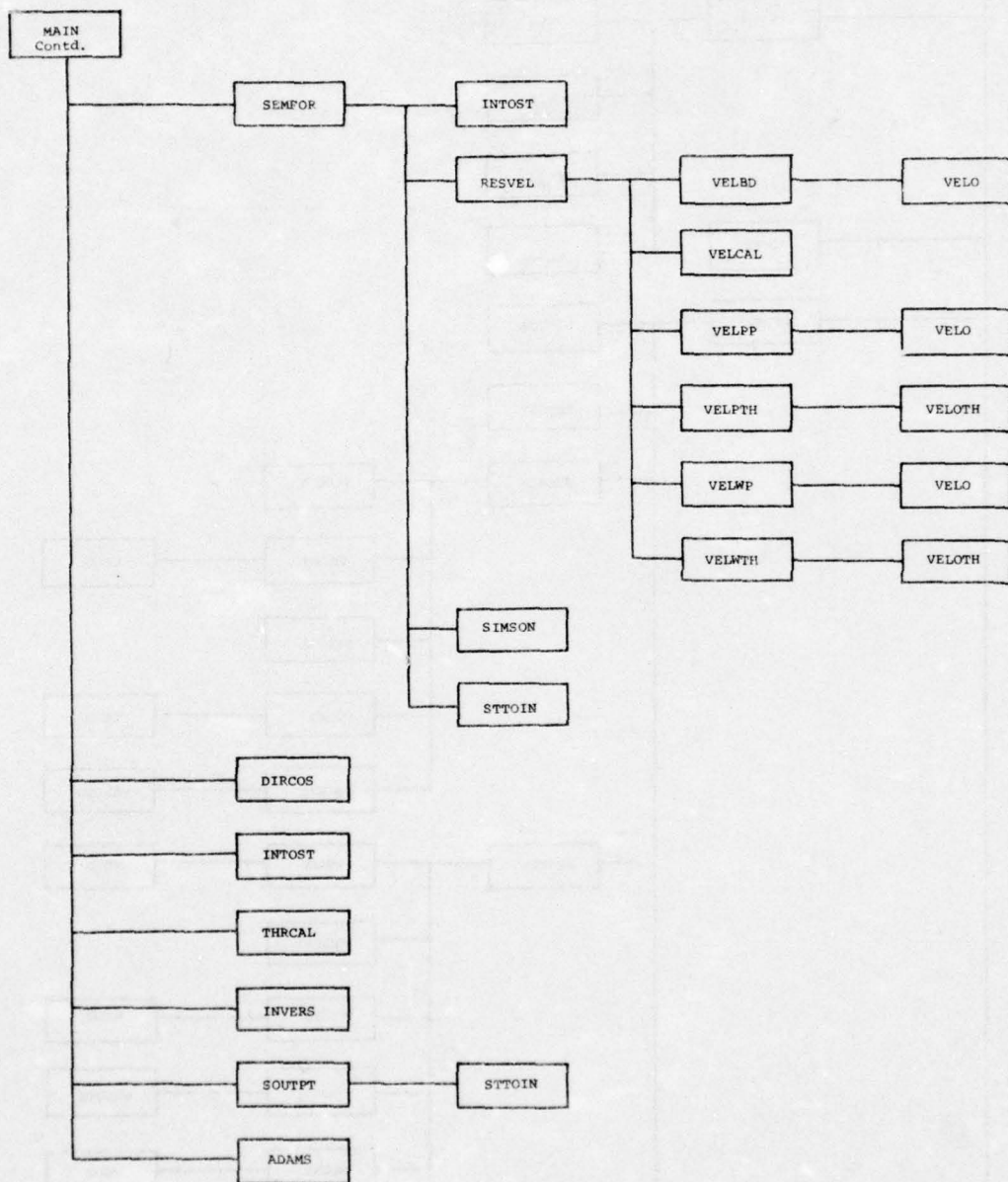
(a) Page 1.

Figure I-2.- Subroutine calling sequence.



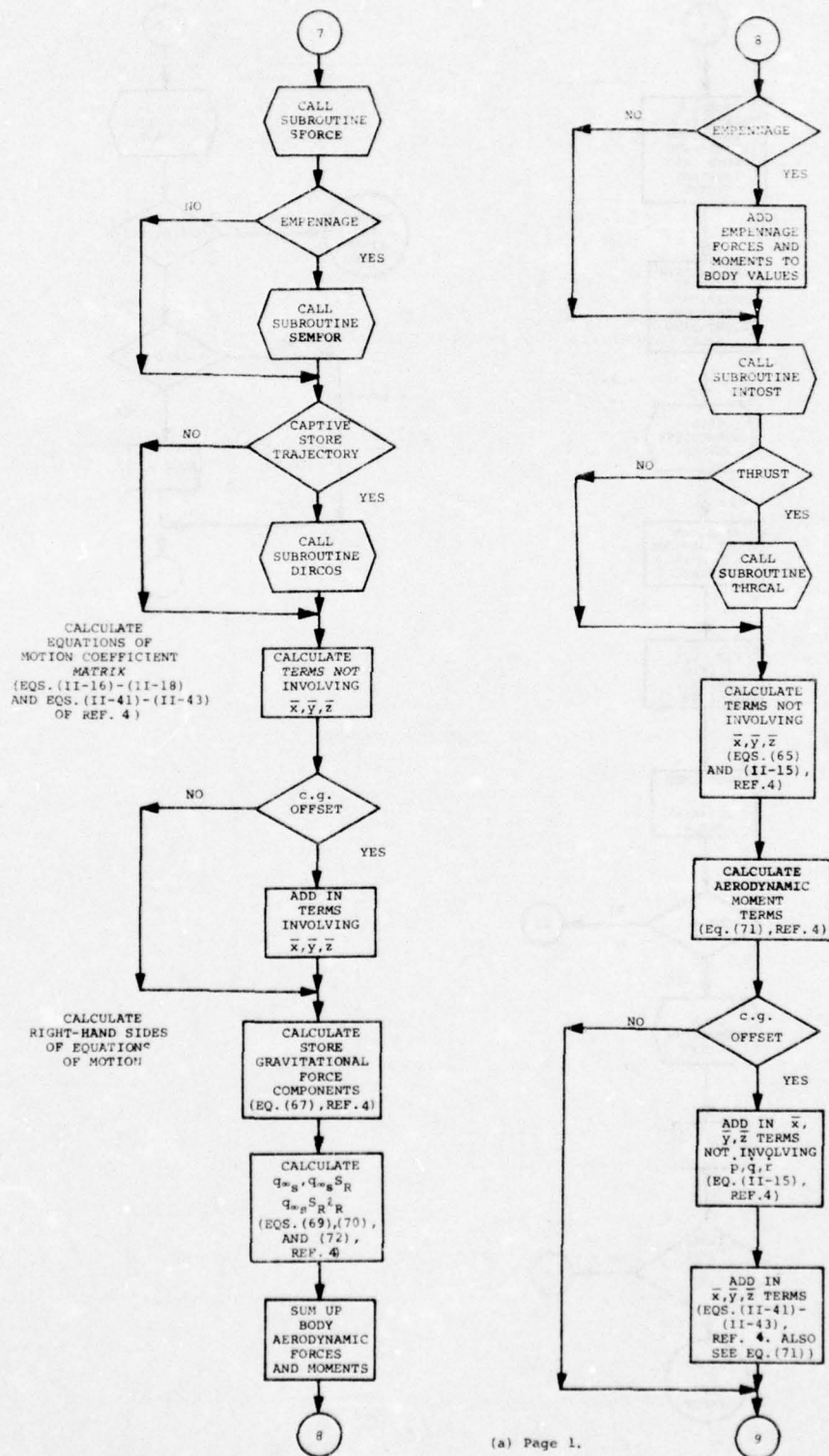
(b) Page 2.

Figure I-2.- Continued.



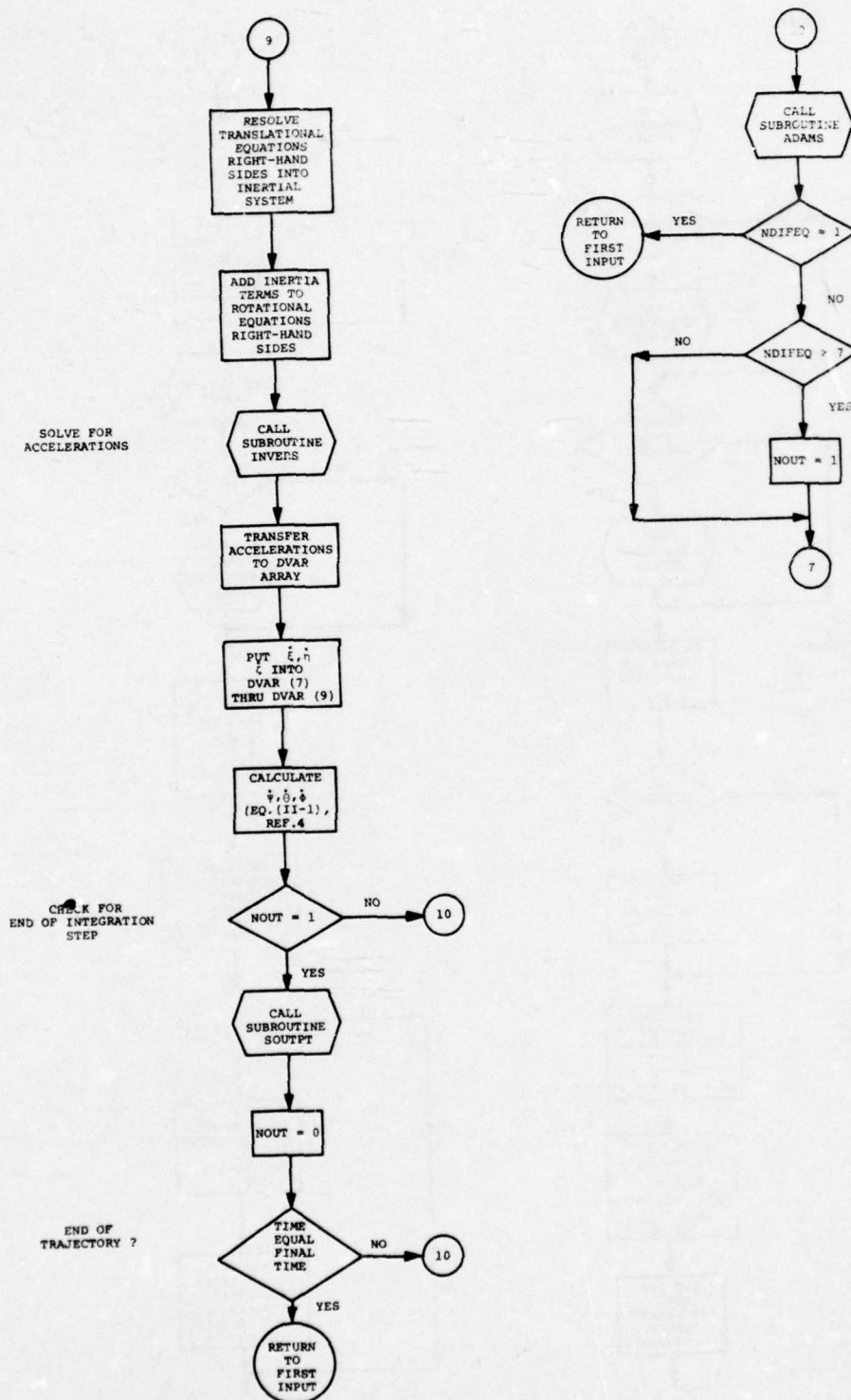
(c) Page 3.

Figure 1-2.- Concluded.



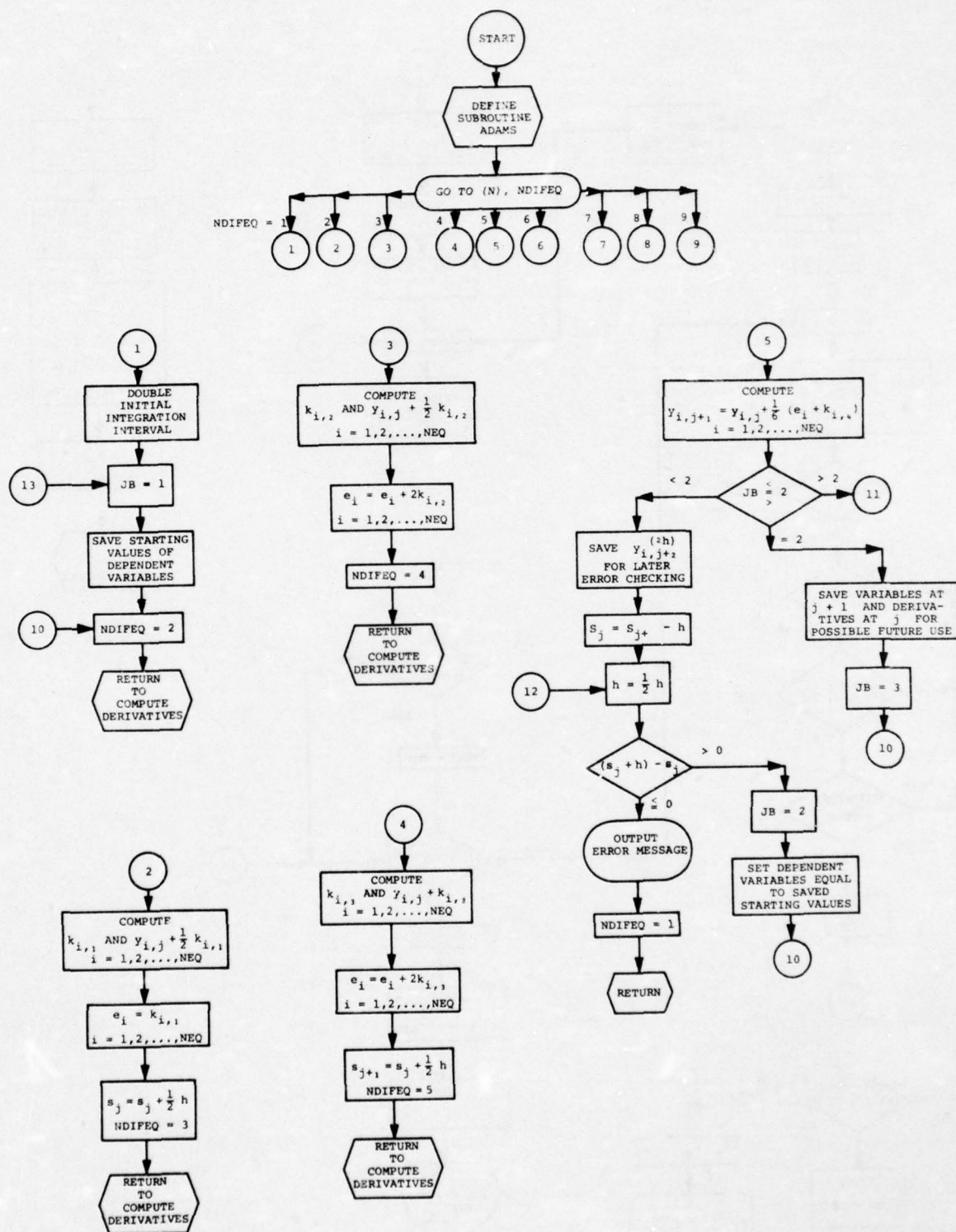
(a) Page 1.

Figure I-3.- Flow chart of integration loop of main program.



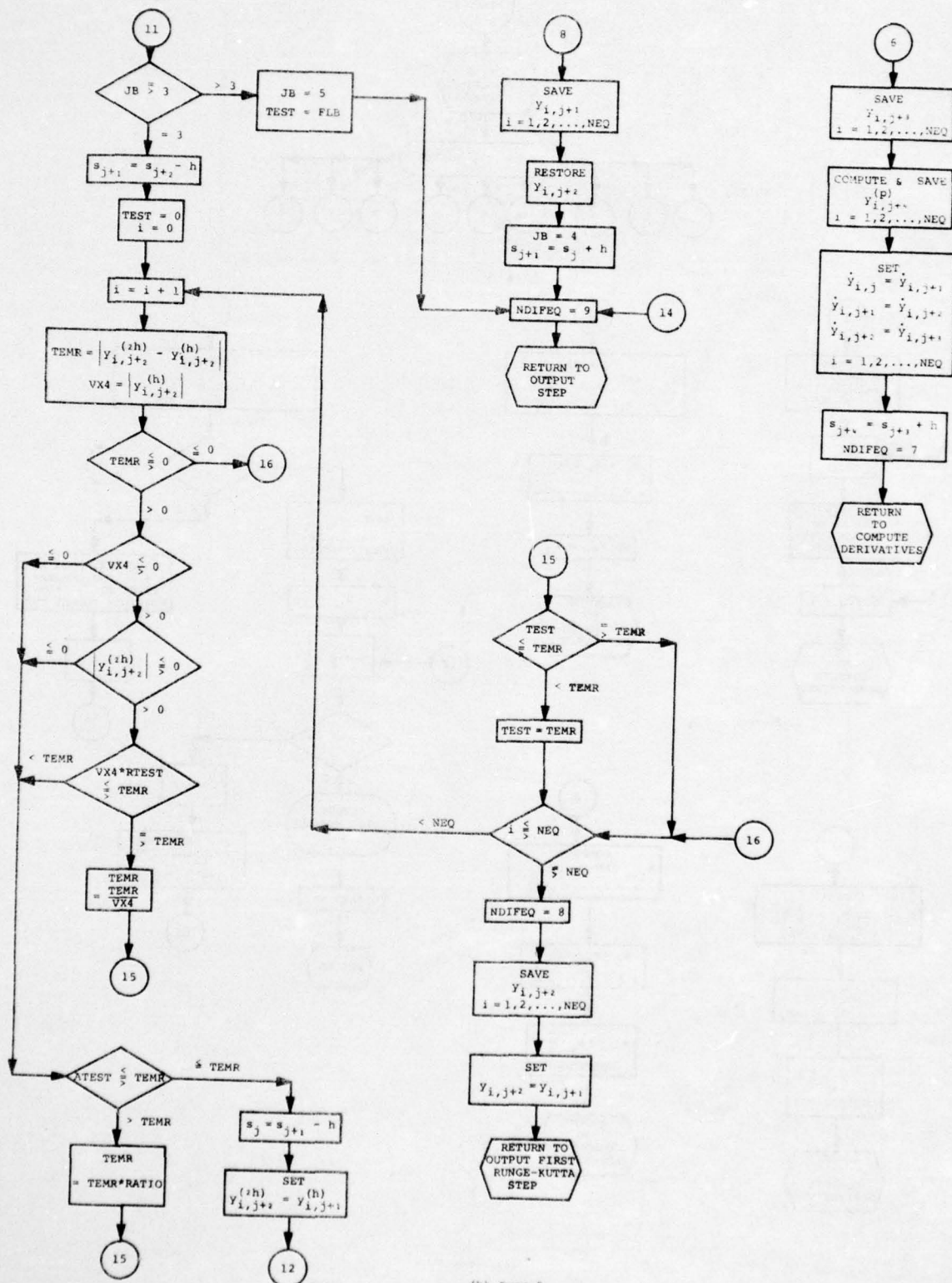
(b) Page 2.

Figure I-3.- Concluded.

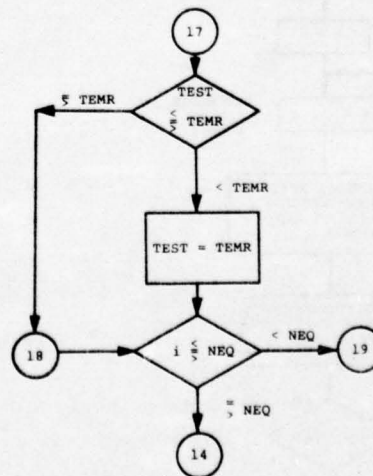
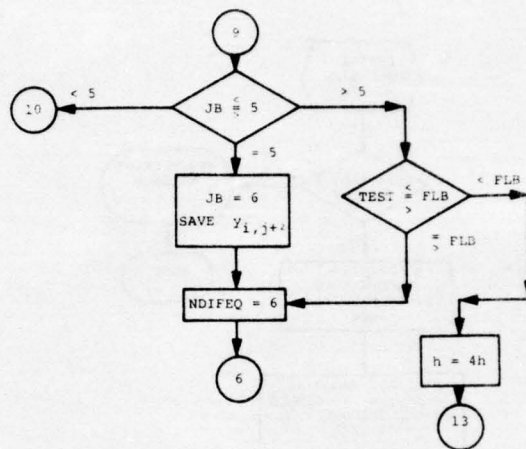
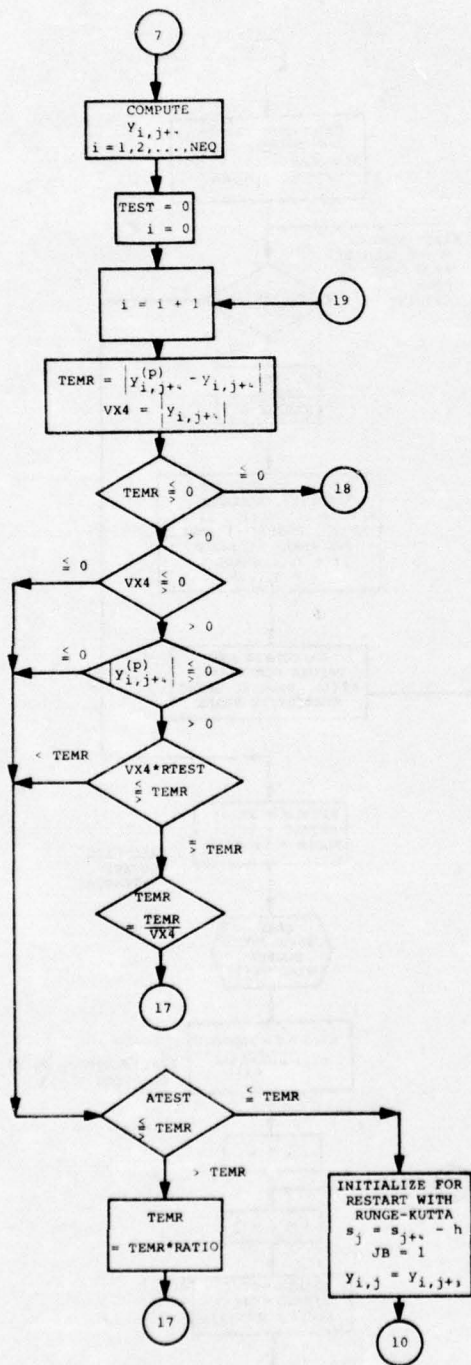


(a) Page 1.

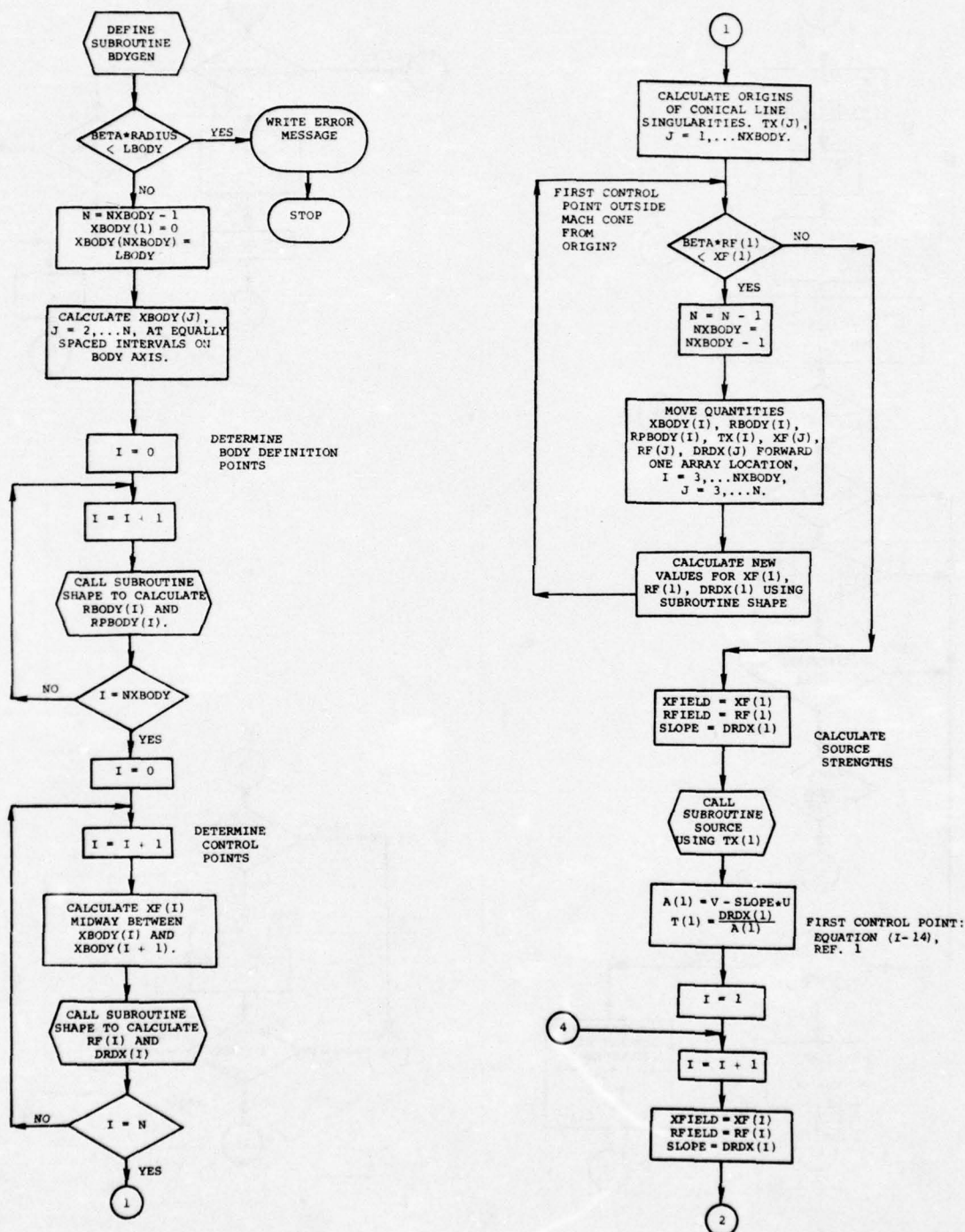
Figure I-4.- Flow chart of subroutine ADAMS.



(b) Page 2.
Figure I-4.- Continued.

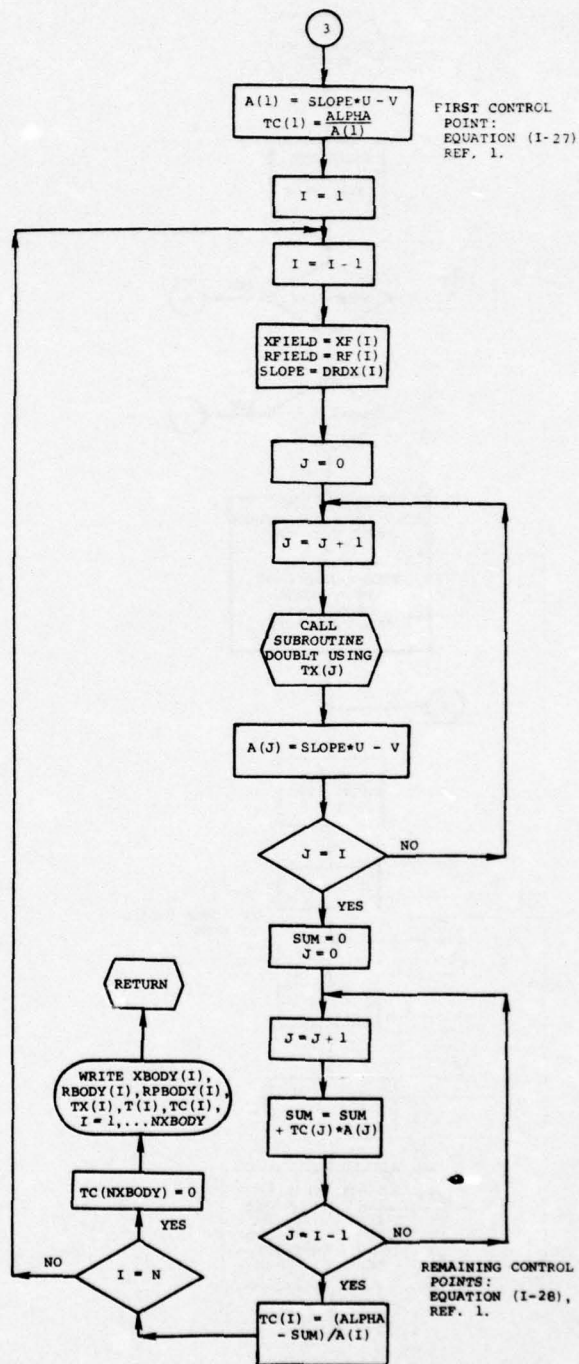
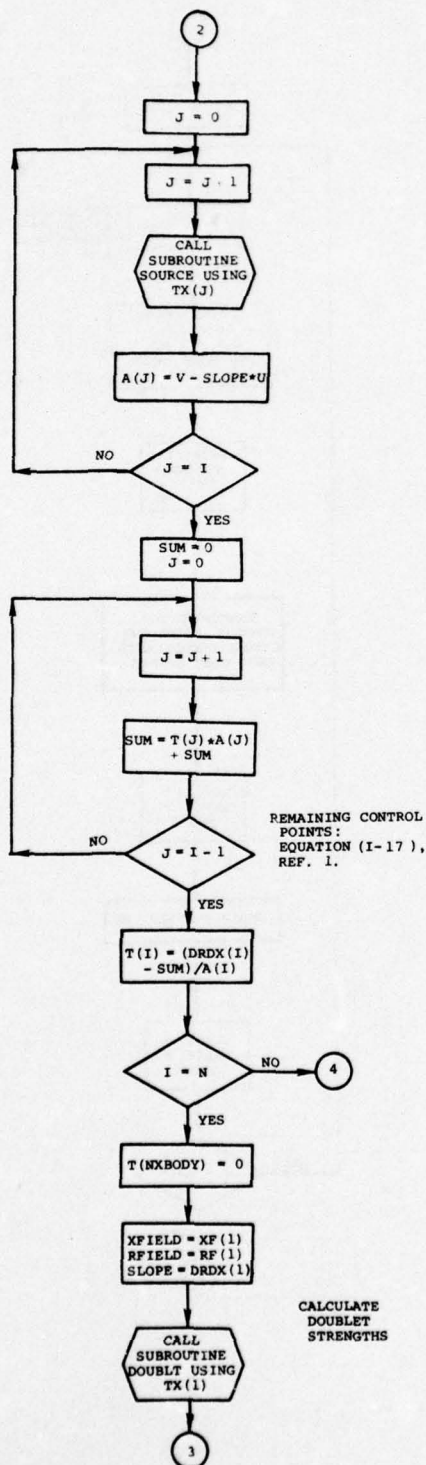


(c) Page 3.
Figure I-4. - Concluded.



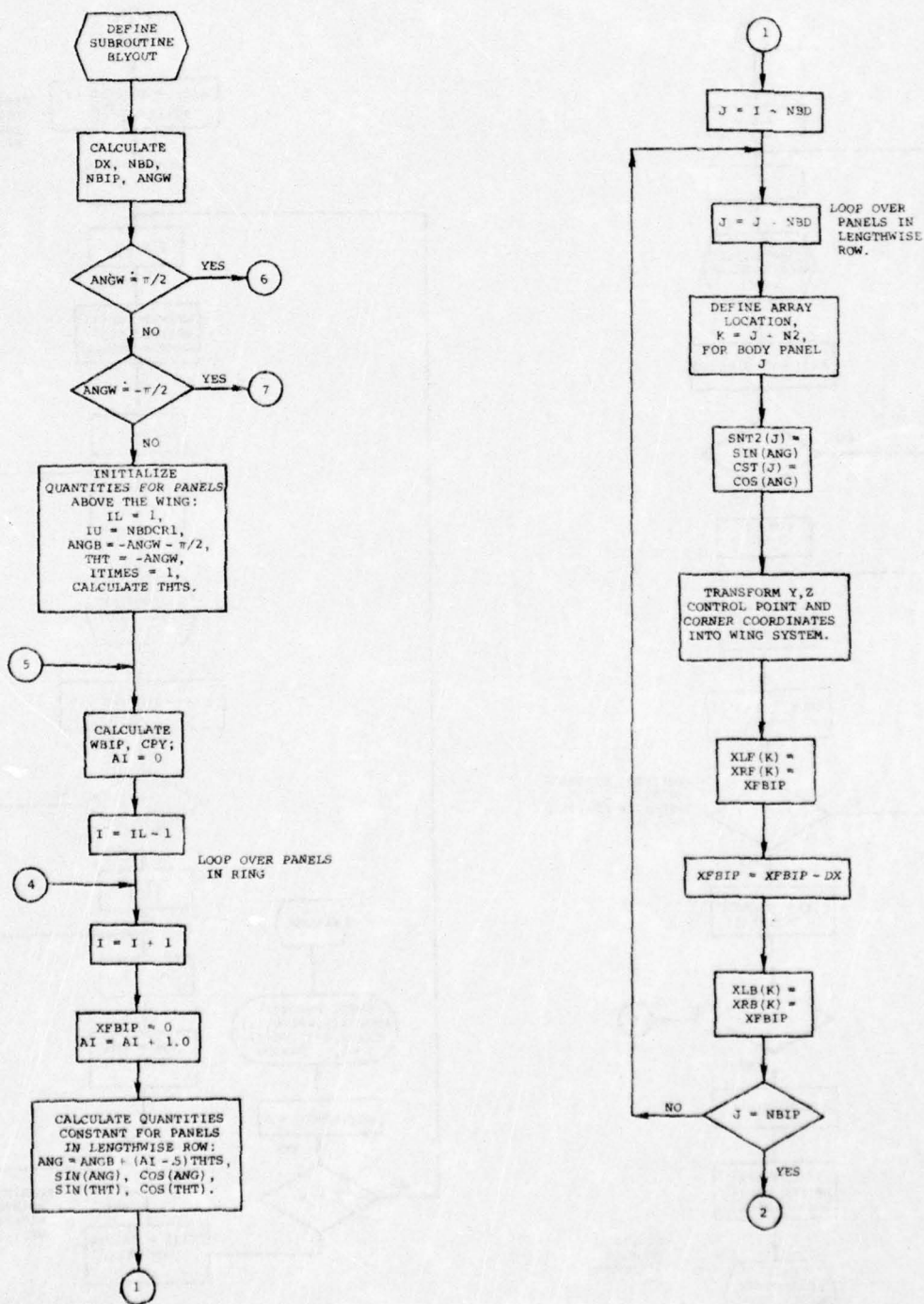
(a) Page 1.

Figure I-5.- Flow chart of su_routine BDYGEN.



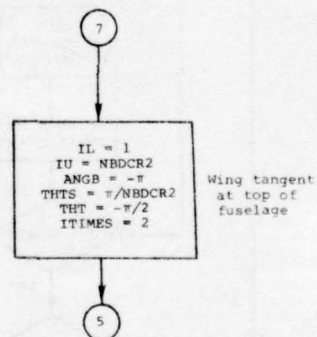
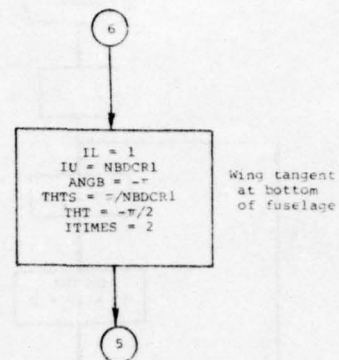
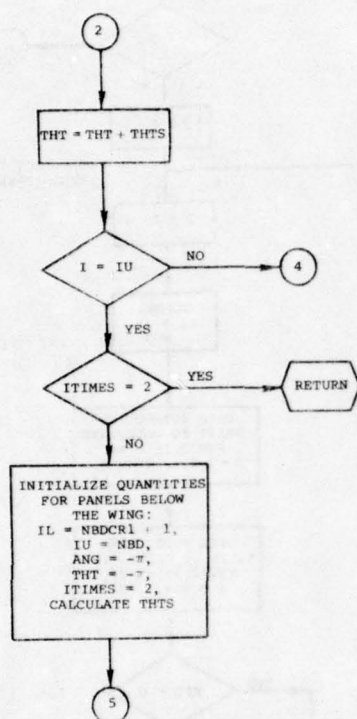
(b) Page 2.

Figure I-5.- Concluded.



(a) Page 1.

Figure I-6.- Flow chart of subroutine BLYOUT.



(b) Page 2.

Figure I-6. - Concluded.

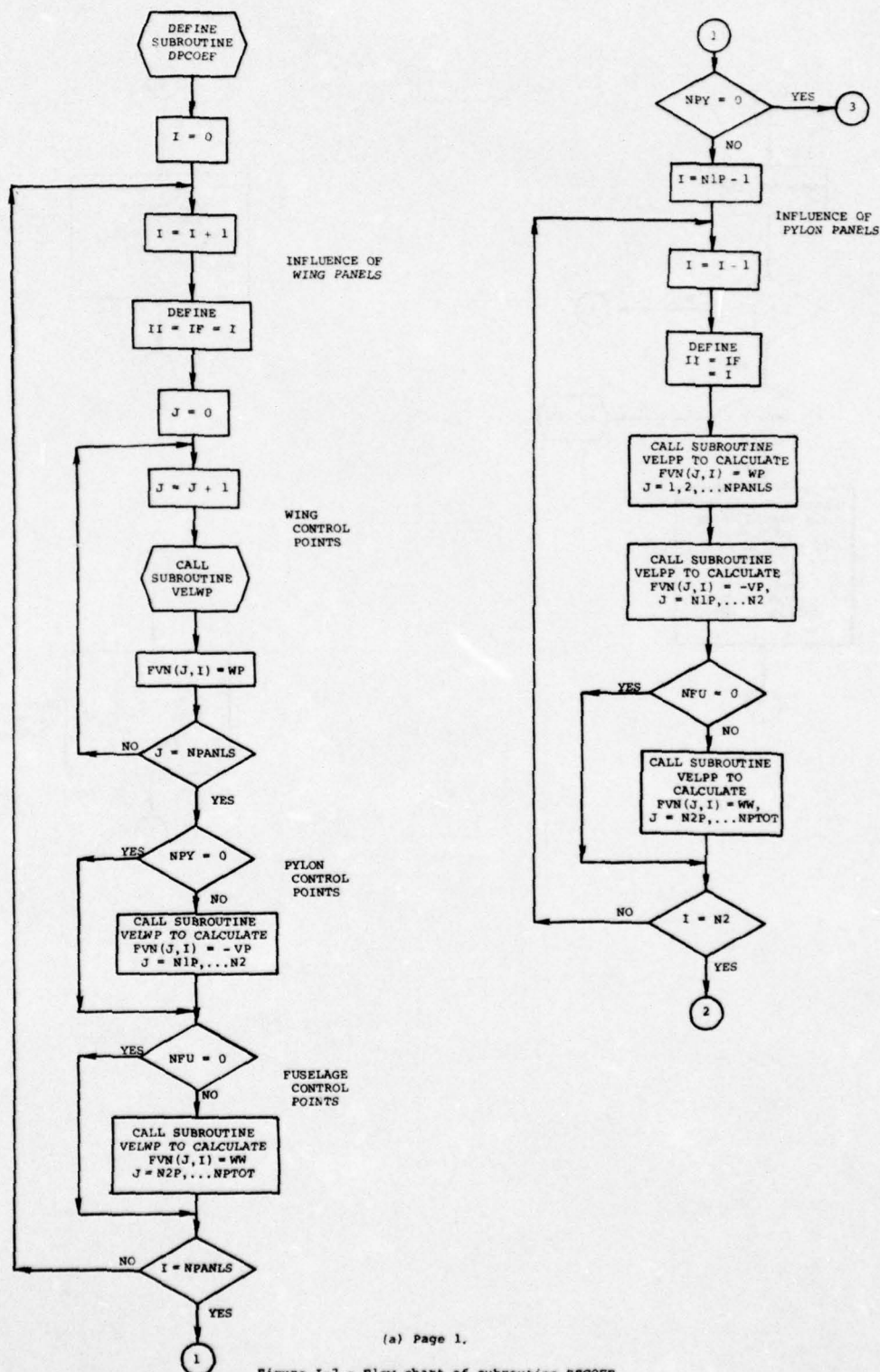
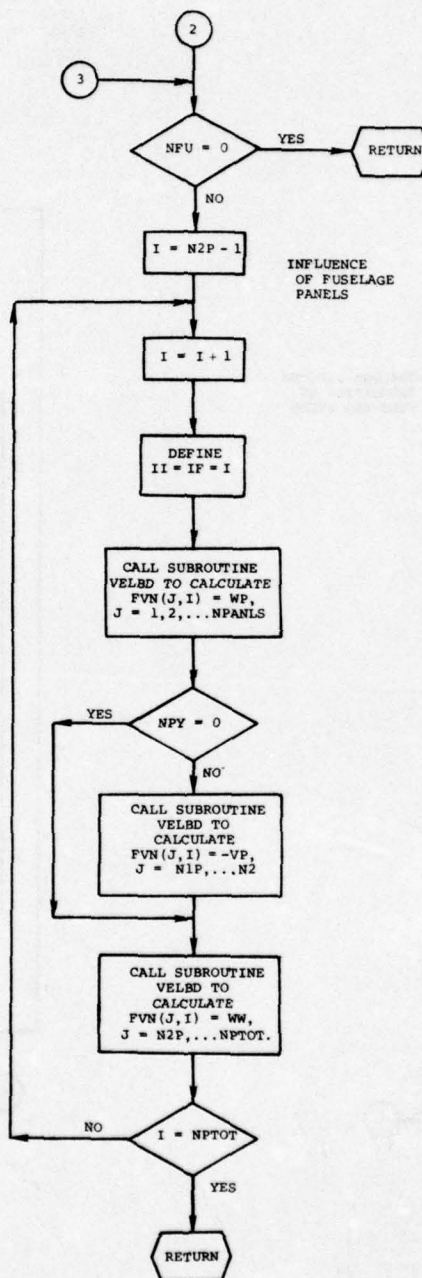
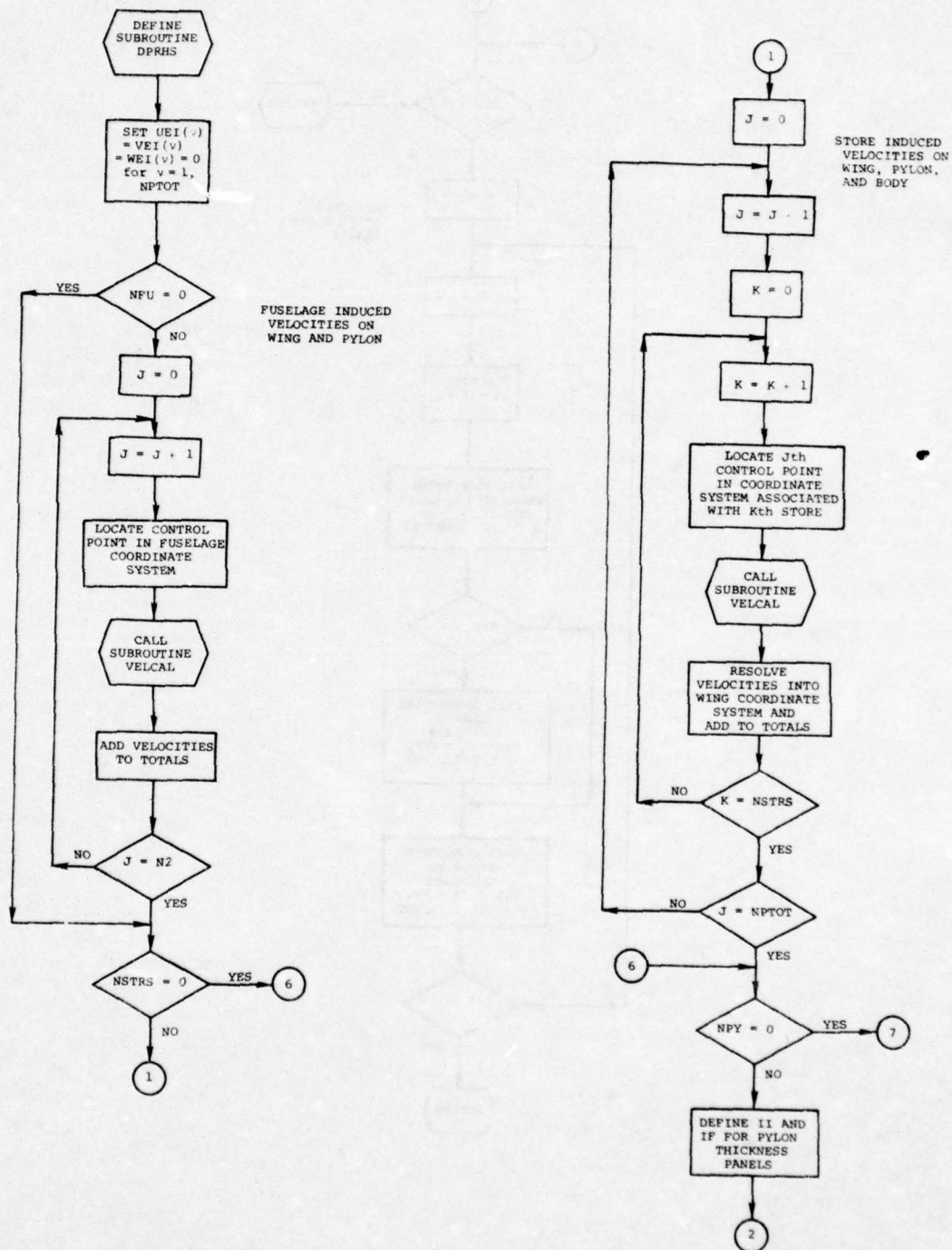


Figure I-7.- Flow chart of subroutine DPCOEF.



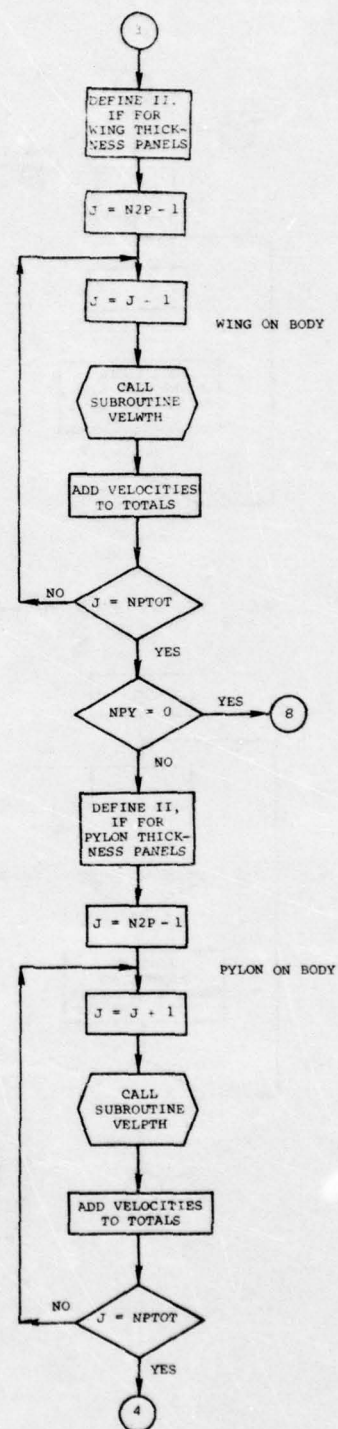
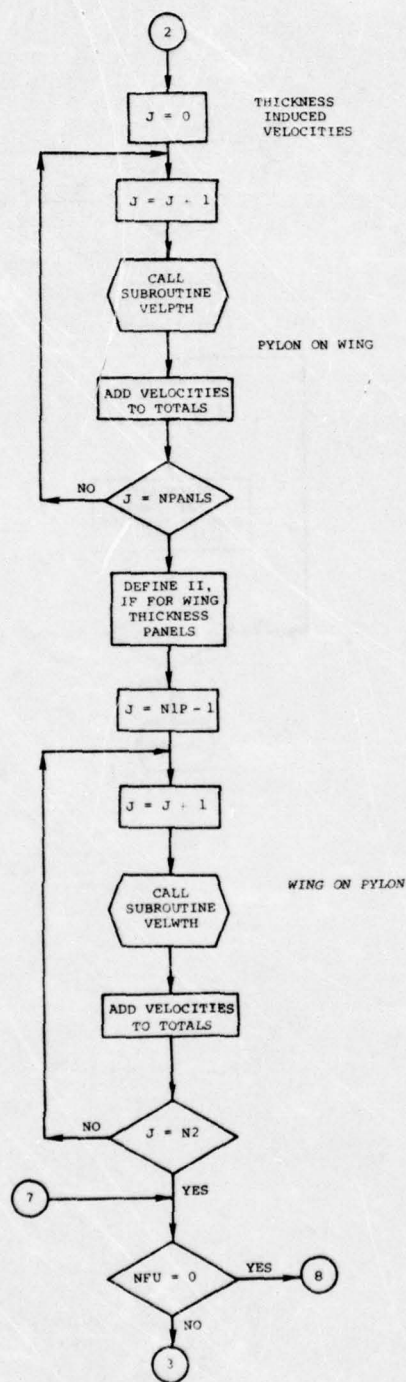
(b) Page 2.

Figure I-7.- Concluded.



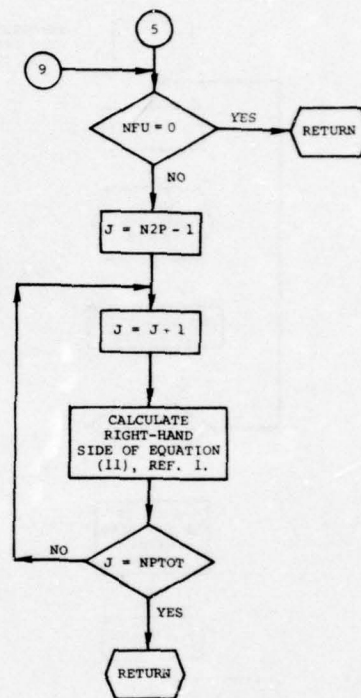
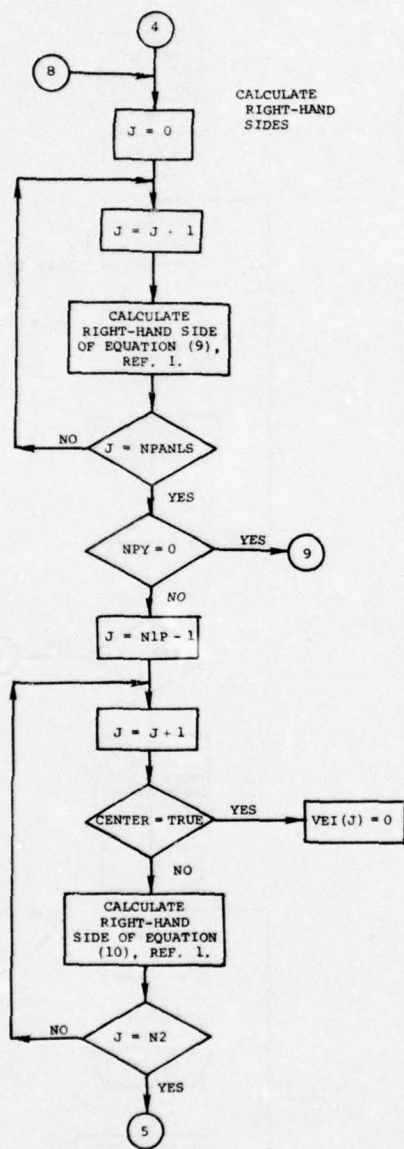
(a) Page 1.

Figure I-8.- Flow chart of subroutine DPRHS.



(b) Page 2.

Figure I-8.- Continued.



(c) Page 3.

Figure I-8. - Concluded.

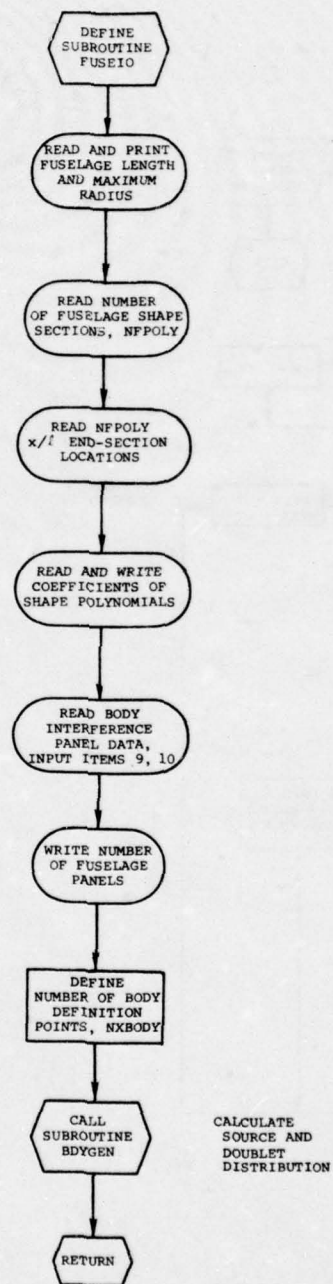
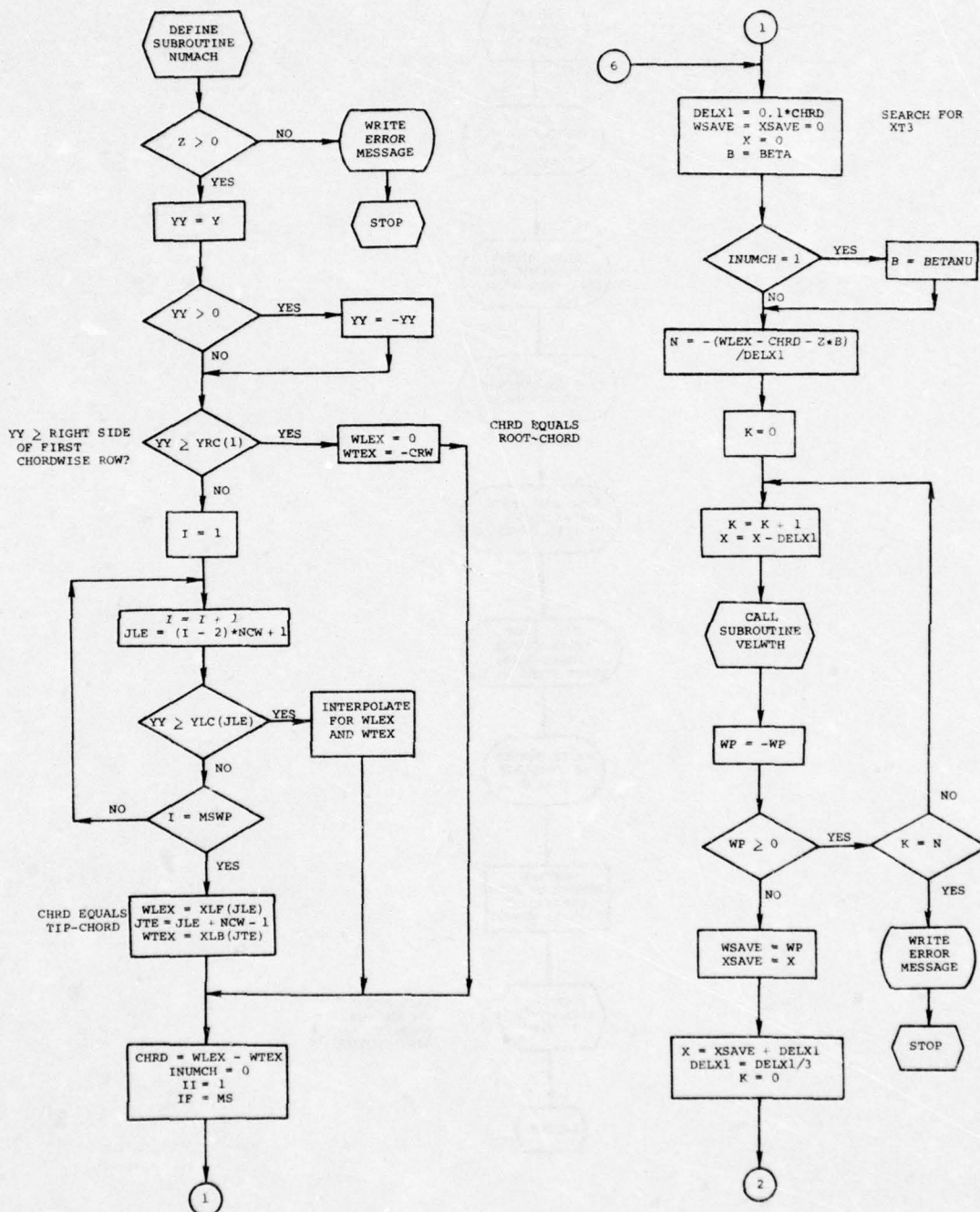
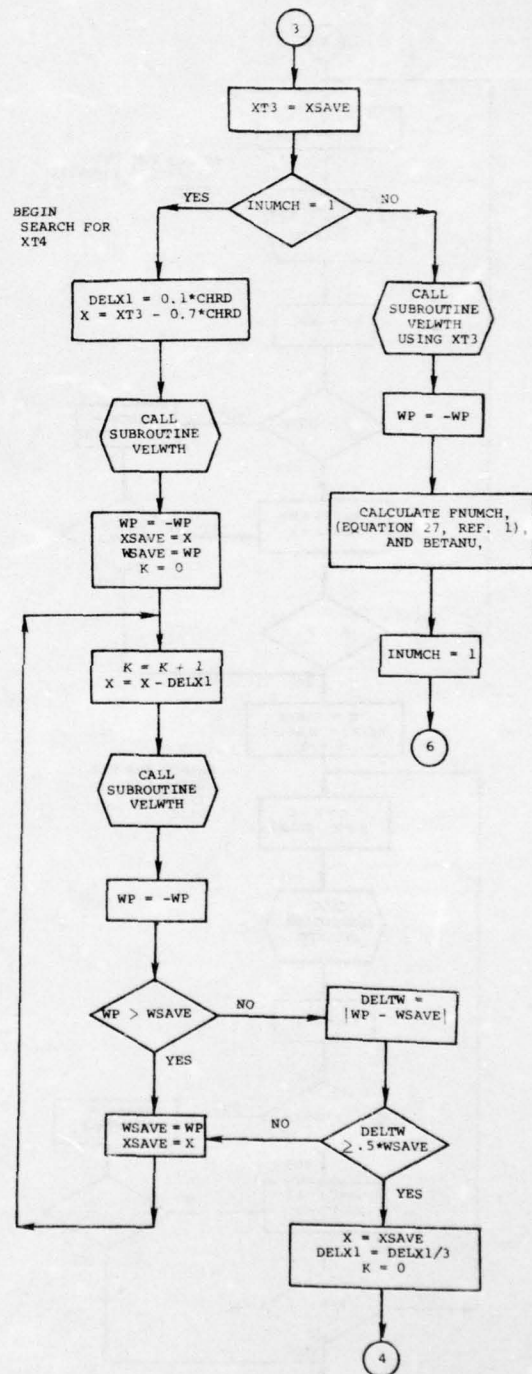
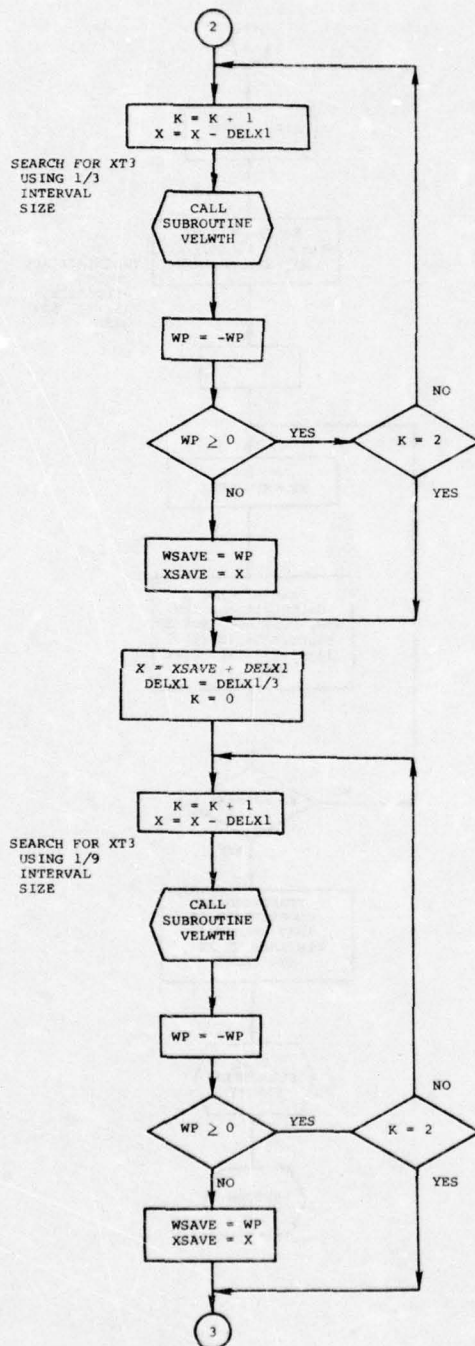


Figure I-9.- Flow chart of subroutine FUSEIO.



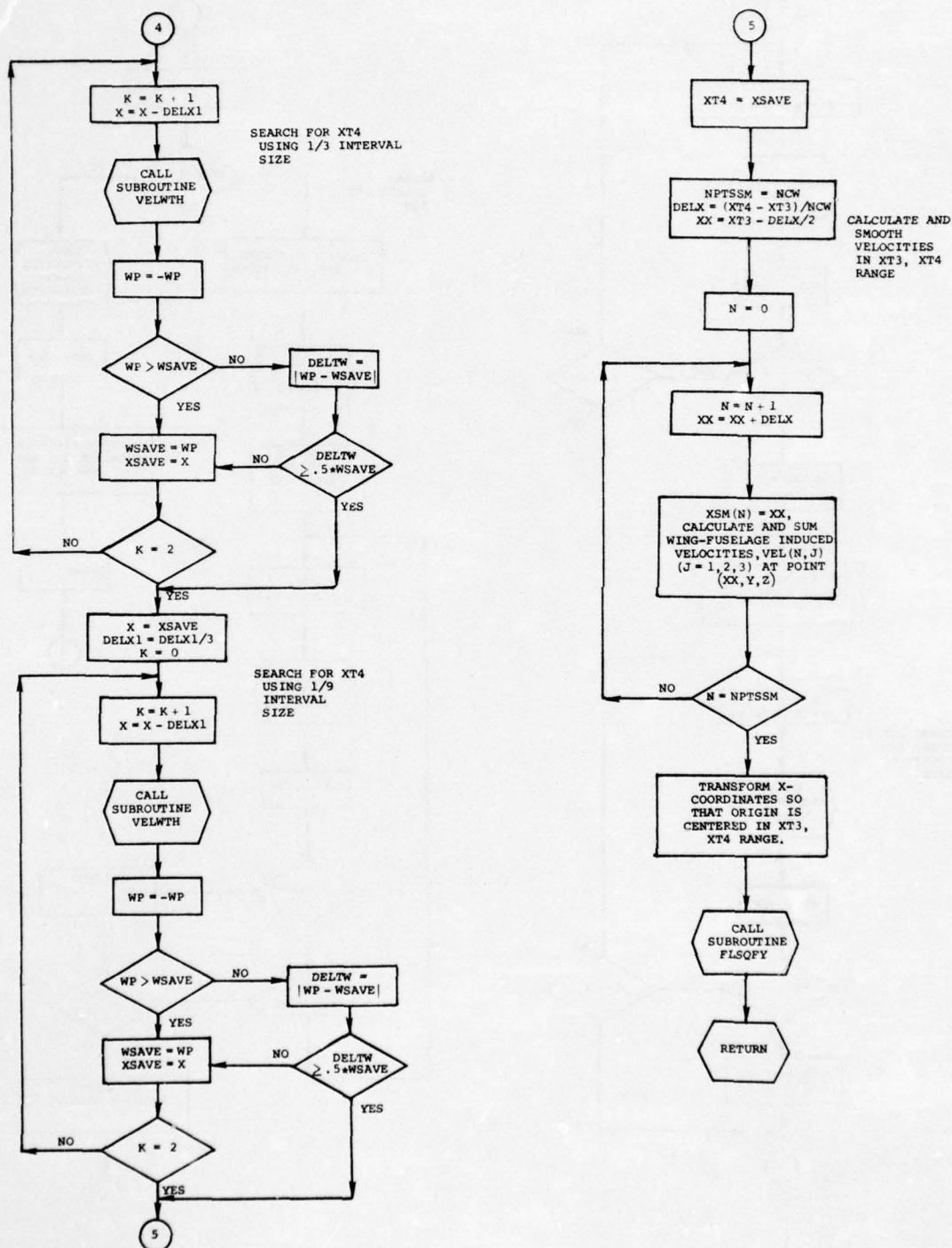
(a) Page 1.

Figure I-10.- Flow chart of subroutine NUMACH.



(b) Page 2.

Figure I-10.- Continued.



(c) Page 3.

Figure I-10.- Concluded.

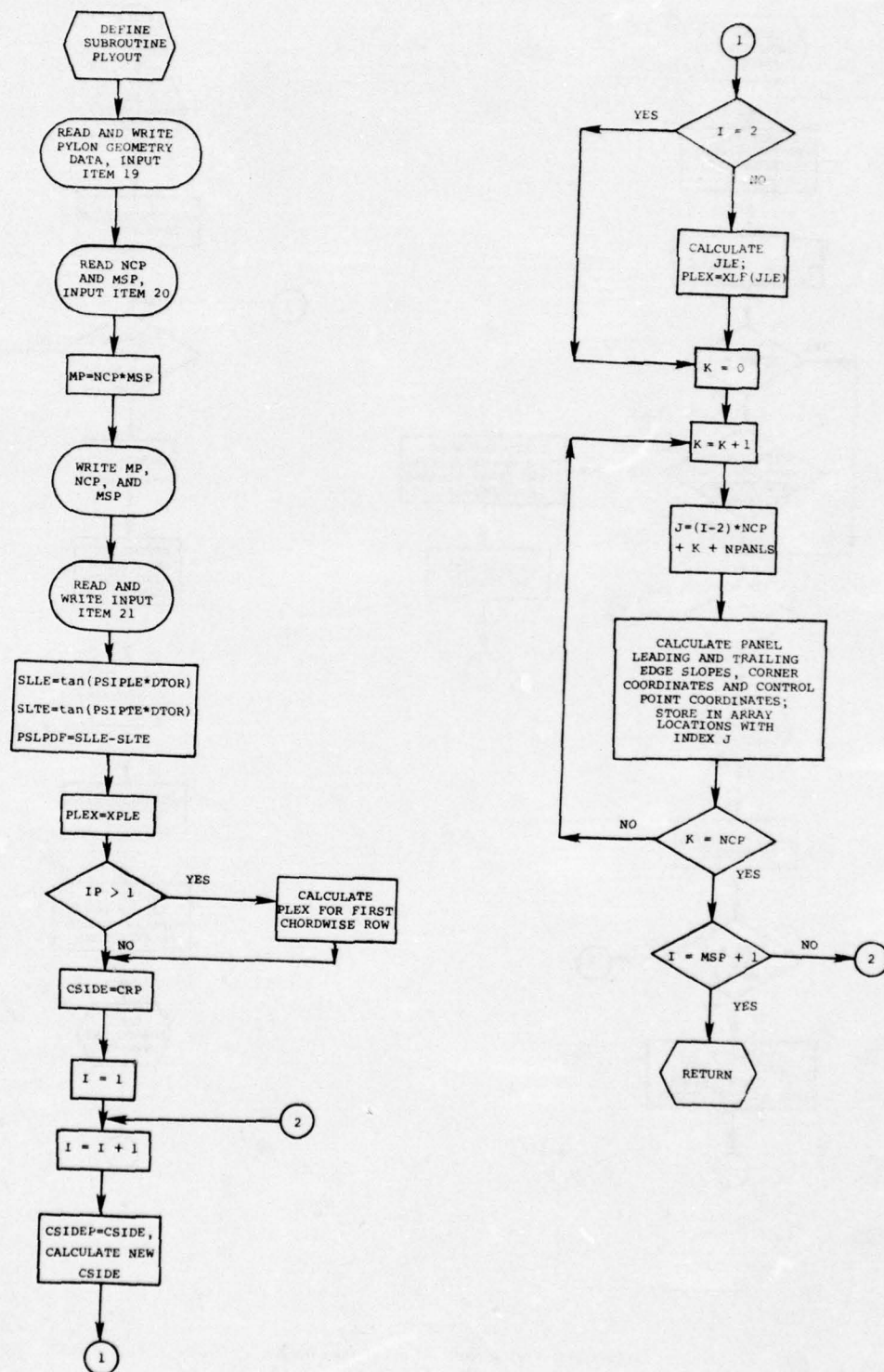
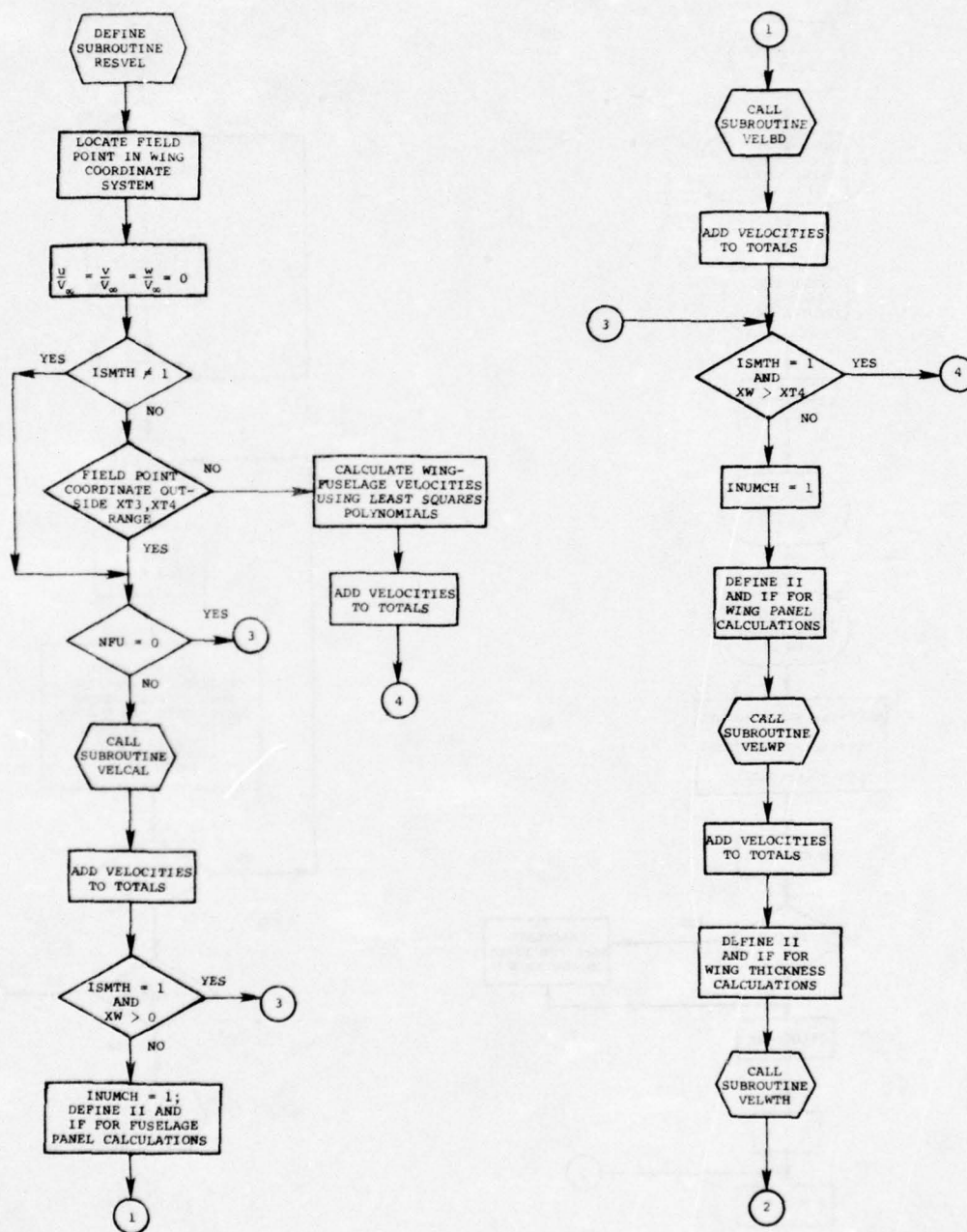
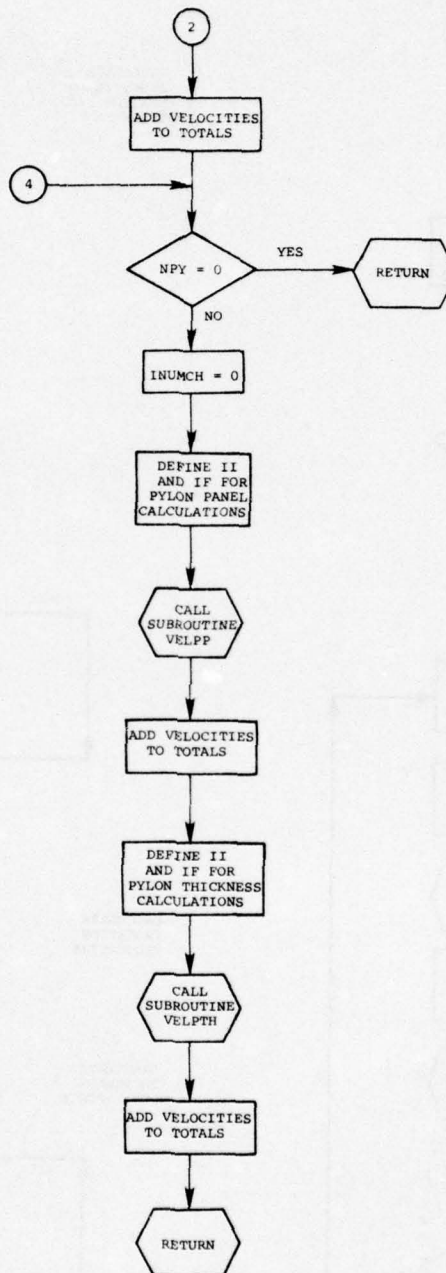


Figure I-11.- Flow chart of subroutine PLYOUT.



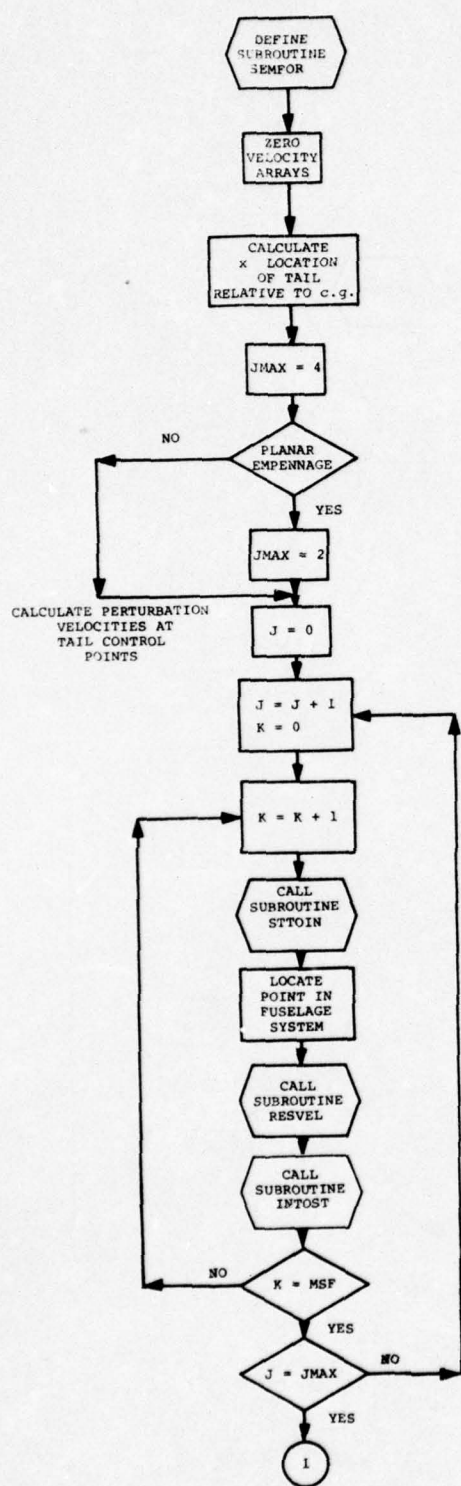
(a) Page 1.

Figure I-12.- Flow chart of subroutine RESVEL.



(b) Page 2.

Figure I-12.- Concluded.



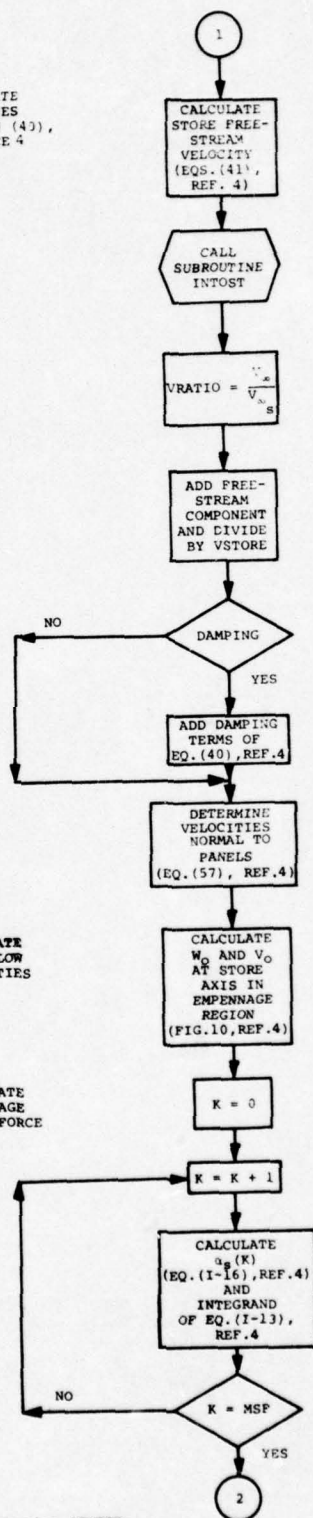
CALCULATE VELOCITIES OF EQUATION (43), REFERENCE 4

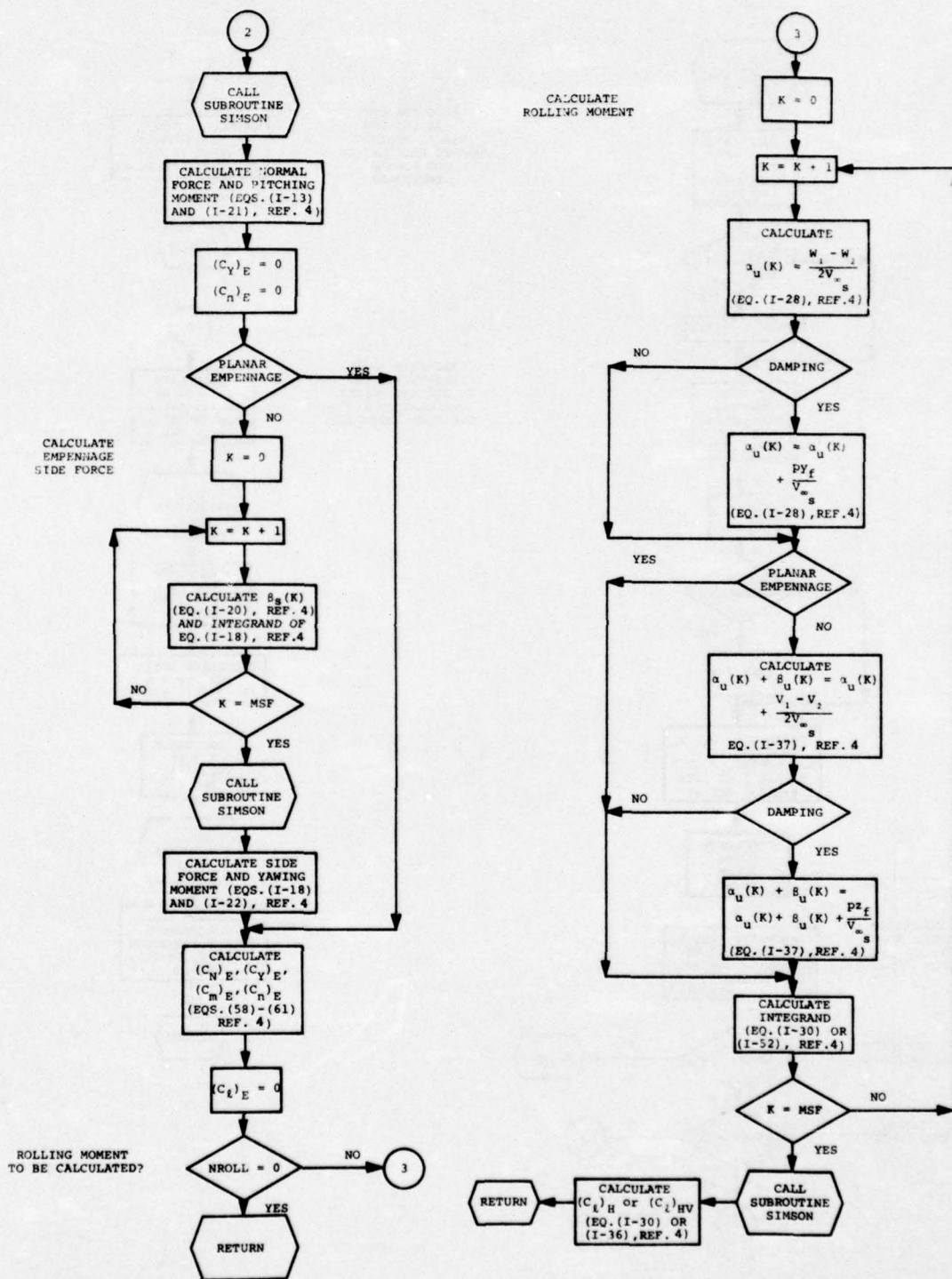
CALCULATE CROSSFLOW VELOCITIES

CALCULATE EMPENNAGE NORMAL FORCE

(a) Page 1.

Figure I-13.- Flow chart of subroutine SEMFOR.





(b) Page 2.

Figure I-13.- Concluded.

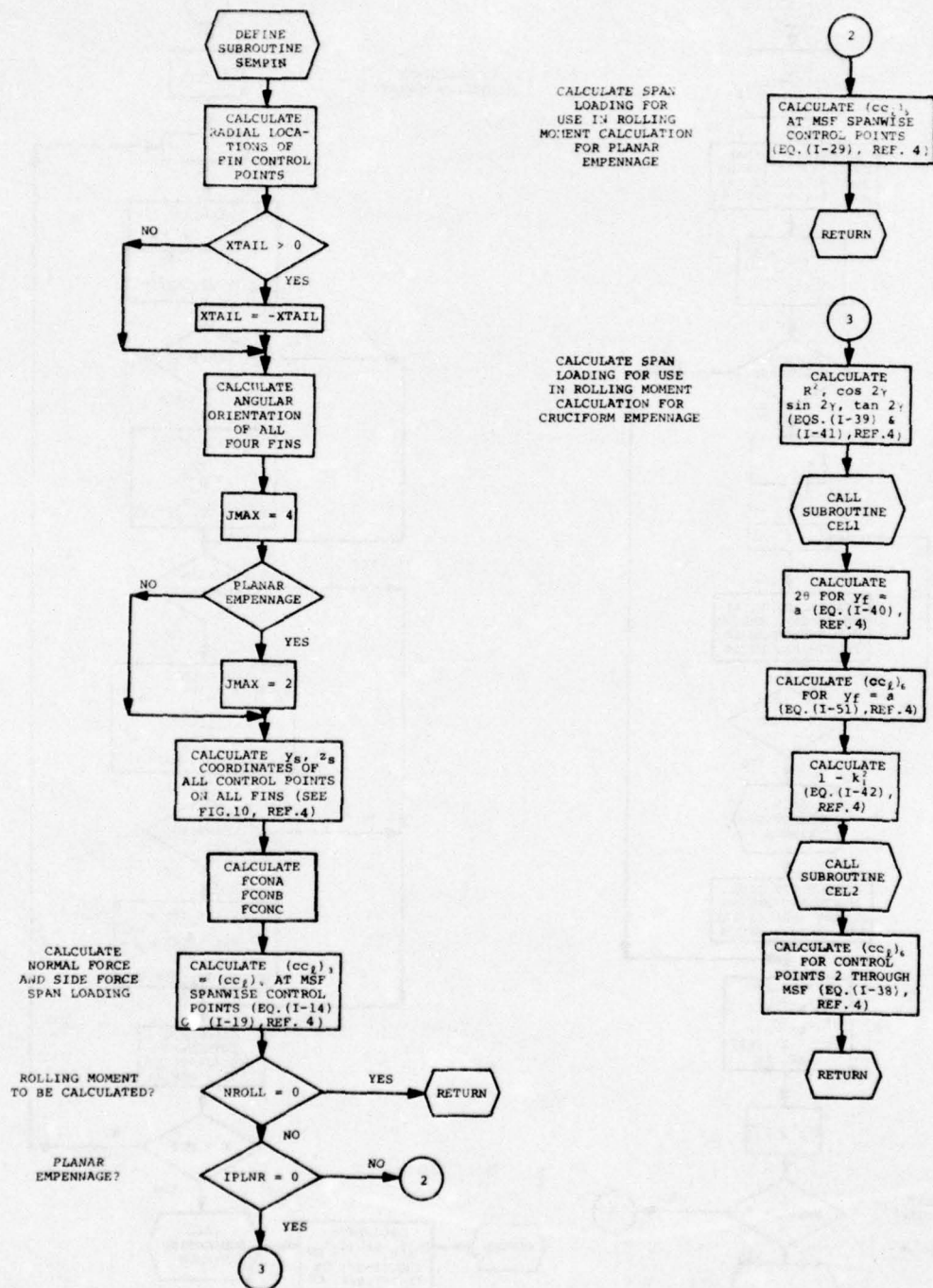
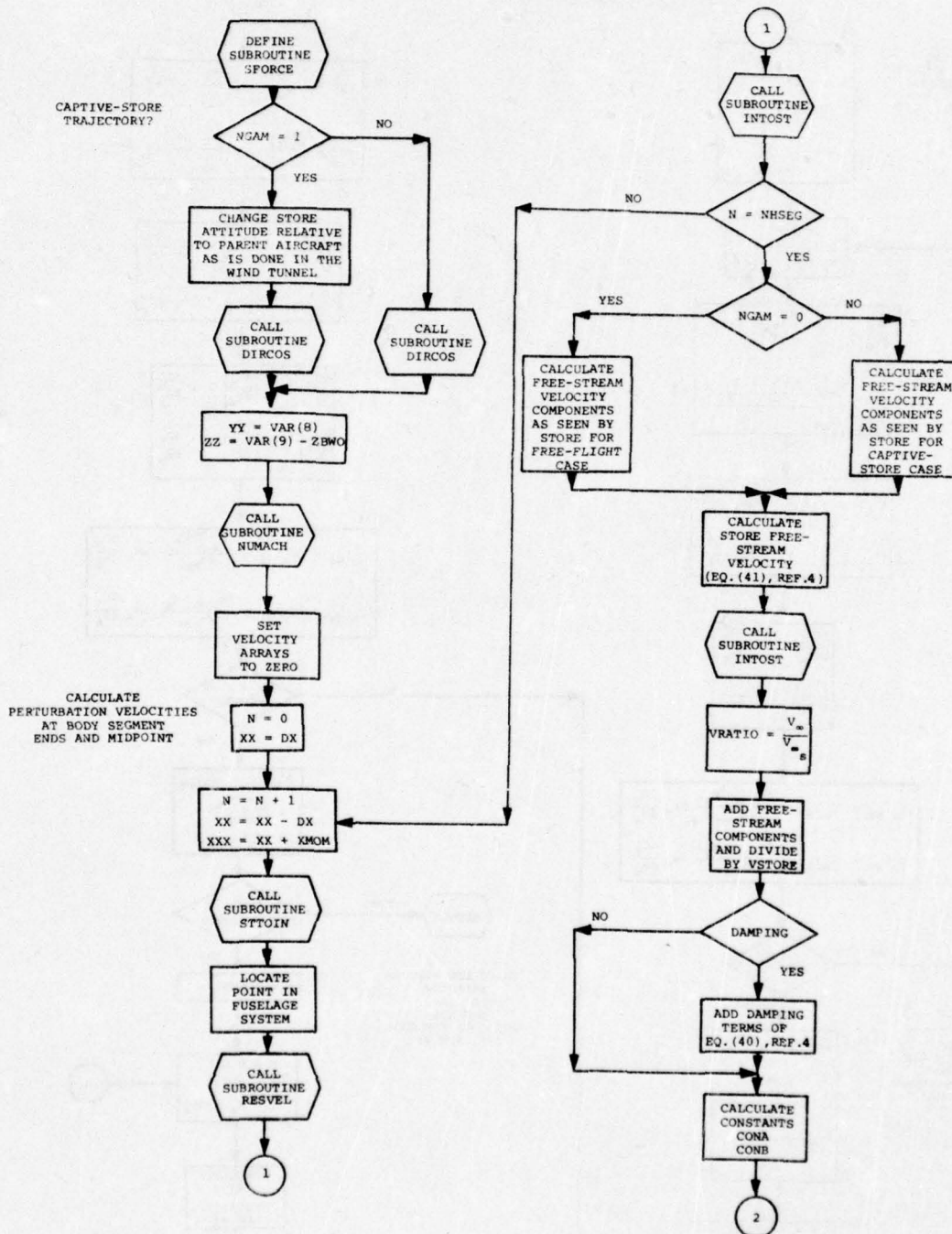
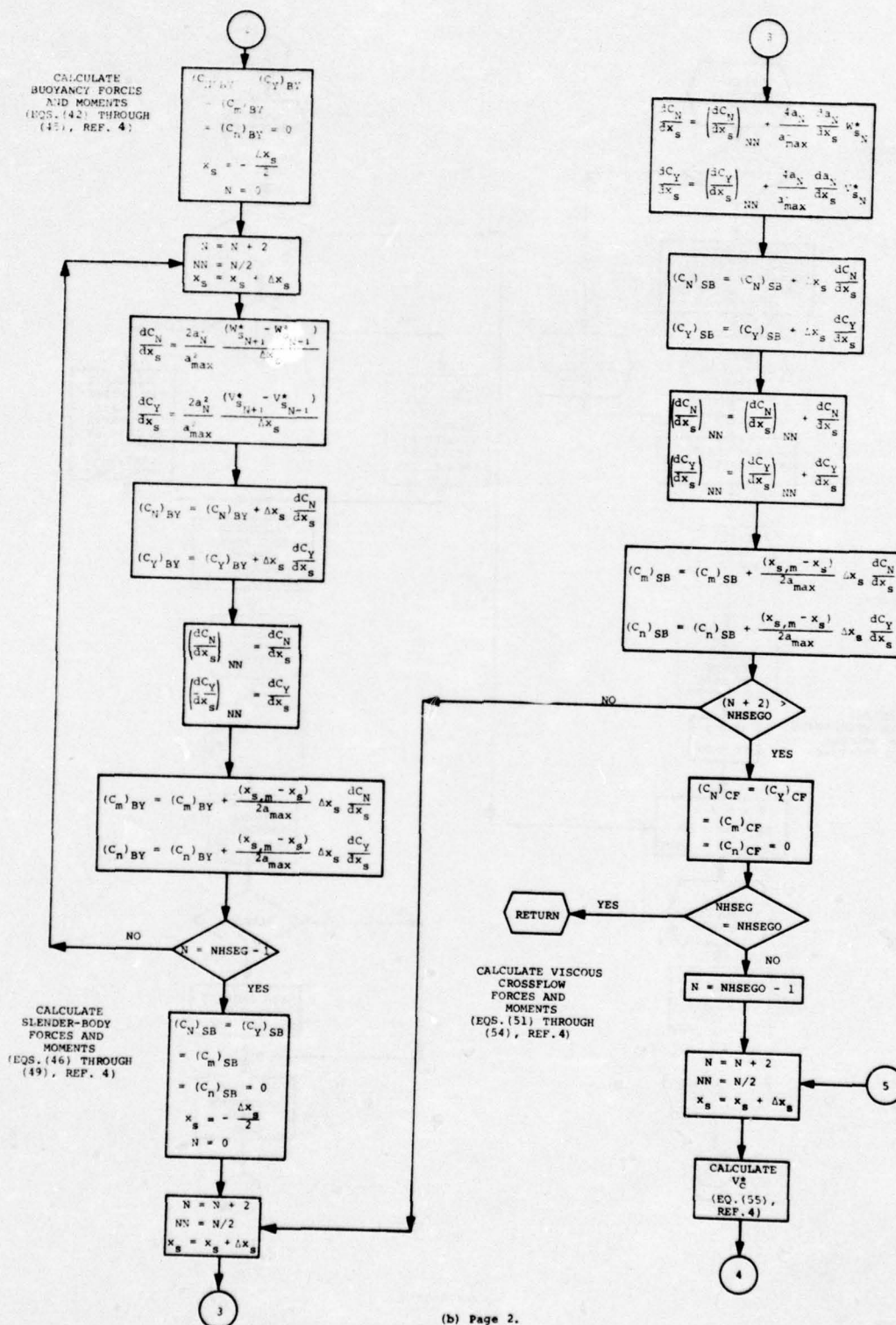


Figure I-14.- Flow chart of subroutine SEMPIN.

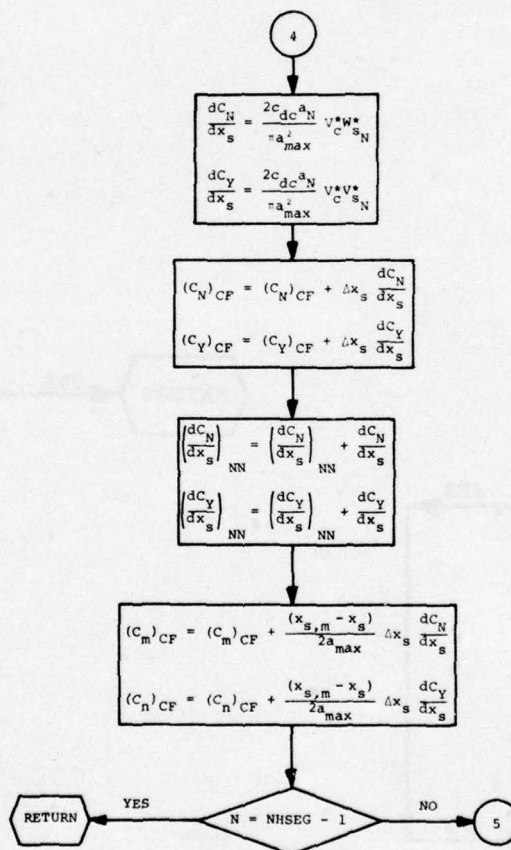


(a) Page 1.

Figure I-15.- Flow chart of subroutine SFORCE.



(b) Page 2.
Figure I-15.- Continued.



(c) Page 3.

Figure I-15.- Concluded.

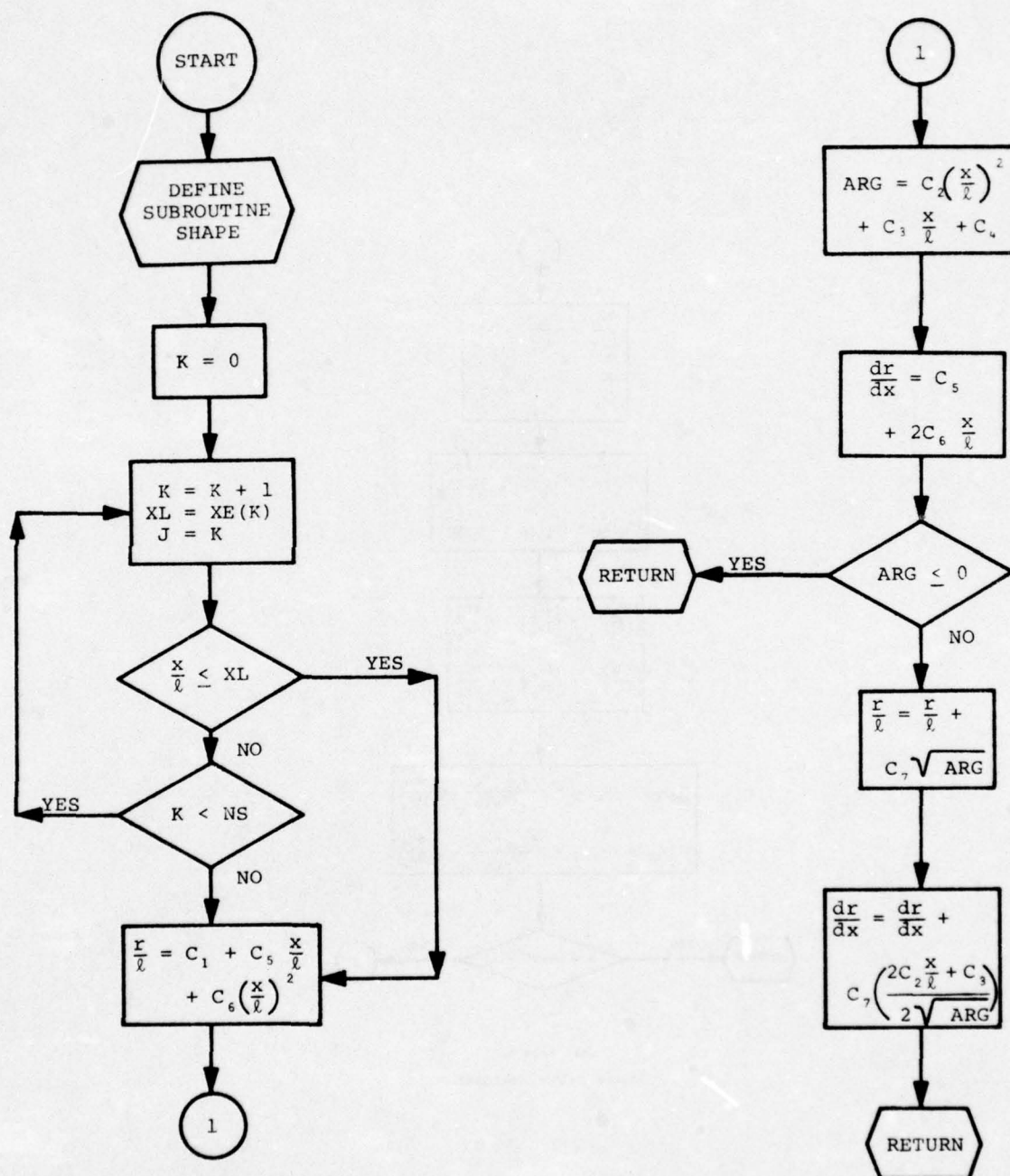


Figure I-16.-Flow chart of subroutine SHAPE.

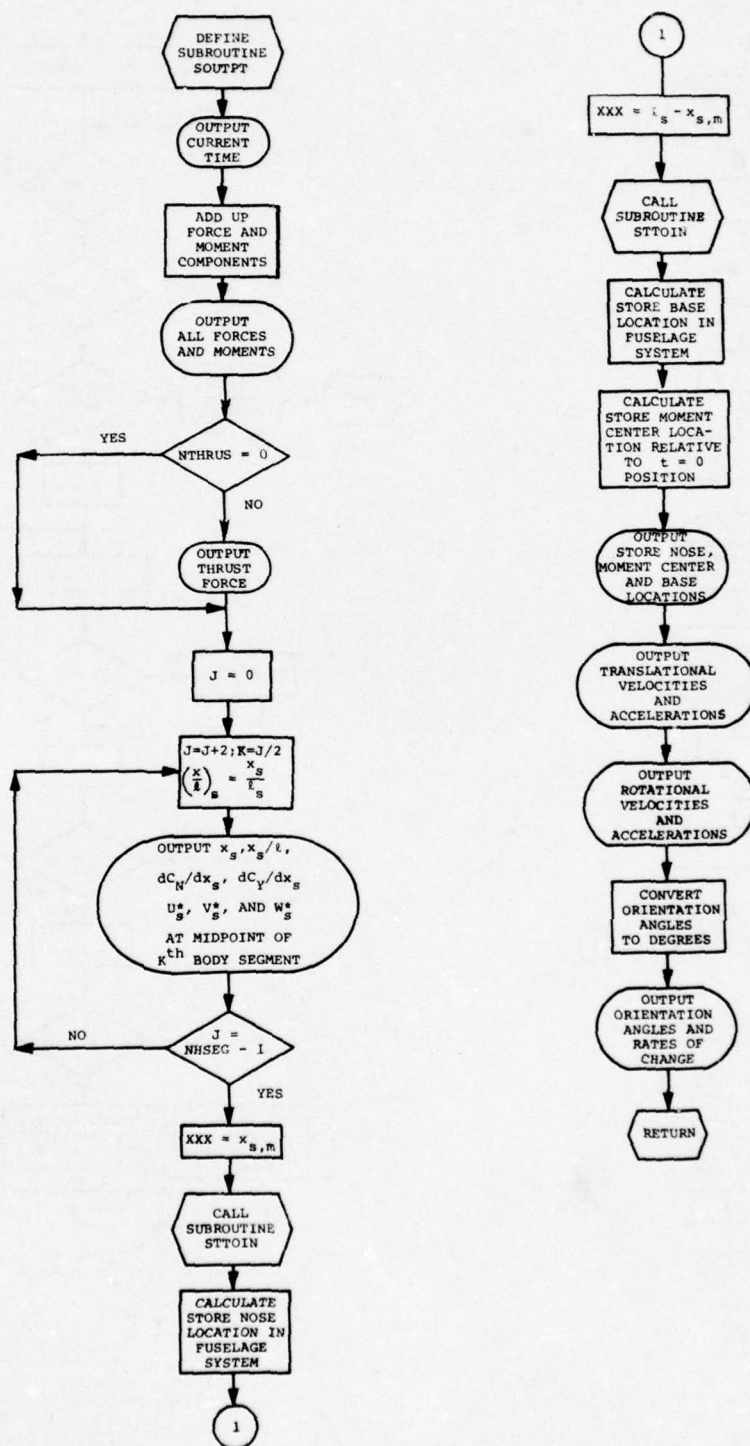
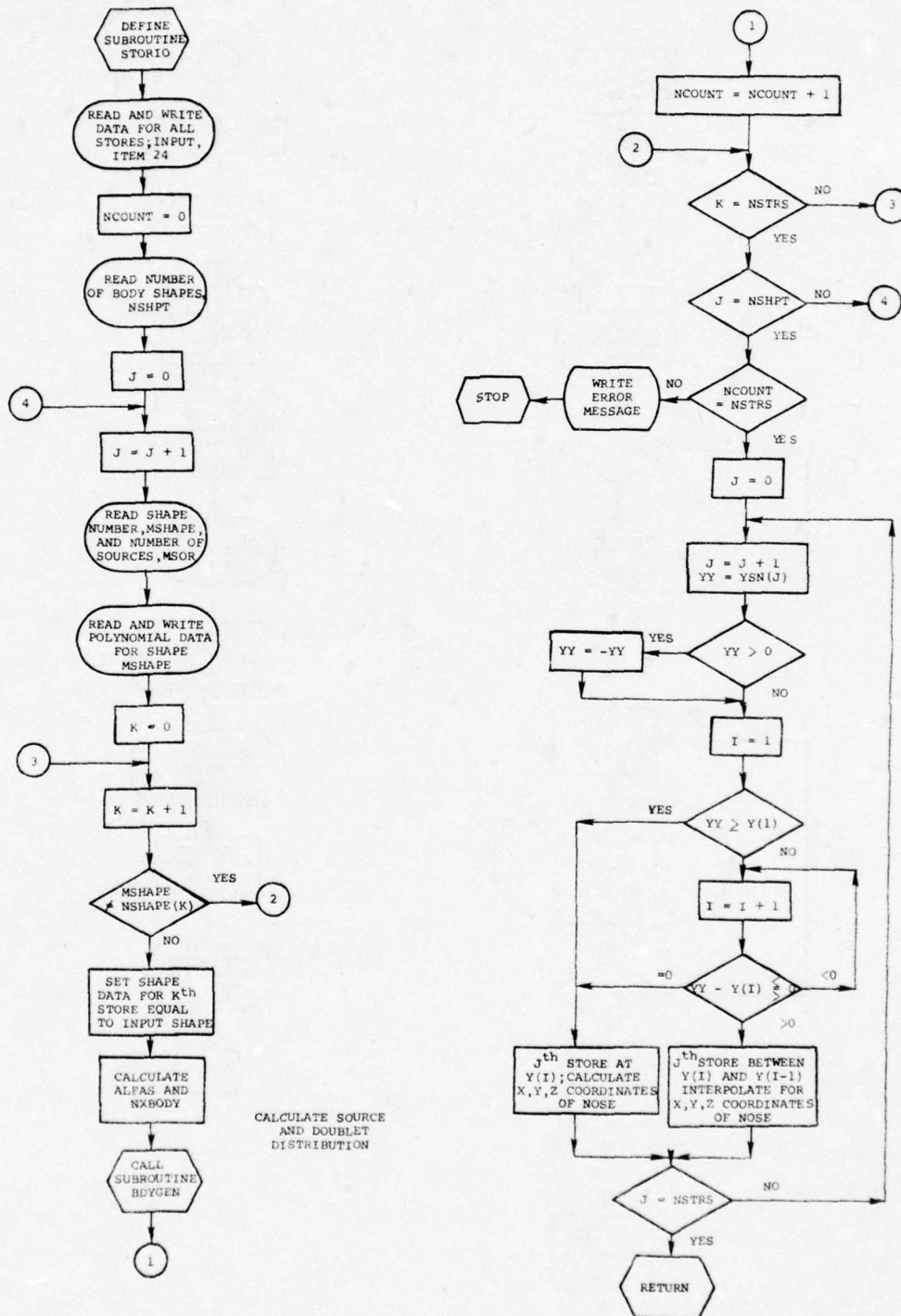
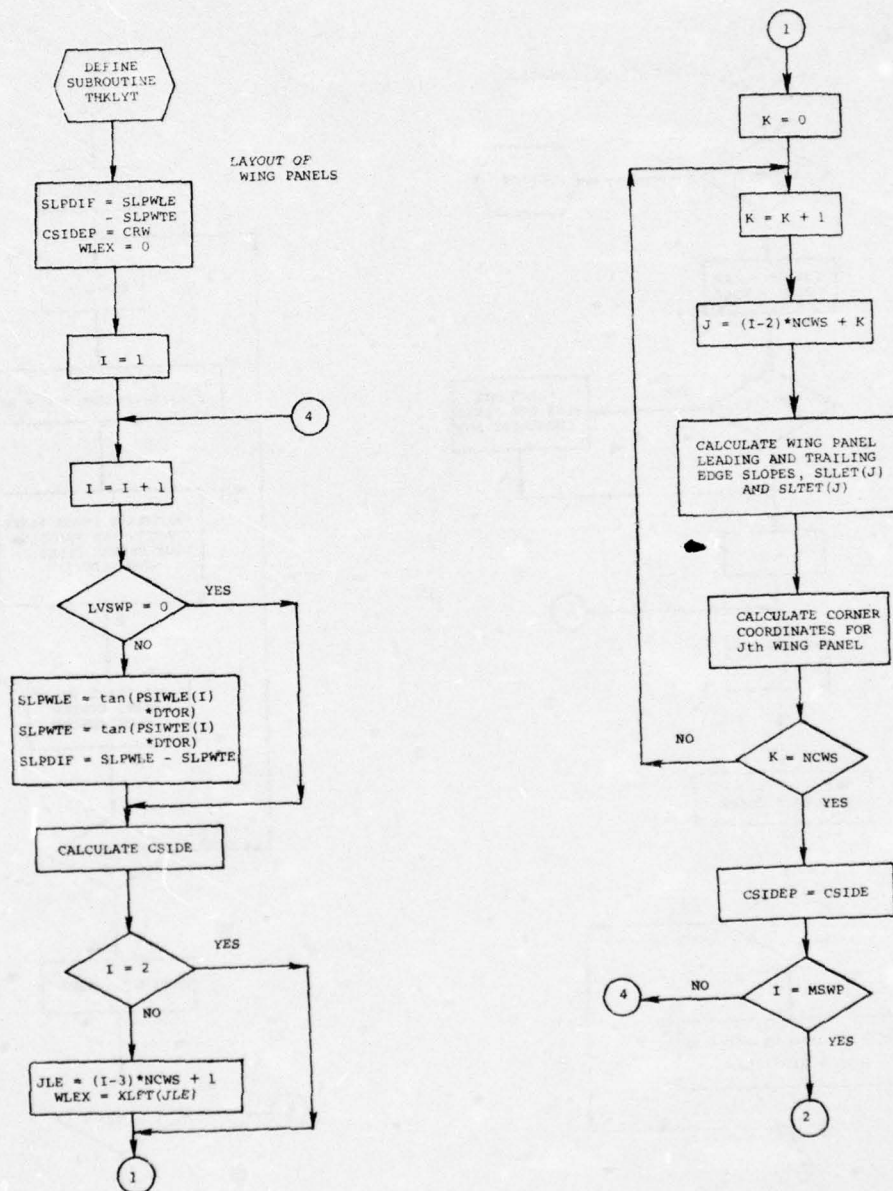


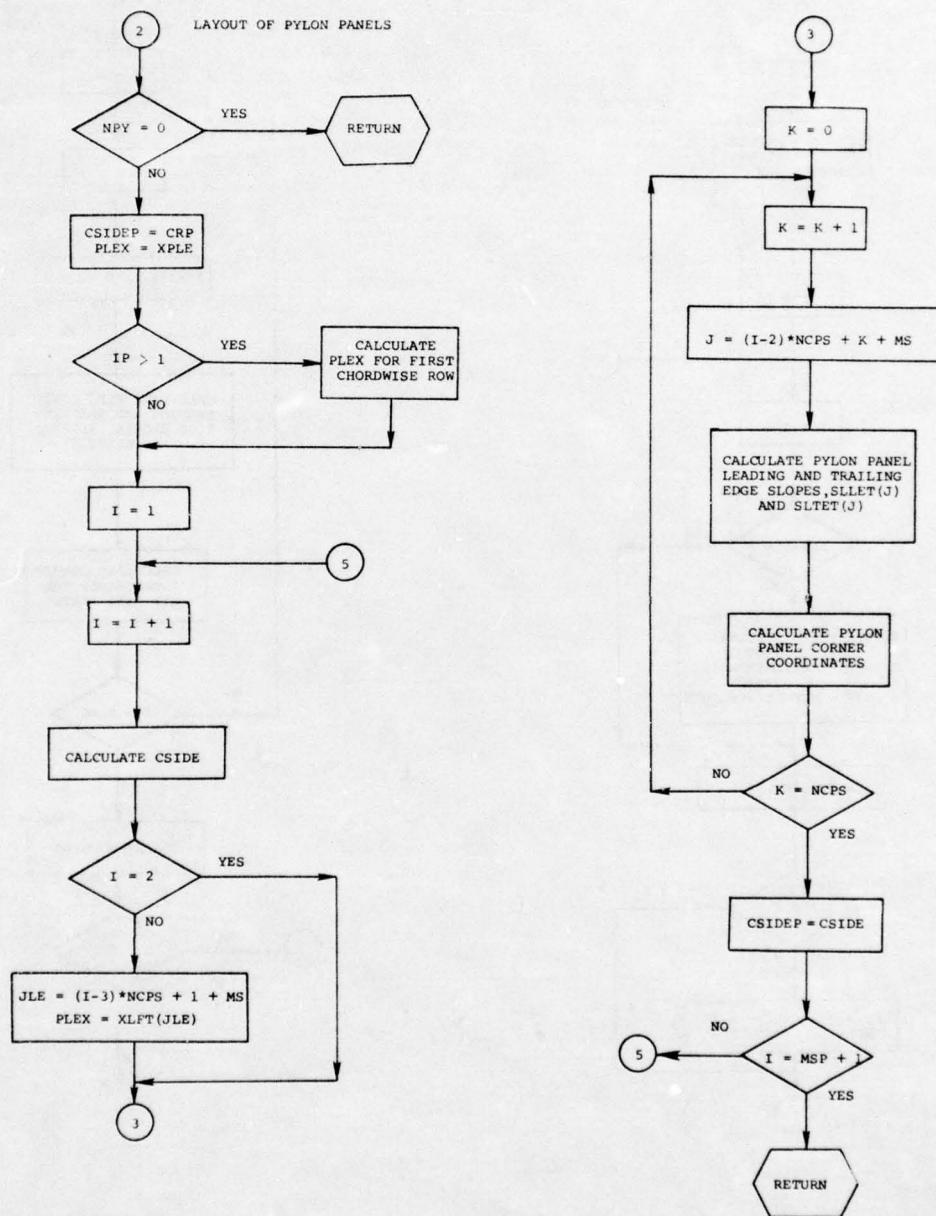
Figure I-17.- Flow chart of subroutine SOUTPT.



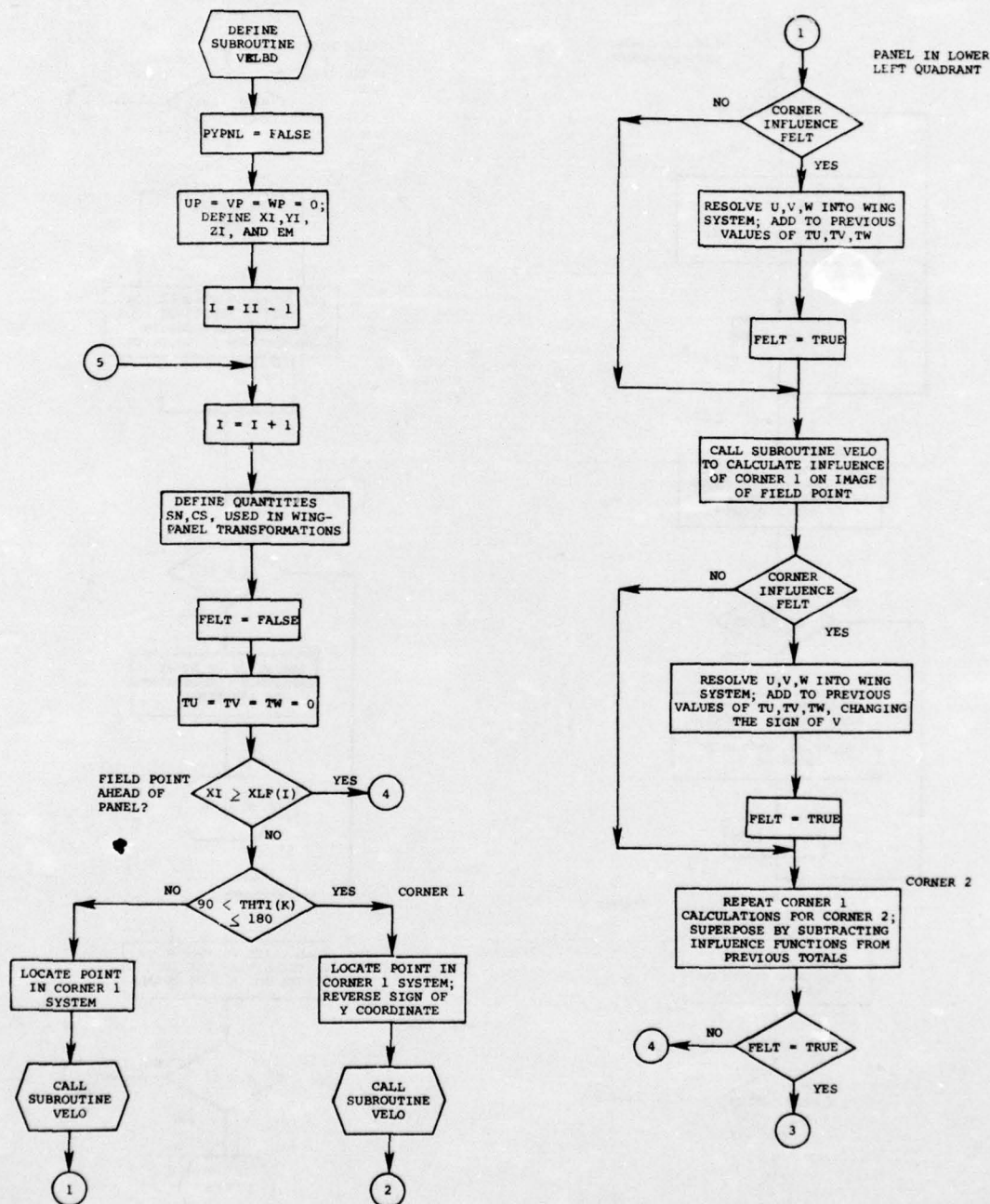


(a) Page 1.

Figure I-19.- Flow chart of subroutine THKLYT.

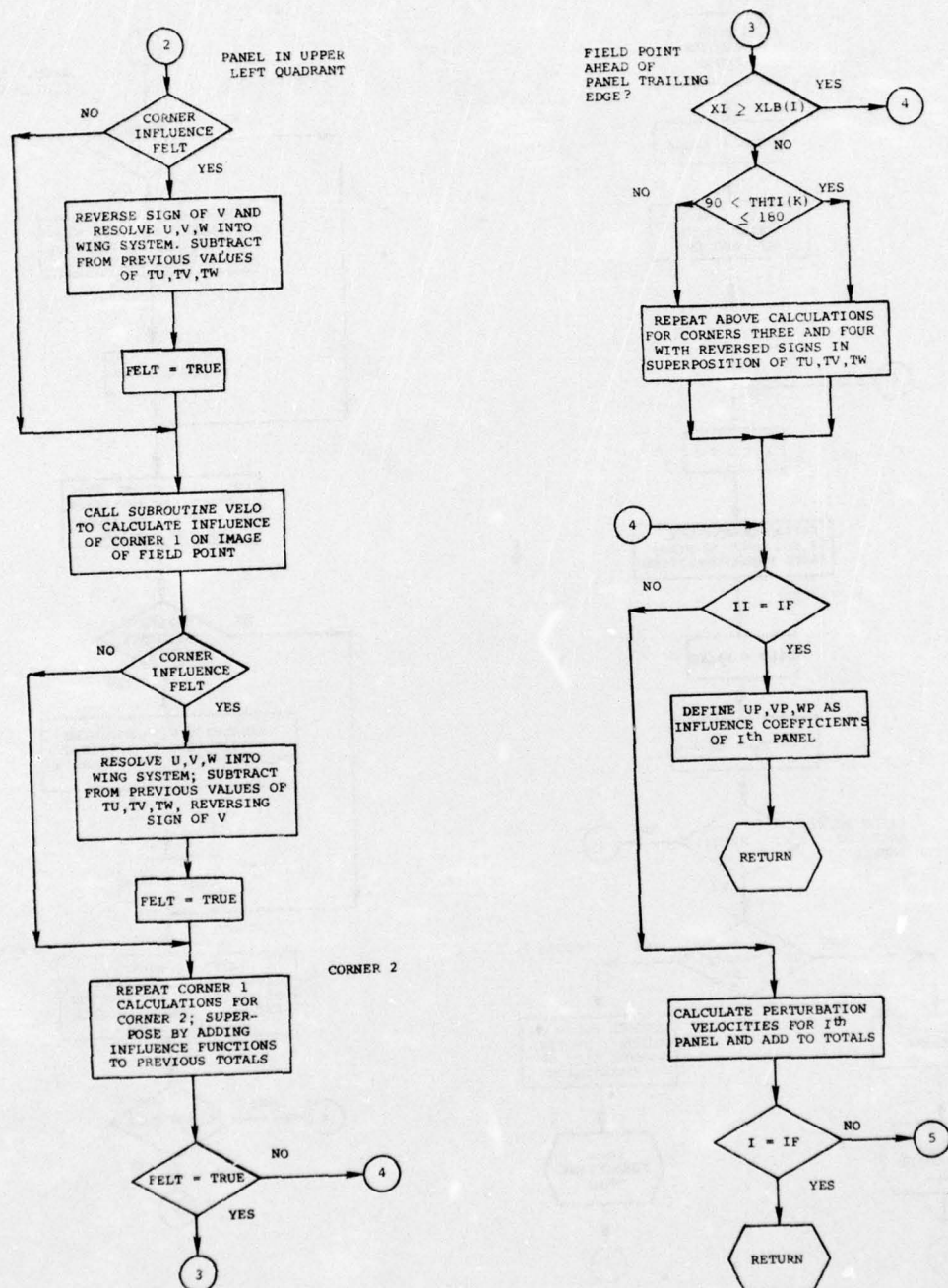


(b) Page 2.
Figure I-19.- Concluded.



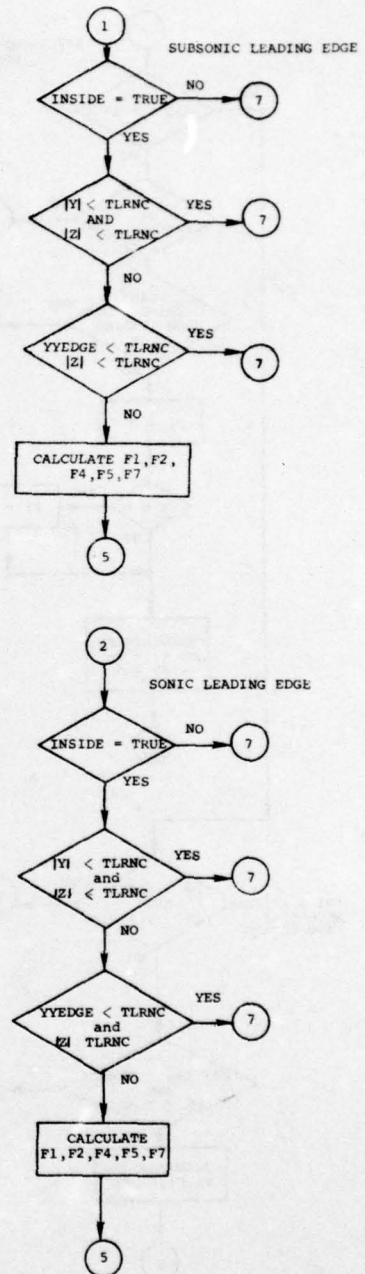
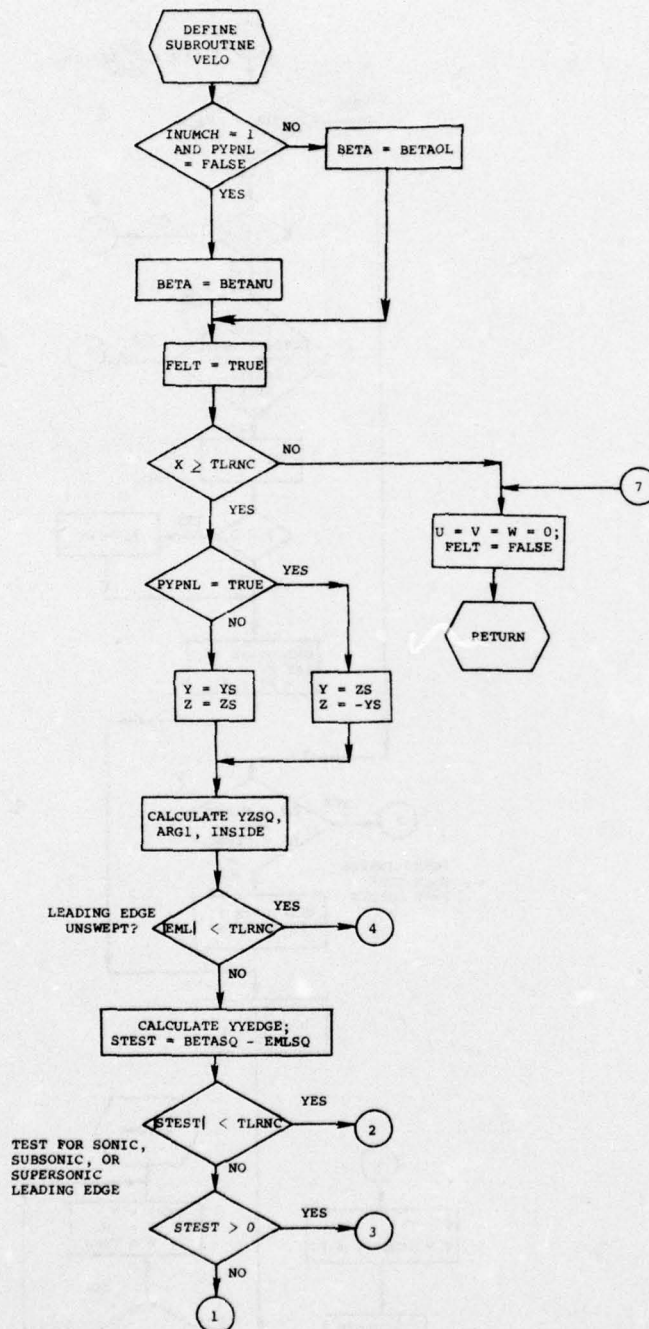
(a) Page 1.

Figure I-20.- Flow chart of subroutine VELBD.



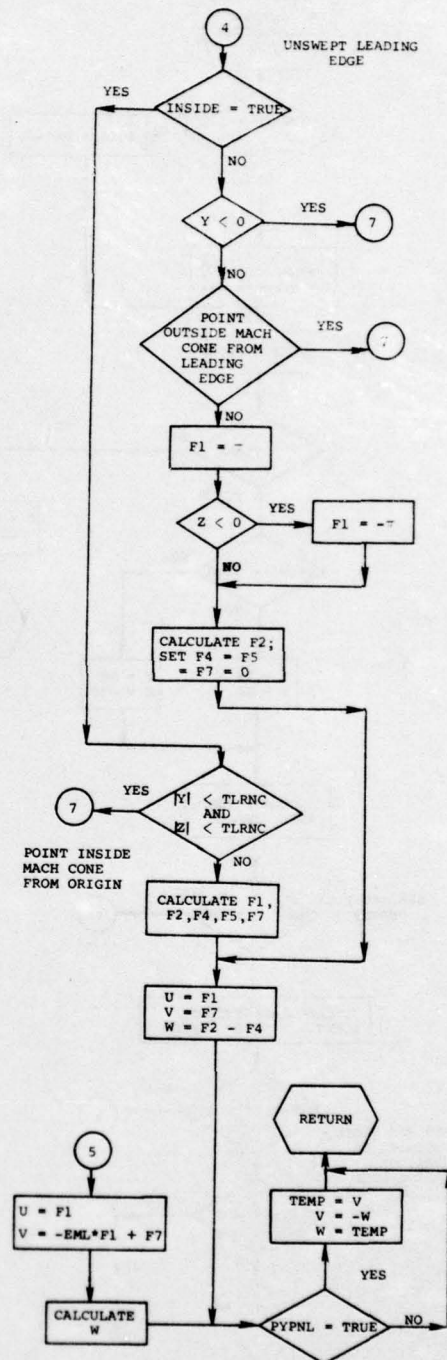
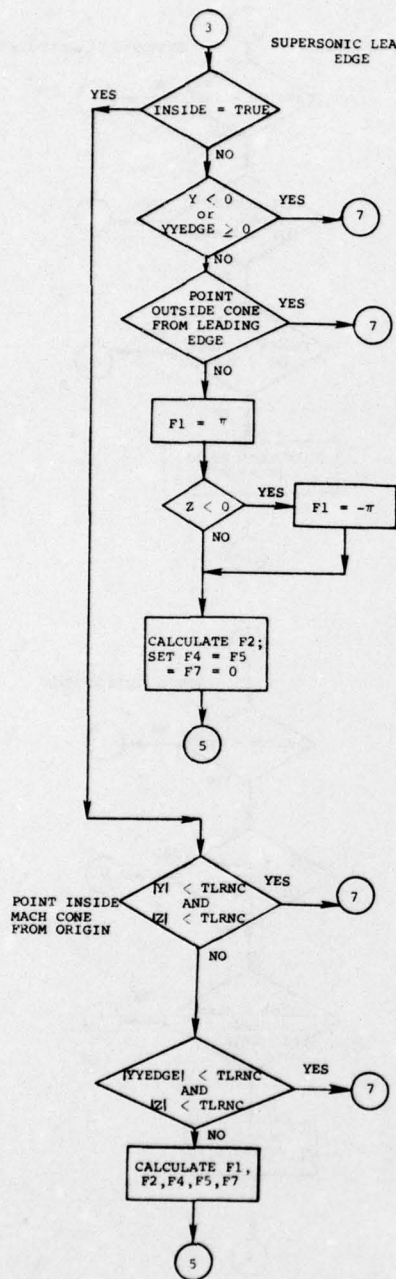
(b) Page 2.

Figure I-20.- Concluded.

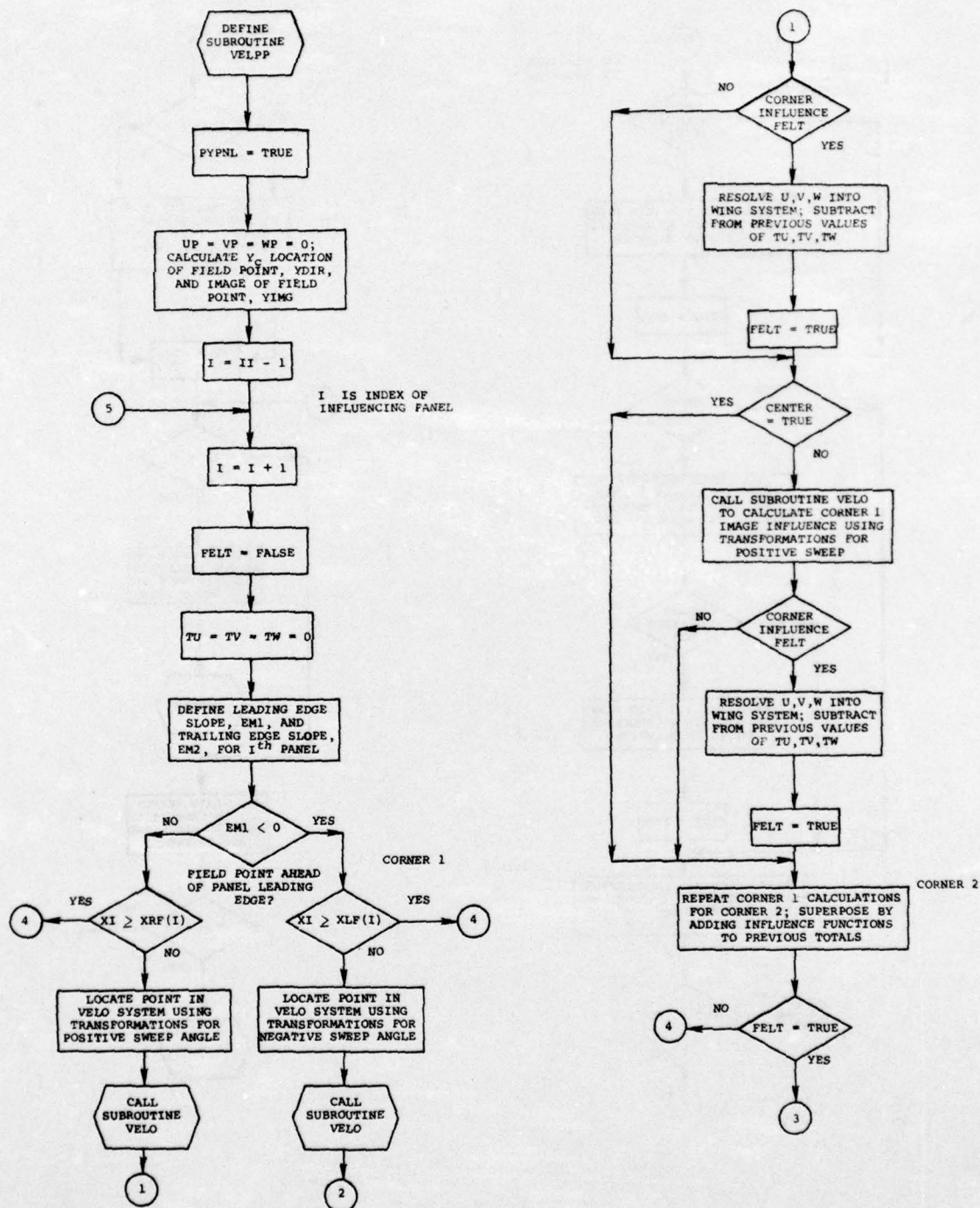


(a) Page 1.

Figure I-21.- Flow chart of subroutine VELO.

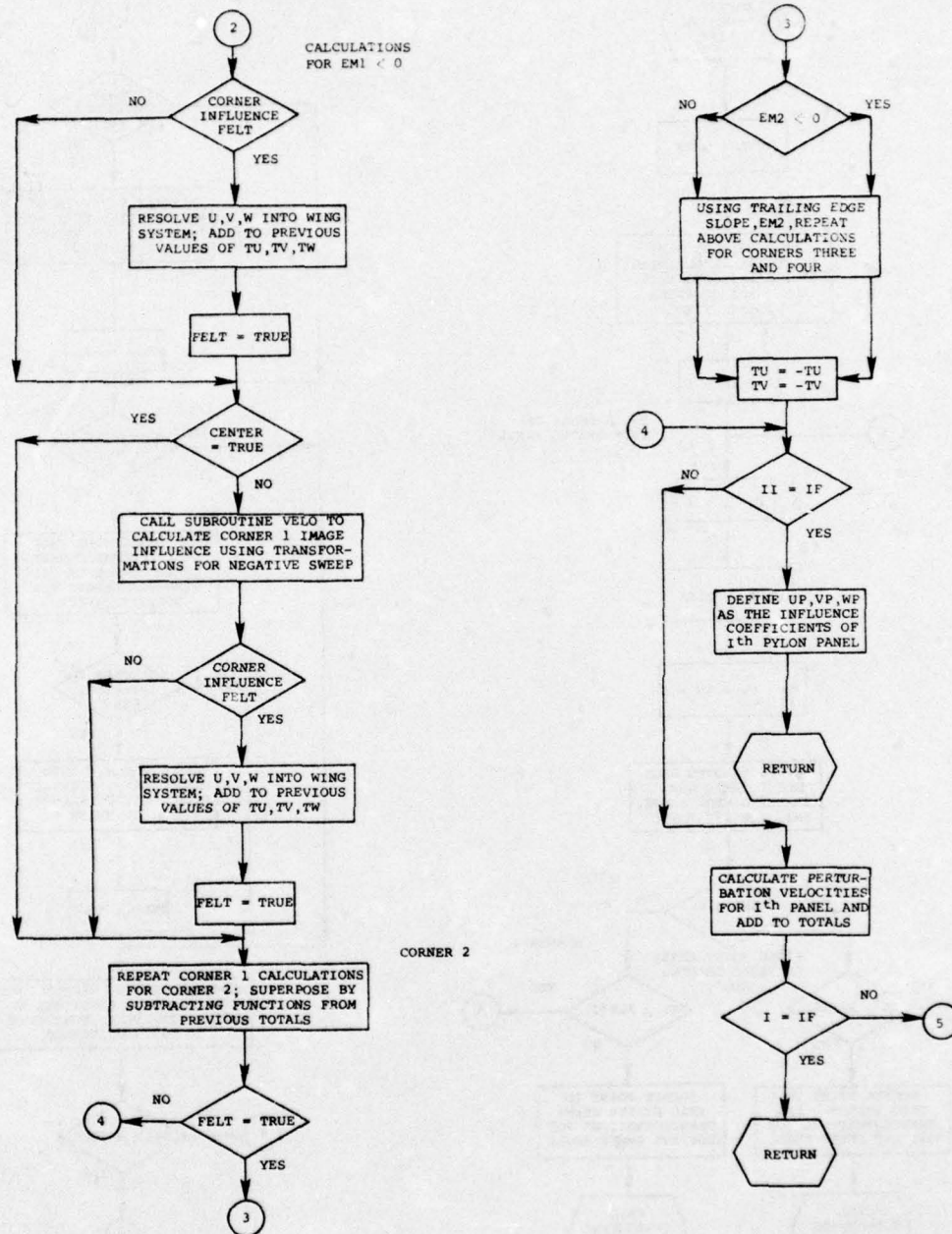


(b) Page 2.
Figure I-21.- Concluded.

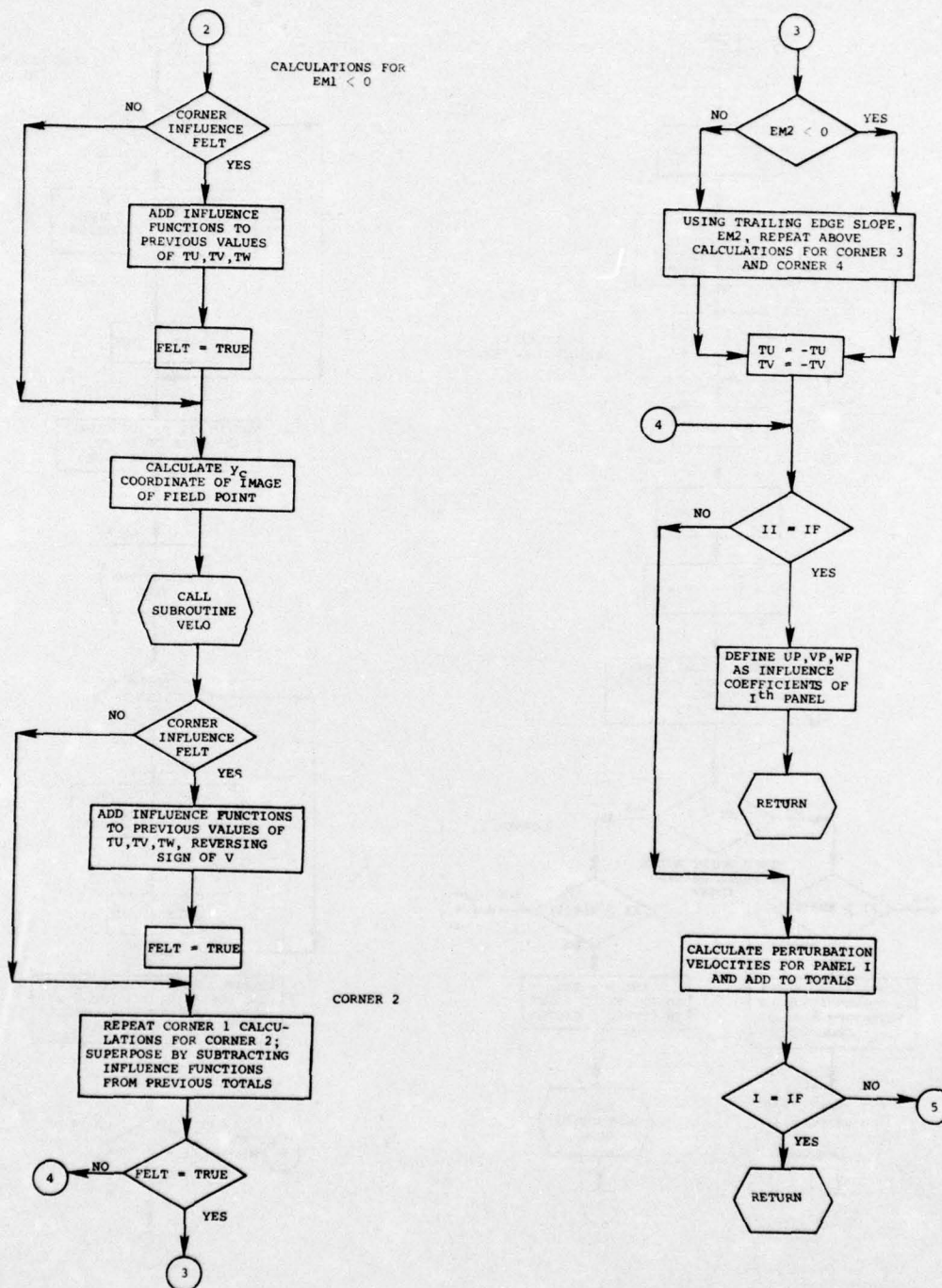


(a) Page 1.

Figure I-22.- Flow chart of subroutine VELPP.



(b) Page 2.
Figure I-22.- Concluded.



(b) Page 2.

Figure I-23.- Concluded.

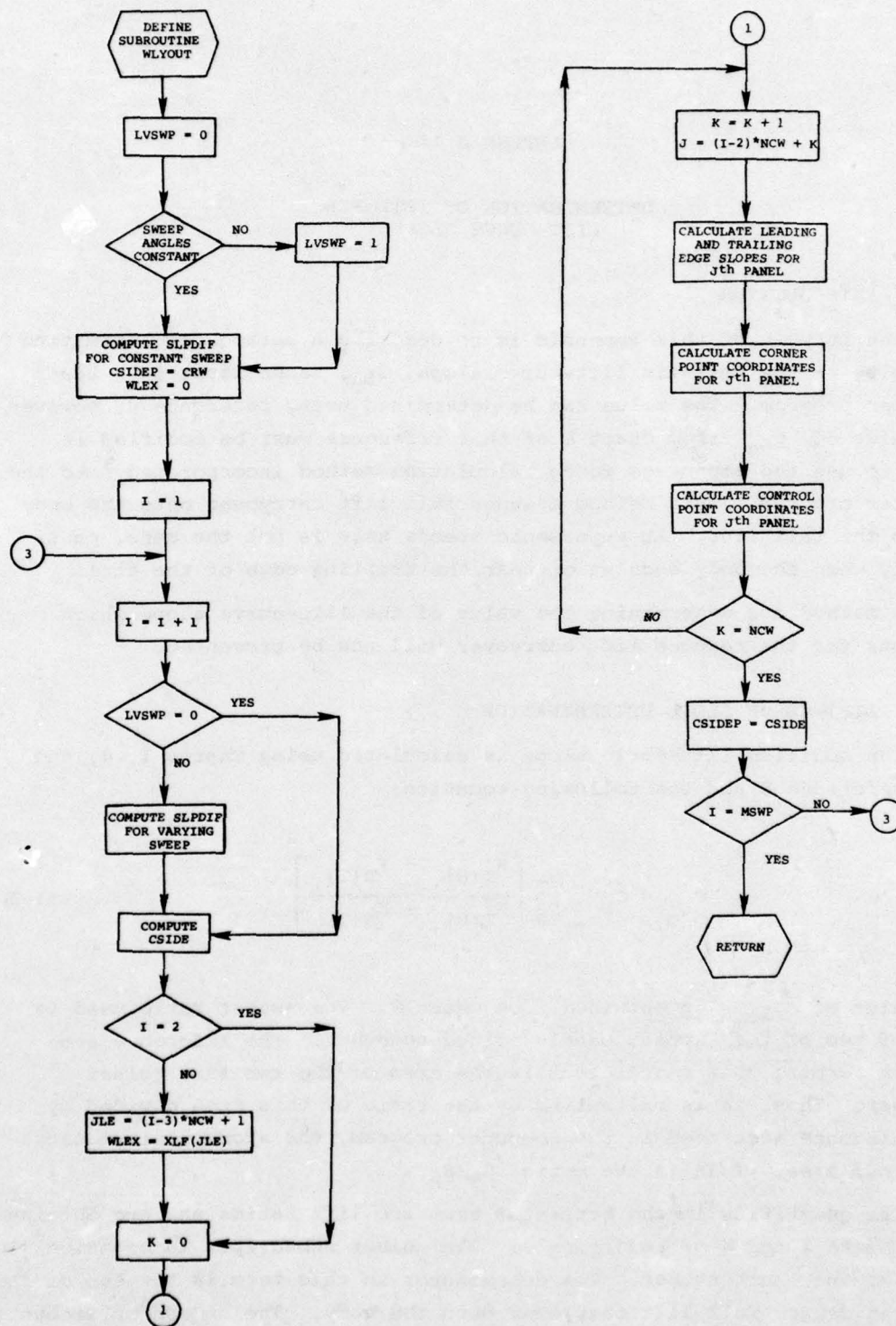


Figure I-24.- Flow chart of subroutine WLYOUT.

APPENDIX II

DETERMINATION OF TAIL-FIN LIFT-CURVE SLOPE

II-1. INTRODUCTION

The purpose of this appendix is to describe a method for estimating the value of the tail-fin lift-curve slope, $C_{L_{\alpha}}$, to be input into the computer program. The value can be determined using reference 8; however, the value of $C_{L_{\alpha}}$ from Chart 8 of that reference must be modified in order to use the empennage force calculation method incorporated into the computer program. This method assumes full lift carryover onto the body due to the tail fins. At supersonic speeds this is not the case, particularly when the body ends at or near the trailing edge of the fins.

A method for determining the value of the lift-curve slope which accounts for the reduced lift carryover will now be presented.

II-2. LIFT-CURVE SLOPE DETERMINATION

The modified lift-curve slope is calculated using Charts 1, 4, and 8 of reference 8 and the following equation:

$$C_{L_{\alpha}} = C_{L_{\alpha T}} \frac{S_T}{S_R} \left[\frac{K_{T(B)1} + K_{B(T)4}}{K_{T(B)1} + K_{B(T)1}} \right] \quad (\text{II-1})$$

The value of $C_{L_{\alpha T}}$ is obtained from Chart 8. The aspect ratio used is that of two of the exposed panels joined together. The reference area used in forming this coefficient is the area of the two fins joined together. Thus, it is multiplied by the ratio of this area divided by the reference area used in the computer program, the store maximum cross-sectional area. This is the ratio S_T/S_R .

The quantities in the bracketed term are lift ratios and are obtained from Charts 1 and 4 of reference 8. The number subscripts in equation (II-1) refer to the chart number. The denominator in this term is the sum of the lift ratios for full lift carryover onto the body. The numerator accounts for only partial lift carryover onto the body. In determining the value of $K_{B(T)4}$ from Chart 4, $(C_{L_{\alpha}})_W$ is $C_{L_{\alpha T}} S_T/S_R$, the quantity multiplying the bracketed term in equation (II-1).

It is recommended that Chart 4 be used for low-aspect-ratio as well as high-aspect-ratio tail fins. Reference 8 recommends that Chart 4 only be used when the aspect ratio parameter defined there is greater than 4.0. The use of this chart in determining $K_{B(T)}$ for values of the aspect ratio parameter of 3.0 and 2.25 has resulted in good agreement with experimental data for the two different stores in uniform flow.

REFERENCES

1. Dillenius, M. F. E., Goodwin, F. K., and Nielsen, J. N.: Prediction of Supersonic Store Separation Characteristics. Vol. I - Theoretical Methods and Comparisons with Experiment. Technical Report AFFDL-TR-76-41, Vol. I, May 1976.
2. Dillenius, M. F. E., Goodwin, F. K., and Nielsen, J. N.: Extension of the Method for Predicting Six-Degree-of-Freedom Store Separation Trajectories at Speeds up to the Critical Speed to Include a Fuselage with Noncircular Cross Section. Vol. I - Theoretical Methods and Comparison with Experiment. Technical Report AFFDL-TR-74-130, Vol. I, Nov. 1974.
3. Goodwin, F. K. and Dillenius, M. F. E.: Extension of the Method for Predicting Six-Degree-of-Freedom Store Separation Trajectories at Speeds up to the Critical Speed to Include a Fuselage with Noncircular Cross Section. Vol. II - Users Manual for the Computer Program. Technical Report AFFDL-TR-74-130, Vol. II, Nov. 1974.
4. Goodwin, F. K., Dillenius, M. F. E., and Nielsen, J. N.: Prediction of Six-Degree-of-Freedom Store Separation Trajectories at Speeds up to the Critical Speed. Vol. I - Theoretical Methods and Comparison with Experiment. Technical Report AFFDL-TR-72-83, Vol. I, Oct. 1974.
5. Goodwin, F. K. and Dillenius, M. F. E.: Prediction of Six-Degree-of-Freedom Store Separation Trajectories at Speeds up to the Critical Speed. Vol. II - Users Manual for the Computer Program. Technical Report AFFDL-TR-72-83, Vol. II, Oct. 1974.
6. Goodwin, F. K., Nielsen, J. N., and Dillenius, M. F. E.: A Method For Predicting Three-Degree-of-Freedom Store Separation Trajectories at Speeds up to the Critical Speed. Technical Report AFFDL-TR-71-81, Nov. 1974.
7. Jorgensen, L. H.: Prediction of Static Aerodynamic Characteristics for Space-Shuttle-Like and Other Bodies at Angles of Attack from 0° to 180°. NASA TN D-6996, Jan. 1973.
8. Pitts, W. C., Nielsen, J. N., and Kaattari, G. E.: Lift and Center of Pressure of Wing-Body-Tail Combinations at Subsonic, Transonic, and Supersonic Speeds. NACA Report 1307, 1957.
9. Perkins, S. C., Jr., Goodwin, F. K.: Data Report for an External Store Test Program Conducted at Supersonic Speeds. Vols. I through VII. Nielsen Engineering & Research, Inc. NEAR TR 103, Dec. 1975.
10. Hildebrand, F. B.: Introduction to Numerical Analysis. McGraw-Hill Book Co., Inc., New York, NY, 1956, Chapter 6.
11. IBM System/360 Scientific Subroutine Package, Version III, Programmers Manual. IBM Corp., GH20-0205-4, August 1970, pp. 372-381.
12. Forsythe, G. E.: Generation and Use of Orthogonal Polynomials for Data-Fitting with a Digital Computer. J. SIAM, Vol. V, No. 2, June 1957, pp. 74-88.

13. Conte, S. D.: Elementary Numerical Analysis. McGraw-Hill Book Co., Inc., New York, NY, 1965, pp. 174-176.
14. Scarborough, J. B.: Numerical Mathematical Analysis. Johns Hopkins Press, Baltimore, 1966, p. 137.